Mathematical Modeling of Liquid/Liquid Hollow Fiber Membrane Contactor Accounting for Interfacial Transport Phenomena: Extraction of Lanthanides as a Surrogate for Actinides

John D. Rogers

August 4, 1994

DISCLAIMER

Abstract

Replace this text with your own abstract.

Contents

1. Membrane and the Membrane Process — A concept

1.1 Background

1.1.1 The Membrane Concept

A membrane in a most general and broadest but rigid sense is: a *region* of discontinuity interposed between two phases [?, page 2]. This region has thicknesses of less than 100 nm to more than a centimeter. Some membrane processes such as the membrane contactors (discussed later) use primarily an interface stabilized in a porous structure to separate two immiscible fluids and transfer mass between the phases. However, this interface, though sometimes visualized as a discrete jump in discontinuity from one phase to another, is in reality a region of steeply or rapidly varying spacial differences between the properties of one phase and another phase. Perhaps a more realistic definition of a membrane is given by Lonsdale [?].

> " a membrane isn't just an object in the abstract, but its definition must embody its function. As the functions we ask membranes to carry out broaden, so must our definition."

Strathmann [?] and Noble and Way [?] elaborate and echo the definition of a synthetic membrane as: a semi–permeable barrier which separates two phases and restricts the transport of various chemical species in a rather specific manner. Strathmann, and Noble and Way suggest that a membrane be defined by what it does, rather than what it is. This statement is due to the properties that a membrane has, the contiguous parts that cause a membrane to exist, and the membranes primary goal and physio/chemical methods and laws by which it accomplishes this goal. In short a membrane is more of a process than a distinct physical entity. The membrane process separates mixtures into components by discriminating on the basis of a physical or chemical attribute, such as molecular size, charge or solubility.

1.1.2 Historical Development of Membrane Process

The processes of separating components in a fluid using membranes is as old as life itself. Mankinds use (or at least recorded use) of membrane technology, usually with little understanding of the process, to separate components in fluids have spanned hundreds of years.

Abbé Nollet in 1748 placed wine in a vessel sealed with an animal bladder and placed the vessel in water. The bladder being more permeable to water than wine swelled and sometimes burst ([?], [?], Kirkothmer, vol 14 1967 p345, [?, p. 27-28]). Through the nineteenth and twentieth centuries, membranes were not used commercially though laboratory use developed physical/chemical theories. van't Hoff developed his limit law using membranes. Data published by Traube and Pfeffer for osmotic pressures of solutions led to understandings of ideal dilute solutions. Maxwell and others used membranes to help develop the kinetic theory of gases. Grahm in the mid 1800's used membranes in the development of theories on separations and gas mobilities and can be considered to of had a considerable initial impact in the field of colloid science which is based in a large part on membrane studies.

Commercial applications of synthetic membrane processes began in the early twentieth century primarily stimulated by the advent of micro porous polymeric materials with graded pore sizes. Later during World War II European water supplies were tested using filters developed under sponsorship of the U. S. Army and later exploited by the Millipore Corporation. In the early 1960's the discovery of Loeb and Sourirajan process for the manufacturing of defect-free, high flux, ultra thin, selective surface films supported on a micro porous support and the infusion of large research funds from the U. S. Department of Interior resulted in commercialization of reverse osmosis and the development of ultrafiltration and micro-filtration [?, p 27-28].

Expanding the Loeb-Sourirajan membrane technology other process were developed for making ultra thin, high-performance membranes. These process of interfacial polymerization or multilayer composite casting and coating allow membranes as thin as 0.1 μm or less. Packaging membranes into spiral wound, hollow-fiber, capillary, and plate-and-frame modules were developed. As a result commercial application of micro filtration, ultrafiltration, reverse osmosis, and electrodialysis were all established and considered developed processes in large plants around the world by the 1980's [?, p 96-97].

There are currently seven types of commercialized membrane processes discussed in the literature: micro filtration, ultrafiltration, reverse osmosis, electrodialysis, gas separation, pervaporation, and liquid membranes (facilitated transport). The first four processes are considered developed processes in that the technology is relatively understood and applied; of these, the first three are related techniques and are pressure driven processes. The electrodialysis process uses a charged membrane to remove or separate ions under an electrical potential difference. Gas separation and pervaporation process are in a developing mode. In this process the membrane is permeable to certain species of gas and not to others in the gas stream. Pervaporation is a process that separates dissolved solvents. Transport in pervaporation is induced by the difference in partial pressure between the liquid feed

solution and permeate vapor on the one side of the membrane.

In the 1980's and 1990's gas-separation technology, pervaporation, and liquid membrane process applications are evolving and expanding. The liquid membrane process particularly facilitated transport is classified by Baker et al. as a "*to be developed*" technology. Liquid membranes (facilitated transport) differ from the other membrane types in that they involve specific chemical reactions like those in extraction. Because of this the separation can be very selective and custom tailored to specific separation operations.

1.1.3 The Liquid Membrane Process

Three types of liquid membranes are under study in the literature: immobilized liquid membrane, emulsion liquid membranes, and membrane contactors.

Emulsion Liquid Membranes: Emulsion liquid membranes or ELMs, whose development is credited to Li in 1968, are multi phase liquid systems of concentric spheres where one phase (phase I) is a droplet encapsulated in an outer immiscible phase (phase II). These concentric spheres or droplets are dispersed in a continuous phase (phase III), immiscible to the outer phase of the droplet. This third phase contains a chemical species to be extracted. Phase II is usually an organic in which a chemically reactive agent or "carrier" is placed and is selectively reactive with a specific species in the continuous phase. A species to be removed reacts with the carrier and the complex diffuses across the membrane where it reacts again and diffuses into the inner phase I. The advantage of this process is that the separations are very fast; but, the emulsion manufacture, separation, and recovery of the internal phase can be difficult and involves a number of operations.

Immobilized liquid Membranes: These membranes are similar to the emulsion membrane in that an organic phase with a carrier species is interposed between two phases both immiscible to the organic phase. The difference lies in that the organic "membrane" of the immobilized liquid membrane is immobilized in the pores of a synthetic micro porous structure with sufficiently small pores to be held there by capillary action. These ILMs are easily made and are normally stable for periods of days, weeks, or maybe months but eventually decay (Cussler in [?, p 244]).

Membrane Contactor: The membrane contactor is another method of facilitated diffusion. This type of membrane basically separates the extraction and stripping process into two units of operation, though variations can keep the two interfaces in the same "module". These variations give it more physical similarity to the ILM. This membrane process uses a micro porous structure or

element like the ILM, but the pores are not impregnated with the organic that actually makes the membrane "active" per se. Two bulk phases immiscible in each other flow on each side of the porous element. The species being extracted are transferred from one phase to the other depending on the physio/chemical properties of the two fluids. Phases are usually an aqueous phase and an organic phase but do not have to be;however, the phases must be immiscible to each other in all proportions for the process to work well. Depending on whether the element is hydrophobic (water hating) or hydrophilic (water liking) determines whether the organic or aqueous phase invades the pores. The contactor performs the same function as a packed tower or liquid/liquid extraction column or centrifugal contactor. Usually the process is counter-current and exhibit the advantages of liquid membranes, but avoid the disadvantages of absorption and extraction. A large area per volume is an advantage and provides for fast separations. They are unaffected by loading, flooding, or by density differences between feed and extract [?, p 248].

Liquid membrane processes are in a development stage and as has been stated in the brief descriptions above they are selective, provide fast separations, but suffer from a major problem of instability. Four main causes of this instability are (see Cussler in [?, p 246]):

Solvent Loss: Is when the solvent making up the active portion of the membrane is lost due to solubility in the adjacent phases. Eventhough the solvents are selected for their immiscible properties in the surrounding phases all fluids are soluble in each other to some extent. Eventually the solvent is lost and the capillary action is not as strong and the membrane ruptures.

Carrier Loss: The solutes as they react with the carrier may make them more soluble in the surrounding fluids and cause loss of the carrier.

Osmotic Imbalances : Facilitated transport can concentrate the solute in the extracting phase or organic membrane sufficiently to cause a large difference in the osmotic pressures causing rupturing or forcing the liquid membrane from the polymer support. This is the chief cause of membrane instability.

Spontaneous Emulsification: The membrane extractants can extract to a small extent the fluids and thus cause the membrane to change characteristics and can cause channeling across the membrane when these fluids are stranded in the membrane.

The membrane contactor avoids many if not all of the stability problems associated with the membranes above. This is basically the result of separating the interfaces associated with the membrane processes. The membrane contactor performances have been excellent

in the laboratory; but, their performance under industrial conditions is only currently being explored. The energy requirements have also to be illuminated.

This study is interested in the membrane process classed as a liquid membrane or facilitated transport technology particularly the sub class category of *membrane contactors*. The membrane contactor is, as Cussler points out: *a hybrid, combining aspects of both conventional extraction and liquid membranes* (Cussler in [?, page 248]).

1.2 Purpose and Scope of This Study

The purpose of this study is threefold

1. To define mathematically the HFM (Hollow Fiber Membrane) contactor separation process by fundamental theoretical laws of physics and chemistry of fuid and mass transport
2. Based on this mathematical model a computer simulation is to be developed that allows the contactor to be simulated under varying conditions with different extractants and species transferred
3. Varify the model using literature and/or experimentally obtained data

The emphasis is primarily to model the extraction of the lantanide and actinide metal compounds from an acid solution. However, the mathematical modeling and simulation should readily extend to other specie extraction needs with input of limited information about the fluids of the system.

1.3 The Membrane Contactor

1.3.1 Description of the Membrane Contactor

The membrane contactor consists of a bundle of small microporous filaments that separate two immiscible phases but allow intimate contact in the porous structure. Analogous to a small shell-and-tube heat exchanger, the HFM's two fluids flow parallel on either side of the filament or "tube" transfering mass instead of heat. Though the filaments are porous, the process is designed such that there is no intentional convective transport through the pores. Instead the porous material acts as a support to facilitate diffusive transfer by the contact of the phases. Material of construction varies and is generally a polyolefin or cellulose ester and is either hydrophobic or hydrophilic. This material property determines where the interface of the two phasese will be located. For a hydrophylic membrane the interface will be in the proximity of the pore entrance on the aqueous side of the membrane. Counter

pressure on the aqueous side is used to keep the non-aqueous phase from flowing into the aqueous phase.

The diagrams in figure ?? show a schematic of the module and also various configurations of types of flow. Most flow configurations are parallel but there has been reports of crossflow experimental work (cf. [?]). Flow is generally parallel for convenience and can be either co-current or countercurrent. A variation of the membrane contactor is the "*contained membrane contactor*" which emulates the immobilized liquid membrane discussed in section 1.1.3. Figure ?? illusrates the contained liquid membrane flow. Where the HFM contactor only has a stripping or extraction stage the contained HFM has both in a single unit. The disadvantage to this module is the difficulty its manufacture and current inablility to model and verify the performance. Ideally the contained liquid membrane would qualitatively be optimal. Once the model and simulator at the fundamental level is developed and working the effort to extend it to the contained HFM may not be as intensive.

1.3.2 Modeling of the Membrane Contactor

The modeling and simulation of liquid membranes, be they emulsion, supported (immobilized), or the membrane contactor are, from an indepth fundamental approach, complex. Extraction of metal compounds from an aqueous phase into an organic phase creates chemical and physical complexities. These complexities involve the formation of an interface with chemical reactions occurring in both phases and at the interface simultaneously and in parallel.

Coupling the reaction mechanism with the diffusion of species through three phases (i.e. aqueous, pores in the membrane, and organic phase) with the mementum effects of the fluid flow internally and externally to the hollow fiber and the characterization of the process elevates in complexity. Because of the complexity at the fundamental level, many workers have used simplified theory of the process and used empirical data to model and simulate the process. Though, the procedures and theory these investigators used are sound they allow only the study of a process for a specific extraction under simplified conditions and only within range of the empirical data (see chapter 5)

1.4 Organization of this Report

This report presents the details of the mathematical modeling as a precursor to the development of a fundamental computer simulation of solvent extraction primarily that used in the nuclear industry using a hollow fiber membrane contactor. Chapter 2 presents the chemistry of solvent and metal extraction with emphasis on the nuclear industry. A literature discussion of the kinetics of metal extracts as it effects the transfer rates and explanations

of experimental procedures and difficulties in determining kinetic and diffusional regimes is presented in chapter ??. Modeling of the membrane contactor in chapter 5 shows the interelationship and critical coupling of the diffusional and (fluid motion) momentum equations that define the membrane contactor model. The theoretical effects of packing or placement of the fibers in a shell and the application of computational geometry concepts of Voronoi diagrams and its theoretical dual the Delaunay Triangulation to the modeling of HFMs are also presented in chapter 5. The concept from geometric computation are used here to define the boundaries between the fibers. One of the most critical aspects of membrane analysis is that of the interface and the theoretical equations that describe it — these are discussed in chapter 6. Necessary data acquasition and possible theretical thermodynamic methods to calculate the necessary input data are given in chapter ??. A summary of the rigorous fundamental model equations and for comparison the simplified theoretical model generally used is presented in chapter ??.

2. METAL EXTACTION

2.1 CHEMISTRY of EXTRACTION

The mass transfer mechanism of the transfer of a metal through an interface of two immiscible fluids is dependent upon the kinetics of the complex formation between the metal and the extractant. The interphase properties that control the transport of the metal species are dependent on the reaction kinetics of metal with the extractant and where it occurs; presumably at the interface if the Damköhler II (Da_{II}) number is low, $Da_{II} \ll 0.1$ (at a $Da_{II} \ll 0.1$ the reaction rate is controlling while at a $Da_{II} \gg 10$ then the molecular diffusion rate is much faster than the reaction rate) (H. J. Bart. Solvenat 1990 page 1229-1344). Between these two values a mixed diffusion regime is evident. The Da_{II} number has been suggested by Bart and Marr to be useful in determining the extraction process to be used (e.g. mixer settlers or columns or perhaps membrane processes). The dominating regime may change depending on the concentrations being delt with. Rogers, Thompson and Thornton (extraction 87 page 15) attribute this switching to interfacial phenomena of build up of complexed species at the interface and the "aging of the interface" with less interfacial turbulence and dependence on the metal species to diffuse to the interface, complex with fresh extractant, and diffuse away. The diffusion of the complexed extractant away from the interface and allowing fresh extractant to diffuse to the interface is an important operation. Thus the reaction mechanism and kinetic analysis is vital to understanding and designing any process for liquid liquid extraction process, particularly the membrane process. In the membrane processes the reaction of the extractant with the metal is referred to as facilitated transport.

2.1.1 Literature Review

The literature is extensive in the area of solvent extraction. In the area of hydormetallurgical and nuclear solvent extraction the literature is contradictory and massive. As we have found out and other authors have stated most studies do not present kinetic or thermodynamic data that is useful in chemical engineering practice and is needed for proper modeling, simulation and design of processes needed for critical separations. Most of the information published is in equilibrium form represented by distribution coefficients of the solute between the organic and aqueous phases. Though this information demonstrates which extractant is useful in certain situations it does not allow any rigorous or first principle design to be formulated. The kinetic data is imperative to model from transient to steady state

situations, upsets in the process, different process conditions such as change in tempeartures and is vital to properly model the diffusion and reaction controlled regimes. Recently (ca. 1990's) information has emerged form the Japanese and a few European laboratories on reporting kinetic information in the extraction of metals. An attempt to obtain from the literature an understanding and glean the scant and illusive and hidden data needed to properly model the extraction of lanthanides and actinides from acidic media is recorded below (albeit incomplete).

General Extraction Considerations

Tarasov and Yagadin (ISECC'88 International Solvent Extraction Conference July 18-24, 1988 Moscow page 8) discuss some results and problems associated with extraction kinetics. Four key questions are brought out

1. What phenomena determine the extraction rate?
2. What peculiarities give the existence of two phases and the interfacial region when chemical reactions proceed?
3. What information or knowledge can be yielded through the studies of extraction kinetics ?
4. Is it possible to control the extraction rate not by adding energy but by using non-traditional techniques?

Three parameters effect the extraction rate: Interfacial area, the driving force of the process, and the resistance of the system to equilibrium. Incorrect consideration of these components and there will be inconsistencies in the study. The resistance can be used to compare different systems. The interface is of critical importance since the mass transfer coefficient is, and the factors affecting it are, concentrated in this region; chemical reactions, accumulation of insoluble products (microdrops, and solid particles) blocking the interface, adsorption and desorption barriers of electric nature, spontaneous interfacial convection i.e. movement of fluids along the interface caused by interfacial tension gradients during mass transfer. The mass transfer coefficient lumps all of the above into one parameter.

Tarasov and Yagadin discuss several regimes and the connections to the transfer rates. The measurement of interfacial properties such as interfacial tension, rheological, electrical and optical properties is seen to be important to a topological scheme of the study of surface reactions. The diffusion regime is important since most of the extractants react almost instantaneously with the extractable substance. Other regimes needed to consider for various systems are: transient regime, kinetic regime, surface reactions, acceleration of

chemical reactions, microheterogeneity zone and condensed interface films, and spontaneous interfacial convection.

Rod (ISECC'88 International Solvent Extraction Conference July 18-24, 1988 Moscow vol 2 page 3-1) discusses extraction kinetics and its chemical engineering application. His first sentence states "Many papers on kinetics of metal extractions are controversial and do not present the rate equations that could be applied in chemical engineering practice." The mechanistic explanation of the extraction plays a minor role. The following points are of primary importance:

a. Kinetic model must intrinsically comprise a very precise description of the equilibrium and reduce to it at zero extraction rate

b. the parameters of the model that depend on the geometrical arrangement and on hydrodynamic conditions (mass transfer coefficients) must be distinguished from the parameters specific to the given extraction system.

The requirement of equilibrium is very important since most mass transfer operations in industrial countercurrent processes occur close to equilibrium. Thus the accurate description of the equilibrium in the kinetic equation is more important than a perfect fit to the extraction rate in regions far from equilibrium. It is also desirable that the extraction and stripping rate be described by the same kinetic model. The authors direct their discussion to a system where extractant A reacts with the extracted component B to form one extractable complex E which is transferred to the organic phase and a component H which is transferred into the aqueous phase (similar to HDEHP). The stoicheometry is $\nu_A\overline{A}$+B- $\overline{E}$ + ν_HH.

Industrial extractants usually have high extraction rates at very low solubility and the extractants of industrial interest occur in the fast reaction regime and the amount extracted depends on the interfacial areas. The film theory is a useful albeit simplified understanding of the mass transfer models for the extraction process. For fast reactions in the diffusional film the relationships for the extraction rate are obtained by integration of the diffusion equations with corresponding reaction terms over the thickness of the film. Physical equilibrium at the interface and chemical equilibrium in the bulk of the phase is usually assumed. *The integration can be performed analytically only for simplest cases of reaction kinetics and only under restrictive assumptions.*

If the formation of the extractable complex is in the aqueous film and then transferred to the organic phase the relations for the extraction rate are very complex, difficult to solve, and validity restricted by the necessary simplifying assumptions. If the solubility of the extractant is very low the reaction occurs in a very thin reaction zone at the interface

the thickness of which is governed by the reaction rate constant (k_r) and of the partition coefficient (D) (i.e. thickness decreases with increasing values of the reaction constant). In the limiting case where $k_r \rightarrow \infty$, $D \rightarrow \infty$, and $\frac{k_r}{D^2} \neq 0$ the reaction zone thickness approaches zero and the concentration at the interface approach equilibrium expressed by the extraction equilibrium constant

$$K = \frac{\overline{c}_{Ei}(c_{Hi})^{\nu_H}}{c_{Bi}(\overline{c}_{Ai})^{\nu_A}} \tag{2.1}$$

and the model representing the rate equation for extraction accompanied by the equilibrium reaction at the interface is

$$K = \frac{\left(\overline{c}_E + \frac{J}{k_E}\right)\left(c_H + \frac{J}{\nu_H k_H}\right)^{\nu_H}}{\left(c_B - \frac{J}{k_B}\right)\left(\overline{c}_A - \frac{J}{\nu_A k_A}\right)^{\nu_A}} \tag{2.2}$$

where A, B, E, H refers to components and c to concentrations, J to extraction rate or flux at the interface, k the mass transfer coefficient, over bar refers to organic phase,ν stoichiometric coefficient.

The authors contend that many works have used an erroneous analogy to homogeneous kinetics where the effects of the reverse reaction on the extraction rate has been often neglected with $\overline{c}_E$ set equal to zero. The concentration at the interface governs the extraction kinetics and the concentration at the interface of the extracted complex may be significant even if the bulk organic phase is at zero concentration especially for high resistance to diffusion in the organic phase.

DEHPA extractants and others have hydrolipophylic character surface activity and can adsorb at the interface and lower the interfacial tension. These surface active agents cause and increase in the rigidity of the interface, increase the viscosity and decrease diffusivity in the vicinity of the phase boundary and decrease the mass transfer considerably. Two models are referenced by the authors to model the interfacial resistance.

1. The barrier model of Whitaker and Pigford Chem. Eng. Res Des 1985 vol 63 p 89. expresses the resistance by a set of adsorption and desorption constants.
2. The hydrodynamic model by Nguyan et al AICHE J 1979 vol 25 p 1015 assumes the interface is of finite thickness with a capacity to accumulate the solute and that equilibrium exist at its boundaries.

Both models imply resistance additivities and an effective mass transfer coefficient $\overline{k}'$ defined by $\frac{1}{\overline{k}'} = \frac{1}{k} + \frac{1}{k_I}$ where $\overline{k}_I$ is the interfacial resistance. When extraction is accompanied by a reaction involving ions the reaction takes place at the aqueous side of the interface and the

transfer of the components crossing the interface is hindered by the interfacial resistance. The authors give the kinetic model for this type of extraction as well as simplifying it under certain circumstances (i.e. if the extractant is in excess, and when the interfacial resistance of the complex is smaller than the mass transfer of the extractant then the diffusion resistances in the aqueous phase can become negligible. Subsequently assuming $\bar{c}_E = 0$ and $c_B = 0$ the extraction mimic rate control by chemical reaction with power kinetics and the rate of re-extraction being dependent only on the concentration of the extracted complex in the organic phase.

I. Kulawik, J. Kulawik, Mikulski (ISECC '88 International Solvent Extraction Conference July 18-24, 1988 Moscow vol 2 page 3-20) discuss the kinetics of the molecular interactions in some extraction systems. The physico-chemical phenomena of extraction is determined by the state of the system inside the phase. The state of the interface is determined by the "work" of the molecules passing across the interface, the orientation of the molecules on the interface, and the formation and gathering of the charged surface active complex on the interface. *This interfacial state will influence the kinetics of the extraction process, the equilibrium in the system, and the value of the partition coefficient of the extraction substance between the two phases.* Measurements of the molecular interactions in the phases and interactions across the interface are necessary to define the state of the system. These authors measured the surface tension of each phase and interfacial tension using the drop weight method and in some cases these parameters were measured as function of temperature to obtain values for entropy and surface energy of the system. The salts NaCl, $CuCl_2$, $ZnCl_2$, $FeCl_3$, $InCl_3$, $TiCl_3$, and $ThCl_4$ were extracted by TBP or acetylacetone from HCl solutions.

Perez de Ortiz and Tatsis (ISECC '88 International Solvent Extraction Conference July 18-24, 1988 Moscow vol 2 page 3-27) Interfacial instabilities in Extractions with Chemical Reaction. Linearized stability analysis is applied to an extractive system with an interfacial chemical reaction. The system consists of two immiscible semi-infinite phases. Solute A in the aqueous phase reacts with component B of the organic phase A+B- P and species A and B are mutually insoluble in the others phase. Therefore the extraction of A takes place only through a chemical reaction at the interface. The *assumptions* are that the system is at steady state and the extractant B is in excess.

The mathematical procedure follows the linearized stability of Sternling and Scriven. A perturbation of the form $F(x,y,t)=f(x)\exp(i\alpha y)\exp(\beta t)$ is imposed on the steady state velocity and concentration profiles and dependence of the growth, β, with the wave number, α, obtained by simultaneous solution of the Navier-Stokes and diffusion equations. The following boundary conditions at the interface are specific to this problem:

(i) the interfacial tension,$\partial\sigma$, may vary with concentration of both A and P:

$$\frac{\partial\sigma o}{\partial y}=\frac{\partial\sigma o}{\partial C_A}\frac{\partial C_A}{\partial y}+\frac{\partial\sigma o}{\partial C_p}\frac{\partial C_p}{\partial y} \tag{2.3}$$

(ii) the interfacial rate of transfer is governed by the reaction kinetics, i.e.

$$N_A=k_1C_AC_B\text{-}k_2C_p \tag{2.4}$$

and

$$D_A\frac{\partial C_A}{\partial x}+h(C_p\text{-}MC_A)=0 \tag{2.5}$$

where

: h = reverse reaction constant

k_1= forward reaction constant

k_2= reverse reaction constant

$M = k_1C_Bk_2$

The authors obtained a characteristic equation by the simultaneous solution of the Navier-Stokes and diffusion equations. Three different cases of the forward reaction constant k_1 and for the same wave number α showed the growth rate constant decreases for k_1 increasing. Thus the reaction rate is a stabilizing factor. A plot of β with α at constant k_1 indicates the fast reaction to be a stabilizing effect. For the wave number investigated, the growth constant is always higher for the reacting system than for the diffusing system until the reaction equilibrium is reached at the interface and the values given by the two models are quite similar. Under similar conditions there may be cases when a system with an intrefacial chemical reaction is more stable than a system with pure diffusion only.

Freiser (Rare Earths Extraction, Preparation and Applications: Proceedings Las Vegas Nev. Feb. 27-March 2, 1989 page 99) discuss the investigation of equilibrium extraction behavior of a variety of chelating extractants. A select group of the tervalent lanthanides were studied to elucidate the selectivity for separation purposes. The equilibrium extraction data (as log K_{ex}) is linearily related to the ionic radius of the tervalent lanthanides ions. The role of adduct formation, steric hindrance, as well as the nature of the bonding atom in the chelate ring represent some of the factors affecting selectivity arising out of the authors database of over 200 individual extraction systems. The separations of the lanthanides is recognized as one of the most difficult inorganic separations. The tervalent lanthanides were used because of their similar behavior and to possibly elucidate understanding of the related actinide ions.

As Freiser has commented, literally hudreds of extractants have been used in liquid extraction processes; and, as time passes a seemingly boundless variation of extractants are being proposed. Each extractant has its own spcificity and favorable properties depending on the separation desired. The organo-phosphorous compounds have been the workhorses of hydrometallurgical extraction industry and also the nuclear fuels reprocessing industry for years. In particular tributal phophates (TBP), di(2-ethylhexyl) phosphoric acid (DEHPA), and more recently the multifunctional dihexyl-N,N-diethylcarbamoylmethylphosphonate (DHDECMP) and octyl(phenyl)—N,N—diisobutylcarbamoylmethylphosphine oxide (CMPO) as well as crown ethers have been employed as extractants for the ferrous, non-ferrous precious metals, rare earths (lanthanide series) and the nuclear (actinide series) metals. This study will emphasize the first three extractants TBP, DEHPA, and DHDECMP. The chemistry and kinetics as presented in the literature is reviewed for various metal extractions to elucidate an understanding of the chemistry of the liquid or solvent extraction process using these three extractants.

DEHPA-di(2-ethylhexyl) phosphoric acid

DEHPA extracts tetra and trivalent metal ions. The acid is a dimer and usually extracts as:

$$M^{n+} + n \cdot XH \cdot HX \rightarrow M(X \cdot HX)_n + n \cdot H^+ \tag{2.6}$$

and the extraction is usually proportional to the nth power of the dimer concentration and inversely proportional to the nth power of the hydrogen ion concentration where n is the valency of the metal (Healy, Radiochemica Acta page 52). DEHPA strongly extracts penta and tetra valent metal species such as Zr, Nb, Ce(IV), Th, Pa and Pu(IV). The extraction of the trivalents are extracted to a much smaller degree on the order of 10^{-6}.

Kizim, Davidov and Larkov (ISECC'88 International Solvent Extraction Conference July 18-24, 1988 Moscow vol 2 page 3-12) discuss the phenomena and kinetics of the extraction of some rare earth and non-ferrous metals by organic acids. Kinetics of extraction discussed in the literature in many cases do not reflect or consider the phenomena of interfacial convection. The formation of condensed interfacial films has been shown to occur in processes of metal extraction of Co, Ni by di-(2-ethylhexyl)phosphoric acid. The authors discuss results of research involving the interfacial phenomena and kinetics of the extraction of Co, Ni, REE(Ce, Pr, Nd, Eu, Gd) by DEHPA in toluene.

The experimental results show the kinetics of accumulation of the main solute in the interfacial layer. For the REE , the interface has a structure made up of emulsion, microemulsions, particles of solid phase and gel metal-organic polymeric molecules. This causes additional diffusional resistances which is higher than the bulk diffusion. Extraction is accompanied

with intrefacial convection which causes a rising of the coefficient of mass-transfer in the initial moment of time after the phases are contacted. As the interface forms the interfacial convection dissipates.

Pichugin, Tarasov, Arutinuyan, Goryachev (ISECC '88 International Solvent Extraction Conference July 18-24, 1988 Moscow vol 2 page 3-26) discuss the hydrodynamical instability in extraction of metals by di(2-ethyl-hexyl) phosphoric acid (D2EHPA). Chemical reactions and mass transfer have a significant effect of the motion pattern of fluids in the interfacial region during extraction of lanthanides and some actinides by D2EHPA. Only under limited conditions, such as when the density and viscosity of medium are independent of the concentration of the substance being transferred, and when capillary forces do not make a significant contribution to the sum of the forces acting on the interface, can the effects of spontaneous interfacial convection be ignored. This fluid motion associated with spontaneous interfacial convection caused by the absence of the above restrictions are closely related with the charge of an electric double layer and interfacial chemical reaction, adsorption processes, surface association and formation of interfacial films. Spontaneous convection has been shown to last long-time periods ($\sim$ 60 secs) after the instant of phase contact. In this case the mass transfer coefficient reaches $8 \times 10^{-2} \frac{cm}{secs}$.

Occurrence of condensed interfacial film along with the spontaneous convection phenomena causes hydrodynamical instability. Gradients of interfacial tension result in oscillatory motion of interface which give rise to convection in the interfacial region. During extraction the convection die out and cease completely after formation at the interface of a continuous condensed interfacial film. The "breakup" of a continuous interfacial film will cause the spontaneous convection to reoccur and the process is periodic in time during extraction. The kinetic curves of extraction verses time show this result (see figure 1 of these authors paper).

Spontaneous convection depend on the values of concentration of extractant and extractive substances. A critical value of concentration exist. If the concentrations values are greater than the critical values then the mass transfer gives rise to breaks of hydrodynamic stability of the interface. The spontaneous convection regime and the rate of extraction is strongly dependent on the ratio of the thickness of layers of contacting phases. A critical value of this ratio occurs for every extraction system. If the value of ratio is equal to the critical value the extremum of extraction rate occurs. If the value of the ratio of thickness is not equal to the critical value spontaneous convection is in the form of circular cells with diameter as high as 1 cm. The value of the Reynolds (Re) number can be as high 150-200. If the ratio of thicknesses equals the critical ratio, hydrodynamical motion is vigorous erruptions. The size of the motion can be as high as 2-3 cm and the minimal value of Re reaches 2000. Drops furnish more hydrodynamical stability than planer interfaces. Thus mass transfer

through plane interfaces was more intense. Additions of surface acting surfactant can give rise to a break of hydrodynamical stability.

Kikařík, Šístková, and Hejná (5 th ISCEC 1968 p 59) give a general mechanism for monacidic organophosphorous extractants

$$M^{m+} + \frac{m+x}{y}(\overline{HA})_y - \overline{MA_m \cdot xHA} + mH^+ \tag{2.7}$$

where M^{m+} is the ion of the extracted metal and HA is the monomeric molecule of the extractant, x is a parameter dependent on the diluent and the extractant interactions (solvation numbers) and are found by the slopes of the $\log D_m - m\log[A-] = f\log([HA])$. Lanthanide(III) form the complex with x=3. No indication of the values for x for higher order valence metals for HDEHP. Sekine (Solvent Extraction Chemistry 1977 page 340) gives a listing of values for various metals in nitric acid for TBP and Ce(IV) has a slope of two where as Ce(III) has a slope of three. Sharma (in Handbook of Solvent extraction p 61) states that this slope method is based on simplifying assumptions one of which is that no polymeric species are formed in either phase. When this polymerization occurs, which is typical of the organophosphoric acids the plot $\log D$ vrs. $\log[RA]$ (HA and RA being synonomous) will then show dramatic curvature. Temperature effects are prevalent in the extraction of cobolt with D2EHPA (another acronym for DEHPA) however nickel does not show this phenomenon with temperature (Handbook of solvent extraction page 62). Sharma also gives the cation exchange reaction (D2EHPA extractant is an example) in a more condensed form

$$M^{n+} + n\overline{RH} - \overline{MR_n} + nH^+ \tag{2.8}$$

Han and Tozawa (Rare Earths Extraction, Preparation and Applications: Proceedings Las Vegas Nev. Feb. 27-March 2, 1989 page 115) developed a thermodynamic model for predicting the distribution coefficients of extracting Sm, Eu, Gd, Tb, Dy, and Ho form acidic chloride solutions into di-2-ethylhexylphosphoric acid and 2-ethylhexyl ester in kerosene respectively. Most investigators use semi-empirical or totally empirical models to predict the distribution coefficients under wide operating conditions. These authors present studies to predict distribution coefficients from initial data. This work assumed that the organophosphorous extractants follow the cation exchange mechanism for the lanthanides in the three valence represented by

$$RE^{3+}_{(aq)} + 3(HX)_{2_{(org)}} - RE(HX_2)_{3_{(org)}} + 3H^+_{(aq)} \tag{2.9}$$

where RE^{3+}, $(HX)_2$ and $RE(HX_2)_3$ refer to the rare earth ion, the dimeric form of the extractant and the rare earth ion complex in the organic phase, respectively. The thermo-

dynamic equilibrium constant K is represented by

$$K = \frac{[RE(HX_2)_3]_{(org)}\,[H^+]^3_{(aq)}}{[RE^{3+}]_{(aq)}\,[(HX)_2]^3_{(org)}} \frac{\gamma^*_{RE(HX_2)_3}\gamma^3_{H+}}{\gamma_{RE^{3+}}\gamma^{*3}_{(HX)_2}} \tag{2.10}$$

where γ and γ^* denote the activity coefficient of corresponding species in the aqueous and organic phases respectively. The formation of the complex of the rare earth ion and the chloride ion is known to be weak until about 2 M chloride conentration and the $RECl^{2+}$ ion is a major player. At 8 M the complex predominates and the thermodynamic stability constant $t_\beta$of the complex must be taken into account.

$$RE^{3+}_{(aq)} + Cl^-_{(aq)} - RECl^{2+}_{(aq)} \tag{2.11}$$

$$t_\beta = \frac{[RECl^{2+}]_{(aq)}}{[RE^{3+}]_{(aq)}\,[Cl^-]_{(aq)}} \frac{1}{\Gamma} \tag{2.12}$$

where

$$\Gamma = \frac{\gamma_{RE^{3+}}\gamma_{Cl^-}}{\gamma_{RECl^{2+}}} \tag{2.13}$$

The distribution coefficient, D, defined to be the ratio of the total concentration of the rare earth ion in the organic phase to that in the aqueous phase is written as

$$D = \frac{[RE(HX_2)_3]_{(org)}}{[RE^{3+}]_{(aq)} + [RECl^{2+}]_{(aq)}} \tag{2.14}$$

and finally the authors give the distribution coefficient by inserting the equalibrium constant equation and the themodynamic stability constant into the above equation

$$D = \frac{\alpha_o \gamma_{RE^{3+}}\,[(HX)_2]^3_{(org)}}{[H^+]^3_{(aq)}\,\gamma^3_{H+}} Q \tag{2.15}$$

where

$$\alpha_o = \frac{1}{1 + t_\beta \Gamma\,[Cl^-]_{(aq)}} \tag{2.16}$$

and

$$Q' = K \frac{\gamma^{*3}_{(HX)_2}}{\gamma^*_{RE(HX_2)_3}} \tag{2.17}$$

note that Q and Q' are related by $\log Q' = \log Q + C\,[\mathrm{RE(HX_2)_3}]^2_{(org)}$ where Q and C are constants and if the activity coefficients of organic species is assumed to vary slightly with concentrations, Q is equal to Q' because C is zero. Taking the log of the distribution coefficient the authors obtain

$$\begin{aligned}\log D \;=\; & \log \alpha_o + \log \gamma_{RE^{3+}} + 3\log\left[(\mathrm{HX})_2\right]_{(org)} - \\ & 3\log\left[\mathrm{H^+}\right]_{(aq)} - 3\log\gamma_{H^+} + \log Q + C\,[\mathrm{RE(HX_2)_3}]^2_{(org)} \end{aligned} \tag{2.18}$$

log Q and C must be obtained from experimental data of the distribution coefficients and adjusting the model distribution coefficient until values of Q and C which are constants give the correct D. The Q and C are constant for that sytem and are used as constants. Activity coefficients obtained from estimations in electrolyte chemistry (i.e. Pitzer eqauation Bromley's or variations there of). Note since the activity coefficients are calculated by concentrations and the concentrations need the activity coefficients to be calculated an iterative procedure is a result.

Sato(page 110 Proceedings of Actinide/Lanthanide Separations 1984) discusses the extraction of uranium(IV), yttrium(III), and lanthanum(III) from HCl with solutions of organophosphorus compounds specifically di-(2-ethylhexyl)-phosphoric acid (DEHPA) or 2-ethylhexylphosphonic acid (EHEHPA) in kerosene. The extraction of actinide and lanthanide metals by these extractants are by a cationic exchange reaction mechanism at low acid concentrations. At high acid concentrations the uranium(VI) and yttrium(III) are extracted into DEHPA by a solvating reaction. Temperature dependency ($10°C$ to $50°C$) is presented for the distribution coefficient, however this is in HCl /DEHPA system and not nitric acid. The distribution coefficient at low acidities is only slightly affected by the chloride ion concentration but shows decreasing trend with increasing pH. This is postulated to be shown by the fact that at low aqueous acidity the species extracted does not contain a chloride ion and is substantiated by infrared spectrophotometry. The equilibrium extraction of U(VI) from hydrochloric acid solutions into DEHPA and EHEHPA is postulated to be an ion-exchange reaction governed by the formation of polymeric species:

$$UO^{2+}_{2_{aq}} + (n+1)(HR)_{2_{org}} - \; (UO_2)_n R_{2(n+1)} H_{2_{org}} + 2nH^+_{aq} \tag{2.19}$$

At higher aqueous acid concentrations the extraction reaction is modeled by a solvating reaction of monomer units similar to TBP (tri-butyl phosphate) viz.

$$UO^{2+}_{2_{aq}} + 2Cl^-_{aq} + m(HR)_{2_{org}} - \; UO_2Cl_2 \cdot 2mHR_{org} \tag{2.20}$$

where $n \geq 1$. Infrared spectroscopy shows that $\mathrm{UO_2(R_2X)_2}$ is extracted species. The extracted species for the yttrium and lanthanum metals are $\mathrm{M(R_2X)_3}$

Choppin(page 176 Proceedings of Actinide/Lanthanide Separations 1984) discusses the redox potential effects at different pH for neptunium and plutonium. He lists the spectrophotometric measurements of the different oxidation states. In general for actinides from valence 3 to 4 the redox is fast and is a simple electron transfer. Cation exchange extractants such as HDEHP (diethylphosphoric acid) shows a separation process due to complexation trends of the different oxidation states of the actinides. Choppin give the basic extraction reaction for cation exchange as

$$M^{+n}X_{i(aq)}^{+(n-i)} + nHS_{(org)} - M^{+n}S_{n_{(org)}} + nH_{(aq)}^{+} + iX_{(aq)}^{-} \tag{2.21}$$

where X is the anion of the aqueous solution which may form actinide complexes (i would increase with the concentration of X), n is the cation charge of the actinide and HS is the acidic form of the extractant. Because of the extraction differences of the different valence states and since actinides or actinide hydrolysis or oxide compounds of the same valence state behave similarly, separations and purifications are possible of the different valences. Keeping them in a specific valence state for removal either by extraction, ion-exchange, or precipitation is the difficulty. The valence states are pH dependent and can be maintained with a suitable strong holding oxidizer. Note that this equation is the same as that presented by Sharma and Kikařík *et al.*

Yoshizuka, Sakamoto, Baba, Inoue, and Nakashio (Ind. Eng. Chem Res. 1992, 31, 1372-1378) review a kinetic study on the extraction of holmium(III) and yttrium(III) with bis(2-ethyl-hexyl)phosphoric acid (D2EHPA) from nitrate media at 303°K using a hollow fiber membrane extractor. Distribution equilibria and interfacial adsorption equilibria of the extractant and its metal complexes between the organic and aqueous phases. The diffusion model with a reaction at the interface reasonably explained the transport effects. The metals used were in the three valence state and are extracted with D2EHPA as follows

$$M^{3+} + 3\overline{H_2R_2} - \overline{MR_3 \cdot 3HR} + 3H^{+} \tag{2.22}$$

where D2EHPA is known to dimerize in aromatic diluents such as benzene and toluene. The extraction equilibrium constant for the above equation is given by $K_{ex} = \frac{[\overline{MR_3 \cdot 3HR}]a_H^3}{[M][H_2R_2]^3} = D_M \frac{a_H^3}{[H_2R_2]^3}$ where M and a_H are the total concentration of metal in the aqueous phase and the hydrogen ion activity calculated by the pH of the aqueous solution. In typical format this equation can be expressed in logarithmic form as

$$\log D_M = 3\log\left(\frac{[\overline{H_2R_2}]}{a_H}\right) + \log K_{ex} \tag{2.23}$$

Plotting experimental data as log D vrs $\log\left(\frac{[\overline{H_2R_2}]}{a_H}\right)$ the K_{ex} values are obtained. The authors calculated the adsorption equilibrium constant assuming that the metal complex at the interface is negligible compared to D2EHPA and the adsorption equilibrium equation is $\overline{H_2R_2}$ - $H_2R_{2(ad)}$ and the adsorption equilibrium constant is given by K_{ad} . The relation between interfacial tension and the concentration of $[H_2R_2]$ in the organic phase K_{ad} is derived from the Gibbs equation for adsorption assuming Langmuir adsorption isotherm

$$\gamma = \gamma_0 - \left(\frac{RT}{S_{ad}}\right) \ln\left(1 + K_{ad}\left[\overline{H_2R_2}\right]\right) \tag{2.24}$$

where γ_0 is the interfacial tension between organic phase and the aqueous phase and S_{ad} is the interfacial area occupied by unit mole of dimeric species of D2EHPA. From experimental results K_{ad} and S_{ad} is obtained by a plot of γ vrs $\log\left[\overline{H_2R_2}\right]$. The interfacial reaction mechanism is proposed

$$M^{3+} + 3H_2R_{2(ad)} - MR^{2+} \cdot HR_{(ad)} + H^+ \qquad K_1 \tag{2.25}$$

$$MR^{2+} \cdot HR_{(ad)} + \overline{H_2R_2} - MR_2^+ \cdot 2HR_{(ad)} + H^+ \qquad K_2 \tag{2.26}$$

$$MR_2^+ \cdot 2HR_{(ad)} + \overline{H_2R_2} \underset{k_3'}{\overset{k_3}{-}} \overline{MR_3 \cdot 3HR} + H^+ \qquad K_3 \tag{2.27}$$

The latter is the rate controlling step as a result of the Yashizuka et al.data. The interfacial reaction rate R is expressed as

$$R = k_3\left[MR_2^+ \cdot 2HR_{(ad)}\right]\left[\overline{H_2R_2}\right] - k_3'\left[\overline{MR_3 \cdot 3HR}\right] a_H \tag{2.28}$$

and assuming Langmuir adsorption isotherm and that the interfacial area occupied by the unit mole of H_2R_2,S_{ad} the interfacial reaction rate R becomes

$$R = \frac{\frac{k_3 K_1 K_2 \left(\frac{K_{ad}}{S_{ad}}\right)[M]\left[\overline{H_2R_2}\right]^3}{a_H^2} - k_3'\left[\overline{MR_3 \cdot 3HR}\right] a_H}{1 + K_{ad}\left[\overline{H_2R_2}\right] + \left(\frac{(K_{ad}K_1[M]\left[\overline{H_2R_2}\right])}{a_H}\right)\left(1 + \frac{K_2\left[\overline{H_2R_2}\right]}{a_H}\right)} \tag{2.29}$$

Yashizuka et al. state that the third and fourth terms in the denominator are considered to be much less than $1 + K_{ad}\left[\overline{H_2R_2}\right]$ since they are complexes adsorbed at the interface and under their experimental conditions the concentration of D2EHPA is much higher than those of the intermediate complexes and the interfacial extraction and stripping rates are

approximately

$$R = \frac{\frac{k_3 K_1 K_2 \left(\frac{K_{ad}}{S_{ad}}\right) [\mathrm{M}] \left[\overline{\mathrm{H_2R_2}}\right]^3}{a_H^2} - k_3' \left[\overline{\mathrm{MR_3 \cdot 3HR}}\right] a_H}{1 + K_{ad} \left[\overline{\mathrm{H_2R_2}}\right]} \tag{2.30}$$

and if the overall forward reaction rate constant is defined to be $k_f = k_3 K_1 K_2 \left(\frac{K_{ad}}{S_{ad}}\right)$ the equation becomes for extraction

$$R = \frac{k_f \left[\frac{[\mathrm{M}] \left[\overline{\mathrm{H_2R_2}}\right]^3}{a_H^2} - \frac{\left[\overline{\mathrm{MR_3 \cdot 3HR}}\right] a_H}{K_{ex}}\right]}{1 + K_{ad} \left[\overline{\mathrm{H_2R_2}}\right]} \tag{2.31}$$

and for stripping

$$R' = \frac{k_3' \left[\left[\overline{\mathrm{MR_3 \cdot 3HR}}\right] a_H - K_{ex} \frac{[\mathrm{M}] \left[\overline{\mathrm{H_2R_2}}\right]^3}{a_H^2}\right]}{1 + K_{ad} \left[\overline{\mathrm{H_2R_2}}\right]} \tag{2.32}$$

The data in the region of high permeabilities for the extraction and stripping were analyzed on the basis of the diffusion model accompanied by an interfacial reaction, taking into account the velocity distributions of the laminar flows in aqueous and organic phases. The authors wrote three diffusion equations for each diffusion regimes, i. e. diffusion through the two bulk phases and the diffusion through the porous media that takes into account the porosity and tortuosity of the porous structures. The authors found that if the ratio of the forward to backward reaction rates k_f to k_3' is equal to the equilibrium constant K_{ex} obtained from extraction kinetics is 7 to 10 times the values obtained from the extraction equilibrium and is explained to be a result of the difference in the ionic strengths of the extraction and stripping aqueous phases.

Cerium Cerium, specifically cerium in the fourth valence state is to be used in this study as a surrogate to Pu(IV). The extraction of Cerium into various extractants has been presented in the literture though little useful kinetic data is available. Below is a literature review of Cerium extraction into DHEPA.

Warf was issued separate U. S. patents for extracting cerium in nitromethane and also in TBP (see Warf under TBP) in the 1949. In order to accomplish this the cerium was kept in the four valence state by the use of sodium bromate in high molar strength nitric acid. *Peppard, Mason and Moline (J Inorg. Nucl Chem 1957 vol 5 pp 141)* extracted Ce(IV) from high molar nitric acids in 1957 and showed that cerium in the four valence state extracted

to a much greater degree in DEHPA (Peppard et al referred to it as HDEHP) than did its valence couple Ce(III).

Bray and partridge (Solvent Extraction Research Proceeding of 5th ICSEC 1968) discuss the extraction into HDEHP of Ce(III) by oxidation to Ce(IV) in concentrated nitric acid solutions. They conclude that the nitrate ion is necessary for rapid oxidation of the Ce(III) in this sytem. The complex formed by this metal and the DEHPA is polymerized and has the formula $CeO_{0.5}NO_3(DEHP)_2$. No mechanism or kinetics were given; though, a distribution curve as a function of nitric acid comparing the extraction of Ce(IV) with Ce(III) is given. The distribution for Ce(III) is minimum between 2 and ~3.5 M HNO_3. The Cerium(IV) distribution is much higher in the acid range of 1 to 5 M HNO_3 than the Ce(III). The ratio of the distribution coefficient of Ce(IV) to Ce(III) is 10,000 at 2 M HNO_3.

Sato (Hydrometallurgy 22(1989)121-140) discusses the extraction efficiency including distribution coefficients as functions of concentrations and temperatures of the lanthanide III series primarily from HCl but does give data on extraction from HNO_3 into DEHPA and EHEHPA in kerosene. For cerium(III) at a concentration of 0.05 $\frac{mol}{dm^3}$ in 0.05 $\frac{mol}{dm^3}$ nitric acid with 0.05 $\frac{mol}{dm^3}$ DEHPA in kerosene Sato observed an enthalpy change of 6 $\frac{kJ}{mol}$.

Uranium *Fatovic, Melex, Polla, Romano(Extraction '87: The recovery of High Value Materials ICHEME symposium Series No. 103 page 29)* used uranyl nitrate hexahydrate to illustrate the extraction kinetics of U(VI) into di-2-ethyl-hexyl phosphoric acid and trioctylphosphineoxide (TOPO) in kerosene and aromatic hydrocarbons. Using a constant area Lewis type mass transfer cell the aqueous to organic K′ and organic to aqueous K transfer. Equilibrium was attained in less than two minutes. The equilibrium data are expressed in terms of distribution ratio D as

$$D = \frac{\text{uranium concetration in the organic phase } (C_U)_o}{\text{uranium concetration in the aqueous phase } (C_U)_{aq}} \tag{2.33}$$

The kinetic data of the concentration vs time was analyzed by assuming a first order reversible reaction for uranium(VI)

$$UO_{2(aq)}^{+2} + 2(HX)_{n_{(org)}} + TOPO_{(org)} \underset{k}{\overset{k'}{\rightleftharpoons}} UO_2 \cdot H_{2n-2} \cdot X_{2n} \cdot TOPO_{(org)} + 2H_{(aq)}^{+} \tag{2.34}$$

and after integration and rearrangement gives for aqueous to organic transfer near time 0 where $C' \sim C'_o$ and the working equation given by is $K' = -\frac{VD}{at}\ln(1 - \frac{c}{C'_o D})$ and for the organic to aqueous transfer near time 0 where $C \sim C_o$ the equation is $k = -\frac{V'}{atD}\ln(1 - \frac{DC'}{C_o})$ where k‘ indicates the rate constants (cm/s) in the aqueous phase to organic phase and k organic phase to aqueous phase respectively; a is the interfacial area and V the volume of the organic and aqueous phases in this case 19.252 cm^2 and 50 cc respectively; t the time

in seconds; C the concentration of uranium in the organic phase after time t in g/dm^3; C′ the uranium concentration in the aqueous phase after time t g/dm^3; C_o is the uranium concentration in the organic phase at t=0 g/dm^3;C'_o the uranium initial concentration in the aqueous phase at t=0 g/dm^3;and D the organic to aqueous distribution ratio ($\frac{O}{A}$). The rate constants k and k′ are time dependent. The authors extrapolated back to zero time (t=0) was performed. The activation energy was calculated using the equation $\log k = -\frac{E}{2.303\,RT}$.

The effects of temperature on the distribution coefficient ratio of U(IV) between phosphoric acid are given. The authors attempted to minimize the contribution of diffusion by using a constant stirring speed in the Lewis cell determined by a plateau of k vrs. stirring speed. The results reveal that the rate constants for the extraction in both directions increase with increasing temperature. The activation energy was estimated via the slope of straight lines on the plot of log k vrs $\frac{1}{T}$ the energy of activation in kcal/mol for various systems studied

system	aqueous to organic	organic to aqueous
4.91 M H_3PO_4; 0.5M D2EHPA-0.125M TOPO		
kerosene w/ 18.3% Aromatics	2.62± 0.46	12.89 ± 0.89
kerosene w/ 0.5% Aromatics and other contaminants	2.92 ± 0.3	
kerosene w/ 18.3 % Aromatics and other contaminants	2.16 ± 0.49	13.22 ± 0.49

Note that the other contaminants are impurities of metals that come in industrial grade phosphoric acids. The ΔH for this system has been determined by Fatovic et al as 10.18 kcal/mol. Others have given a ΔH of 10.38 kcal/mol for the H_3PO_4 in the kerosene with 18.3 % aromatics and no contaminants determined from equilibrium data. For the system with contaminants and 18.3 % aromatics a value for ΔH using kinetic data was 11.06 kcal/mol and equilibrium data 9.53 kcal/mol. The effect of concentration of phosphoric acids on the aqueous to organic transfer constants at 40°C showed that the rate constants increased form 3.4 $\times 10^{-4}$ to 1.15 $\times 10^{-3}$ $\frac{cm}{sec}$.

Brčić, Fetović, Meleš, Romano (ISECC '88 International Solvent Extraction Conference July 18-24, 1988 Moscow vol 2 page 3-15) report on a study conducted on the rate constants for the interphase transfer of uranium(VI) from phosphoric acid solution by D2EHPA (di-2-ethyl-hexyl phosphoric acid) and TOPO (tri-n-octyl phosphine oxide) in non-aromatic kerosene. The heat of reaction is calculated from van't Hoff's equation at 26.53 $\frac{kJ}{mol}$ and the activation energy for the forward reaction is 38.73 $\frac{kJ}{mol}$ and for the reverse reaction 13.12 $\frac{kJ}{mol}$. The heat of reaction is the difference of the activation energies and was calculated at 25.61 $\frac{kJ}{mol}$. The chemical reaction of uranium controls the transfer of uranium from the

organic into the aqueous phase. The rate of transfer of the uranium is a strong function of phosphoric acid concentration.

DHDECMP dihexyl–N,N–diethylcarbamylmethylene phosphonate

Kwinta, David and Metzger (page 31 Proceedings of Actinide/Lanthanide Separations 1984) discuss the extraction of rare earths in bi-functional extractant dihexyl–*N,N*–diethylcarbamylmethylene phosphonate (DHDECMP). They state that the di-(2–ethylhexylphosphoric acid (HDEHP) presents some inconveniences with insufficient selectivity, and the need of relatively low acidity. These authors state that the extraction equilibrium into toluene is very fast and the quasi- total reaction (authors words) will not require more than 2 minutes as determined by a distribution vrs shaking time plot for lutetium (Lu z=71). The distribution relation for the lanthanide III elements (Ce(III), Eu(III), and Y(III)) used in the study was determined to be $D = k(\text{DHDECMP})^3$ and is stated to be in good agreement with other literature values (see McIssac and Baker INEL-ICP 1180 1979). Cerium III is included in this work for extraction distribution.

Impurities in the DHDECMP are the most critical factors affecting stripping efficiencies. The distribution coefficient decreases when the solute concentration increases. This is illustrated with Ce(III) in the authors figure 4. The distribution coefficient decreases when the temperature increases. A plot of $log\,\text{D}$ vrs. $\frac{1}{T}$ gives a van't Hoff relationship for the activation enthalpy in 6 N acidity of $\Delta\text{H}^\circ = -27\ \frac{\text{kJ}}{\text{mole}}$. Like other metal extraction processes salting out effects are present when nitrate salts are added to the aqueous solution; but, also increase the distribution coefficient of other elements that may be present. The structure of extracted complex of the lanthanide(III) elements is suggested to be $\text{M}(\text{NO}_3)_2(\text{DHDECMP})_3$.

Mitsugashira, Maki and Suzuki (page 91 Proceedings of Actinide/Lanthanide Separations 1984) discuss the bi-functional dibutyl–*N,N*–diethylcarbamoylmethylene phosphonate (DBDECMP) and the dihexyl homologue dihexyl–*N,N*–diethylcarbamylmethylene phosphonate (DHDECMP) in a benzene diluent for the extraction of Th(IV), Am(III) and Cm(III) form perchloric (HClO_4) and nitric (HNO_3) acids. To understand the extraction mechanism of metal ions from an acid media it is necessary to examine the interaction of the extractant and the acid. The extraction mechanism of HNO_3 and HClO_4 is different. The mechanism for DBDECMP is given to be

$$\overline{\text{BP}} + nH^+ + nNO_3^- \underset{k_2}{\overset{k_1}{\rightleftharpoons}} \overline{\text{BP}(\text{HNO}_3)_n} \tag{2.35}$$

where BP is DBDECMP and the over bar distinguishes the organic phase. $k_1 = 0.33\text{M}^{-2}$ and $k_2 = 0.0043\text{M}^{-4}$. The authors suggest that the kinetic constants given reproduce

the nitric acid extraction for both DBDECMP and DHDECMP. The authors suggest that since no difference between the constants exist the acid is attached to a functional groups basicity is independent of the substitution butyl or hexyl group. Though we will not use the $HCLO_4$, it is interesting to note that the same conclusion was reached in regards to the extraction behavior of the two extractants with this acid also. These authors did not report a third phase forming in the nitric acid DBDECMP or DHDECMP as have other investigators using these extractants with aliphatic hydrocarbons instead of the benzene as used by these authors. The perchloric acid system did show a third phase formation in the DBDECMP system at acid concentrations greater than 2.5 M; but, they did not see any third phase formation in the DHDECMP until an acid concentration less than 5 M. The authors postulate that the nitric acid suppresses the third phase in the organic phase.

Distributon coefficients for the actinides of interest in this article are given as functions of concentrations of organic extractant, NO_3^- , ClO_4^-, and pH. The slopes of the distribution curves for nitric acid are identical to those reported by previous authors. The distribution coefficients for Am(III) in DHDECMP need to be corrected for the decrease in $\overline{[DHDECMP]}$ caused by nitric acid extraction. The authors conclude that the extracted Am(III) contains one extra nitric acid in the organic phase. Th(IV) does not extract with an extra nitrate anion. Thus for DBDECMP the extraction reactions for Th(IV) and Am(III) are given by these authors as

$$x\overline{BP} + M^{n+} + (n+m)X^- + mH^+ \underset{K_{ex,X}}{-} \overline{(BP)_xMX_n(HX)_m} \tag{2.36}$$

The authors suggest that for Cm(III) the same values for $K_{ex,X}$ as given by them for Am(III) can be used to evaluate extraction behavior. The values for n, x, m, and $K_{ex,X}$ are valid at $[NO_3^-]$ <2M. The following table is a partial listing from these authors table 2 for these values.

X^-	M	n	x	m	$\frac{K_{ex,X}}{M^{-n-x-2m}}$	
					DBDECMP	DHDECMP
NO_3^-	Th(IV)	4	2	0	$8 \cdot 10^5 \pm 2 \cdot 10^4$	$6 \cdot 10^4 \pm 2 \cdot 10^4$
	Am(III)	3	3	1	30 ± 10	25 ± 7

Brossard, Kwinta and Schwander(page 126 Proceedings of Actinide/Lanthanide Separations 1984) investigate the extraction of americium in DHDECMP. Influence of metal concentration, aqueous phase acidity, and DHDECMP concentration is studied. The effects of temperature are discussed but not in any detail. Synergistic effects of TBP are negligible.

The effects of the acidity of the aqueous phase is governed by two relations

$$\beta_e = \frac{A_e^\circ - A_e}{A_e} \quad \text{and} \quad \beta_r = \frac{A_r^\circ + A_e - A_r}{A_r} \tag{2.37}$$

where

A_e° is the acidity of the solution before Am extraction

A_e is the acidity of the solution after Am extraction

A_r° is the acidity of the aqueous phase used for stripping Am

A_r is the acidity of the aqueous phase after stripping Am

The Am distribution coefficient decreases as the temperature increases. For a DHDECMP concentration of 0.8 M these authors obtained a ratio of 3±1 for the distribution ratio for Am at 20°C and 60°C. Other literature reported in this article give a ratio of 5. However, this shows a great dependency of D on temperature.

TBP Tri-Butyl Phosphate

Naylor and Eccles (ISECC'88 International Solvent Extraction Conference July 18-24, 1988 Moscow page 31) gives a plenary evaluation of TBP as an extractive solvent for the nuclear fuels cycle. TBP is very popular though it can be classified as a moderate metal extractant and has been used since the 1940's as the "workhorse" of extractants. Its cost is kept in line because of the commercial demand in other areas. TBP is used as a plasticiser, anti oxidant or catalyst and in anti-foaming agents, hydraulic fluids and fire retardant. TBP's affinity for metals derives mainly from its phosphoryl group the oxygen forms coordinate links with cations $(C_4H_9O)_3P{=}O{\rightarrow}M$. TBP forms adducts such as that with U(VI) to give $UO_2(NO_3)_2{\cdot}2TBP$. The nitrates are extracted as neutral molecular species with a definite number of attached TBP molecules. The complexes for the actinides and the lanthanides as well are established as: trivalent, $M(NO_3)_3{\cdot}3TBP$; tetravalent $M(NO_3)_4{\cdot}2TBP$; hexavalent, $MO_2(NO_3)_2{\cdot}2TBP$. The mechanism given by these authors is one of simple complex formation:

$$MO^{2+}_{2(aq)} + 2NO^{-}_{3(aq)} + 2TBP_{(org)} - MO_2(NO_3)_2 \cdot 2TBP_{(org)} \tag{2.38}$$

$$M^{4+}_{(aq)} + 4NO^{-}_{3(aq)} + 2TBP_{(org)} - M(NO_3)_4 \cdot 2TBP_{(org)} \tag{2.39}$$

the nitrato complex may be substantially formed in the aqueous phase. Thermodynamic and kinetic data for the extraction of uranium indicate the extraction is exothermic. The

rates in the forward direction increase with increasing TBP concentration, but those in the reverse direction (back washing) decrease. The effect of temperature on the extraction of actinides is small, although back washing from the loaded solvent is encouraged by higher temperature. The difference in extractability due to different valency states is utilized to effect separations between elements in the actinide series and elements in the lanthanide series. At high concentrations of nitric acid (>6 M) the nitrates compete with the metal species for extraction. TBP is susceptible to hydrolysis and yields dibutyl phosphate (DBP) monobutyl phosphate (MBP), and phosphoric acid. The first hydrolysis step in the extraction process is the most critical. Ionizing radiation cause decomposition of TBP and result in the formation of DBP, MBP, H_3PO_4,and various gases H_2,CH_4,C_2H_4, alcohols and other hydrocarbons. The degradations products complex more strongly with the metals and cause metal losses, reduced decontamination of the products, and solvent containing metal products. Precipitates may also form and may negatively influence the interfacial mass transfer.

Rogers, Thompson and Thornton (Extraction '87: The recovery of High Value Materials ICHEME symposium Series No. 103 page 15) discuss the time dependence of mass transfer of uranyl nitrate between nitric acid and tri-butyl phosphate. Interfacial turbulence is discussed in regards to surface renewal accompanying the transport process. Chemical reactions occurring at the liquid liquid interface during the extraction of uranyl nitrate, plutonium nitrate and nitric acid by TBP are

$$\begin{aligned} UO_2^{++} + 2NO_3^- + 2TBP &- UO_2(NO_3)_2 \cdot 2TBP \\ PU^{+4} + 4NO_3^- + 2TBP &- PU(NO_3)_4 \cdot 2TBP \\ H^+ + NO_3^- + TBP &- HNO_3 \cdot TBP \end{aligned} \tag{2.40}$$

and the determination of the interfacial transfer kinetics in these systems has been investigated by independent workers (reviews of these investigations will be discussed latter). A difference of opinion as whether the mass transfer is diffusion or kinetically controlled is evident in the comparison of these papers. The authors comment that only two studies cited by them were macro concentrations of uranyl ion and that the **mass transfer mechanism at low concentrations may be different than that at high macro concentrations.** For uranyl nitrate the authors state that values for the activation energy of the forward reaction range from 10 $\frac{kJ}{mol}$ to 23 $\frac{kJ}{mol}$. The authors maintain that these values are indicative of a diffusional control mechanism.

Rogers et al. work used a quasi-steady state droplet technique to study the time dependent behavior or mass transfer coefficients of uranyl nitrate from aqueous phase into an organic phase of TBP and odorless kerosene at 25° C. As the interface ages the mass transfer coefficient decreases and is associated with a corresponding decrease in the frequency of

interfacial disturbances. This dampening has been suggested by Ruckenstein(Int J. Heat Mass Trans. 11 1753(1968)) as a result of the liquid elements taking part in the surface renewal process become more and more saturated and consequently the interfacial renewal weaker. Sawistowski (Trans Inst Chem Engrs 412, 174 (1963)) suggest that the increase in interfacial tension when liquid eddies of bulk phase arrive at the interface cause the dampening of interfacial turbulence. The authors suggest that the exact reason for the dampening is not known but postulate that it is caused by a buildup of complexed species $UO_2(NO_3)_2 \cdot 2TBP$ at the interface.

> *As the interfacial turbulence decays the rate of mass transfer will ultimately depend on the diffusion of the complexed species across the interface and possibly the diffusion of free TBP molecules to the interface. Thus mass transfer becomes a totally diffusion controlled process.*

The interfacial tensions of this system increases with higher solute concentrations (Thompson ICHEME Symposium Series 88 (231)1984). These authors found that after an extended period of time (600 secs) the mass transfer coefficients become a constant value and the transport process is primarily a diffusional regime although some interfacial turbulence exists. These authors also noted that the back extraction from the organic did not show any visible Marangoni interfacial turbulence and also showed no time dependence of the mass transfer coefficients. In conclusion the differences in the mass transfer coefficients reported in the literature for the same systems is a result of the time dependence on the interfacial turbulence and interface age.

Hughes and Lawson (Extraction '87: The recovery of High Value Materials ICHEME symposium Series No. 103 page 37) develop and discuss a mechanism for the co extraction of uranium and nitric acid by TBP. These authors describe a phenomenon of nitric acid "equilibrium overshoot". This phenomenon is a result of the nitric acid concentration in the organic being higher than predicted equilibrium concentrations. These authors propose that the overshoot be predicted by

$$E = \frac{\text{Equilibrium concentration of nitric acid in the organic phase (no uranium)}}{\text{Equilibrium concentration of nitric acid in the organic phase (with uranium)}} \quad (2.41)$$

Note that as the uranium concentration is increased the uranium ions displace the nitrates into the aqueous phase and the uranium is extracted. Co-extraction in kinetic experiments in the literature indicate the overshoot factor, E, typically within the range 1<E<3. The mechanism for the extraction is given by

$$HNO_{3_{(aq)}} + TBP_{(org)} \xrightarrow{k_1} HNO_3 \cdot TBP_{(org)} \quad (2.42)$$

$$2(HNO_3 \cdot TBP)_{(org)} + UO_2(NO_3)_{2(aq)} \xrightarrow{k_2} UO_2(NO_3)_2 \cdot TBP_{(org)} + 2HNO_{3(aq)} \quad (2.43)$$

$$UO_2(NO_3)_{2(aq)} + 2TBP(org) \xrightarrow{k_3} UO_2(NO_3)_2 \cdot TBP_{(org)} \quad (2.44)$$

2.2 Summary

3. KINETICS of METAL EXTRACTION

3.1 INTRODUCTION to RATES of METAL EXTRACTION

Solvent extraction is commonly applied as an equilibrium process, but the rate at which equilibrium is achieved is of paramount importance. The rate at which equilibrium is attained between two phases which are initially not at equilibrium depends on the degree of extent in which the concentration in the two phases initially differ from those attained at equilibrium. That is, the rate that extraction reaches equilibrium depends on the chemical potential of the metal in the two phases (page 89 Solvent extraction Principles and Application to Process Metallurgy Part I Ritcey and Ashbrook).

Most processes currently in use are designed by equilibrium data. The design of a process is dependent on the throughput of that process. The chemical reaction kinetics determines the size and type of extractors to be used. These process can be designed by the use of equilibrium data since the hydrodynamics and fast kinetics of the systems allow very rapid approaches to equilibrium. This is somewhat of a paradox, since membrane processes like the ones considered in this study are rate processes. The separation is accomplished by a driving force, not by equilibrium between phases (*Noble and Way ACS 347 Liquid Membranes Theory and Appls. 1986 p1*). The rate of metal extraction is largely determined by interfacial chemistry. Kinetics of solvent extraction of metal species is a function of both the kinetics of the chemical reaction occurring in the system and the rates of diffusion of the species present in the two phases.

Generally, metal extraction is governed by mass transfer and diffusion rates which are on the whole, fairly rapid. Most reactions involving ionic type reaction are rapid, whereas the rates of reaction involving chelate formation can vary over considerable range. There are primarily two regimes of extraction — the kinetic regime and the diffusion regime. A third and more complex regime is termed the mixed regime. This regime is a combination of the two primary regimes. Most laboratory apparatus are designed to give a combination mass transfer rate, or a diffusional transfer rate, or a kinetic transfer rate. The separation of the transport rates for the different regimes is difficult albeit impossible in the same experimental apparatus. In general to accomplish this the system hydrodynamics are changed to eliminate diffusional effects. Thus, as the hydrodynamic conditions change for each apparatus, the rates obtained may not accurately reflect a processes actual transport rate for a specific regime.

The interface plays a most vital role in two phase mass transport. Different models have been developed for transport at interfaces. The two phase film is a simple model and illustrates quite well, the mechanistic aspects of the solvent extraction process. In most published modeling and simulation works the two film theory model has been used extensively for two phase systems. In the two film model the hydrodynamics determines the thicknesses of the differential film on either side of the interface. These different transport models will be discussed in detail later in the interface section of this study.

Most of the current extraction processes i.e. pulsed columns, centrifugal contactors, etc. are well stirred and the diffusion mechanism may not be of importance except at or close to the interface. When the hydrodynamics is such that this film thickness approaches zero, diffusion contributions to the rate of extraction can be small or insignificant and many times are justifiably neglected. This is not so with membranes where the bulk fluids are in intimate contact only at a single interface and flow in both phases is primarily in a laminar flow regime and diffusional and kinetic regimes may be affecting the transfer of mass.

3.2 SIMPLE MECHANISMS of METAL EXTRACTION

Solvent exchange and complex formation are special cases of nucleophilic substitution reactions (Principles and Practices of Solvent Extraction page167 1992). The rate at which solvent molecules are exchanged between the primary solvation shell of a cation and the bulk solvent is of primary importance in the kinetics of complex formation from aquo-cations.

The dependence of the kinetics on the chemical reactions can be understood by considering that the final products of any extraction process are usually in a chemical state different from the initial unreacted species. The extraction of neutral metal complexes as in the solvation environment produce completely different metal species in the extraction or stripping phase than in the original phase. The extraction of a metal cation from an aqueous solution by chelating extractant has more complex mechanism than the simpler solvating complex. The solvating mechanism also has these additional complexities. These complexities manifest themselves in where the reactions take place i.e. the bulk phases or the interface. Reactions occurring in the bulk phases are homogenous reactions. The interface reactions are analogous to heterogeneous reactions. In general, the distribution processes between immiscible liquid phases of extraction of metal ions performed at very low concentrations, can be treated as first-order reversible reactions when the value of the equilibrium (partition) coefficient is not very high (Danesi in Principles of Solvent Extraction page 166).

3.2.1 Rate Controlling Extraction Regimes

As mentioned earlier there exists transport extraction regimes. In a well stirred system solvent extraction kinetics can be controlled only by slow chemical reactions or only by diffusion through the interfacial film (in the two film model). When one or more of the chemical reactions is sufficiently slow in comparison to the diffusion to and away from the interface such that the diffusion can be considered instantaneous, the solvent extraction kinetics occur in a kinetic regime. This can occur when the process is well mixed with moderately slow chemical reactions or the reactions are rapid but the diffusion coefficients are comparatively slow. Danesi gives a limiting value for the diffusion coefficients in liquids as $10^{-4}cm^2s^{-1}$ and the depth of the diffusion films is never less than 10^{-4} cm. Danesi does not elaborate on the origination of these numbers. In contrast, if the chemical reactions are very fast compared to the diffusional processes the solvent extraction kinetics are defined to occur in the diffusional regime. The rate of extraction is described in terms of the interfacial film diffusion.

A combination of these regimes, where the diffusion and reaction rates are comparable the solvent extraction kinetics are defined to take place in a mixed diffusional — kinetic regime. This is a most complicated case, since the rate of extraction must be described in terms of both diffusional processes and chemical reactions, and a complete mathematical description is obtained only by simultaneously solving the differential equations of diffusion and those of chemical kinetics.

Determining the transport regime is very difficult. Even when the apparatus is designed to obtain a specific regime transfer rate, the hydrodynamics of the system may be a parameter that may not be capable of sufficient adjustment to allow the regime to be correctly studied. This is illustrated in a stirred cell where the diffusion film is not sufficiently small enough to make diffusion so fast as to be neglected relative to the chemical reactions. This effect is called "slip effect" and depends on the specific hydrodynamic conditions of the apparatus in which the extraction takes place and simulates a kinetic regime (Danesi ISEC 83 p 1-3 and Danesi in Principles of Solvent Extraction page 182) . Thus, many workers who have reported kinetic transport data often times conflict with each others interpretation of the extraction regime.

Kinetic Regime

The kinetics of solvent extraction can be described in terms of chemical reactions occurring in the bulk phases or at the interface. In many metal extractions, extraction is by ligand substitution reactions, and the rate laws similar to those for complexation reactions in solution may be expected. During most extraction processes, coordinated water molecules

or ligands are substituted in part or wholly by molecules of a more oganophilic ligand (the extractant) or of the organic diluent (ibid page 182). The hydrophobic extractants, with little solubility in the aqueous phase, are strong surfactants as are most extractants, and the ligand substitution reaction may and generally does take place at the interface.

As with all reactions the slowest step in the process is rate determining and controls the overall rate of the system. Danesi presents three possible cases that can occur and the development of the rate equations assuming the extraction of a monovalent cation M^+ with a weakly acidic solvent extraction reagent.

$$M^+ + HA(org) - MA(org) + H^+ \tag{3.1}$$

The equilibrium constant, K_{ex}, is given by

$$K_{ex} = \frac{\left[\overline{MA}\right]_{eq} [H^+]_{eq}}{\left[\overline{HA}\right]_{eq} [M^+]_{eq}} \tag{3.2}$$

where M^+ is the monovalent metal ion HA is the organic extractant in monomeric form. MA is the metal extractant complex and H^+ is the hydrogen ion. The overbar distinguishes the organic phase as does a (org) subscripted or not. The equalibrium state is indicated by a subscript eq and brackets indicate concentration.

Case 1. *The rate-determining step of the extraction reaction is the aqueous phase complex formation between the metal ion and the anion of the extracting reagent.*

For a monovalent metal species extraction in this regime for case 1

$$M^+ + A^- \underset{k_{-1}}{\overset{k_1}{-}} MA \qquad \text{(slow)} \tag{3.3}$$

and a reaction rate expression:

$$\text{rate} = -\frac{d\,[M^+]}{dt} = k_1\,[M^+]\,[A^-] - k_{-1}\,[MA] \tag{3.4}$$

where $[A^-]$ is the dissociated acidic monomeric extractant and k_i is the reaction rate constant for reaction i. The following equilibrium constraints are used to derive the rate in terms of easily measurable concentrations

$$1.\quad \overline{HA} - HA; K_{DB} = \frac{\left[\overline{HA}\right]}{[HA]} \tag{3.5}$$

$$2.\quad \mathrm{HA} - \quad \mathrm{B^+ + H^+; K_a} = \frac{[\mathrm{B^-}]\,[\mathrm{H^+}]}{[\mathrm{HA}]} \tag{3.6}$$

$$3.\quad \mathrm{MA} - \quad \mathrm{MA(org); K_{DM}} = \frac{\left[\overline{\mathrm{MA}}\right]}{[\mathrm{MA}]} \tag{3.7}$$

where K_{DB} and K_{DM} are the distribution or equalibrium coefficients for the extractant and the metal extractant complex respectively between the organic and aqueous phases. K_a is the dissassociation equalibrium constant for the acidic extractant. The rate expression can be obtained by substituting equations 3.5 through 3.7 into equation 3.4

$$\text{rate} = k_1 \frac{K_a}{K_{DB}} \frac{[\mathrm{M^+}]\left[\overline{\mathrm{HA}}\right]}{[\mathrm{H^+}]} - \frac{k_{-1}}{K_{DM}}\left[\overline{\mathrm{MA}}\right] \tag{3.8}$$

The the rate constants of the aqueous complex formation can be obtained if values for the apparent rate constants $k_1 \frac{K_a}{K_{DB}}$ and $\frac{k_{-1}}{K_{DM}}$ of the extraction reaction can be evaluated. This means that K_a, K_{DB},and K_{DM} need to be known. The values of the apparent rate constants are determined from the slope of straight lines obtained by plotting

$$\ln \frac{[\mathrm{M^+}] - [\mathrm{M^+}]_{\mathrm{eq}}}{[\mathrm{M^+}]_0 - [\mathrm{M^+}]_{\mathrm{eq}}} \text{ vs } t \tag{3.9}$$

where the subscript 0 indicates initial concentrations in the aqueous phase and t is time. In general experimental data is obtained for $\mathrm{M^+}$ as a function of $\left[\overline{\mathrm{HA}}\right]$ at constant $[\mathrm{H^+}]$, or a function of $[\mathrm{H^+}]$ at constant $\left[\overline{\mathrm{HA}}\right]$, and of $\left[\overline{\mathrm{MA}}\right]$ at constant $[\mathrm{H^+}]$ and $\left[\overline{\mathrm{HA}}\right]$. The experimental conditions are chosen such that the reaction can be assumed first order (Danesi in Principles and Practice of Solvent Extraction). As in subsequent cases the rate of extraction is independent of the specific interfacial area $\overline{a}, Q$ the area of diffusion, and volume of the phases V.

Case 2. *The rate-determining step of the extraction reaction is the interfacial formation of the complex between the metal ion and the interfacially adsorbed extracting reagent.* The rate determining step of the extraction can be written as

$$\mathrm{M^+ + A^-(ad)} \underset{k_{-2}}{\overset{k_2}{\rightleftharpoons}} \mathrm{MA(ad)} \qquad \text{(slow)} \tag{3.10}$$

where (ad) indicates species adsorbed at the liquid–liquid interface. The rate of reaction which follows is

$$\text{rate} = -\frac{\mathrm{d}\,[\mathrm{M^+}]}{\mathrm{d}t} = k_2 \overline{a}_w\,[\mathrm{M^+}]\,[\mathrm{A^-}]_{\mathrm{ad}} - k_{-2}\overline{a}_O\left[\overline{\mathrm{MA}}\right]_{\mathrm{ad}} \tag{3.11}$$

where $\overline{a}_w$ and $\overline{a}_O$ represent the specific interfacial areas of the aqueous or water phase and the organic phases respecitvely or the ratio of Q cm^2 and the volumes of the aqueous V_w and organic V_O. For simplicity at this point $V_w = V_O = V$ and $\frac{Q}{V} = \overline{a}_w = \overline{a}_O = \overline{a}$. The adsorption at the interface is obtained from the Langmuir's adsorption law:

$$[\mathrm{HA}]_{\mathrm{ad}} = \frac{\alpha_2 \frac{\boxed{\mathrm{HA}}}{\gamma}}{1 + \frac{\boxed{\mathrm{HA}}}{\gamma}} \tag{3.12}$$

The Langmuir adsorption constants α_2 and γ are specific for each system. Two regions of adsorption can be identified at the interface:

1. Ideal case where $1 \gg \frac{\boxed{\mathrm{HA}}}{\gamma}$ yielding

$$[\mathrm{HA}]_{\mathrm{ad}} = \frac{\alpha_2}{\gamma}\left[\overline{\mathrm{HA}}\right] = \alpha\left[\overline{\mathrm{HA}}\right] \tag{3.13}$$

2. Complete interface saturation with extractant molecules where $1 \ll \frac{\boxed{\mathrm{HA}}}{\gamma}$ yielding

$$[\mathrm{HA}]_{\mathrm{ad}} = \alpha_2 \tag{3.14}$$

Extractants exhibit strong surface active properties, equation 3.14 is valid for the entire concentration range of general interest in practical studies and the interface becomes fully saturated with extractant molecules when their bulk concentration is as low as 10^{-3} M (Danesi page 186). The following instantaneously established equilibria have to be accounted for:

1. $\mathrm{HA(org)} - \quad \mathrm{HA(ad)}$ (3.15)

adsorption of the extractant molecules at the interface described by Langmuir's Law

2. $\mathrm{HA(ad)} - \quad \mathrm{B^-} + \mathrm{H^+}; \mathrm{K}_a^* = \frac{[\mathrm{B^-}]_{\mathrm{ad}}[\mathrm{H^+}]}{[\mathrm{HA}]_{\mathrm{ad}}}$ (3.16)

interfacial dissociation of the extractant (involving no interfacial adsorption of the dissociated protons)

3. $\mathrm{MA(ad)} + \mathrm{HA(org)} - \quad \mathrm{MA(org)} + \mathrm{HA(ad)}; \mathrm{K}_{\mathrm{ex}}^o = \frac{\left[\overline{\mathrm{MA}}\right][\mathrm{HA}]_{\mathrm{ad}}}{\left[\overline{\mathrm{MA}}\right][\mathrm{HA}]}$ (3.17)

fast replacement at the interface of the interfacially adsorbed metal complex with bulk molecules of the extractant.

Equations 3.12, 3.16, and 3.17 are inserted into equation 3.11 and obtain

$$\text{rate} = k_2\overline{a}\alpha_2 K_a^* \left[\mathrm{M}^+\right]\left[\mathrm{H}^+\right]^{-1} - \frac{k_{-2}\overline{a}}{K_{\mathrm{ex}}^O}\alpha_2 \left[\overline{\mathrm{MA}}\right]^{-1}\left[\overline{\mathrm{HA}}\right] \tag{3.18}$$

which holds for a fully saturated interface, and

$$\text{rate} = k_2\overline{a}\alpha K_a^* \frac{\left[\mathrm{M}^+\right]\left[\overline{\mathrm{HA}}\right]}{\left[\mathrm{H}^+\right]} - \overline{a}\frac{k_{-2}}{K_{\mathrm{ex}}^O}\alpha\left[\overline{\mathrm{MA}}\right] \tag{3.19}$$

which holds for ideal adsorption. The equilibrium constant of the extraction reaction, equation 3.2 is equal to

$$K_{ex} = \frac{k_2 K_a^* K_{ex}^o}{k_{-2}} \tag{3.20}$$

for both ideal adsorption and for a saturated interface. The expression for K_{ex} is derived from equation 3.18 or 3.19 since at equilibrium the forward rate equals the reverse rate.

The concentration dependency for the rate of case 1 (equation 3.8) and equation 3.19 is the same. The difference of these two scenarios is that the second deals with the interface and is directly proportional the interfacial area case 1 has no dependency on the interfacial area. This has been experimentally verified in the literature . A plot of the apparent rate constant of the forward rate of extraction versus $\overline{a}$ must yield a straight line through the origin of the axes when case 2 holds.

Equation 3.18 shows a zero reaction order relative to $\left[\overline{\mathrm{HA}}\right]$ in the forward extraction rate, reflecting the complete saturation of the interface with the extracting reagent. Case 2 is more difficult to analyze for the rate constants since the interfacial parameters (α, α_2, K_a^*, K_{ex}^o) are difficult to obtain.

Case 3. *There are two interfacial rate-determining steps. consisting in: (1) formation of an interfacial complex between the interfacially adsorbed molecules of the extractant and the metal ion; (2) transfer of the interfacial complexes from the interface to the bulk organic phase and simultaneous replacement of the interfacial vacancy with bulk organic phase and simultaneous replacement of the interfacial vacancy with bulk organic molecules of the extractant.* This mechanism has two possibilities or sub cases. (1) reaction of dissociated anion of the extractant and (2) the reaction with the undissociated extractant.

Case 3.1 The first mechanism is

$$\mathrm{M}^+ + \mathrm{A}^-(\mathrm{ad}) \underset{k_{-3}}{\overset{k_3}{-}} \mathrm{MA(ad)} \qquad \text{(slow)} \tag{3.21}$$

$$\mathrm{MA(ad)+HA(org)} \underset{k_{-4}}{\overset{k_4}{\rightleftharpoons}} \mathrm{HA(ad)+MA(org)} \qquad \text{(slow)} \tag{3.22}$$

and the rate equations holding for the two slow steps are:

$$\text{rate 1} = \overline{a}k_3 \left[\mathrm{M^+}\right] \left[\mathrm{B^-}\right]_{\mathrm{ad}} - \overline{a}k_{-3} \left[\mathrm{MA}\right]_{\mathrm{ad}} \tag{3.23}$$

$$\text{rate 2} = \overline{a}k_4 \left[\mathrm{MA}\right]_{\mathrm{ad}} \left[\overline{\mathrm{HA}}\right] - \overline{a}k_{-4} \left[\mathrm{HA}\right]_{\mathrm{ad}} \left[\overline{\mathrm{MA}}\right] \tag{3.24}$$

When the metal concentration is sufficiently low and the concentration of the interfacially adsorbed metal complex is consequently low, for the stationary condition at $[\mathrm{MA}]_{\mathrm{ad}}$,

$$\text{rate 1} = \text{rate 2} \tag{3.25}$$

Thus, using equations 3.23, 3.24 and 3.25 and using the instantaneously established equilibria for the interfacial dissociation of the extractant (equation 3.16) for $[\mathrm{A^-}]_{\mathrm{ad}}$ then $[\mathrm{MA}]_{\mathrm{ad}}$ can be determined. Considering that for a fully saturated interface $[\mathrm{HA}]_{\mathrm{ad}} = \alpha_2$ the equation for $[\mathrm{MA}]_{\mathrm{ad}}$

$$\left[\mathrm{MA}\right]_{\mathrm{ad}} = \frac{k_3 K_a^* \alpha_2 \left[\mathrm{M^+}\right] \left[\mathrm{H^+}\right]^{-1} + k_{-4} \alpha_2 \left[\overline{\mathrm{MA}}\right]}{k_{-3} + k_4 \left[\overline{\mathrm{HA}}\right]} \tag{3.26}$$

substituting this value of $[\mathrm{MA}]_{\mathrm{ad}}$ into either equation 3.23 or 3.24 gives the rate equation

$$\text{rate} = \frac{\overline{a}k_3 k_4 K_a^* \alpha_2 \left[\mathrm{M^+}\right] \left[\mathrm{H^+}\right]^{-1}}{k_{-3} + k_4 \left[\overline{\mathrm{HA}}\right]} - \frac{\overline{a}k_{-3} k_{-4} \alpha_2 \left[\overline{\mathrm{MA}}\right]}{k_{-3} + k_4 \left[\overline{\mathrm{HA}}\right]} \tag{3.27}$$

again at equilibrium the rate(forward)=rate(reverse) and the equilibrium constant is

$$K_{ex} = \frac{k_3 k_4 K_a^*}{k_{-3} k_{-4}} \tag{3.28}$$

The following comparison of the rate equations for the above derived cases in the kinetic regime

- A homogenous reaction in the aqueous phase with the anion of the extractant

$$\text{rate} = k_1 \frac{K_a}{K_{DB}} \frac{\left[\mathrm{M^+}\right] \left[\overline{\mathrm{HA}}\right]}{\left[\mathrm{H^+}\right]} - \frac{k_{-1}}{K_{DM}} \left[\overline{\mathrm{MA}}\right] \qquad \text{equation 3.8 case 1}$$

- Interfacial reaction with the anion of the extractant, which is ideally adsorbed at the interface

$$\text{rate} = k_2\bar{a}\alpha K_a^* \frac{[M^+]\left[\overline{HA}\right]}{[H^+]} - \bar{a}\frac{k_{-2}}{K_{ex}^O}\alpha\left[\overline{MA}\right] \qquad \text{equation 3.19 case 2 ideal}$$

- Two sequential interfacial reactions: the first one being the reaction with the anion of the extractant, which is ideally adsorbed at the interface; the second one being the slow desorption of the interfacial complex from the interface.

$$\text{rate} = \frac{\bar{a}k_3k_4K_a^*\alpha_2[M^+][H^+]^{-1}}{k_{-3}+k_4\left[\overline{HA}\right]} - \frac{\bar{a}k_{-3}k_{-4}\alpha_2\left[\overline{MA}\right]}{k_{-3}+k_4\left[\overline{HA}\right]} \qquad \text{equation 3.27 case 3.1}$$

shows that if $\left[\overline{HA}\right]$ is sufficiently small to allow the approximation $k_4\left[\overline{HA}\right] \ll k_{-3}$ into the denominator of equation 3.27 the three rate equations have exactly the same concentration dependence on $[M^+]$, $\left[\overline{HA}\right]$, $[H^+]$, although the extraction mechanisms are characterized by different rate-determining steps. The difference among these mechanisms can be seen only by measuring the dependence of the rate of extraction on the specific interfacial area, $\bar{a}$, and by using the broadest possible concentration range of the reactants. If a dependence on $\bar{a}$ exists, case 1 can be excluded. If in addition the reaction rate becomes first order then becomes zero order when $\left[\overline{HA}\right]$ increases, case 2 can also be ruled out.

Case 3.2. When the interfacially reactive species are the undissociated molecules of the extractant adsorbed at the interface (i.e., the first rate determining step of the two step mechanism is the reaction between the metal ion M^+ and HA(ad)), the following equations will hold:

$$M^+ + HA(ad) \underset{k_{-3}^*}{\overset{k_3^*}{\rightleftharpoons}} MA(ad) + H^+ \qquad \text{(slow)} \tag{3.29}$$

$$MA(ad) + HA(org) \underset{k_{-4}}{\overset{k_4}{\rightleftharpoons}} HA(ad) + MA(org) \qquad \text{(slow)} \tag{3.30}$$

The rate equation for these slow steps are

$$\text{rate 1} = \bar{a}k_3^*[M^+][HA]_{ad} - k_{-3}^*\bar{a}[MA]_{ad}[H^+] \tag{3.31}$$

$$\text{rate 2} = \bar{a}k_4^*[MA]_{ad}\left[\overline{HA}\right] - \bar{a}k_{-4}[HA]_{ad}\left[\overline{MA}\right] \tag{3.32}$$

and assuming the equilibrium state (rate 1= rate 2) and introducing the same substitution as in case 3.1 i.e. ($[A^-]_{ad} = K_a^* \frac{[HA]_{ad}}{[H^+]}$) for the fully saturated interface

$$[MA]_{ad} = \frac{\alpha_2 k_3^* [M^+] - \alpha_2 k_{-4} \overline{[MA]}}{k_{-3}^* [H^+] + k_4 \left[\overline{HA}\right]} \tag{3.33}$$

and inserting this into equation 3.32 gives

$$\begin{aligned} \text{rate} &= \text{rate (forward)} - \text{rate (reverse)} \\ &= \frac{\overline{a} k_3^* k_4 \alpha_2 [M^+] \left[\overline{HA}\right]}{k_{-3}^* [H^+] + k_4 \left[\overline{HA}\right]} - \frac{\overline{a} k_{-3}^* k_{-4} \alpha_2 \overline{[MA]} [H^+]}{k_{-3}^* [H^+] + k_4 \left[\overline{HA}\right]} \end{aligned} \tag{3.34}$$

when the simplification of $k_4 \left[\overline{HA}\right] \ll k_{-3}^* [H^+]$ is applied then equation 3.34 has the same concentration dependence of $[M^+]$, $\left[\overline{HA}\right]$, and $[H^+]$ as equations 3.8 and 3.19

$$\text{rate} = k_1 \frac{K_a}{K_{DB}} \frac{[M^+] \left[\overline{HA}\right]}{[H^+]} - \frac{k_{-1}}{K_{DM}} \left[\overline{MA}\right] \text{ equation 3.8 case1}$$

$$\text{rate} = k_2 \overline{a} \alpha K_a^* \frac{[M^+] \left[\overline{HA}\right]}{[H^+]} - \overline{a} \frac{k_{-2}}{K_{ex}^O} \alpha \left[\overline{MA}\right] \text{ equation 3.19 case 2 ideal}$$

Unlike case 3.1 the logarithmic plot of equation of the forward rate divided by the metal ion concentration vrs. $[H^+]$ is not linear.

Note that these cases, as presented and derived by Danesi, exemplify the differences, ambiguities, complexities and diversities of metal extraction systems. Many other mechanisms can occur in the absence of diffusional contributions. Other physicochemical properties can also effect the transport mechanism. For example, appreciable water solubility and weak adsorption at the interface of the extacting reagent generally favor class 1 mechanisms. High water insoluble and strongly interfacially adsorbed chelating extractant increase the possibility that cases 2 and 3 may describe the mechanism of extraction.

A special note should be included here. As will be discussed later in sections 3.3.2 page 69, 3.206 page 83, and 3.3.2 page 85 the use of the Langmuir isotherm in the form as used by Danesi in the above derivations is questioned as to its correctness in form and context for this process. The assumptions in the derivation of the Langmuir isotherm are: (1) assumes equalibrium between adsorption rate and desorption rate which is contrary to the last reaction in the last case and its subcases where the adsorption and desorption

reaction is slow and partially controlling; (2) a single specie adsorption isotherm is used where two species are vying for the same surface spots. The extractant is a reversably adsorbed/desorbed specie as is the formed neutral metal extractant complex. Once formed the metal extractant complex will act similar to a catalyst poison competing for the sites but not reacting. How strongly it competes will depend on the system but will probably be strongly effected by the relative concentration of the metal complex and the extractant in the organic phase as is suggested by the overall rate equations.

Diffusional Regime

In a two film model for mass transport between two phases a stagnant film thickness δ_w or δ_o is defined on either side of the interface. The interface is assumed to have no thickness. Three resistances are defined to account for the diffusional contributions as R_w — the water or aqueous side diffusion contribution; R_o — the organic side diffusion; R_i — the resistance across the interface. This is the most popular model to explain mass transfer between two different phases, though it is inappropriate in some cases as will be discussed later. This model is introduced here to help explain the diffusional regime.

The resistances are assumed to occur completely in the stagnant films on either side of the interface. These resistances are linearly additive to give a total resistance R as $R = R_w + R_i + R_o$. This equation is true for steady state situations. An assumption, that in the absence of rigid interfacial films causes R_i to be negligible compared to R_w and R_o, simplifies the development of this model for metal extraction. This latter assumption is basically a very ideal and more often than not an unrealistic assumption. The interface, as has been mentioned several times, is a most critical and important aspect of two phase separations. Thus, the interface will be discussed, in detail, later in this study .

Like his development of the kinetic regime, Danesi also develops two cases for the diffusional regime assuming two film theory. These two cases are:

Case 1. *The interfacial partition between the two phases of uncharged species is fast. The rate is controlled by the diffusion to and away from the interface of the partitioning species.* In the absence of an interfacial resistance, the partition equilibrium of an arbatrary specie A between the aqueous and organic phase, occurring at the interface, can be always considered as an instantaneous process. The partition coefficient is the ratio of measured concentration of the metal species in the organic phase to that of the measured concentration in the aqueous phase at interfacial equilibrium. Mathematically this is developed below;

$$A - A_{(org)} \tag{3.35}$$

with an extraction equilibrium distribution constant K_{DA}, reached at $t = \infty$;

$$A - A_{(org)} \quad \text{(fast)} \tag{3.36}$$

The interfacial equilibrium, holds at any time (subscript indicates species in contact with the interface); thus

$$K_{DA} = \frac{[\bar{A}]_{eq}}{[A]_{eq}} = \frac{[\bar{A}]_i}{[A]_i} \tag{3.37}$$

The symbol $[\ ]_i$ indicates concentrations at the extreme limit of the diffusional film (i.e., volume concentrations in the region in direct contact or very close to the liquid–liquid interface). Because of the fast nature of the distribution reaction, local equilibrium always holds at the interface.

The diffusional regime is developed by using Fick's diffusion law at both sides of the interface under steady state and linear concentration gradients.

$$J_w = -D_A \frac{\partial [A]}{\partial x} = -D_A \frac{([A]_i - [A])}{\delta_w} \tag{3.38}$$

$$J_O = -D_{\bar{A}} \frac{\partial [\bar{A}]}{\partial x} = -D_{\bar{A}} \frac{([A] - [A]_i)}{\delta_O} \tag{3.39}$$

$D_{\bar{A}}$ and D_A are the diffusion coefficients of the distributing species in the aqueous and organic layers, respectively. At steady state the fluxes $J_w = J_O = J$ and by setting

$$\Delta_w = \frac{\delta_w}{D_A}, \qquad \Delta_O = \frac{\delta_O}{D_{\bar{A}}} \tag{3.40}$$

Solving equations 3.38 and 3.39 for the interfacial concentrations to yield

$$[A]_i = [A] - J\Delta_w \tag{3.41}$$

$$[\bar{A}]_i = J\Delta_O + [\bar{A}] \tag{3.42}$$

Inserting equations 3.41 and 3.42 into equation 3.37 and considering the correlation between flux and rate (i.e. $-\frac{dc_1}{dt}\frac{V_1}{Q} = +\frac{dc_2}{dt}\frac{V_2}{Q} = J$ where Q is the area of the diffusion film and V_1 and V_2 are well stirred reservoir volumes and J is the flux) the following is given by Danesi's development;

$$\text{rate} \quad = \quad -\frac{d[A]}{dt} = \text{rate (forward)} - \text{rate (reverse)}$$

$$= \frac{\bar{a}K_{DA}[A]}{K_{DA}\Delta_w + \Delta_O} - \frac{\bar{a}[\bar{A}]}{K_{DA}\Delta_w + \Delta_O} \tag{3.43}$$

The diffusion – controlled, extraction kinetics of A, therefore, can be described as a pseudo – first – order rate process with apparent rate constants

$$k_1 = \frac{K_{DA}}{K_{DA}\Delta_w + \Delta_O}, \qquad k_{-1} = \frac{1}{K_{DA}\Delta_w + \Delta_O} \tag{3.44}$$

The rate equation is indistinguishable from that of an extraction process occurring in kinetic regime, which is controlled by a slow, interfacial partition reaction:

$$A \underset{k_{-1}}{\overset{k_1}{\rightleftharpoons}} A_{(org)} \quad \text{(slow)} \tag{3.45}$$

Equation 3.43 can be integrated to obtain

$$\ln \frac{[A]_O - [A]_{eq}}{[A] - [A]_{eq}} = \frac{\bar{a}(K_{DA}+1)}{K_{DA}\Delta_w + \Delta_O} t = \bar{a}(k_1 + k_{-1})\, t \tag{3.46}$$

If K_{DA} is very high (i.e. the partition of A in favor of the organic phase

$$k_1 \sim \frac{D_A}{\delta_w} \qquad \text{and} \qquad k_{-1} \sim 0 \tag{3.47}$$

and the extraction rate is controlled only by the aqueous-phase diffusional resistance. However, if K_{DA} is very small, then $k_1 \sim 0$ and

$$k_{-1} \sim \frac{D_{\bar{A}}}{\delta_w} \tag{3.48}$$

the rate is controlled by the organic phase diffusional resistance.

Case 2. *A fast reaction between the metal cation and the undissociated extracting reagent occurs at the interface (or in proximity of the interface). The rate is controlled by the diffusion to and away from the interface of the species taking part in the reaction*

For example in a monovalent cation extraction, the stoichiometry is represented by the equation:

$$M^+ + HA(org) - MA(org) + H^+ \tag{3.49}$$

with equilibrium extraction constant K_{ex}. The chemical reaction occurring at or near the interface is considered to always at equilibrium, although bulk phases reach this condition

only at the end of the extraction process. The condition of interfacial (local) equilibrium is expressed by

$$M_i^+ + HA_i(org) - MA_i(org) + H_i^+ \qquad \text{(fast)} \tag{3.50}$$

with interface equilibrium constant K_i which alternatively can be written as the sum of the two equilibria.

$$M_i^+ + HA_i(org) - MA_i(org) + H_i^+, \qquad K_1 = \frac{\left[\overline{MA}\right]_i}{[M^+]_{i[A^-]i}} \tag{3.51}$$

$$HA_i(org) - H_i^+ + B_i^-(org), \qquad K_2 = \frac{[A^-]_i [H^+]_i}{\left[\overline{HA}\right]_i} \tag{3.52}$$

with

$$K_{ex} = K_1 K_2 = \frac{\left[\overline{MA}\right]_{eq} [H^+]_{eq}}{\left[\overline{HA}\right]_{eq} [M^+]_{eq}} = \frac{\left[\overline{MA}\right]_i [H^+]_i}{\left[\overline{HA}\right]_i [M^+]_i} = K_i \tag{3.53}$$

Like case 1 above, the rate of extraction can be obtained by considering the diffusional fluxes through the diffusion films of M^+, H^+, MA, and HA, expressed through the Fick's law, and introducing the chemical reaction, equation 3.50 as boundary condition to the differential equations describing diffusion through the aqueous and organic diffusion films. Applying these laws and equations along with the simplifying assumptions of steady state and linear concentration gradients the rate of diffusional extraction of the monovalent metal M^+ can be derived.

$$J_{M^+} = -D_{M^+} \frac{\partial [M^+]}{\partial x} = -D_{M^+} \frac{([M^+]_i - [M^+])}{\delta_w} \tag{3.54}$$

$$J_{H^+} = -D_{H^+} \frac{\partial [H^+]}{\partial x} = -D_{H^+} \frac{([H^+]_i - [H^+])}{\delta_w} \tag{3.55}$$

$$J_{\overline{MA}} = -D_{\overline{MA}} \frac{\partial \left[\overline{MA}\right]}{\partial x} = -D_{\overline{AB}} \frac{\left(\left[\overline{MA}\right] - \left[\overline{MA}\right]_i\right)}{\delta_O} \tag{3.56}$$

$$J_{\overline{HA}} = -D_{\overline{HA}} \frac{\partial \left[\overline{HA}\right]}{\partial x} = -D_{\overline{HA}} \frac{\left(\left[\overline{HA}\right] - \left[\overline{HA}\right]_i\right)}{\delta_O} \tag{3.57}$$

These four fluxes are not independent and at steady state are related by the condition:

$$J_{M^+} = J_{H^+} = -J_{\overline{MA}} = -J_{\overline{HA}} \tag{3.58}$$

Relating again the correlation between flux and rate

$$-\frac{\mathrm{d}\,[M^+]}{\mathrm{d}\,t}\frac{V}{Q} = J = J_{M^+} \tag{3.59}$$

solving equations 3.54—3.57 for the interfacial concentrations $[\ ]_i$ and introducing the simplification that the diffusion coefficients depend only on the nature of the phase or

$$\Delta_w = \frac{\delta_w}{D_{M^+}} = \frac{\delta_w}{D_{H^+}}, \qquad \Delta_O = \frac{\delta_O}{D_{\overline{MA}}} = \frac{\delta_O}{D_{\overline{HA}}} \tag{3.60}$$

the following is obtained

$$[M^+]_i = [M^+] - J\,\Delta_w \tag{3.61}$$

$$[H^+]_i = [H^+] + J\,\Delta_w \tag{3.62}$$

$$\left[\overline{MA}\right]_i = \left[\overline{MA}\right] + J\,\Delta_O \tag{3.63}$$

$$\left[\overline{HA}\right]_i = \left[\overline{HA}\right] - J\,\Delta_O \tag{3.64}$$

Equations 3.61 — 3.64 are inserted into equation 3.53 to yield

$$K_{ex} = \frac{\left(\left[\overline{MA}\right] + J\,\Delta_O\right)\left([H^+] + J\,\Delta_w\right)}{\left([M^+] - J\,\Delta_w\right)\left(\left[\overline{HA}\right] - J\,\Delta_O\right)} \tag{3.65}$$

Thus the above equation can be solved for the flux J and an expression for the extraction rate as a function of the four concentration variables in the bulk phases, the equilibrium constant of the extraction reaction, and the two diffusional parameters Δ_w and Δ_O. At low fluxes the J^2 term from equation 3.65 can be neglected and J isolated.

$$\begin{aligned} \text{rate} &= \text{rate(forward)} - \text{rate(reverse)} = -\frac{d\,[M^+]}{dt} = J\,\overline{a} \\ &= \frac{\overline{a}K_{ex}\,[M^+]\left[\overline{HA}\right]}{\Delta_w\left(\left[\overline{MA}\right] + K_{ex}\left[\overline{HA}\right]\right) + \Delta_O\left([H^+] + K_{ex}\,[M^+]\right)} \\ &\quad - \frac{\overline{a}\left[\overline{MA}\right][H^+]}{\Delta_w\left(\left[\overline{MA}\right] + K_{ex}\left[\overline{HA}\right]\right) + \Delta_O\left([H^+] + K_{ex}\,[M^+]\right)} \end{aligned} \tag{3.66}$$

the terms containing $[M^+]$ and $\left[\overline{MA}\right]$ can be neglected in the denominator of equation 3.66. In practice this means that $\left[\overline{HA}\right]$ and $[H^+]$ are constant with time and their initial and equilibrium concentrations are essentially the same. The rate equation then becomes

$$\text{rate} = \frac{\bar{a}K_{ex}[M^+]\left[\overline{HA}\right]}{\Delta_w K_{ex}\left[\overline{HA}\right]_{eq} + \Delta_O [H^+]_{eq}} - \frac{\bar{a}\left[\overline{MA}\right][H^+]_{eq}}{\Delta_w K_{ex}\left[\overline{HA}\right]_{eq} + \Delta_O [H^+]_{eq}} \tag{3.67}$$

By dividing the numerators and denominators by $[H^+]_{eq}$ and setting

$$K^*_{ex} = \frac{K_{ex}\left[\overline{HA}\right]_{eq}}{[H^+]_{eq}} \tag{3.68}$$

where K^*_{ex} is the conditional equilibrium constant of equilibrium given by equation 3.49 at constant $[H^+]$ and $\left[\overline{HA}\right]$

$$\text{rate} = \frac{\bar{a}K^*_{ex}[M^+]}{\Delta_w K^*_{ex} + \Delta_O} - \frac{\bar{a}\left[\overline{MA}\right]}{\Delta^*_{wK_{ex}} + \Delta_O} \tag{3.69}$$

comparing this to equation 3.43 rate $= \frac{\bar{a}K_{DA}[A]}{K_{DA}\Delta_w + \Delta_O} - \frac{\bar{a}[\bar{A}]}{K_{DA}\Delta_w + \Delta_O}$ an observation is made that this is the same equation with K_{DA} being replaced with K^*_{ex}. The rate of extraction of species present at high dilution in a system of fixed composition is the simple distribution of an uncharged species between two immiscible phases.

Mixed Diffusional—Kinetic Regime

When the reaction velocity is comparable to the diffusional process through the interfacial films then a mixed regime is evident and the other two regimes are limiting cases of this more general one. A full description of the extraction kinetics of a mixed regime requires that the equations of diffusion and of chemical kinetics be solved simultaneously. When the reactions occur as homogenous reactions i. e. in the bulk phase or thin films surrounding the interface then the differential equations describing the diffusional processes and the rate of formation of different chemical species need to be solved simultaneously. When the chemical reactions occur at the interface and can be described as heterogeneous, the rates of the chemical reactions appear in the boundary conditions of the differential diffusion equations. The chemical kinetics at the interface must be known from separate experiments carried out in a pure kinetic regime. The interfacial rate laws cannot be known a priori and have to be derived from kinetic experiments. In some cases this has been avoided by assuming that the interfacial rate laws are simply related to the reaction stoichiometry or

by trying to empirically derive information on the interfacial reactions through fitting, to experimental data obtained in a mixed regime, analytical solutions of differential equations that take into account both diffusion and chemical reactions (Danesi page 199). Danesi explains that

> "...unfortunately both of the above procedures can lead to erroneous interpretations, as in only a few cases can the rate laws be correctly derived from stoichiometric considerations, and when too many variables (e.g., rate constants, rate laws, and diffusional parameters) are simultaneously adjusted to fit experimental data, many alternative models can usually satisfy the same equations. Therefore, it is important that the boundary condition of the diffusion equations (i.e., the interfacial rate laws) be derived by separate, suitable experiments..."

Danesi derives a very simple (mathematically) case where the solvent extractant is adsorbed at the interface and has extremely low water solubility.

Case 1. *The interfacial partition reaction between the two phases of uncharged species is slow. The rate is controlled both by the slow partition reaction and by diffusion to and away from the interface of the partitioning species.*

This case is very similar to case 1 in the diffusional regime section of this study, section 3.2.1. Note that the assumptions here are those of steady state diffusion and linear concentration gradients through the diffusion films. The slow interfacial chemical reaction and the corresponding interfacial flux, J_i are

$$\mathrm{A}_i \underset{k_{-1}}{\overset{k_1}{\rightleftharpoons}} \mathrm{A}_i(\mathrm{org}) \tag{3.70}$$

$$J_i = k_1 [A]_i - k_{-1} \left[\overline{A}\right]_i \tag{3.71}$$

Note that $[A]_i$ and $\left[\overline{A}\right]_i$ are at equilibrium only at the end of the extraction process and at steady state

$$J = J_w = J_o = J_i \tag{3.72}$$

where J is the flux on the w— water side film, o— organic side film or i— the interface.

$$\begin{aligned} \text{rate} &= -\frac{d[A]}{dt} = \text{rate (forward)} - \text{rate (reverse)} \\ &= \frac{\bar{a}k_1[A]}{k_1\Delta_w + k_{-1}\Delta_O + 1} - \frac{\bar{a}k_{-1}[\bar{A}]}{k_1\Delta_w + k_{-1}\Delta_O + 1} \end{aligned} \tag{3.73}$$

comparing this with equation 3.43 (the rate is controlled by the diffusion to and from the interface) indicates that the presence of slow interfacial chemical reaction shows up as an additional term in the denominator of the rate laws. Note also that the pure kinetic and diffusional regimes are limitations of equation 3.73. If the rate constants are large i.e. fast reactions then equation 3.73 can be divided and multiplied by k_{-1} and $\frac{k_1}{k_{-1}} = K_{\mathrm{DA}}$ and $(k_{-1})^{-1}$ can be neglected for fast rates relative to the other terms in the denominator an equation identical to equation 3.43 is obtained for which only diffusion controls the partition rate. At the other limiting end when interfacial film diffusion is fast and the reactions are slow then $1 \gg (k_1 \Delta_w + k_{-1} \Delta_o)$ and the rate equation becomes equal to

$$\text{rate} = \overline{a} k_1 [\mathrm{A}] - \overline{a} k_{-1} \left[\overline{\mathrm{A}}\right] \tag{3.74}$$

3.2.2 INTERPRETATION

The interpretation and comparisons between the kinetic equations and the diffusion equations as presented by Danesi illustrates that :

> the rate laws obtained for a system in a kinetic regime controlled by slow two-step interfacial chemical reactions and for a system in diffusional regime controlled by slow film diffusion processes coupled to an instantaneous reaction occurring at the interface have the same functional dependence on the concentrations variables when low fluxes and low metal concentrations are involved.

Danesi Clarifies:

> Diffusional contributions to the extraction rate, a fast extraction reaction occurring with a simple stoichiometry can mimic a two step interfacial chemical reaction occurring in absence of diffusional contributions. This type of ambiguity, in the past has led solvent extraction chemists (including Danesi) to sometimes erroneously derive extraction mechanisms invoking a series of two slow interfacial chemical reactions as rate determining steps in systems for which the two phases were insufficiently stirred. However, a distinction between the two cases can occasionally be made if it is possible to conduct kinetic experiments in which the values of δ_w and δ_O are varied. When the rate is independent of δ_w and δ_O, the equation for kinetic regime describes the rate extraction. Nevertheless, since the film thickness never seem to go to zero, the ambiguity may not be resolved.

3.3 MORE COMPLEX MECHANISMS

The derivations of the monovalent mechanisms in the previous section was developed by Danesi (Principles and Practice of solvent extraction chapter 5) and reproduced here to introduce the simpler characteristics of the complex mechanistic behavior of solvent extraction. The literature is as varied in mechanisms as it is in the emmense volume of types of extractants developed over the last forty to fifty years to remove, separate, and purify metallic species from aqueous bearing process streams. The trend has been to develop extractants selective to a specific metal under specific conditions over other metals in the process streams and thus effect a separation. Flow sheets for these processes can be quite extensive and elaborate. In this section the development of the more complex multivalent extraction kinetic mechanisms and rate will be presented along with discussions of the diffusional models to explain metal extraction. The three valence metal will be emphasized here since these are the more stable configuration for a great number of the Lanthanide and Actinide series. An analytical model for the extraction rate of the three valence and a general m valence metal is developed when the mathematics and algebra are amenable.

3.3.1 Liquid Ion Exchange

Acidic, extractants, or cationic liquid ion exchangers, extract metals by a cation–exchange mechanism, in which hydrogens of the extractant are exchanged for metal ions. Examples of these types of extractants are phosphoric acids, phosphonic acids, carboxylic acids, and sulphonic acids. The general chemical mechanism is

$$M^{m+} + \overline{mHA} - \overline{MA_m} + mH^+. \tag{3.75}$$

where m is the valence of the metal being extracted and also the stoichimetric variable. The most useful acidic type metal extractant is organic derivatives of phosphorus acids. This group includes esters of orthophosphoric, phosphonic and phosphinic acids. Of these, alkylphosphoric acids have proved to be the most versatile, especially di(2 — ethylhexyl)phosphoric acid (D2EHPA or DEHPA) (solvent extraction page 98 Ritcey and Ashbrook). DEHPA has been one of the most versatile extractants in metal extraction. DEHPA has good chemical stability because of its size and moderate branching, generally good kinetics of extraction, good loading and stripping characteristics, low solubility in the aqueous phase, and availability in commercial quantities (Ritcey and Ashbrook page 98 and Roddy and Coleman page 64) though recently a number of companies manufacturing this extractant have ceased to carry it in the U. S. This is primarily due to its replacement with the bidentate and polydentate phosphonate compounds that have better selectivity.

Equation 3.75 is a simple form of metal extraction by D2EHPA. Like many of the acidic extractants DEHPA forms dimers as shown in figure———— which complicates the

extraction mechanism. At low metal loading in the organic phase extraction is considered to occur as indicated in equation 3.76.

$$M^{m+} + \overline{m(HA)_2} - \overline{M(A \cdot HA)_m} + mH^+ \tag{3.76}$$

where HA represents DEHPA, n is the valence of the metal, M. At higher metal loading extraction occurs as in equation 3.75. This is a typically accepted mechanism presented in the literature for most transition metals, lanthanides and actinides proposed by Peppard and workers. However, as the valence charge of metals increase the extractability of the metal also increases. Because of this the above equation may not hold for higher valence elements such as thorium(IV) and cerium(IV) etc. since DEHPA extracts these to a greater extent. Kolařík (in 5 th ISCEC 1968 p 59) gives an overall equilibrium formula for a monoacidic organophosphorus extractant

$$M^{m+} + \frac{m+x}{y}\overline{(HA)}_y - \overline{MA_m \cdot xHA} + mH^+ \tag{3.77}$$

where M^{m+} is the ion of the extracted metal and HA is the monomeric molecule of the extractant species. As pointed out in the previous section, this overall extraction equilibria contains several individual equilibria mechanisms i. e. dissociation, self-association, and partition of the extractant species, the formation and partition of simple complexes MA_m, and the addition of the HA molecules to MA_m with the formation of the adduct complex $\overline{MA_m \cdot xHA}$.

Using the above more general equation for the overall cationic exchange mechanism we will make use of an equilibrium concept at the interface to obtain a value for x. The acidic extractant DEHPA is dimeric in the organic phase y in equation 3.77 is equal to 2. Equation 3.77 will become

$$M^{m+} + \frac{m+x}{2}\overline{(HA)}_2 \underset{k_{-1}}{\overset{k_1}{\rightleftharpoons}} \overline{MA_m \cdot xHA} + mH^+ \tag{3.78}$$

The overall equilibrium coefficient for extraction for the above reaction is given by

$$K_{ex} = \frac{\left[\overline{MA_m \cdot xHA}\right][H^+]^m}{[M^{m+}]\left[\overline{(HA)}_2\right]^{\frac{m+x}{2}}} \tag{3.79}$$

The distribution coefficient is defined to be the ratio of the total metal concentration or activity (regardless of form or complex) in the organic phase to that in the aqueous phase.

$$D = \frac{\left[\overline{MA_m \cdot xHA}\right]}{[M^{m+}]} = K_{ex}\frac{\left[\overline{(HA)}_2\right]^{\frac{m+x}{2}}}{[H^+]^m} \tag{3.80}$$

Taking the logarithm of equation 3.80

$$\log\left(\mathrm{D}\ [\mathrm{H}^+]^m\right) = \log K_{ex} + \left\{\frac{m+x}{2}\right\}\log\left[(\overline{\mathrm{HA}})_2\right] \tag{3.81}$$

A log–log plot of D $[\mathrm{H}^+]^m$ versus $(\overline{\mathrm{HA}})_2$ gives a straight line with an intercept of $\log K_{ex}$ and a slope of $\frac{m+x}{2}$. Since for a specific metal the valence m will be known and from the slope x can be obtained. In subsequent sections the usefulness of equilibrium data for the reactions known to occur will be used. The x value calculated is the number of undissociated monomeric molecules of the extractant that surrounds or complexes with the metal ion. K_{ex} is also equal to the ratio of the forward and reverse reactions or $\frac{k_1}{k_{-1}}$.

3.3.2 Kinetic Regime

As mentioned in the kinetic regime portion of section 3.2.1 various controlling mechanisms can be developed.

Case 1: The controlling step in the extraction between the metal cation and an organic acidic reagent (extractant) which is rapidly solubilized in the aqueous phase can be mechanistically described by the following equilibria:

Distribution or Partition of the organic extractant between the two phases

$$[\mathrm{HA}]_{(\mathrm{org})} \overset{K_D}{-} [\mathrm{HA}] \qquad \text{fast} \qquad \mathrm{K}_D = \frac{[\mathrm{HA}]_{(\mathrm{org})}}{[\mathrm{HA}]} \tag{3.82}$$

where K_D is the distribution equalibrium constant for HA between the phases. Generally for acidic extractants alkylphosphoric acid or carboxylic acid is present as monomer in aqueous solutions but mainly as dimer in nonpolar organic solvents (SEKINE pp187). Thus y is generally 2.

Formation of Complexes

$$[\mathrm{M}^{m+}] + [\mathrm{HA}] \underset{k_{-1}}{\overset{k_1}{-}} \left[\mathrm{MA}^{(m-1)+}\right] + [\mathrm{H}^+] \qquad \text{slow} \tag{3.83}$$

$$K_1 = \frac{\left[\mathrm{MA}^{(m-1)+}\right][\mathrm{H}^+]}{[\mathrm{M}^{m+}][\mathrm{HA}]}$$

$$\left[\mathrm{MA}^{(m-1)+}\right] + [\mathrm{HA}] \underset{k_{-2}}{\overset{k_2}{-}} \left[\mathrm{MA}_2^{(m-2)+}\right] + [\mathrm{H}^+] \tag{3.84}$$

$$K_2 = \frac{\left[\mathrm{MA}_2^{(m-2)+}\right][\mathrm{H}^+]}{\left[\mathrm{MA}^{(m-1)+}\right][\mathrm{HA}]}$$

$$\left[MA_2^{(m-2)+}\right] + [HA] \underset{k_{-3}}{\overset{k_3}{-}} \left[MA_3^{(m-3)+}\right] + [H^+]$$
$$K_3 = \frac{\left[MA_3^{(m-3)+}\right][H^+]}{\left[M^{(m-2)+}\right][HA]} \tag{3.85}$$

$$\vdots$$

$$\left[MA_{m-1}^{+}\right] + [HA] \underset{k_{-m}}{\overset{k_m}{-}} [MA_m] + [H^+] \qquad K_m = \frac{[MA_m][H^+]}{\left[M_{m-1}^{+}\right][HA]} \tag{3.86}$$

For which the overall formation constant is

$$K_f = K_1K_2K_3\cdots K_{m-1}K_m = \prod_{i=1}^{m} K_i = \frac{[MA_m][H^+]^m}{[M^{m+}][HA]^m} \tag{3.87}$$

The self association of the extractant or polymerization of some weak acid extractants such as HDEHPA (which forms a dimer in the organic phase) is accomplished by forming intermolecular hydrogen bonds in the organic phase where in the aqueous phase form hydrogen bonds with water and are present primarily as the monomer (SEKIN solvent extraction chemistry p 122).

$$[yHA]_{(org)} - [H_yA_y]_{(org)} \qquad \text{fast} \qquad K_{poly} = \frac{[H_yA_y]_{(org)}}{[HA]_{(org)}^{y}} \tag{3.88}$$

This polymerization phenomena can also occur between other types of extractants and cause a synergistic affect of extraction.

The distribution of the metal extraction species

$$[MA_m] - [MA_m]_{org} \qquad \text{fast} \qquad K_{MA_m} = \frac{[MA_m]_{org}}{[MA_m]} \tag{3.89}$$

and for the self adduct formation to satisfy the coordination saturation demand by adding one or several molecules of the undissociated acid HA. The complex formed is

$$[MA_m]_{org} + x\,[HA]_{org} - [MA_m \cdot x\,(HA)]_{org} \quad \text{fast}$$
$$K_{add\ (org)} = \frac{[MA_m \cdot x(HA)]_{org}}{[MA_m]_{org}[HA]_{org}^{x}} \tag{3.90}$$

At this point assumptions are necessary to develop the chemical kinetic rate equations.

ASSUMPTION 1: The only metal species that is extracted into the organic phase is the fully complexed MA_m and that the intermediate species in equations 3.83 through 3.86 are not extracted.

ASSUMPTION 2: At this point only one slow step will be assumed in the aqueous phase, that of equation 3.83. All other reactions of the complex formations are rapid.

Therefore equation 3.83 is the controlling step and the reaction mechanism is :

$$[M^{m+}] + [HA] \underset{k_{-1}}{\overset{k_1}{=}} \left[MA^{(m-1)}\right] + [H^+] \tag{3.91}$$

and the reaction rate expression for this controlling step:

$$\text{rate} = -\frac{d\,[M^{+m}]}{dt} = k_1\,[M^{+m}]\,[HA] - k_{-1}\left[MA^{(m-1)+}\right][H^+] \tag{3.92}$$

Using equations 3.84 through 3.86 an equilibrium constant can be derived for this series of complex reactions

$$K_{comp_1} = \frac{[MA_m]\,[H^+]^{m-1}}{\left[MA^{(m-1)+}\right][HA]^{m-1}} \tag{3.93}$$

and from this the $\left[MA^{(m-1)+}\right]$ can be solved

$$\left[MA^{(m-1)+}\right] = \frac{[MA_m]\,[H^+]^{m-1}}{K_{comp_1}\,[HA]^{m-1}}\,. \tag{3.94}$$

The rate equation becomes

$$\text{rate} = k_1\,[M^{+m}]\,[HA] - k_{-1}\frac{[MA_m]\,[H^+]^m}{K_{comp_1}\,[HA]^{m-1}} \tag{3.95}$$

from equation 3.89 for distribution of the metal extraction species

$$[MA_m] = \frac{[MA_m]_{org}}{K_{MA_m}}$$

and the rate equation

$$\text{rate} = k_1\,[M^{+m}]\,[HA] - k_{-1}\frac{[MA_m]_{org}\,[H^+]^m}{K_{MA_m}K_{comp_1}\,[HA]^{m-1}} \tag{3.96}$$

using the equation for the distribution of the acidic extractant between phases equation 3.82

$$[HA] = \frac{[HA]_{org}}{K_D}$$

the rate equation becomes

$$\text{rate} = \mathrm{k_1}\,[\mathrm{M}^{+m}]\,\frac{[\mathrm{HA}]_{\mathrm{org}}}{\mathrm{K}_D} - \mathrm{k_{-1}}\frac{[\mathrm{MA}_m]_{\mathrm{org}}\,[\mathrm{H}^+]^m}{K_{MA_m}K_{comp_1}\left(\frac{[\mathrm{HA}]_{\mathrm{org}}}{\mathrm{K}_D}\right)^{m-1}} \tag{3.97}$$

substituting equation 3.90 for the equilibrium of the adduct formation of the extracted metal complex in the organic phase

$$[\mathrm{MA}_m]_{\mathrm{org}} = \frac{[\mathrm{MA}_m \cdot x\,(\mathrm{HA})]_{\mathrm{org}}}{K_{add(\mathrm{org})}\,[\mathrm{HA}]^x_{\mathrm{org}}}$$

the rate equation is transformed to

$$\begin{aligned}\text{rate} \;=\; & \frac{\mathrm{k_1}}{\mathrm{K}_D}\,[\mathrm{M}^{+m}]\,[\mathrm{HA}]_{\mathrm{org}} \\ & -\frac{\mathrm{k_{-1}K}_D^{m-1}}{\mathrm{K}_{MA_m}\mathrm{K}_{comp_1}\mathrm{K}_{add(\mathrm{org})}}\,\frac{[\mathrm{MA}_m \cdot x\,(\mathrm{HA})]_{\mathrm{org}}\,[\mathrm{H}^+]^m}{\left([\mathrm{HA}]_{\mathrm{org}}\right)^{x+m-1}}\end{aligned} \tag{3.98}$$

Assuming that the acidic organic polymerizes in a nonpolar organic solvent or diluent then equation 3.88 is used to account for this phenomenon

$$[\mathrm{HA}]_{(\mathrm{org})} = \left(\frac{[\mathrm{H}_y\mathrm{A}_y]_{(\mathrm{org})}}{K_{poly}}\right)^{\frac{1}{y}}$$

and the rate equation once again is modified to reflect this

$$\begin{aligned}\text{rate} \;=\; & \frac{\mathrm{k_1}}{\mathrm{K}_D}\,[\mathrm{M}^{+m}]\left(\frac{[\mathrm{H}_y\mathrm{A}_y]_{\mathrm{org}}}{\mathrm{K}_{poly}}\right)^{\frac{1}{y}} \\ & -\frac{\mathrm{k_{-1}K}_D^{m-1}}{\mathrm{K}_{MA_m}\mathrm{K}_{comp_1}\mathrm{K}_{add(\mathrm{org})}}\,\frac{[\mathrm{MA}_m \cdot x\,(\mathrm{HA})]_{\mathrm{org}}\,[\mathrm{H}^+]^m}{\left(\frac{[\mathrm{H}_y\mathrm{A}_y]_{\mathrm{org}}}{\mathrm{K}_{poly}}\right)^{\frac{x+m-1}{y}}}\end{aligned} \tag{3.99}$$

or

$$\begin{aligned}\text{rate} \;=\; & \frac{\mathrm{k_1}}{\mathrm{K}_D\,(K_{poly})^{\frac{1}{y}}}\,[\mathrm{M}^{+m}]\left([\mathrm{H}_y\mathrm{A}_y]_{(\mathrm{org})}\right)^{\frac{1}{y}} \\ & -\frac{\mathrm{k_{-1}K}_D^{m-1}K_{poly}^{\frac{x+m-1}{y}}}{K_{MA_m}K_{comp_1}K_{add(\mathrm{org})}}\,\frac{[\mathrm{MA}_m \cdot x\,(\mathrm{HA})]_{\mathrm{org}}\,[\mathrm{H}^+]^m}{\left([\mathrm{H}_y\mathrm{A}_y]_{(\mathrm{org})}\right)^{\frac{x+m-1}{y}}}\end{aligned} \tag{3.100}$$

$[MA_m \cdot x\,(HA)]_{org}$	—	is a measurable or determinable quantity
$[H_yA_y]_{(org)}$	—	is known or determinable
$[M^{+m}]$	—	is known

The polymerization number y is known by the type of acid or extractant used. For example HDEHPA is a dimer in nonpolar organic solvents thus y is 2. The adduct number x is determined by a plot as given on page 53. However, the various equilibrium constants are not known but can be obtained from literature or suitable experiments and plots. Note that equation 3.100 is zero at equilibrium i. e.

$$\begin{aligned} \text{rate} &= 0 \\ &= \frac{k_1}{K_D\,(K_{poly})^{\frac{1}{y}}}\,[M^{+m}]\left([H_yA_y]_{(org)}\right)^{\frac{1}{y}} \\ &\quad -\frac{k_{-1}K_D^{m-1}K_{poly}^{\frac{x+m-1}{y}}}{K_{MA_m}K_{comp_1}K_{add(org)}}\,\frac{[MA_m \cdot x\,(HA)]_{org}\,[H^+]^m}{\left([H_yA_y]_{(org)}\right)^{\frac{x+m-1}{y}}} \end{aligned} \tag{3.101}$$

and thus

$$\frac{k_1K_{MA_m}K_{comp_1}K_{add(org)}}{K_D\,(K_{poly})^{\frac{1}{y}}\,k_{-1}K_D^{m-1}K_{poly}^{\frac{x+m-1}{y}}} = \frac{[MA_m \cdot x\,(HA)]_{org}\,[H^+]^m}{[M^{+m}]\left([H_yA_y]_{(org)}\right)^{\frac{1}{y}}\left([H_yA_y]_{(org)}\right)^{\frac{x+m-1}{y}}} \tag{3.102}$$

which simplifies to

$$\frac{k_1K_{MA_m}K_{comp_1}K_{add(org)}}{k_{-1}K_D^mK_{poly}^{\frac{x+m}{y}}} = \frac{[MA_m \cdot x\,(HA)]_{org}\,[H^+]^m}{[M^{+m}]\left([H_yA_y]_{(org)}\right)^{\frac{x+m}{y}}} \tag{3.103}$$

which is equal to the equilibrium coefficient k_{ex} compare with equation 3.79 page 52. Note that the equilibrium coefficient does not equal just the ratio of the forward and reverse reaction rate constants since the other reactions of the mechanism do have an affect on the equilibrium. Using the definition of the distribution coefficient for the metal, D= $\frac{[MA_m \cdot x(HA)]_{org}}{[M^{+m}]}$ and $K_{eq,ex}$ defined to be $\frac{k_1K_{MA_m}K_{comp_1}K_{add(org)}}{k_{-1}K_D^mK_{poly}^{\frac{x+m}{y}}}$ then the distribution between the bulk phases can be derived as

$$D = K_{eq,ex}\frac{\left([H_yA_y]_{(org)}\right)^{\frac{x+m}{y}}}{[H^+]^m} \tag{3.104}$$

Equations 3.101 through 3.104 are equilibrium equations. These equations can only be used where the process or unit operation is assured to be an equilibrium process.

Case 1-a: Additionally the extractant can dissociate in the aqueous phase and cause an additional reaction. If for the moment this reaction in the aqueous phase is assumed to occur completely and rapidly then additional cases need be considered.

$$[\mathrm{HA}]_{(\mathrm{org})} \overset{K_D}{-} [\mathrm{HA}] \qquad \text{fast} \qquad \mathrm{K}_D = \frac{[\mathrm{HA}]_{(\mathrm{org})}}{[\mathrm{HA}]} \tag{3.105}$$

$$[\mathrm{HA}] \overset{K_a}{-} [\mathrm{H}^+] + [\mathrm{A}^-] \qquad \text{fast} \qquad K_a = \frac{[\mathrm{H}^+]\,[\mathrm{A}^-]}{[\mathrm{HA}]} \tag{3.106}$$

$$\mathrm{M}^{m+} + \mathrm{A}^- \underset{k_{-2}}{\overset{k_2}{-}} \mathrm{MA}^{(m-1)+} \qquad \text{slow} \tag{3.107}$$

$$\mathrm{MA}^{(m-1)+} + \mathrm{A}^- \overset{K_2}{-} \mathrm{MA}_2^{(m-2)+} \tag{3.108}$$

$$\mathrm{MA}_2^{(m-2)+} + \mathrm{A}^- \overset{K_3}{-} \mathrm{MA}_3^{(m-3)+} \tag{3.109}$$

$$\vdots$$

$$\mathrm{MA}_{m-1}^{+} + \mathrm{A}^- \overset{K_3}{-} \mathrm{MA}_m \tag{3.110}$$

The rate law for equation 3.107 is

$$r = k_2 [\mathrm{M}^{m+}]\,[\mathrm{A}^-] - k_{-2} \left[\mathrm{MA}^{(m-1)+}\right] \tag{3.111}$$

and from equations 3.108 through 3.110 a total complex formation constant can be obtained

$$K_{comp_2} = \frac{[\mathrm{MA}_m]}{\left[\mathrm{MA}^{(m-1)+}\right][\mathrm{A}^-]^{m-1}} \tag{3.112}$$

and the term $\left[\mathrm{MA}^{(m-1)+}\right]$ solved for and the rate equation becomes

$$r = k_2 [\mathrm{M}^{m+}]\,[\mathrm{A}^-] - \frac{k_{-2}}{K_{comp_2}} \frac{[\mathrm{MA}_m]}{[\mathrm{A}^-]^{m-1}} \tag{3.113}$$

using the equilibrium constant for the dissociation of the acid extractant in the aqueous phase

$$K_a = \frac{[\mathrm{H}^+]\,[\mathrm{A}^-]}{[\mathrm{HA}]} \tag{3.114}$$

and solving for $[A^-]$

$$[A^-] = \frac{K_a [HA]}{[H^+]} \tag{3.115}$$

$$r = k_2 [M^{m+}] \frac{K_a [HA]}{[H^+]} - \frac{k_{-2}}{K_{comp_2}} \frac{[MA_m]}{\left(\frac{K_a [HA]}{[H^+]}\right)^{m-1}} \tag{3.116}$$

$$r = k_2 [M^{m+}] \frac{K_a [HA]}{[H^+]} - \frac{k_{-2}}{K_{comp_2}} \frac{[MA_m] [H^+]^{m-1}}{(K_a [HA])^{m-1}} \tag{3.117}$$

substituting the equilibrium equations as before since none of these change, give the following rate law equation

$$\begin{aligned} rate \;=\; & \frac{K_a k_2}{K_D} \frac{[M^{m+}] [HA]_{org}}{[H^+]} \\ & - \frac{k_{-2} K_D^{m-1}}{K_{MA_m} K_{comp_2} K_a^{m-1} K_{add(org)}} \frac{[MA_m \cdot x\,(HA)]_{org} [H^+]^{m-1}}{[HA]_{org}^{m+x-1}} \end{aligned} \tag{3.118}$$

or assuming polymerization of extractant in the organic phase

$$\begin{aligned} rate \;=\; & \frac{K_a k_2}{K_D K_{poly}^{\frac{1}{y}}} \frac{[M^{m+}] [H_y A_y]_{org}^{\frac{1}{y}}}{[H^+]} \\ & - \frac{k_{-2} K_D^{m-1} K_{poly}^{\frac{m+x-1}{y}}}{K_{MA_m} K_{comp_2} K_a^{m-1} K_{add(org)}} \frac{[MA_m \cdot x\,(HA)]_{org} [H^+]^{m-1}}{[H_y A_y]_{org}^{\frac{m+x-1}{y}}} \end{aligned} \tag{3.119}$$

Case 1—b: Parallel Reactions Assuming that the undissociated and dissociated forms of the extracting reagent react in parallel *viz.* the reaction velocities of these two mechanisms occurring in the aqueous phase are comparable and that they occur together then the rate of reaction with the metal cation M^{m+} is given by the following

$$\begin{aligned} rate \;=\; & \{k_1 [M^{m+}] [HA] + k_2 [M^{m+}] [A^-]\} \\ & - \left\{k_{-1} \left[MA^{(m-1)+}\right] [H^+] + k_{-2} \left[MA^{(m-1)+}\right]\right\} \end{aligned} \tag{3.120}$$

simplifying

$$rate = [M^{m+}]\{k_1[HA] + k_2[A^-]\} - \left[MA^{(m-1)+}\right]\{k_{-1}[H^+] + k_{-2}\} \tag{3.121}$$

using 3.94 to solve for $\left[MA^{(m-1)+}\right]$ and placing this into equation 3.121 results in

$$rate = [M^{m+}]\{k_1[HA] + k_2[A^-]\} - \frac{[MA_m][H^+]^{m-1}}{K_{comp_1}[HA]^{m-1}}\{k_{-1}[H^+] + k_{-2}\} \tag{3.122}$$

NOTE: $K_{comp_1} \neq K_{comp_2}$ since these are obtained using different reaction mechanisms. However, for the term $\left[MA^{(m-1)+}\right]$ to be equal in the same "pot" so as to say, it is necessary for the equations to be equivalent. This is shown in the following

$$\left[MA^{(m-1)+}\right] = \frac{[MA_m][H^+]^{m-1}}{K_{comp_1}[HA]^{m-1}} = \frac{[MA_m]}{K_{comp_2}^{m-1}[A^-]} \tag{3.123}$$

and that $[A^-] = \frac{K_a[HA]}{[H^+]}$ where by

$$\left[MA^{(m-1)+}\right] = \frac{[MA_m][H^+]^{m-1}}{K_{comp_1}[HA]^{m-1}} = \frac{[MA_m]}{K_{comp_2}\left[\frac{K_a[HA]}{[H^+]}\right]^{m-1}} \tag{3.124}$$

and therefore

$$\left[MA^{(m-1)+}\right] = \frac{[MA_m][H^+]^{m-1}}{K_{comp_1}[HA]^{m-1}} = \frac{[MA_m][H^+]^{m-1}}{K_{comp_2}K_a^{m-1}[HA]^{m-1}} \tag{3.125}$$

and finally

$$K_{comp_1} = K_{comp_2}K_a^{m-1}\ . \tag{3.126}$$

K_{comp_1} will be used for conciseness, but it should be noted that an equivalency does exist.

Using equation 3.89 $[MA_m] = \frac{[MA_m]_{org}}{K_{MA_m}}$ the parallel equation is adjusted for this equilibrium reaction

$$\begin{aligned} rate &= [M^{m+}]\{k_1[HA] + k_2[A^-]\} \\ &\quad - \frac{[MA_m]_{org}[H^+]^{m-1}}{K_{MA_m}K_{comp_1}[HA]^{m-1}}\{k_{-1}[H^+] + k_{-2}\} \end{aligned} \tag{3.127}$$

and the dissociation equation $[A^-] = \frac{K_a[HA]}{[H^+]}$

$$rate = [M^{m+}]\left\{k_1[HA] + k_2\frac{K_a[HA]}{[H^+]}\right\}$$

$$-\frac{[MA_m]_{org}[H^+]^{m-1}}{K_{MA_m}K_{comp_1}[HA]^{m-1}}\{k_{-1}[H^+]+k_{-2}\} \tag{3.128}$$

and the distribution of the extractant between the two phases $[HA]=\frac{[HA]_{org}}{K_D}$

$$\begin{aligned} rate &= [M^{m+}]\left\{k_1\frac{[HA]_{org}}{K_D}+k_2\frac{K_a[HA]_{org}}{K_D[H^+]}\right\} \\ &\quad -\frac{[MA_m]_{org}[H^+]^{m-1}}{K_{MA_m}K_{comp_1}\left[\frac{[HA]_{org}}{K_D}\right]^{m-1}}\{k_{-1}[H^+]+k_{-2}\} \end{aligned} \tag{3.129}$$

simplifying

$$\begin{aligned} rate &= [M^{m+}][HA]_{org}\frac{\left(k_1+k_2\frac{K_a}{[H^+]}\right)}{K_D} \\ &\quad -\frac{K_D^{m-1}(k_{-1}[H^+]+k_{-2})}{K_{MA_m}K_{comp_1}}\frac{[MA_m]_{org}[H^+]^{m-1}}{[HA]_{org}^{m-1}} \end{aligned} \tag{3.130}$$

Case 1-c: Hydrolyzed metal ion Many times the metal ion will be hydrolyzed where the controlling mechanism is

$$M(OH)^{(m-1)+}\underset{k_{-1}^*}{\overset{k_1^*}{-}}MA^{(m-1)+}+H_2O \quad \text{slow} \tag{3.131}$$

Danesi (CRC Critical REviews vol 10 iss 1 1980 page 34) gives the reaction rates for a cation of valence 3 (without proof). The rate equations are converted here to a general valence cation

$$r=\frac{k_1^*k_h}{K_D}\frac{[M^{m+}][HA]_{org}}{[H^+]}-\frac{k_{-1}^*K_D^{m-1}}{K_{MA_m}K_{comp_1}}\frac{[MA_m]_{org}[H^+]^{m-1}}{[HA]_{org}^{m-1}} \tag{3.132}$$

here Danesi defines k_h as the first hydrolysis constant of the metal cation. He then gives the parallel reaction rates (without proof) for a cation of valence 3 and again is presented here in a general form as

$$\begin{aligned} rate &= [M^{m+}][HA]_{org}\frac{\left(k_1+k_1^*\frac{K_h}{[H^+]}\right)}{K_D} \\ &\quad -\frac{K_D^{m-1}(k_{-1}[H^+]+k_{-1}^*)}{K_{MA_m}K_{comp_1}}\frac{[MA_m]_{org}[H^+]^{m-1}}{[HA]_{org}^{m-1}} \end{aligned} \tag{3.133}$$

These rates for hydrolysis are reproduced here without proof but are proven very similarly to 3.130; infact, equation 3.130 and 3.133 are the same equation except for the equilibrium constants. The $[H^+]$ term in the product $\frac{[MA_m]_{org}[H^+]^{m-1}}{[HA]^{m-1}_{org}}$ is raised to the $m-1$ power here. Danesi's paper gives this term raised to the first power. It is believed this is possibly a printing error since in my deriving the hydrolysis equation (not shown) the above equation was obtained and verified.

Since these parallel rate laws are equal in context it is difficult albeit impossible to determine the reacting species from the rate laws and is referred to as "proton ambiguity" (Danesi CRC reviews page 35). The rate laws as given by equations in Case 1, Case 1-a, and Case 1-b can be validated by plotting the reverse and forward rates verses the concentrations of the various species. If the rate laws hold straight lines of integer slopes will be obtained. In the case of the parallel reactions two straight lines will be obtained with a transition region (curvature) between the two regions. No controlling steps in the above cases involve transport across the interface and therefore the rates will be independent of the interfacial area and the volume of aqueous and organic phases.

Again, these rate laws are valid when the extracting reagent exhibits some solubility in the aqueous phase and its adsorption at the interface is negligible (Danesi CRC reviews). The above rate laws should be emphasized were derived assuming first order kinetics with respect to all the species. There has been significant evidence that in the literature that this is not a considerably inappropriate assumption. However, there is also considerable controversy as to the contrary. The determination of kinetic data and order is empirical and there seems to be a lack of kinetic information and studies in the solvent extraction community of higher order mechanisms than first order. Hanson, Hughes and Marsland (ISEC 74) present a discussion that no true kinetic regime exists.

Case 2: Controlling Steps Occur at the Interface The cases described and derived in this section are done so assuming the rate determining steps are across the interface. Slow interfacial reactions can be found when the extractant exhibits low solubility in the aqueous phase and has substantial surfactant qualities. The driving force for the transfer of the interfacial complex into the organic phase is the stronger surface activity of the reagent which replaces the less surface active metal complex at the interface. Though not included at this time this strong driving force phenomenon may induce the marangoni effect which inturn may improve the mass transfer process.

The following mechanistic reactions can be visualized to occur:

1. Interfacial partition of the extractant is the slow step

(a) An additional slow step is in the aqueous phase of the metal reacting with the undissociated extractant

(b) An additional slow step is in the aqueous phase of the metal reacting with the dissociated extractant

(c) All of the above steps are slow and in parallel

2. The controlling reaction occurs at the interface forming the metal extractant complex with the adsorbed extractant

   (a) undissociated extractant

      i. slow addition of additional ligand molecule(s) at the interface

      ii. slow adsorption — desorption process of the interfacial complex and extractant

      iii. all of the above are slow and in parallel

   (b) dissociated extractant

      i. slow addition of additional ligand molecule(s) at the interface

      ii. slow adsorption — desorption process of the interfacial complex and extractant

      iii. all of the above are slow and in parallel

   (c) All of the Mechanisms are slow

3. The slow controlling reactions occur at the interface and in the aqueous phase.

The above need to be taken into account when an **extraction rate** is to be determined in the kinetic regime only. This means that the diffusional transport is so rapid that it is negligible. However these rate equations are necessary for the reaction term in the transport equation.

Case 2-1: Interfacial Partition of the extractant The following is the mechanism associated with this case

> Interfacial partition of the organic extractant between the organic and aqueous phases

$$[\mathrm{HA}]_{org} \underset{k_{-1}^*}{\overset{k_1^*}{-}} [\mathrm{HA}] \quad \text{slow} \tag{3.134}$$

Formation of Complexes

$$[\mathrm{M}^{m+}] + [\mathrm{HA}] \underset{k_{-1}}{\overset{k_1}{-}} \left[\mathrm{MA}^{(m-1)+}\right] + [\mathrm{H}^+] \qquad K_1 = \frac{\left[\mathrm{MA}^{(m-1)+}\right][\mathrm{H}^+]}{[\mathrm{M}^{m+}][\mathrm{HA}]} \tag{3.135}$$

$$\left[\mathrm{MA}^{(m-1)+}\right] + [\mathrm{HA}] \underset{k_{-2}}{\overset{k_2}{-}} \left[\mathrm{MA}_2^{(m-2)+}\right] + [\mathrm{H}^+] \qquad K_2 = \frac{\left[\mathrm{MA}_2^{(m-2)+}\right][\mathrm{H}^+]}{\left[\mathrm{MA}^{(m-1)+}\right][\mathrm{HA}]} \tag{3.136}$$

$$\left[\mathrm{MA}_2^{(m-2)+}\right] + [\mathrm{HA}] \underset{k_{-3}}{\overset{k_3}{-}} \left[\mathrm{MA}_3^{(m-3)+}\right] + [\mathrm{H}^+] \qquad K_3 = \frac{\left[\mathrm{MA}_3^{(m-3)+}\right][\mathrm{H}^+]}{\left[\mathrm{M}^{(m-2)+}\right][\mathrm{HA}]} \tag{3.137}$$

$$\vdots$$

$$\left[\mathrm{MA}_{m-1}^{+}\right] + [\mathrm{HA}] \underset{k_{-m}}{\overset{k_m}{-}} [\mathrm{MA}_m] + [\mathrm{H}^+] \qquad K_m = \frac{[\mathrm{MA}_m]\,[\mathrm{H}^+]}{\left[\mathrm{M}_{m-1}^{+}\right][\mathrm{HA}]} \tag{3.138}$$

Distribution or partition of the metal/extractant complex between the aqueous organic phases

$$[\mathrm{MA}_m] \underset{k_{-2}^*}{\overset{k_2^*}{-}} [\mathrm{MA}_m]_{\mathrm{org}} \qquad K_{MA_m} = \frac{[\mathrm{MA}_m]_{\mathrm{org}}}{[\mathrm{MA}_m]} \tag{3.139}$$

The accumulation of [HA] in the aqueous phase is given by a mass balance

$$\begin{aligned} \frac{d\,[\mathrm{HA}]}{dt} \;=\; & \frac{a_{org}}{V_{org}} k_1^* [\mathrm{HA}]_{org} - \frac{a_{aq}}{V_{aq}} k_{-1}^* [\mathrm{HA}] \\ & -k_1 [\mathrm{M}^{m+}][\mathrm{HA}] + k_{-1}\left[MA^{(m-1)+}\right][H^+] \\ & -k_2 \left[\mathrm{MA}^{(m-1)+}\right][\mathrm{HA}] + k_{-2}\left[MA^{(m-2)+}\right][H^+] \\ & -k_3 \left[\mathrm{MA}_2^{(m-2)+}\right][\mathrm{HA}] + k_{-3}\left[MA_3^{(m-3)+}\right][H^+] \\ & -k_4 \left[\mathrm{MA}_3^{(m-3)+}\right][\mathrm{HA}] + k_{-4}\left[MA_4^{(m-4)+}\right][H^+] \end{aligned}$$

$$\vdots$$

$$-k_{m-1}\left[\mathrm{MA}_{m-2}^{2+}\right][\mathrm{HA}] + k_{1-m}\left[MA_{m-1}^{+}\right][H^+]$$

$$-k_m\left[\mathrm{MA}_{m-1}^{+}\right][\mathrm{HA}] + k_{-m}\left[MA_m\right][H^+] \tag{3.140}$$

$$\frac{d\left[\mathrm{M}^{m+}\right]}{dt} = k_{-1}\left[\mathrm{MA}^{(m-1)+}\right][H^+] - k_1\left[\mathrm{MA}^{m+}\right][\mathrm{HA}] \tag{3.141}$$

$$\begin{aligned}\frac{d\left[\mathrm{M}^{(m-1)+}\right]}{dt} &= k\left[\mathrm{M}^{m+}\right][\mathrm{HA}] - k_{-1}\left[\mathrm{MA}^{(m-1)+}\right][\mathrm{H}^+] \\ &\quad -k_2\left[\mathrm{MA}^{(m-1)+}\right][\mathrm{HA}] + k_{-2}\left[\mathrm{MA}_2^{(m-2)+}\right][\mathrm{H}^+] \end{aligned} \tag{3.142}$$

$$\begin{aligned}\frac{d\left[\mathrm{MA}_2^{(m-2)+}\right]}{dt} &= k_2\left[\mathrm{MA}^{(m-1)+}\right][\mathrm{HA}] - k_{-2}\left[\mathrm{MA}_2^{(m-2)+}\right][\mathrm{H}^+] \\ &\quad -k_3\left[\mathrm{MA}_2^{(m-2)+}\right][\mathrm{HA}] + k_{-3}\left[\mathrm{MA}_3^{(m-3)+}\right][\mathrm{H}^+] \end{aligned} \tag{3.143}$$

$$\begin{aligned}\frac{d\left[\mathrm{MA}_3^{(m-3)+}\right]}{dt} &= k_3\left[\mathrm{MA}_2^{(m-2)+}\right][\mathrm{HA}] - k_{-3}\left[\mathrm{MA}_3^{(m-3)+}\right][\mathrm{H}^+] \\ &\quad -k_4\left[\mathrm{MA}_3^{(m-3)+}\right][\mathrm{HA}] + k_{-4}\left[\mathrm{MA}_4^{(m-4)+}\right][\mathrm{H}^+] \end{aligned} \tag{3.144}$$

$$\vdots$$

$$\begin{aligned}\frac{d\left[\mathrm{MA}_{m-1}^{+}\right]}{dt} &= k_{m-1}\left[\mathrm{MA}_{m-2}^{m+}\right][\mathrm{HA}] - k_{1-m}\left[\mathrm{MA}_{m-1}^{+}\right][\mathrm{H}^+] \\ &\quad -k_m\left[\mathrm{MA}_{m-1}^{+}\right][\mathrm{HA}] + k_{-m}\left[\mathrm{MA}_m\right][\mathrm{H}^+] \end{aligned} \tag{3.145}$$

Equations 3.142 through 3.145 can be reduced in form to

$$\begin{aligned}\frac{d\left[\mathrm{MA}_i^{(m-i)+}\right]}{dt} &= k_i\left[\mathrm{MA}_{i-1}^{(m-i+1)+}\right][\mathrm{HA}] - k_{-i}\left[\mathrm{MA}_i^{(m-i)+}\right][\mathrm{H}^+] \\ &\quad -k_{i+1}\left[\mathrm{MA}_i^{(m-i)+}\right][\mathrm{HA}] \\ &\quad +k_{-(i+1)}\left[\mathrm{MA}_{i+1}^{m-(i+1)}\right][\mathrm{H}^+] \end{aligned} \tag{3.146}$$

for $i = 1$ to $m-1$. The rate expression for the metal complex concentration in the aqueous phase is

$$-\frac{d\left[\mathrm{MA}_m\right]}{dt} = k_m\left[\mathrm{MA}_{m-1}^{+}\right][\mathrm{HA}] - k_{-m}\left[\mathrm{MA}_m\right][\mathrm{H}^+] - k_2^*\left[\mathrm{MA}_m\right] + k_{-2}^*\left[\mathrm{MA}_m\right] \tag{3.147}$$

As can be seen from the above, the extraction of a metal can become quite involved and complex. Each individual reaction is not particularly complex but to derive an overall rate expression the model can become very elaborate and may in retrospect become so unwieldy that its purpose is severely negated. Danesi (Critical Reviews in Analytical Chemistry 1980 page 35) and most other published works on modeling the kinetics of extraction chemistry use the psuedo kinetic constants as given by k_1^*, k_{-1}^*, k_2^*, k_{-2}^* previously to describe the mass transfer across the interface in the kinetic regime. The above scenario, for the extraction of metals, assumes the second reaction is irreversible and a psuedo steady state or stationary state exists for the intermediate [HA]. This may occur if HA is sufficiently reactive or if the rate $\frac{d[HA]}{dt}$ is very small which says that the concentration of HA in the aqueous phase is constant or does not accumulate to any appreciable level compared to $\left[\overline{HA}\right]$ and $[MA^{2+}]$ i.e. $[HA] \ll \left[\overline{HA}\right] + [MA^{2+}]$. Therefore from a material balance

$$\left[\overline{HA}\right] + \left[MA^{2+}\right] + [HA] = \left[\overline{HA}\right]_0 \tag{3.148}$$

where $\left[\overline{HA}\right]_0$ is the concentration of $\left[\overline{HA}\right]$ initially. If $[HA] \ll \left[\overline{HA}\right] + [MA^{2+}]$ is valid then $\left[\overline{HA}\right] + [MA^{2+}] = \left[\overline{HA}\right]_0$ which yields $\frac{d[MA^{2+}]}{dt} = -\frac{d\left[\overline{HA}\right]}{dt}$ which means that $\frac{d[HA]}{dt} = 0$. This is a very strict condition. When this is applied to the following mechanism

$$\left[\overline{HA}\right] \underset{k_{-1}}{\overset{k_1}{\rightleftharpoons}} [HA] \quad \text{slow} \tag{3.149}$$

$$[HA] + \left[M^{+3}\right] \underset{k_{-2}}{\overset{k_2}{\rightleftharpoons}} \left[MA^{2+}\right] + [H^+] \quad \text{slow} \tag{3.150}$$

then it is possible to solve for $\frac{d[MA^{2+}]}{dt}$ as functions of concentrations which are known such as bulk concentrations. Using the full material balance and not setting the derivatives or rates of the products and reactants equal to each other then a solution can be obtained and Danesi's example for a metal of valence 3 and an irreversalbe reaction in the aqueous phase is a special case of this reaction scheme. The following is the derivation of the determination of the rate of formation of $[MA^{2+}]$ assuming the mechanism of equations 3.149 and 3.150.

$$\frac{d\left[\overline{HA}\right]}{dt} = \frac{k_{-1}A[HA]}{V_{aq}} - \frac{k_1 A\left[\overline{HA}\right]}{V_{org}} \tag{3.151}$$

$$\frac{d[HA]}{dt} = -\frac{k_{-1}A[HA]}{V_{aq}} + \frac{k_1 A\left[\overline{HA}\right]}{V_{org}} + k_{-2}\left[MA^{2+}\right][H^+] - k_2[HA]\left[M^{+3}\right] \tag{3.152}$$

The concentration of $\left[\overline{HA}\right]$ is initially $\left[\overline{HA}\right]_0$ and will be equal to the sum of the concentration of the unreacted reactants and products formed $\left[\overline{HA}\right] + [MA^{2+}] + [HA] = \left[\overline{HA}\right]_0$ or $[MA^{2+}] = \left[\overline{HA}\right]_0 - [HA] - \left[\overline{HA}\right]$ this assumes the initial concentration of the intermediates and products are zero. $[MA^{2+}]_0 = [HA]_0 = 0$. Assuming that the stationary state hypothesis is valid for the time derivative of [HA] and for the mass balance i.e. $[HA] \ll \left[\overline{HA}\right] + [MA^{2+}]$. This states that the rate of accumulation of [HA] with time is small or insignificant compared with the sum of the rates of accumulation with respect to time for the other reactants and products. The magnitude of the [HA] is also insignificant when compared with the sum of the concentrations of the other reactants and products. Thus $[MA^{2+}] = \left[\overline{HA}\right]_0 - \left[\overline{HA}\right]$ assuming $[HA] \cong 0$ or very small.

$$\frac{d[HA]}{dt} \cong 0 \cong \frac{k_1 A \left[\overline{HA}\right]}{V_{org}} - \frac{k_{-1} A [HA]}{V_{aq}} + k_{-2} \left[MA^{2+}\right] [H^+] - k_2 [HA] \left[M^{+3}\right] \quad (3.153)$$

inserting the material balance solved for $[MA^{2+}]$ into equation 3.153 and rearrangement to solve for [HA]

$$[HA] = \frac{V_{aq}}{V_{org}} \frac{\left(k_{-2} \left[\overline{HA}\right]_0 [H^+] V_{org} - k_{-2} \left[\overline{HA}\right] [H^+] V_{org} + k_1 A \left[\overline{HA}\right]\right)}{k_{-1} A + k_2 [M^{+3}] V_{aq}} \quad (3.154)$$

From the mechanism the rate equation for $[MA^{2+}]$ is

$$\frac{d[MA^{2+}]}{dt} = k_2 \left[M^{+3}\right] [HA] - k_{-2} \left[MA^{2+}\right] [H^+] \quad (3.155)$$

and again using the material balance for $[MA^{2+}]$

$$\frac{d[MA^{2+}]}{dt} = k_2 \left[M^{+3}\right] [HA] - k_{-2} \left(\left[\overline{HA}\right]_0 - \left[\overline{HA}\right]\right) [H^+] \quad (3.156)$$

$$\frac{d[MA^{2+}]}{dt} = k_2 \left[M^{+3}\right] [HA] - k_{-2} [H^+] \left(\left[\overline{HA}\right]_0 - \left[\overline{HA}\right]\right) \quad (3.157)$$

inserting equation 3.154 into equation 3.157

$$\frac{d[MA^{2+}]}{dt} = \frac{V_{aq} V_{org} \left(\frac{Ak_1}{V_{org}} k_2 [M^{+3}] \left[\overline{HA}\right] + \frac{Ak_{-1}}{V_{aq}} k_{-2} [H^+] \left[\overline{HA}\right] - \frac{Ak_{-1}}{V_{aq}} k_{-2} [H^+] \left[\overline{HA}\right]_0\right)}{V_{aq} V_{org} \left(\frac{Ak_{-1}}{V_{aq}} + k_2 [M^{+3}]\right)} \quad (3.158)$$

combining terms and setting

$$K_1 = \frac{Ak_1}{V_{org}} \qquad K_{-1} = \frac{Ak_{-1}}{V_{aq}} \qquad K_2 = k_2\left[M^{+3}\right]$$

the general equation is found for the 1:1 complex rate for a metal of valence 3

$$\frac{d\left[MA^{2+}\right]}{dt} = \frac{\left[\overline{HA}\right]K_1K_2 + K_{-1}k_{-2}\left[H^+\right]\left(\left[\overline{HA}\right] - \left[\overline{HA}\right]_0\right)}{K_{-1} + K_2} \tag{3.159}$$

If the reverse reaction of equation 3.150 is extremely small or $k_{-2} \cong 0$ (note that this makes stripping impossible) making the term

$$K_{-1}k_{-2}\left[H^+\right]\left(\left[\overline{HA}\right] - \left[\overline{HA}\right]_0\right) \ll \left[\overline{HA}\right]K_1K_2$$

then equation 3.159 reduces to

$$\frac{d\left[MA^{2+}\right]}{dt} = \frac{\left[\overline{HA}\right]K_1K_2}{K_1 + K_2} \tag{3.160}$$

which is the same as given by Danesi and other authors on kinetic works for equation 3.150 being irreversible (see also Esperson Chemical Kinetics and Reaction Mechanisms and Connors Chemical Kinetics). The above derivation assumes that *quasi-steady-state approximation,* also referred to as the *stationary state hypothesis* or *Bodenstein approximation* is valid.

The restriction that the intermediate rates are negligible or set to zero is more restrictive than necessary since from the rate equation for [HA]

$$\frac{d[HA]}{dt} = K_1\left[\overline{HA}\right] - (K_{-1} + K_2)[HA] + k_{-2}\left[MA^{2+}\right]\left[H^+\right] \tag{3.161}$$

using the material balance for $[MA^{2+}]$ and solving for [HA] one obtains

$$[HA] = \frac{(K_1 - k_{-2})\left[\overline{HA}\right] + k_{-2}\left[\overline{HA}\right]_0 - \frac{d[HA]}{dt}}{K_{-1} + K_2 - k_{-2}\left[H^+\right]} \tag{3.162}$$

and the criteria that $\frac{d[HA]}{dt} \ll (K_1 - k_{-2})\left[\overline{HA}\right] + k_{-2}\left[\overline{HA}\right]_0$ is sufficient and necessary for the quasi steady state to be valid. Setting the derivative to zero is sufficient but may be overly restrictive and cause mathematical inconsistencies. Also if $(k_2 + k_{-1}) \gg (k_1 + k_{-2})$ then [HA] will be small as compared to $\left(\left[\overline{HA}\right] + \left[MA^{2+}\right]\right)$; however, without a sufficient

supply of [HA] then $[MA^{2+}]$ will be small also. Thus k_1 needs to be sufficiently greater than k_{-1} for the reaction to proceed.

It should be noted that in the above case the controlling reaction is assumed to be the $1:1$ complex formation and thus the rate of extraction is assumed to be approximated by the rate of formation of the MA^{2+} or $MA^{(m-1)+}$ species. The complete and general extraction rate can be quite complex if not impossible to obtain analytically. This was attempted using the method given by Froment and Bischoff (page 72–73) with a very extensive equation being obtained. This equation could not be algebraically reduced to a form that would give the limiting cases of an irreversable reaction in the second step or the summations of the rate constants in the denominator. Both manual algebraic manipulations and the use of Mathematica computer algebraic system was used to obtain an equation in the measurable quantities. The intermediate concentration [HA] is a polynomial to the m power as is $[H^+]$. Thus the ability to solve for [HA] explicitely in terms of $\left[\overline{MA}_3\right]$ was not possible which thwarted the attempt to get a meaningful general analytical equation even for a metal of valence of three.

Interface Reactions Interfacial reactions occur when there is no distribution or partial distribution of the extractant between the phases and the extractant organizes itself along the interface. This is especially true for a cationic extractant that has a polar and a non-polar head and tail. The polar or more soluble portion of the extractant hydrogen bonds with the water in the aqueous phase at the interface. The interface becomes a structured molecular layer of extractant molecules. Horwitz and others have suggested that the water at the interface becomes structured also in an "ice-like" character. This phenomenon will be discussed in the interfacial section of this study.

Based upon this qualitative argument a surface is formed of adsorbed or "condensed" extractant at the interface between two highly immiscible phases. The extractant itself both forms and reacts with the metal ion sufficiently to form a neutral complex which then desorbs and diffuses into the bulk of the organic phase and more extractant is adsorbed at the vacated site. This interface or surface is unusual in respect to ordinary view of a surface in catalysis or adsorbtion since in a solid, a well defined surface boundary exists to which a species adsorbs. However, the theories purported in catalyis and adsorption processes can be extended here liquid/liquid extraction.

Adsorption and Chemisorption Two types of adsorption have been recognized in the literature for many years. Physical adsorption or *physiosorption* is a physical process generally attributed to van der Wals forces between molecules and is always exothermic. *Chemisorption* on the other hand is a chemical process that entails a rearrangement of

electrons and thus has an activation energy and is typically exothermic often much more exothermic than the physical adsorption but not always. Thermodynamically adsorption is a more ordered state and the entropy change and enthalpy is negative (Bond Heterogeneous Catalysis p 13, Satterfield page 27). Chemisorption leads at most to a monolayer coverage of the available sites. Chemisorption and physiosorption can occur together but any adsorbed layers beyond the first must be presumed to be physically adsorbed.

In the solvent extraction of metals the reaction of the metal with the extractant at the interface could cause an increase in entropy requiring adjustments which could mean interactions between adsorbates at different sites and/or desorption of the complex. Thus many schemes as to how metals are extracted when the extraction reaction takes place at the interface can be proposed. The derivations of an overall rate of extraction can become tedious and mathematically and algebraically laborious albeit impossible to obtain especially for more than one reaction step occurring. Therefore in general when more than one step is inherent in the overall reaction scheme then the steps are combined or lumped if possible.

The rates of adsorption are generally very rapid. The derivation of the overall rate equation for this case requires that a relationship between the amount of substance adsorbed on the surface and its bulk concentrations or activity at equilibrium be known. The relationship that does this is the adsorption isotherm. This is done for several reasons: (1) to provide a framework for describing the extent and strength of adsorption of molecules on sufraces in quantiative terms; (2) provide the bases of a useful method for representing the kinetics of surface catalysed reactions; and (3) to open the way to a powerful technique for estimating the surface area (Bond page15). The Langmuir isotherm is generally used to model the adsorption of the extractant at the interface. This model assumes a three step process: 1) adsorption chemisorption of the active extractant on the interface or surface, 2) reaction at the interface, and 3) desorption of the prodeucts from the interface or surface. This model of adsorption on a surface was originally derived from kinetic gas theory of a gas adsorbing on a solid catalyst and is present in catalyst theory. It is valid for liquid/solid systems (Butt Reaction Kinetics and Reactor Design page 139) and has been extended in the solvent extraction literature for liquid/liquid interactions. A theoretical proof of the validity of this extension to the liquid/liquid state has not been found in the literature and will not be established here the extension is assumed without proof..

The Langmuir isotherm adsorption theory assumes that every site on the surface has the same energy of interaction and is not effected by the presence or absence of sorbate molecules on adjoining sites. This is a very restrictive assumption for real surfaces of solids but may not be for the formation of liquid/liquid surfaces or interfaces if interactions between the adsorbed species is not present. Many other adsorption isotherm models have been proposed and are a result of modifying the Langmuir isotherm to reflect differently the distribution

of the energy of adsorption in the heat of chemisorption term present in the constants of the Langmuir isotherm theory.

One such nonideal isotherm is the Freundlich isotherm which distributes the heat of chemisorption in an exponential way. This type of isotherm was originally empirical and is a power model

$$\Theta_A = cP_A^{\frac{1}{n}} \tag{3.163}$$

where n > 1 and the parameters n and c usually both decrease with increasing temperature and Θ_A is the fraction of sites on the surface covered by species A, P_A is the pressure of species A (note for liquids this is the activity of A or the concentration of A assuming ideality). The Freundlich isotherm distributes the energy of adsorption logarithmically or exponentially decreasing with coverage. This particular isotherm has been derived from a statistical and thermodynamic derivation which gives an interpretation of n as a constatnt representing the mutual interfaction of adsorbed species (Saterfield, Heterogeneous Catalysis Practice p 38).

Another nonideal isotherm is the Timken (or Slygin-Frumkin) isotherm postulates that the heat of chemisorption decreases linearly with surface coverage (Butt p 146, Saterfield, Heterogeneous Catalysis Practice p 38). The Langmuir isotherm is used more extensively in solvent extraction because of its simplicity compared to the other isotherms, the adsorption is of the extractant to the surface is assumed ideal, and there is less empirical collection of data necessary to obtain the parameters.

The derivation of an overall rate equation for a heterogeneous reaction at a surface or interface usually uses the Langmuir-Hinshelwood, or the Rideal-Ely versions of the Langmuir mechanism. Both of these techniques assume three consecutive reaction steps like the Langmuir mechanism: adsorption of reactants, surface reaction, and desorption of products. Each step may be complicated by such effects as dissociation of adsorbed compounds —adsorption of only one reactant or all reactants — and an extremely large number of combinations (Bischoff and Froment I&EC fundamentals Aug 1962 p 195-200) as well as the laborious and tedious and more often than not impossible task of expressing the overall rate equation as a product of a linear driving force divided by a resistance for multiple controlling steps . Thus the use of the techniques intoduced by Hougen and Watson (Ind. and Eng. Chem. May 1943 p 529-541) and Yang and Hougen(Chem Eng Progress March 1950) and the assumption of a single controlling step to simplify the mathematics has been incorporated in the heterogeneous kinetic literature. Though these methods help to derive a mathematical rate expression the one controlling step may not or can not be justified (Bischoff and Froment I&EC Fundmtls. vol 1 no 3 1962).

The Langmuir Henshelwood mechanism assumes the reaction at the interface is between two adorbed molecules on the surface. The Rideal–Ely mechanism assumes the reaction is between an adsorbed species and a "free" species close to the surface or intrface. It should be noted that both of these mechanisms goes on in metal extraction. That is the active extractant adsorbs at the interface, the metal cation reacts with a molecule of the extractant for the 1:1 complex, other adsorbed extractant molecules react with the charged complex until it is neutralized, and the neutral complex is desorbed from the surface into the bulk of the organic phase. This will be discussed more fully in a moment.

Many real reactions as immediately discussed above can involve the formation and disappearance of several intermediates on the surface and a mechanistically rigorous formulation can become so complex as to lose most of its utility (Satterfield pa 54). Boudart (Boudart AICHEJ 1972) adresses this problem and suggests that one step is the rate determining one and that one intermediate is present in significant amounts compared to the others. However, as a reaction proceeds one step may gain controll over another previously controlling step. In the transition between these "controlling regime steps" more than one controlling step can occur and a combination of the rates of surface reaction and desorption will invalidate the assumption of more than one controlling step (Bischoff and Froment I&EC Fundamentals 1962).

Danesi (CRC Critical reviews page 35) give the following mechanism for adsorption and reaction at the interface for a 3 valence metal:

$$\text{r1} \quad \left[M^{3+}\right] + [HA]_{ad} \underset{k_{-1}}{\overset{k_1}{-}} \left[MA^{2+}\right]_{ad} + [H^+] \tag{3.164}$$

$$\text{r2} \quad \left[MA^{2+}\right]_{ad} + [HA]_{ad} \underset{k_{-2}}{\overset{k_2}{-}} \left[MA_2^+\right]_{ad} + [H^+] \tag{3.165}$$

$$\text{r3} \quad \left[MA_2^+\right]_{ad} + [HA]_{ad} \underset{k_{-3}}{\overset{k_3}{-}} [MA_3]_{ad} + [H^+] \tag{3.166}$$

$$\text{r4} \quad [MA_3]_{ad} + 3\left[\overline{HA}\right] \underset{k_{-4}}{\overset{k_4}{-}} \left[\overline{MA_3}\right] + 3[HA]_{ad} \tag{3.167}$$

The rate equations are

$$r_1 = k_1 a \left[M^{3+}\right][HA]_{ad} - k_{-1} a \left[MA^{2+}\right]_{ad}[H^+] \tag{3.168}$$

$$r_2 = k_2 a \left[MA^{2+}\right]_{ad}[HA]_{ad} - k_{-2} a \left[MA_2^+\right]_{ad}[H^+] \tag{3.169}$$

$$r_3 = k_3 a \left[MA_2^+\right]_{ad}[HA]_{ad} - k_{-3} a [MA_3]_{ad}[H^+] \tag{3.170}$$

$$r_4 = k_4 a \left[MA_3\right]_{ad} \left[HA\right]_{ad}^3 - k_{-4} a \left[MA_3\right] \left[\overline{HA}\right]^3 \quad (3.171)$$

Where r1, r2, r3 and r4 refer to reaction 1, reaction 2 etc. Note that reaction r4 is not an elementary or fundamental reaction step and is actually two steps: the adsorption of extractant at the interface; and, the desorption of the metal complex. Thus, r4 is in reality two steps

$$\text{r4a} \quad \left[MA_3\right]_{ad} \underset{k_{-d}}{\overset{k_d}{\rightleftharpoons}} \left[\overline{MA_3}\right] \quad (3.172)$$

$$\text{r4b} \quad 3\left[\overline{HA}\right] \underset{k_{-a}}{\overset{k_a}{\rightleftharpoons}} 3\left[HA\right]_{ad} \quad (3.173)$$

with the rate equations being

$$r_{4a} = k_d a \left[MA_3\right]_{ad} - k_{-d} a \left[MA_3\right] \quad (3.174)$$

$$r_{4b} = k_a a \left[HA\right]_{ad}^3 - k_{-a} a \left[\overline{HA}\right]^3 \quad (3.175)$$

However, in certain instances the combination of reactions r_{4a} and r_{4b} can be useful in the derivation of overall rate expressions where the adsorption and desorption from the interface are slow as well as the reaction at the interface. Note that all reaction steps are second order except for r4a and r4b which are first and third order respectively as written in these elementary reaction steps. One or any number of the above steps could be rate controlling. Danesi uses the Langmuir Isotherm in his derivation of an overall reaction rate assuming different controlling steps. He derives four scenarios. There are fourteen possible rate schemes that could controll the overall rate of extraction in the mechanism originally proposed by Danesi. In the case of using the adsorption and desorption steps there would be thirty one possible schemes of controlling rate steps. In the four that Danesi derives he uses at most two controlling steps. Boudart (Boudart AICHEJ 1972 and Kinetics of Chemical Processes 1991, Bischoff and Froment I&EC FUnd 1962) discuss the use of at most two controlling steps. Froment ilustrates that for a two step controlled adsorption – reaction – desorption mechanism the equation is rather complicated and cannot be written as a linear equation in the bulk specie concentrations. Additionally, for simple first order systems i.e. $A - B$ a general equation can be derived assuming no controlling step (see Froment and Bischoff Chemical Reactor Design 1990 and Aris Elementary Chemical Reactor Analysis 1989 pp 121). The derivation by Aris uses matrix linear algebra techniques and is a concise method. For the second order mechanisms presented above no easy method of solution for an overall reaction rate is available.

Danesi uses the Langmuir isotherm for a single specie being adsorbed at the surface i.e. the extractant which allows a relationship between the surface concentration of the adsorbed extractant and the concentration of the extractant in the bulk of the organic phase. The form of the Isotherm that he uses is

$$[\mathrm{HA}]_{ad} = \frac{\alpha_2 \frac{\boxed{\mathrm{HA}}}{\gamma}}{1 + \frac{\boxed{\mathrm{HA}}}{\gamma}} \tag{3.176}$$

where α_2 and γ are Langmuir adsorption constants. Though, Danesi does not explain what these constants are it may be valuable to understand the origin of these constants and the Langmuir isotherm.

The Langmuir Law assumes that the rate of adsorption and desorption of a specie at a surface are the same or the equilibrium state exists. Therefore, for species A interacting with a surface

$$[A] \underset{k_{des}}{\overset{k_{ads}}{=}} [A]_{ads}$$

$$\left(\frac{dn_A}{dt}\right)_{ads} = \left(\frac{dn_A}{dt}\right)_{des}$$

If θ_A is defined to be the fraction of occupied "sites" on which adsorption is possible (i.e. $\frac{[A]_{ads}}{[A]_{\max}}$ — where $[A]_{\max}$ is the maximum amount of A that can be adsorbed) then the rate of adsorption is proportional to the rate of molecular collisions with the unoccupied sites (satterfield p 36).

$$\left(\frac{dn_A}{dt}\right)_{ads} = k_{ads}\,(1-\theta_A)\,[A]$$

The rate of desorption is proportional to the number of molecules adsorbed

$$\left(\frac{dn_A}{dt}\right)_{des} = k_{des}\theta_A$$

and thus

$$k_{ads}\,(1-\theta_A)\,[A] = k_{des}\theta_A$$

solving for θ_A

$$\theta_A = \frac{k_{ads}\,[A]}{k_{des} + k_{ads}\,[A]}$$

rearranging

$$\theta_A = \frac{\frac{k_{ads}}{k_{des}}[A]}{1 + \frac{k_{ads}}{k_{des}}[A]}$$

$\frac{k_{ads}}{k_{des}}$ is the adsorption equilibrium constant called K or $\frac{1}{\gamma}$ to be consistne with Danesi (also derived in Bischoff and Froment page 68) and using the definition of θ_A

$$\theta_A = \frac{[A]_{ads}}{[A]_{\max}} = \frac{\frac{[A]}{\gamma}}{1 + \frac{[A]}{\gamma}}$$

and thus

$$[A]_{ads} = \frac{[A]_{\max}\frac{[A]}{\gamma}}{1 + \frac{[A]}{\gamma}} = \frac{\alpha_2\frac{[A]}{\gamma}}{1 + \frac{[A]}{\gamma}} \tag{3.177}$$

where $\alpha_2 = [A]_{\max}$ following Danesi and γ is the inverse of the equilibrium constant of adsorption and can be expressed in and Arrehnieus form

$$K = \frac{1}{\gamma} = A\exp^{\frac{\lambda}{RT}} \tag{3.178}$$

where λ is the heat of adsorption. A large value of K implies strong adsorption or bonding and the greater is the surface coverage at a fixed temperature.

Danesi uses equation 3.177 in his derivation of the overall rate equations. This is an oversimplification of the problem. From reaction r4 or (r4a and r4b) two species actually compete for the "sites" or adsorption locations on the surface or interface. In order to take this into account additional terms in the denominator are needed. If the fraction of surface area or sites occupied by A is again taken to be θ_A and θ_B is the fraction of sites occupied by species B and the adsorption reaction mechanism can be considered as

for species A

$$A + s \underset{k_{-1}}{\overset{k_1}{-}} As$$

where s is the acitve sites and the equilibrium equation is

$$k_1 C_A (1 - \theta_A - \theta_B) = k_{-1}\theta_A$$

and

$$B + s \underset{k_{-2}}{\overset{k_2}{-}} Bs$$

$$k_2 C_B (1 - \theta_A - \theta_B) = k_{-2}\theta_B$$

which give two equations in two unknowns and solving for θ_A and θ_B

$$\theta_A = \frac{K_A C_A}{1 + K_A C_A + K_B C_B} \tag{3.179}$$

$$\theta_B = \frac{K_B C_B}{1 + K_A C_A + K_B C_B} \tag{3.180}$$

where K_A and K_B are the equilibrium constants $\frac{k_1}{k_{-1}}$ and $\frac{k_2}{k_{-2}}$ respectively. Using equations 3.179 and 3.180 an overall reaction rate can be determined. Since the adsorption B is reversible it can be thought of as an inhibitor. As the concentration of B becomes large the concentration of A on the surface becomes smaller and the concentration of B on the surface larger and since A adsorbed on the surface is the reactive species the reaction is inhibited. This can be extended to an arbitraty number of inhibitors or competing adsorbates

$$\theta_A = \frac{K_A C_A}{1 + \sum K_i C_i} \tag{3.181}$$

$$\theta_j = \frac{K_j C_j}{1 + \sum K_i C_i}$$

where $K_i C_i$ account for the n species competing for adsorption on the active sites. These extended Langmuir isotherms are proposed to give more exacting though certainly more complex equations than the ones using the Langmuir isotherm as in equation 3.177. The derivations for the overall rate equations using the extended Langmuir isotherm equations 3.179 and 3.180 will be presented for only the four schemes as presented by Danesi. Danesi's final equations will be presented for comparison but with limited derivations.

It should be noted that Yoshizuka et. al (Ind Eng Chem res 1992 p 1372-1378) conducted interfacial tension experiments with D2EHPA extracting Holmium and Yttrium, valence 3 Lanthanide metals, and showed that the metal complexes are scarcely adsorbed while the D2EHPA is strongly adsorbed. This suggests that Danesi's use of the single specie Langmuir isotherm to derive the overall extraction rates may be valid when the acidic extractant Bis(2–ethylhexyl) phosphoric Acid in aromatic diluents is used. Yoshizuka et. al use the single specie adsorption isotherm and the second ligand reaction to the neutral complex as the controlling steps i.e.

$$MA_2^+ \cdot 2HA_{(ad)} + \overline{H_2A_2} - MA_3 \cdot 3HA + H^+$$

The mechanism in these authors work show a dimeric acid extractant adorbing at the interface and not the monomeric formulation used in this study and Danesi's work.

Case 2-2-a: reaction r1 slow or controlling with remainder in equalibrium Danesi shows using the Langmuir Isotherm with one species adsorbing on the surface $[\mathrm{HA}]_{ad} = \frac{\alpha_2 \frac{[\overline{\mathrm{HA}}]}{\gamma}}{1+\frac{[\overline{\mathrm{HA}}]}{\gamma}}$ and derives the rate equations for ideal adsorption as

$$\overrightarrow{V}_0 = ak_1\alpha_1 \left[\mathrm{M}^{+3}\right] \left[\overline{\mathrm{HA}}\right] \tag{3.182}$$

$$\overleftarrow{V}_0 = \frac{k_{-1}a\alpha_1}{K_{e,2}K_{e,3}K_{e4}} \frac{\left[\overline{\mathrm{MA}_3}\right] [\mathrm{H}^+]^3}{\left[\overline{\mathrm{HA}}\right]^2} \tag{3.183}$$

where $\overrightarrow{V}_0$, and $\overleftarrow{V}_0$ are rate velocities in the forward and reverse directions and $\alpha_1 = \frac{\alpha_2}{\gamma}$. For ideal adsorption the criteria of $\frac{[\overline{\mathrm{HA}}]}{\gamma} \ll 1$ is meet and the Langmuir single species adsoption equation becomes $[\mathrm{HA}]_{ad} = \alpha_2 \frac{[\overline{\mathrm{HA}}]}{\gamma} = \alpha_1 \left[\overline{\mathrm{HA}}\right]$ which is a form of a Henry's law that is the adsorbed concentration is proportional to the concentration in the bulk. When $1 \ll \frac{[\overline{\mathrm{HA}}]}{\gamma}$ then $[\mathrm{HA}]_{ad} = \alpha_2$ or the adsorbed species is constant this is the surface saturation region. Generally with strong surfactants the surface is saturated with the extracting species even when the bulk concentration is very low 10^{-4} or 10^{-5} M (Danesi page 35). For the saturated interface adsorption region Danesi gives the forward and reverse reactions as

$$\overrightarrow{V}_0 = ak_1\alpha_2 \left[\mathrm{M}^{+3}\right] \tag{3.184}$$

$$\overleftarrow{V}_0 = \frac{k_{-1}a\alpha_2}{K_{e,2}K_{e,3}K_{e4}} \frac{\left[\overline{\mathrm{MA}_3}\right] [\mathrm{H}^+]^3}{\left[\overline{\mathrm{HA}}\right]^3} \tag{3.185}$$

Danesi's equations before the limiting Langmuir Isotherm constraints are used or

$$\overrightarrow{V}_0 = ak_1 \left[\mathrm{M}^{+3}\right] [\mathrm{HA}]_{ad} \tag{3.186}$$

$$\overleftarrow{V}_0 = \frac{k_{-1}a}{K_{e,2}K_{e,3}K_{e4}} \frac{\left[\overline{\mathrm{MA}_3}\right] [\mathrm{H}^+]^3 [\mathrm{HA}]_{ad}}{\left[\overline{\mathrm{HA}}\right]^3} \tag{3.187}$$

and combining these as $\overrightarrow{V}_0 - \overleftarrow{V}_0 = r$ or the combined reversible reaction rate will give the

following expression

$$r = \frac{ak_{-1}\left[\mathrm{HA}\right]_{ad}\left(K_{e,1}K_{e,2}K_{e,3}K_{e4}\left[\mathrm{M}^{+3}\right]\left[\overline{\mathrm{HA}}\right]^3 - \left[\mathrm{H}^{+}\right]^3\left[\overline{\mathrm{MA}_3}\right]\right)}{K_{e,2}K_{e,3}K_{e4}\left[\overline{\mathrm{HA}}\right]^3} \tag{3.188}$$

after simplification and inserting the Langmuir single adsorption species equation (equation 3.177) we obtain

$$r = \frac{a\alpha_2 k_{-1}\left(K_{e,1}K_{e,2}K_{e,3}K_{e4}\left[\mathrm{M}^{+3}\right]\left[\overline{\mathrm{HA}}\right]^3 - \left[\overline{\mathrm{MA}_3}\right]\left[\mathrm{H}^{+}\right]^3\right)}{K_{e,2}K_{e,3}K_{e4}\left(\gamma\left[\overline{\mathrm{HA}}\right]^2 + \left[\overline{\mathrm{HA}}\right]^3\right)} \tag{3.189}$$

Equation 3.189 is equal to zero at equalibrium and reduces to

$$K_{e,1}K_{e,2}K_{e,3}K_{e4} = \frac{\left[\overline{\mathrm{MA}_3}\right]\left[\mathrm{H}^{+}\right]^3}{\left[\mathrm{M}^{+3}\right]\left[\overline{\mathrm{HA}}\right]^3} = K_{eq} \tag{3.190}$$

Where K_{eq} is the overall equalibrium for the overall reaction

$$\left[\mathrm{M}^{+3}\right] + 3\left[\overline{\mathrm{HA}}\right] - \left[\overline{\mathrm{MA}_3}\right] + 3\left[\mathrm{H}^{+}\right]$$

Note that equation 3.189 contains the form of popular Hougan -Watson equations for complex reactions at surfaces (see Hougen Watson Industrial and Engineering Chemistry May 1943, Yang and Hougen Chemical Engineering Progress March 1950, Butt Reactions and Reactor Design, Satterfield Heterogeneous Catalysis in Practice, Froment and Bischof Chemical reactor analysis and design). The form of this equation for the overall reaction rate is

$$r = \frac{(\text{kinetic factor})\,(\text{driving-force or potential term})}{(\text{adsorption term})} \tag{3.191}$$

The driving force or potential term is the term that drives the rate to equilibrium at which time no further change in chemical potental exists. The other terms are a result of the kinetics of the system and is generally any thing other than the potential term and the adsorption term. The adsorption term is the term that enters from the adsorption at the interface or surface. Equation 3.189 is nonlinear and becomes complex for the overall reaction where more than two reactions are controlling are at least of the same magnitude in velocity. The Hougen-Watson form is also difficult to obtain for multiple reactions with higher order reactions than one (see Bischoff and Froment Ind and EC Fund 1962).

As has been stated previously Danesi used the Langmuir isotherm derived for a single

specie adsobing at a surface. The following derivation uses the Langmuir isotherm derived for competing specie for the surface sites. The species adsorbing at this surface are the extractant $\left[\overline{\mathrm{HA}}\right]$ - $[\mathrm{HA}]_{ad}$ and the metal complex, $\left[\overline{\mathrm{MA}_3}\right]$ - $[\mathrm{MA}_3]_{ad}$, formed by the reaction at the interface but which is desorbed reversably at the interface. The overbar denotes the organic phase and *ad* the adsorbed species at the interface.

Using reaction r1 and assuming that it is controlling and reactions r2, r3, r4a, and r4b are in equilibrium and that the relationship of the adsorption species are given by the Langmuir Isotherm law

$$\theta_A\alpha_2 = [\mathrm{HA}]_{ad} = \frac{K_{e,HA}\left[\overline{\mathrm{HA}}\right]\alpha_2}{1 + K_{e,HA}\left[\overline{\mathrm{HA}}\right] + K_{e,MA_3}\left[\overline{\mathrm{MA}_3}\right]}$$

$$\theta_B\alpha_2 = [\mathrm{MA}_3]_{ad} = \frac{K_{e,MA_3}\left[\overline{\mathrm{MA}_3}\right]\alpha_2}{1 + K_{e,HA}\left[\overline{\mathrm{HA}}\right] + K_{e,MA_3}\left[\overline{\mathrm{MA}_3}\right]}$$

thus $\left[\mathrm{MA}^{2+}\right]_{ad} = \frac{\left[\mathrm{MA}_2^+\right]_{ad}[\mathrm{H}^+]}{K_{2e}[\mathrm{HA}]_{ad}}$ where $K_{2e} = \frac{k_2}{k_{-2}}$ and $\left[\mathrm{MA}_2^+\right]_{ad} = \frac{[\mathrm{MA}_3]_{ad}[\mathrm{H}^+]}{K_{3e}[\mathrm{HA}]_{ad}}$ where $K_{3e} = \frac{k_3}{k_{-3}}$ and $K_{e,HA}$, K_{e,MA_3} are the equalibrium constants for species HA and MA_3 respecitvely between the bulk organic phase and the surface or interface. Inserting these equations into equation r1 we obtain

$$r = \frac{ak_{-1}\left(\alpha_2^2 K_{1e}K_{2e}K_{3e}K_{e,HA}^3\left[\mathrm{M}^{+3}\right]\left[\overline{\mathrm{HA}}\right]^3 - K_{e,MA_3}\left[\overline{\mathrm{MA}_3}\right][\mathrm{H}^+]^3\,\Xi\right)}{\alpha_2 K_{2e}K_{3e}K_{e,HA}^2\left[\overline{\mathrm{HA}}\right]^2\left(1 + K_{e,HA}\left[\overline{\mathrm{HA}}\right] + K_{e,MA_3}\left[\overline{\mathrm{MA}_3}\right]\right)} \tag{3.192}$$

where

$$\Xi = \left(1 + 2\left(K_{e,HA}\left[\overline{\mathrm{HA}}\right] + K_{e,MA_3}\left[\overline{\mathrm{MA}_3}\right]\right) + \left(K_{e,HA}\left[\overline{\mathrm{HA}}\right] + K_{e,MA_3}\left[\overline{\mathrm{MA}_3}\right]\right)^2\right)$$

$$\Xi = \left(1 + K_{e,HA}\left[\overline{\mathrm{HA}}\right] + K_{e,MA_3}\left[\overline{\mathrm{MA}_3}\right]\right) \tag{3.193}$$

or Setting $r = 0$ for equalibrium here gives a different more complex equation

$$K_{eq} = \frac{\alpha_2^2 K_{1e}K_{2e}K_{3e}K_{e,HA}^3}{K_{e,MA_3}\left(1 + K_{e,HA}\left[\overline{\mathrm{HA}}\right] + K_{e,MA_3}\left[\overline{\mathrm{MA}_3}\right]\right)^2} \tag{3.194}$$

In equation 3.194 the equalibrium constant is dependent on the nonliner combination of the equalibrium constants for each reaction and the equalibrium constant of the adsorbing species as well as the number of or amount of adsorption space available for adsorption (α_2) and the bulk concentrations of the adsorbing species competing for the adsorption sites.

Case 2-2-b: reactions r1 and r2 slow or controlling with remainder in equalibrium Based on the Langmuir theory of adsorption, reaction, and desorption and using equations 3.164, 3.165,3.166,3.172, and 3.173 on page 73 and assuming that r1 and r2 are controlling

$$r_1 = k_1 a \left[M^{+3}\right] [HA]_{ad} - k_{-1} a \left[MA^{+2}\right]_{ad} [H^+] \tag{3.195}$$

$$r_2 = k_2 a \left[MA^{+2}\right]_{ad} [HA]_{ad} - k_{-2} a \left[MA_2^{+}\right]_{ad} [H^+] \tag{3.196}$$

Again Danesi uses the Langmuir isotherm for a single species absorbing to obtain an overall rate expression for this case his equations for the ideal adsorption case are

$$\overrightarrow{V}_0 = \frac{k_1 k_2 a \alpha_1 \left[M^{+3}\right] \left[\overline{HA}\right]^2}{k_{-1} [H^+] + k_2 \alpha_1 \left[\overline{HA}\right]} \tag{3.197}$$

$$\overleftarrow{V}_0 = \frac{\frac{k_{-1}k_{-2}}{K_{e,3}K_{e4}} a \alpha_1 \left[\overline{MA_3}\right] [H^+]^3}{k_{-1} [H^+] \left[\overline{HA}\right] + k_2 \alpha_1 \left[\overline{HA}\right]^2} \tag{3.198}$$

where $\overrightarrow{V}_0$, and $\overleftarrow{V}_0$ are rate velocities in the forward and reverse directions respectively. For the saturated interface adsorption region Danesi gives the forward and reverse reactions as

$$\overrightarrow{V}_0 = \frac{k_1 k_2 a \alpha_2 \left[M^{+3}\right]}{k_1 [H^+] + k_2 \alpha_2} \tag{3.199}$$

$$\overleftarrow{V}_0 = \frac{\frac{k_{-1}k_{-2}}{K_{e,3}K_{e4}} a \alpha_2^2 [MA_3] [H^+]^3}{\left(k_{-1} [H^+] \left[\overline{HA}\right] + k_2 \alpha_2\right) \left[\overline{HA}\right]^3} \tag{3.200}$$

Danesi's equations before the limiting Langmuir Isotherms constraints are used or

$$\overrightarrow{V}_0 = \frac{k_1 k_2 a \left[M^{+3}\right] [HA]_{ad}^2}{k_{-1} [H^+] + k_2 [HA]_{ad}} \tag{3.201}$$

$$\overleftarrow{V}_0 = \frac{\frac{k_{-1}k_{-2}}{K_{e,3}K_{e4}} a \left[\overline{MA_3}\right] [H^+]^3 \left[\overline{HA}\right]^{-3} [HA]_{ad}^2}{k_{-1} [H^+] + k_2 [HA]_{ad}} \tag{3.202}$$

and combining these as $\overrightarrow{V}_0 - \overleftarrow{V}_0 = r$ or the combined reversible reaction rate will give the following expression

$$r = \frac{a\left(K_{3e}K_{4e}k_2k_1\left[M^{+3}\right]\left[HA\right]_{ad}^2\left[\overline{HA}\right]^3 - k_{-1}k_{-2}\left[H^+\right]^3\left[\overline{MA_3}\right]\left[HA\right]_{ad}^2\right)}{k_{-1}\left[H^+\right] + k_2\left[HA\right]_{ad}} \tag{3.203}$$

after simplification and inserting the Langmuir single adsorption species equation (equation 3.177) we obtain

$$r = \frac{a\alpha_2^2k_{-1}k_{-2}\left(K_{3e}K_{4e}K_{2e}K_{1e}\left[M^{+3}\right]\left[\overline{HA}\right]^3 - \left[\overline{MA_3}\right]\left[H^+\right]^3\right)}{\left[\overline{HA}\right]\left(k_{-1}\left[H^+\right]\gamma^2 + \gamma\left(2k_1\left[H^+\right] + k_2\alpha_2\right)\left[\overline{HA}\right] + \left(k_{-1}\left[H^+\right] + k_2\alpha_2\right)\left[\overline{HA}\right]^2\right)} \tag{3.204}$$

Note again that this equation contains the form as put forth in the popular Hougan - Watson equations for complex reactions at surfaces. Equation 3.204 like before is nonlinear and comparison between this equation and equation 3.189 shows the increasing degree of complexity associated with obtaining the overall reaction where more than one reaction is controlling are at least of the same magnitude in velocity.

As before I will derive the equation for this case using the Langmuir isotherm derived for competing specie for surface sites. The species adsorbing at this surface are the extractant $\left[\overline{HA}\right]$ - $[HA]_{ad}$ and the metal complex, $\left[\overline{MA_3}\right]$ - $[MA_3]_{ad}$, formed by the reaction at the interface but which is desorbed reversably at the interface. The overbar denotes the organic phase and *ad* the adsorbed species at the interface.

Applying the stationary states to the rate of change of the intermediate $\left[MA^{+2}\right]_{ad}$

$$\frac{d\left[MA^{+2}\right]_{ad}}{dt} = 0 = r_1 - r_2$$

$\left[MA^{+2}\right]_{ad}$ can be determined

$$\left[MA^{+2}\right]_{ad} = \frac{k_1\left[M^{+3}\right]\left[HA\right]_{ad} + k_{-2}\left[MA_2^+\right]_{ad}\left[H^+\right]}{k_2\left[HA\right]_{ad} + k_{-1}\left[H^+\right]}$$

r_3 equation 3.166 will be used in equilibrium to obtain $\left[MA_2^+\right]_{ad}$ therefore $r_3 = 0$ and $\left[MA_2^+\right]_{ad} = \frac{[MA_3]_{ad}[H^+]}{K_{3e}[HA]_{ad}}$ where $K_{3e} = \frac{k_3}{k_{-3}}$ and for competing adsorption species two Lang-

muir isotherms are needed. These are taken from eqations 3.179 and 3.180

$$\theta_A\alpha_2 = [\mathrm{HA}]_{ad} = \frac{K_{e,HA}\left[\overline{\mathrm{HA}}\right]\alpha_2}{1 + K_{e,HA}\left[\overline{\mathrm{HA}}\right] + K_{e,MA_3}\left[\overline{\mathrm{MA_3}}\right]}$$

$$\theta_B\alpha_2 = [\mathrm{MA_3}]_{ad} = \frac{K_{e,MA_3}\left[\overline{\mathrm{MA_3}}\right]\alpha_2}{1 + K_{e,HA}\left[\overline{\mathrm{HA}}\right] + K_{e,MA_3}\left[\overline{\mathrm{MA_3}}\right]}$$

where α_2 is the total amount of surface area or sites available for adsorption. Using the above series of equations we obtain values for the indeterminable species at the surface: $[\mathrm{MA}^{+2}]_{ad}$, $\left[\mathrm{MA}_2^{+}\right]_{ad}$, $[\mathrm{MA_3}]_{ad}$, and $[\mathrm{HA}]_{ad}$ in the measurable bulk concentrations. Inserting these various parameters from the above equations reveals the following equation.

$$r = \frac{a\left(K_{e,HA}^3 k_1 k_2 \alpha_2^2 [\mathrm{M}^{+3}]\left[\overline{\mathrm{HA}}\right]^3 - k_{-1}k_{-2}[\mathrm{H}^+]^3 K_{e,MA_3}\left[\overline{\mathrm{MA_3}}\right]\left(\Psi^2 + 2K_{e,MA_3}\Psi\left[\overline{\mathrm{MA_3}}\right] + K_{e,M}^2\right.\right.}{\left(K_{e,HA}k_{-1}K_{e3}\left[\overline{\mathrm{HA}}\right][\mathrm{H}^+]\left(\Psi + K_{e,MA_3}\left[\overline{\mathrm{MA_3}}\right]\right)^2 + \alpha_2 K_{e,HA}^2 K_{e3}k_2\left[\overline{\mathrm{HA}}\right]^2\left(\Psi + K_{e,MA_3}\right.\right.}$$

where $\Psi = \left(1 + K_{e,HA}\left[\overline{\mathrm{HA}}\right]\right)$

$$r = \frac{ak_{-1}k_{-2}\left(K_{e,HA}^3 K_{e1}K_{e2}\alpha_2^2[\mathrm{M}^{+3}]\left[\overline{\mathrm{HA}}\right]^3 - K_{e,MA_3}\left[\overline{\mathrm{MA_3}}\right][\mathrm{H}^+]^3\left(\Psi + K_{e,MA_3}\left[\overline{\mathrm{MA_3}}\right]\right)^2\right)}{K_{e,HA}K_{e3}\left(k_{-1}\left[\overline{\mathrm{HA}}\right][\mathrm{H}^+]\left(\Psi + K_{e,MA_3}\left[\overline{\mathrm{MA_3}}\right]\right)^2 + \alpha_2 K_{e,HA}k_2\left[\overline{\mathrm{HA}}\right]^2\left(\Psi + K_{e,MA_3}\left[\overline{\mathrm{MA_3}}\right]\right)\right)}$$

$$r = \frac{ak_{-1}k_{-2}\alpha_2^2\left(K_{e1}K_{e2}K_{e,HA}^3[\mathrm{M}^{+3}]\left[\overline{\mathrm{HA}}\right]^3 - K_{e,MA_3}[\mathrm{H}^+]^3\left[\overline{\mathrm{MA_3}}\right]\Omega^2\right)}{\alpha_2^2\Omega K_{e,HA}K_{e3}\left(k_{-1}\left[\overline{\mathrm{HA}}\right][\mathrm{H}^+]\Omega + k_2 K_{e,HA}\left[\overline{\mathrm{HA}}\right]^2\right)}$$

where $\Omega = \frac{\Psi + K_{e,MA_3}\left[\overline{\mathrm{MA_3}}\right]}{\alpha_2} = \frac{1 + K_{e,HA}\left[\overline{\mathrm{HA}}\right] + K_{e,MA_3}\left[\overline{\mathrm{MA_3}}\right]}{\alpha_2}$

$$r = \frac{ak_{-1}k_{-2}\alpha_2\left(K_{e1}K_{e2}K_{e,HA}^3[\mathrm{M}^{+3}]\left[\overline{\mathrm{HA}}\right]^3 - K_{e,MA_3}[\mathrm{H}^+]^3\left[\overline{\mathrm{MA_3}}\right]\Omega^2\right)}{\left[\overline{\mathrm{HA}}\right]K_{e,HA}K_{e3}\left(\Psi + K_{e,MA_3}\left[\overline{\mathrm{MA_3}}\right]\right)\left(k_{-1}[\mathrm{H}^+]\Omega + k_2 K_{e,HA}\left[\overline{\mathrm{HA}}\right]\right)} \tag{3.205}$$

Equation 3.205 is similar to equation 3.204 but is different in various terms. The form of the equation in respect to the driving potential, the kinetic term, and the adsorption term are still present, but unequal due to the different Langmuir mechanism chosen to derive the equation. Note in comparing the two equations $K_{e,HA} = \frac{1}{\gamma}$.

Case 2-2c: r1 and r4 slow remainder in equalibrium adsorption and desorption are slow

$$r_1 = k_1 a \left[M^{3+}\right] [HA]_{ad} - k_{-1} a \left[MA^{2+}\right]_{ad} [H^+] \quad \text{slow} \quad (3.206)$$

$$r_2 = k_2 a \left[MA^{2+}\right]_{ad} [HA]_{ad} - k_{-2} a \left[MA_2^+\right]_{ad} [H^+] \quad \text{fast} \quad (3.207)$$

$$r_3 = k_3 a \left[MA_2^+\right]_{ad} [HA]_{ad} - k_{-3} a [MA_3]_{ad} [H^+] \quad \text{fast} \quad (3.208)$$

$$r_4 = k_4 a [MA_3]_{ad} [HA]_{ad}^3 - k_{-4} a \left[\overline{MA_3}\right] \left[\overline{HA}\right]^3 \quad \text{slow} \quad (3.209)$$

Danesi states here that the adsorption and desorption are to be slow reactions and the Langmuir iso herm is to be used for the relationship to reformulate the adsorbed concentration quantities in measurable quantities. This is contradictory. The Langmuir isotherm equation that Danesi uses is a single species adsorption isotherm that was derived assuming equilibrium between adsorbed specie and the bulk concentration of the specie. Though it can be used here if one assumes, incorrectly, that the quantity $[MA_3]_{ad}$ is not in equilibrium with the quantity of that specie in the bulk of the liquid and does not reversibly compete for the adsorption sites on the surface. Thus the desorption of $[MA_3]_{ad}$ is basically irreversible. This is inappropriate since in metal extraction the reversability is necessary to strip the organic of the metal.

The derivation of an overall rate equation for the extraction of high valence metals in which two or more intrinsic rates are controlling develops equations algebraically complex. In this particulary case a fifth power of $[HA]_{ad}$ is involved. Froment and Bischoff (I&EC Fundamentals 1962) derives a rather unwieldy equation for a mixed first and second order reversible consecutive heterogeneous reaction with two steps controlling. Here we essentially have three steps controlling *e.g.* adsorption; surface reaction; and desorption of the product species. To illustrate we chose r_1 and r_4 as controlling steps with r_2 and r_3 in equalibrium and the assumption is used that $r_1 \cong r_2$. Thus from the equalibrium steps

$$\left[MA_2^+\right]_{ad} = \frac{k_{-3} [H^+] [MA_3]_{ad}}{k_3 [HA]_{ad}} = \frac{[H^+] [MA_3]_{ad}}{K_{3,e} [HA]_{ad}} \quad (3.210)$$

and

$$\left[MA^{+2}\right]_{ad} = \frac{[H^+]^2 [MA_3]_{ad}}{K_{2,e} K_{3,e} [HA]_{ad}^2} \quad (3.211)$$

and from the two controlling steps set equal to each other and inserting equations 3.210

and 3.211 for the respective quantities $[MA_3]_{ad}$ is obtained.

$$[MA_3]_{ad} = \frac{k_1 [M^{3+}] [HA]_{ad} + k_{-4} \left[\overline{MA_3}\right] \left[\overline{HA}\right]^3}{\frac{k_{-1}}{K_{2,e}K_{3,e}} \frac{[H^+]^3}{[HA]_{ad}^2} + k_4 \left[\overline{HA}\right]^3} \tag{3.212}$$

The total coverage of the interface with adsorbed species is given by

$$c_t = [HA]_{ad} + [MA_3]_{ad} + \frac{[H^+] [MA_3]_{ad}}{K_{3,e} [HA]_{ad}} + \frac{[H^+]^2 [MA_3]_{ad}}{K_{2,e}K_{3,e} [HA]_{ad}^2} \tag{3.213}$$

Substituting $[MA_3]_{ad}$ of equation 3.212 into 3.213 gives the following equations

$$c_t = [HA]_{ad} \left(\frac{\left(k_1 [M^{3+}] + k_{-4} \left[\overline{MA_3}\right] [HA]_{ad}^2\right) \left(K_{2,e}K_{3,e} [HA]_{ad}^2 + K_{2,e} [H^+] [HA]_{ad} + [H^+]^2\right)}{k_{-1} [H^+]^3 + k_4 K_{2,e}K_{3,e} \left[\overline{HA}\right]^3 [HA]_{ad}^2} \right) \tag{3.2}$$

When the numerator is expanded a fifth order polynomial is formed in $[HA]_{ad}$ and is not ameanable to factoring. It is probable that many of the roots of the equation are in the complex range and have no physical meaning here. The real root of $[HA]_{ad}$ is substituted into the following equation for reaction r4:

$$r = \frac{a [HA]_{ad}^3 \left(k_1 k_4 K_{2,e}K_{3,e} [M^{3+}] \left[\overline{HA}\right]^3 - k_{-1}k_{-4} \left[\overline{MA_3}\right] [H^+]^3\right)}{k_{-1} [H^+]^3 + k_4 K_{2,e}K_{3,e} \left[\overline{HA}\right]^3 [HA]_{ad}^2}$$

Danesi obtains the forward and reverse reactions for the fourth reaction step as follows

for the forward reaction:

$$\overrightarrow{V}_0 = \frac{k_1 k_4 a [M^{3+}] \left[\overline{HA}\right]^3 [HA]_{ad}^3}{\frac{k_{-1}}{K_{2,e}K_{3,e}} \frac{[H^+]^3}{[HA]_{ad}^2} + k_4 \left[\overline{HA}\right]^3} \tag{3.215}$$

and the reverse reaction:

$$\overrightarrow{V}_0 = \frac{k_{-1}k_{-4}a \left[\overline{MA_3}\right] [H^+]^3 [HA]_{ad}}{\frac{k_{-1}}{K_{2,e}K_{3,e}} \frac{[H^+]^3}{[HA]_{ad}^2} + k_4 \left[\overline{HA}\right]^3} \tag{3.216}$$

and Danisi use the Langmuir isotherm here to eliminate $[HA]_{ad}$. This is felt to be incorrect in this circumstance since it is contrary to the adsorption being a slow reaction and contrary to the first reaction equaling the fourth reaction and thus influencing and controlling the overall reaction rate.

Case 2-2d: reaction 1 and 4 slow; reaction 2 and 3 fast with a slow parallel step also in the aqueous phase. In all of the cases in this section and indeed in any metal extraction from aqueous phases hydrolyzed metals can react with the extractant as well as metals complexed with nitrates or chlorides in solutions with mineral acids. This particular case is a combination of Case 2-2a and 2-2c. The extracting reagent is partially solubilized in the aqueous phase and adsorbed at the liquid-liquid interface and the metal cation is present also in its hydrolyzed form the following mechanism will be simultaneously in effect (Danesi CRC 1980).

$$\left.\begin{aligned} &[M^{3+}] + [HA] \underset{k_{-1}}{\overset{k_1}{-}} [MA^{2+}] + [H^+] \\ &\left[M(OH)^{2+}\right] + [HA] \underset{k_{-2}}{\overset{k_2}{-}} [MA^{2+}] + [H_2O] \end{aligned}\right\} \text{homogeneous parallel reactions} \quad (3.217)$$

$$\left.\begin{aligned} &[M^{3+}] + [HA]_{ad} \underset{k_{-3}}{\overset{k_3}{-}} [MA^{2+}]_{ad} + [H^+] \\ &\left[M(OH)^{2+}\right] + [HA]_{ad} \underset{k_{-2}}{\overset{k_2}{-}} [MA^{2+}]_{ad} + [H_2O] \end{aligned}\right\} \text{interfacial parallel reactions} \quad (3.218)$$

$$[MA_3]_{ad} + 3\left[\overline{HA}\right] \underset{k_{-4}}{\overset{k_4}{-}} \left[\overline{MA_3}\right] + 3[HA]_{ad} \quad (3.219)$$

As in the previous case Danesi uses the Langmuir isotherm and again its use in this case with the adsorption and desorption reactions assumed to be slow is opinioned to be incorrect. The algebraic equations as a result of the above reactions need to be solved simultaniously making use of the Bodenstein approximation and the equalibrium concept of the other reaction steps. Again this will prove an impossible task since the equations will produce a polynomial in the adsorbed specie of higer power than three and incapable of factorization to solve for the adsorbed intermediate. Thus the case is relegated to numerical solutions of simultaneous differential equations.

Summary

The kinetic regime as reviewed in this chapter can be extremely complex expecially for metals with valences higher than 2. Thus suitably derived analytical solutions for the overall rate equations are not available. This becomes even more obvious when one considers that the above derivations do not account for extracting reagents undrgoing association and dissociation which many of the later discussions did not consider. The derivations also did not consider non ideality of the complexes in the solutions being used; thus, the concentration quatities need be replaced by activities when non–ideal behavoir is present. In all of the cases in this section and indeed in any metal extraction from aqueous phases

hydrolyzed metals can react with the extractant as well as metals complexed with nitrates or chlorides in solutions with mineral acids.

3.3.3 Diffusional Regime

Psuedo rate constants in conjunction with the actual kinetic rate equations used above may allow the determination of an overall rate of extraction for a solute from one phase to another for well mixed tanks or "compartments". This concept is different from typical chemical engineering models (see for example Cussler Diffusion:Mass Transfer in fluids) for mass transfer and is generally used in the modeling of biological systems (Long personal January 22, 1994, Building Brading Jones and Tomita Smooth Muscles page 69).

In a compartment model, a rate constant is used instead of a mass transfer coefficient. Basically the model is represented as two tanks in series being well–mixed, and the transfer being a first order linear process. The constants can be thought of as "exchange" coefficients and are not really the same as conventional mass transfer coefficients. The transfer of mass is more complex at the micro scale than the lumped parameter mass transfer model suggests. Mass transfer in any system is a phenomenon created by the actual chemical potential imbalance across the interface. In some manner the interaction between the species in solution in one phase is broken and another interaction is formed in the other phase between the transferred species in order to drive the system to a state of more order or equilibrium.

The kinetically derived model as in the case 1 in section ?? through 3.3.2 pages ??—61 assumes that there is no resistance or adsorbtion at the interface. These two techniques of modeling the transfer of mass can be related for simple systems but the relationships as a single rate equation are difficult and complex in more extensive systems. To illustrate this the mass transfer of an acidic species transferring from one phase to another is shown below.

Mass Transfer without reaction using exchange coefficients Assume two phases are placed in contact with each other and these phases are immiscible and a solute initially contained only in the first phase and has a slight solubility in the second phase.

$$\left[\overline{\mathrm{HA}}\right] \underset{k_{II}}{\overset{k_I}{-}} [\mathrm{HA}]$$

$$n_{\overline{\mathrm{HA}}} = V_I \left[\overline{\mathrm{HA}}\right]$$
$$n_{\mathrm{HA}} = V_{II} [\mathrm{HA}]$$
$$n_{\overline{\mathrm{HA}}} + n_{\mathrm{HA}} = \text{constant}$$

The accumulation of a species of HA in phase II is

$$V_I \frac{d[\mathrm{HA}]}{dt} = k_I A \left[\overline{\mathrm{HA}}\right] - k_{II} A [\mathrm{HA}] = \vec{N} = K_{II} A \left(\left[\overline{\mathrm{HA}}\right] - [\mathrm{HA}]\right)$$

where K_{II} will be defined to be the overall mass "exchange" coefficient

$$K_{II} = \frac{k_I \left[\overline{\mathrm{HA}}\right] - k_{II} [\mathrm{HA}]}{\left(\left[\overline{\mathrm{HA}}\right] - [\mathrm{HA}]\right)} \Longrightarrow K_{II} = K_{II}\left(\left[\overline{\mathrm{HA}}\right], [\mathrm{HA}]\right)$$

and when $[\mathrm{HA}] = 0, K_{II} = k_I$ and

and when $\left[\overline{\mathrm{HA}}\right] = 0, K_{II} = k_{II}$ where k_I and k_{II} are exchange coefficients and are not true mass transfer coefficients unless $\left[\overline{\mathrm{HA}}\right] = 0$ or $[\mathrm{HA}] = 0$. At equilibrium the distribution coefficient can be found from the fact that

$$V_I \frac{d[\mathrm{HA}]}{dt} = 0 = k_I A \left[\overline{\mathrm{HA}}\right] - k_{II} A [\mathrm{HA}] = \vec{N} = K_{II} A \left(\left[\overline{\mathrm{HA}}\right] - [\mathrm{HA}]\right)$$

and therefore

$$k_I \left[\overline{\mathrm{HA}}\right] = k_{II} [\mathrm{HA}]$$

and

$$K_d = \frac{k_I}{k_{II}} = \frac{[\mathrm{HA}]}{\left[\overline{\mathrm{HA}}\right]}$$

Danesi uses the mass exchange constants to get a rate equation for the following mechanism

$$\left[\overline{\mathrm{HA}}\right] \underset{K_{-1}^*}{\overset{K_1^*}{\rightleftharpoons}} [\mathrm{HA}] \quad \text{slow} \tag{3.220}$$

$$[\mathrm{HA}] + \left[\mathrm{M}^{+3}\right] \overset{K_2^*}{\rightarrow} \left[\mathrm{MA}^{2+}\right] + [\mathrm{H}^+] \quad \text{slow}$$

the rate of formation for the solute in the second phase is given by

$$\frac{d[\mathrm{HA}]}{dt} = 0 = K_1 \left[\overline{\mathrm{HA}}\right] - (K_{-1} + K_2)[\mathrm{HA}]$$

$$\frac{d[\mathrm{MA}^{2+}]}{dt} = \frac{K_1 K_2}{(K_{-1} + K_2)} \left[\overline{\mathrm{HA}}\right]$$

with $K_1 = \frac{K_1^* A}{V_{org}}, K_{-1} = \frac{K_{-1}^* A}{V_w}$, and $K_2 = K_2^* [M^{+3}]$ and when $V_{org} = V_w$ and $K_{-1} \gg K_2$, then

$$\frac{d[MA^{2+}]}{dt} = \frac{K_1}{K_{-1}} K_2 \left[\overline{HA}\right]$$

which is similar to the first term of equation 3.97. The first term in equation 3.97 is the forward rate or the irreversible reaction of equation 3.220 when $\frac{K_1}{K_{-1}} = \frac{K_1^*}{K_{-1}^*} = \frac{1}{K_D}$ where K_D in this case equals $\frac{[\overline{HA}]}{[HA]}$ and when the irreversible reaction constant is much faster than the reversible partition exchange coefficient i.e. $K_2 \gg K_{-1}$ then the rate of formation of the first metal complex (which is assumed to be the slowest here) is

$$\frac{d[MA^{2+}]}{dt} = K_1^* \frac{A}{V_{org}} \left[\overline{HA}\right]$$

and therefor the rate will be controlled by the rate of the partition of the extractant and by the interfacial area even-though the complex formation does not occur at the interface.

This simple scenario illustrates the use of the psuedo kinetic rate constants or exchange coefficients and also shows how once derived into a single rate equation other scenarios can be obtained assuming knowledge of the rate constants. This scenario also assumes a priori knowledge of the controlling steps. If all the steps of the mechanism were to have rate constants of similar or comparable magnitude then the appropriate individual rate equations given by equations 3.140 through 3.147 would have to be solved simultaneously.

Mass Transfer with reaction

The concept that a pure kinetic regime exits is fictional though in some cases the concept can be approched empirically and thus a model simplified considerably. As represented in the derivation above a relationship between the kinetic regime and the mass transfer physical regime may be obtained. The validity of doing this may ve quesionable since the two regimes are different in concept. Most of the chemical engineering literature use mass transfer coefficients with a chemical reaction and not the psuedo rate constants or "exchange coefficients" of the kinetic regime. The principle behind this is a concentration difference as the driving force for mass transfer across the interface. This concentration difference is the difference between the bulk phase concentration and the interfacial concentration. If the reaction is sufficiently fast that most of the reaction occurs in the film region close to the interface the two film theory needs to be modified to take this into account.

Assuming the two film theory which implies steady state, the balance over the aqueous film or continuity equation for the foregoing reaction mechanism (equations 3.134 through 3.138

for a 3 valence metal extraction

$$D_{\mathrm{HA}}\frac{d^2\left[\mathrm{HA}\right]}{dy^2} = r_{\mathrm{HA}} = k_2\left[\mathrm{HA}\right]\left[\mathrm{M}^{+3}\right] - k_{-2}\left[\mathrm{MA}^{2+}\right]\left[\mathrm{H}^{+}\right] \tag{3.221}$$

,

$$D_{\mathrm{M}^{+3}}\frac{d^2\left[\mathrm{M}^{+3}\right]}{dy^2} = r_{\mathrm{M}^{+3}} = k_2\left[\mathrm{HA}\right]\left[\mathrm{M}^{+3}\right] - k_{-2}\left[\mathrm{MA}^{2+}\right]\left[\mathrm{H}^{+}\right] \tag{3.222}$$

and

$$D_{\mathrm{MA}^{2+}}\frac{d^2\left[\mathrm{MA}^{2+}\right]}{dy^2} = r_{\mathrm{MA}^{2+}} = k_{-2}\left[\mathrm{MA}^{2+}\right]\left[\mathrm{H}^{+}\right] - k_2\left[\mathrm{HA}\right]\left[\mathrm{M}^{+3}\right] \tag{3.223}$$

$$D_{\mathrm{MA}_2^{+}}\frac{d^2\left[\mathrm{MA}_2^{+}\right]}{dy^2} = r_{\mathrm{MA}_2^{+}} = k_{-3}\left[\mathrm{MA}_2^{+}\right]\left[\mathrm{H}^{+}\right] - k_3\left[\mathrm{HA}\right]\left[\mathrm{MA}^{2+}\right] \tag{3.224}$$

$$D_{\mathrm{MA}_3}\frac{d^2\left[\mathrm{MA}_3\right]}{dy^2} = r_{\mathrm{MA}_3} = k_{-4}\left[\mathrm{MA}_3\right]\left[\mathrm{H}^{+}\right] - k_4\left[\mathrm{HA}\right]\left[\mathrm{MA}_2^{+}\right] \tag{3.225}$$

note that $D_{HA}\frac{d^2[\mathrm{HA}]}{dy^2} = D_{\mathrm{M}^{+3}}\frac{d^2[\mathrm{M}^{+3}]}{dy^2} = -D_{\mathrm{MA}^{2+}}\frac{d^2[\mathrm{MA}^{2+}]}{dy^2}$ the boundary conditions at

$$\begin{array}{lrcll}
\text{at } y = 0 \text{ (the interface)}: & [\mathrm{HA}] & = & [\mathrm{HA}]_i & \\
& [\mathrm{M}^{+3}] & = & [\mathrm{M}^{+3}]_i & \\
& [\mathrm{MA}^{+2}] & = & [\mathrm{MA}^{+2}]_i & i \text{ interface} \\
\text{at } y = y_l: & [\mathrm{HA}] & = & [\mathrm{HA}]_b & b \text{ bulk} \\
& [\mathrm{M}^{+3}] & = & [\mathrm{M}^{+3}]_b & \\
& [\mathrm{MA}^{+2}] & = & [\mathrm{MA}^{+2}]_b &
\end{array}$$

the rate of accumulation in the aqueous phase of HA is

$$\frac{d\left[\mathrm{HA}\right]}{dt} = \frac{k_{aq}A_{aq}}{V_{aq}}\left(\left[\mathrm{HA}\right]_i - \left[\mathrm{HA}\right]\right) - \left(k_2\left[\mathrm{HA}\right]\left[\mathrm{M}^{3+}\right] - k_{-2}\left[\mathrm{MA}^{2+}\right]\left[\mathrm{H}^{+}\right]\right) \tag{3.226}$$

where k_{aq} is the mass transfer coefficient in the aqueous phase and the accumulation of HA on the organic side is

$$\frac{d\left[\overline{\mathrm{HA}}\right]}{dt} = \frac{k_{org}A_{org}}{V_{org}}\left(\left[\overline{\mathrm{HA}}\right] - \left[\overline{\mathrm{HA}}\right]_i\right) \tag{3.227}$$

where $\left[\overline{\mathrm{HA}}\right]_i$, $[\mathrm{HA}]_i$ are the concentration of HA at the interface on the organic and aqueous phase sides. If the interface is assumed to be in equilibrium i.e. there is no accumulation of

HA at the interface then a partition or distribution coefficient following a Henry's linearity law could be assumed valid.

$$P_{HA} = \frac{\left[\overline{\mathrm{HA}}\right]_i}{[\mathrm{HA}]_i} \tag{3.228}$$

The system of differential equations models the mass transfer of the organic extractant across the interface from the organic to the aqueous phase with a series reaction in the aqueous phase. The reaction is sufficiently slow enough in the aqueous phase to occur away from the interface and sufficiently fast to allow significant completion in the film. The system of equations does not have an analytical or closed form solution (Secor and Beutler AICHEJ 1967 p365-373, Bischoff and Frometn p 613-615). Contrarily a slow reaction where an insignificant amount of the reaction occurs in the film and the majority of the reaction occurs in the bulk phase can be readily solved analytically and has been repeatedly in the literature (Ortiz and Ortiz Chem. Eng Process 27(1990) 13-18, H. Komiyama and H. Inoue Chemical Enginer. Sci. V 35 (1980), V. Rod The Chemical Engineering Journal 20(1980), Wang and Wu Chemical engr. Sc. 46(2) 1991). Rod attempts an approximation of the solution reaction in the film which gives the exact solution for the two limiting cases of

1. reversible pseudo first order reaction
2. instantaneous reversible reaction

Hughes and Rod (Hydormetallurgy 12(1984) claim, probably rightfully so, that no true kinetic regime exists regardless of the apparatus involved. They derive a pseudokinetic regime equation for the maximum attainable flux for fast reactions that occur in the film of a liquid–liquid interface using concepts from Astarita.

$$N_A = \frac{(k_R D_A)^{\frac{1}{2}}}{P_A} c_B^{\frac{1}{2}} \overline{c}_A \tag{3.229}$$

Where k_R is the reaction rate constant for an irreversible fast reaction $A + B \xrightarrow{k_R} C$; D_A is the diffusion coefficient for species A through the aqueous phase; P_A is the partition coefficient for species A between the two liquid phases; $\overline{c}_A$ is the organic phase concentration of species A; and c_B is the concentration of B in the aqueous phase.

A great deal of discussion has been put forth here in elaboration of the theory of mass transfer across an interface with a chemical reaction in the aqueous phase. The literature is replete with works on this subject. Evenso, most works assume an irreversible moderately fast first order reaction which simplifies the process considerably or that the reaction happens solely at the interface. If the phases are completely immiscible then a heterogenous reaction at the interface is applicable. Some extracting system phases may be so

immiscible with each other that they may be approximated sufficiently with reactions at the interface. It is unlikely that a metal extractant will be entirely immiscible or that the phases do not distribute at all. Astarita has developed a general model for a fast, diffusion controlled reaction for which solutions for various cases of irreversible reactions have been obtained. Astarita's (Astarita Mass Transfer with Chemical Reaction 1967) equation as given by Hanson, Hughes and Marsland (ISEC 74 p2401—2415) is

$$\overline{R} = \sqrt{2D_A \int_{[A]_b}^{[A]_i} r(A) d[A]} \tag{3.230}$$

where $\overline{R}$ is the transfer rate per unit interfacial area

$[A]_b$ is the bulk concentration of A in the phase in which the reaction takes place
$[A]_i$ is the interfacial concentration of A in that phase
D_A is the diffusion coefficient of A through the phase
$r(A)$ is the rate of the reaction with respect to A

Metal extraction processes must be reversible to permit extraction and stripping. Hanson et al have developed a rate equation using Astarita's method for reversible reactions. Because of the importance of this case these authors derivation bears elaboration and repeating here:

Consider, as before the extraction process in which an extractant, HA, transfers into the aqueous phase where it reacts with a solute, M^{m+}

$$M^{m+} + mHA \underset{k_2}{\overset{k_1}{\rightleftharpoons}} MA_m + mH^+ \tag{3.231}$$

and the elementry reaction the rate equation will be

$$r = k_1 [M^{m+}] [HA]^m - k_2 [MA_m] [H^+]^m \tag{3.232}$$

The following are concepts associated with this process

- The extractant and the complex will be in chemical equilibrium in the bulk of the aqueous phase and each will be in individual mass transfer equilibrium at the interface.
- The two film theory is time invariant or steady state and the quantity entering the phase must be equivalent to the complex leaving i.e. no accumulation
- A material balance on the extractant anion shows that for every mole of HA entering then $\frac{1}{m}$ moles of MR_m must leave. and this equivalence exists at every plane parallel to the interface within the reaction zone

- Based on the above the rate of transfer of the complex will be $\frac{1}{m}$ times the rate of transfer of the extractant and will be in the opposite direction.

$$\overline{R}_{MA_m} = -\frac{1}{m}\overline{R}_{HA} \tag{3.233}$$

- The solubilities of the extractant and complex in the aqueous phase are probably low then the solute, M^{m+}, and hydrogen ions will be present in the reaction zone in great excess relative to the other reactants and the change in their concentration will be very small and their concentrations can be considered constant and equal to their bulk concentrations

Hanson et al give the general rate of transfer for HA as

$$\overline{R}_{HA} = \sqrt{\begin{array}{c} 2D_{HA}\left\{k_1\frac{[M^{m+}]_b}{m+1}\left([HA]_i^{m+1} - [HA]_b^{m+1}\right) - k_2[H^+]_b^m\left(\frac{\delta}{m}[HA]_i^2 + [MA_m]_i[HA]_i\right)\right. \\ \left. + k_2[H^+]_b^m\left(\frac{\delta}{m}[HA]_i + [MA_m]_i\right)[HA]_b + \frac{k_2\delta}{2m}[H^+]_b^m\left([HA]_i^2 - [MA_m]_i^2\right)\right\} \end{array}} \tag{3.2}$$

In Equation 3.234 δ is defined to be the ratio of the diffusivities of the extractant to the complex $\frac{D_{HA}}{D_{MA_m}}$. This eqation can be simplified with the following assumptions

- The bulk concentration of the extractant in the aqueous phase will be very small and as $[HA]_b \to 0$ then $[HR]_i \gg [HA]_b$
- The effect of the reverse reaction is negligible in the extraction stage. Usually this can be justified if conditions are chosen to minimize the reverse reaction.

$$\overline{R}_{HA} = \sqrt{\frac{2D_{HA}k_1[M^{m+}]_b[HA]_i^{m+1}}{m+1}} \tag{3.235}$$

and according to Hanson et al this is the eqation of the psuedo n^{th} order irreversible reaction derived by Dankwerts

- Since the phases have been assumed to be in equilibrium at the interface and also that all resistance to mass transfer lies in the aqueous phase we can write $\frac{[HA]_{org}}{[HA]_i} = \phi_{HA}$ where $[HA]_{org}$ is the extractant concentration in the bulk organic phase and ϕ_{HA} is the partition coefficient for the extractant and thus

$$\overline{R}_{HA} = [HA]_i^{\frac{m+1}{2}}\sqrt{\frac{2D_{HA}k_1[M^{n+}]_b}{m+1}} = \left(\frac{[HA]_{org}}{\phi_{HA}}\right)^{\frac{m+1}{2}}\sqrt{\frac{2D_{HA}k_1[M^{n+}]_b}{m+1}} \tag{3.236}$$

and from equation 3.233 then

$$\overline{R}_{MA_m} = -\frac{1}{m}\left(\frac{[HA]_{org}}{\phi_{HA}}\right)^{\frac{m+1}{2}}\sqrt{\frac{2D_{HA}k_1\left[M^{n+}\right]_b}{m+1}} \tag{3.237}$$

The stripping equation is obtained similarly assuming the following mechanism

$$MA_m + mH^+ - M^{m+} + mHA$$

and the reaction rate is

$$r_{MA_m} = k_2\left[MA_m\right]\left[H^+\right]^m - k_1\left[M^{m+}\right]\left[HA\right]^m \tag{3.238}$$

Integrating Fick's first law of diffusion

$$\begin{array}{rcl} -D_{MA_m}\frac{d[MA_m]}{dx} & = & \frac{D_{HA}}{m}\frac{d[HA]}{dx} \\ [MA_m]-[MA_m]_i & = & \frac{1}{m}\frac{D_{HA}}{D_{MA_m}}\left([HA]_i-[HA]\right) \end{array} \tag{3.239}$$

and using this in equation 3.238 and Astarita's equation (equation 3.230) gives

$$\overline{R}_{MA_m} = \sqrt{\begin{array}{c} 2D_{MA_m}\left\{k_2\frac{\left[H^+\right]_b^m}{2}\left([MA_m]_i^2-[MA_m]_b^2\right)+\frac{\delta}{m(m+1)}k_1\left[M^{m+}\right]_b[HA]_i^{m+1}\right. \\ \left.-\frac{\delta}{m(m+1)}k_1\left[M^{m+}\right]_b\left([HA]_i+\frac{m}{\delta}[MA_m]_i-\frac{m}{\delta}[MA_m]_b^{m+1}\right)\right\} \end{array}} \tag{3.240}$$

and making the assumptions of negligible bulk phase concentration of MA_m and negligible back reaction reduces to the Dankwerts' equation again

$$\overline{R}_{MA_m} = \frac{[MA_m]_{org}}{\phi_{MA_m}}\sqrt{D_{MA_m}k_2\left[H^+\right]^m} \tag{3.241}$$

From Hanson et al work it is apparent that the partition coefficient is an important parameter for metal extraction. Also as the authors point out the overall rates have fractional orders eventhough the actual chemical reactions are simple thus the fractional overall orders obtained from experimental results reported in the literature may be in the existence of mass transfer resistance rather than complex reaction mechanism (Hanson et al). This model could be used to determine the diffusion coefficient if the partition coefficient, rate constants, and concentrations are known.

A further observation is the difference between this model for transfer across the interface using mass transfer with a reaction in the film and the psuedo kinetic method presented by Danesi. It is difficult, at least for this engineer to imagine a pure kinetc concept of mass transfer across an interface. The development of an analytical general kinetic rate model for metal extraction is difficult and tedious for reversable reaction mechanisms that consist

of a number of intermediate steps. This is witnessed in the Kinetic Regime section of this study (see section 3.3.2).

4. Nomenclature for Chapter 3

$M^{[]}$	Metal Species ([ ] valence #)
$MB^{\pm}$	Metal extractant complex $\pm$ superscript valence charge
k	reaction rate constant
HB, HA	monomeric acidic extractant
H^+	Hydrogen ion
K	equalibrium constant
B^-	dissociated acidic extractant
K_{DB}	distribution constant; equalibrium contant of extractant between organic and aqueous phase
K_{DM}	distribution constant for the metal extractant complex between the organic and aqueous phases
t	time
$\overline{a}$	specific interfacial area
Q	the area of diffusion
V	Volume of phases
(ad)	adsorption species at surface or interface
(org)	organic phase
R	gas constant
R	resistance
$\overline{R}$	transfer rate
T	temperature
a	area of transfer

A	arbutrary species area; Arrehenious coeeficient
J	diffusional flux
$\mathfrak{D}$	diffusion coefficient (subscript indicates specific specie)
D	distribution coefficient
c_i	concentration of specie i
m	stoichemetric valence of metal
y	polymerization number
x	co-ordination saturation number (or adduct number)
MA_m	neutral metal extractant complex for a metal of valence m
K_{comp_1}	equalibrium constant given by equation 3.93 page 55
K_{comp_2}	equalibrium constant given by equation ??
K_a	dissociation equalibrium constant for acid extractant
r	reaction rate
s	reaction sites
c_j	concentration of species j
$\overrightarrow{V}_0$	forward initial reaction velocity
$\overleftarrow{V}_0$	reverse initial reaction velocity

Greek

α_2	Langmuir adsorption Isotherm coefficient (total sites of adsorption)
γ	Langmuir Isotherm coefficient $= \frac{1}{K_{ads}}$
α or α_1	$=\frac{\alpha_2}{\alpha}$
θ_A	fraction of occupies sites for specie $\frac{[A]_{ads}}{[A]_{max}}$
δ	film thickness
∞	infinity
Δ_w	$\frac{\delta_w}{D_A}$

Δ_o	$\frac{\delta_o}{D_A}$
λ	heat of adsorption
ϕ	partitioning coefficient

Subscript

org	organic phase
e, eq	equalibrium
ex	extraction
1, 2, ...	reaction number
0 (zero)	initial conditions at time zero
ad	adsorbed species at surface or interface
w	aqueous or water phase
o	organic phase
max	maximum
des	desorption
i	interfac; species counter
add	adduct
poly	polymeric
MA_m	neutral metal extractant complex for a metal of valence m

Superscript

+	positive valence
-	negative valence
*, o,	indices for extraction or adsorbtion equalibrium coefficients (see equations 3.16 and 3.17

Acronyms

D2EHP, DEHP, HDEHPA } Diethylhexylphosphoric acid

5. Modeling the Membrane Contactor

5.1 The Liquid/Liquid Membrane Extractor

As previously defined, a membrane is a semi–permeable barrier between two phases defined by what it does and not by what it is. The membrane separation is a rate process accomplished by a driving force, not equilibrium between the phases [?]. In section 1.1.3 three different types of liquid/liquid extractors or membranes were introduced. Of primary interest to this study are the immobilized or supported liquid membranes and the membrane contactor. The emulsion liquid membrane is discussed in a relative and historical sense. These membrane processes allow a fast and selective separation of chemical species due to high mass transfer surface area to volume ratios. Compared with polymer membranes the diffusion coefficients of these membranes are much greater. Their greater selectivity is brought about by the use of a mobile carrier initiating the facilitated transport process to enhance the separation.

A large number of works have been published in this area for various separations. Noble and Way [?] give a good overview of this technology. Boyadzhiev [?] also review the technology of liquid membranes. The liquid pertraction (as Boyadzhiev refers to liquid membranes) is simple conceptually but complex theoretically. The membranes are made up of two miscible or partially miscible liquids separated by a third, immiscible, phase. These three phases create interfaces on either side of the inner phase. The mass transfer and kinetics at interfaces is quite complex and has been addressed frequently in the literature but is still not well understood. The interface will be addressed separately in the discussions of this study.

The membrane contactor has been described in section chapter 1 as a microporous structure that separates two immiscible fluids while mass transfer between the phases is accomplished. The membrane contactor is a unit that separates the extraction and stripping stages of the membrane process into two separate processes. Other membrane process have these processes inherently inseparable. The microporous structure is actually a hollow small diameter cylindrical filament made of various synthetic (or in some rare cases natural) material with microscopic pores that are filled either with an organic phase or aqueous phase depending on the material that the filament is made. A hdrophobic material will cause the organic or more non-polar fluid to invade and fill the pores and eventually permeate to the opposite side of the filament unless counteracted by another force. The contactor in reality

is a number of these filaments packed into a container, generally cylidrical itself, that allows flow of one of the fluids outside the filaments refered to as tubes or lumin and the other fluid to flow inside the lumin. The only contact allowed is at the interface of the two fluids via the pore structure (see figure —1). This container packed with these hollow fiber filiments is refered to as the membrane contactor module.

Previous literature or modeled it as a module through empiracle phenomenological correlations of the mass transfer processes through a resistance theory where the membrane is assumed to be a separate phase resistance and not modeled as the interface with adsorption and reaction at the interface in the porous structure of the fiber walls [?], [?], [?], [?], [?], [?], [?], [?], [?], [?], [?], [?], [?], [?], [?], [?], [?],[?], [?]. From these example referenced literature the field has been active for over twenty years, but is still not developed at the fundamental kinetic, transport, and interfacial approach though there has been efforts forward in this area. For example the references [?], [?], [?], [?], [?], [?], [?], [?], [?], [?], [?], [?], [?], [?], [?] have completed more fundamental mathematical and/or computer simulation studies. Yoshizuka et al modeled the contactor membrane process as a single fibere concentrically inside another cylinder from a fundamental simulation approach. In this study the more fundamental modeling of the module will be used to approach a more realistic simulation of the module itself. The transport equations for the shell side, tube side, and in the pore structure of the filament wall is developed and resembles very closely the transport models of a shell and tube heat exchanger and thus the theory can, in places be developed as analogous to the heat exchanger transport model..

To properly understand the modeling of the membrane contactor, the diffusive transport mechanisms associated with membranes will be discussed and then the modeling of porous structures will be discussed. The governing equations for the diffusion in each phase of the module will be presented (i.e. the lumen side, the porous structure, and the shell side). The shell side transport becomes complicated since the flow, though assumed laminar, is parallel to the axis of a bundle of fibers contained within a hull. Thus the shell side flow is much like the shell side flow of fluid through a rod cluster in a shell and tube heat exchanger. The velocity profile in the shell side is a critical factor in the design of a shell and tube heat exchanger. Because of the well known analogous behavior of the transport properties (mass, energy and momentum) it is proposed here that this will also be apparent in the mass transfer through microporous hollow fibers. The geometry of the fiber placement is also critical. As will be presented the fibers are placed randomly and accounting for this complicates the modeling further.

5.1.1 Membrane Diffusive Transport Mechanisms

The transport across a membrane can be divided into three divisions [?], [?]

1. Simple or passive diffusion
2. Facilitated diffusion
3. Active Transport

The first category is the ordinary mass transfer (molecular diffusion) most familiar to engineers and scientists and is the movement of a substance from a region of high concentration to a region of low concentration. This type of transport is characterized by the chemical potential gradients of the diffusing species without the presence of carrier molecules or diffusion coupled chemical reactions. The transport rate is proportional to the solubility and diffusivity of the substance. In contrast the other two categories of facilitated diffusion and active transport use a molecule to complex or react and "diffuse" the species against its concentration gradient.

In facilitated, also called passive carrier transport, and active transport the diffusing species reacts in a region (phase) with a carrier molecule forming a complex. This complex then moves down its concentration gradient to another region where it releases the species. This uptake and release reaction proceeds in an equilibrium setting and energy input is not required. Active transport, is similar to facilitated transport but the transport is against the concentration gradient or chemical potentials. Without further energy input this would violate the second law of themordynamics.

Active transport phenomenon is accomplished within the constraints of thermodynamics by utilizing energy input from chemical reactions. The use of chemical reactions is common to the facilitated and active transport. The facilitated transport generally uses one or maybe two reactions to accomplish the transport at or near an interface. The active transport, however, uses a series of complex reactions in the membrane to accomplish the transport against the normal gradient potentials. Simply put, for active transport a catalyst exist at one side of the membrane where the diffusive species reacts with the carrier with the aid of the catalyst. At the other side of the membrane another catalyst decomposes the complex of species and carrier into separate species. At this side of the membrane the local concentration is higher inside the membrane than on the outside and the species diffuses through the interface or membrane wall. Active transport is primarily a natural biological phenomena where the catalyst is an enzyme. The facilitated transport is the mechanism of the metals extraction and concentration to be studied here.

As discussed previously (chapter 1) liquid membranes tend to be unstable because of dissolution, osmotic forces, and inverted micelles. A method to improve membrane stability is to chemically bind the mobile carrier within the membrane [?].

The reaction for a liquid membrane is generally carried out at or close to the interface. This reaction constitutes part of the boundary condition for the transport equations [?]. A system of second order nonlinear differential equations usually are needed to describe the concentration field within the membrane [?]. The modeling literature for the liquid membrane has been briefly discussed. Schultz et al [?], [?] discuss the mechanistic aspects, mathematical aspects and analysis, and characteristic regims of carrier mediated transport in membranes. Their emphasis was/is on the constant diffusivity, steady state behavior, homogeneous chemico-diffusion model for membrane transport.

5.2 Current State of the Art Models

5.2.1 Film Theory

In the previous section a number of published works were referenced that used a simplified theory and empirical correlations to model transport in membrane processes, specifically hollow fiber membrane contactors. A number of assumption are needed for this model [?]:

1. Steady state mass transfer at equilibrium.
2. No immiscible displacement taking place through the pores (i.e. no convective flow through the membrane).
3. Solute is present in high dilution so that diffusion induced convetion perpendicular to the interface can be neglected.
4. Aqueous organic interface at the opposite pore throat of the wetting pase (i.e. for hydrophobic membrane this is at the aqueous membrane interface for hydrophylic this is on the organic membrane interface)
5. Uniform pore size and wetting characteristics throughout the membrane.
6. Negligible influence of aqueous organic interface curvature on solute distribution coefficient rate of solute transfer and interfacial area.
7. No chemical reaction.
8. Solute transport in the aqueous phase and the organic phase outside the membrane may be described by simple film-type mass transfer coefficients without bulk flow correction.
9. The diffusion of solute i through the wetting phase filled pore may be described by means of a membrane transfer coefficient k_{imo} based on the total area of the membrane

(including porous and nonporous sections). Note that this is different for the type of material used i.e. hydrophobic or hydrophylic.

10. No solute transport through nonporous sections of the membrane.
11. The aqueous and organic film resistances may be combined with the membrane pore diffusion resistance as a one dimensional series of diffusion resistances.
12. Solute distribution coefficient m_i is constant over the relevent concentration range and the two liquids are essentially insoluble in each other.

The simplified model is an example of the classical two film theory presented in all classical mass transfer textbooks [?, page 146], [?], [?, chapter 21], [?]. Sirkar and co-workers have used this model extensively in their work on membrane separations. The film theory provides a simple insight of the resistances to mass transfer at an interface without an enormous amount of mathematics. There are several disadvantages to using the two film theory. One is that the type of membrane (hydrophobic or hydorphilic) and the direction of transfer as well as whether the organic is inside the tube or outside the tube has to be known *a priori*. If this is known then the solute flux terms can be formalized in terms of individual mass transfer coefficients and converted to an overall mass transfer coefficient. To calculate the overall transfer coefficient the area should be based upon the diameter where the aqueous-organic phase interface is located [?], [?], [?], [?]. Consider a hydrophobic fiber with mass transfer from the aqueous phase (tube side) to the organic phase (shell side) then the flux is written (reference figure ??)

$$\begin{aligned} N_i \pi d_{ti} &= k_{i(aq_t)} \pi d_{i(t)} \left(c_{i(aq_b)} - c_{i(aq_{int})} \right) \\ &= k_{i(m_o)} \pi d_{t(lm)} \left(c_{i(o_{int})} - c_{i(o_m)} \right) \\ &= k_{i(o_s)} \pi d_{t(o)} \left(c_{i(o_m)} - c_{i(o_b)} \right) \\ &= K_o \pi d_{i(t)} \left(c^*_{i(o)} - c_{i(o_b)} \right) \\ &= K_w \pi d_{i(t)} \left(c_{i(aq_b)} - c^*_{i(aq)} \right) \end{aligned} \tag{5.1}$$

where $k_{i(\ )}$ are the individual mass transfer coefficients calculated using appropriate area; K_γ overall mass transfer coefficient based on the repective phase given as the subscript γ; $c_{i(\ )}$ are the concentrations at specific locations given by the subsccripts in the parenthesis; d is the respective diameter to calculate the appropriate area; subscripts i is the specie transferred, t tube side, o the organic phase, m the membrane phase, b respective bulk phase, aq the aqueous phase, int the interface locale, lm log mean, s shell side of the fiber; and for the superscript $*$ is the equilibrium value with the concentration in the opposite phase. Making use of the assumed equalibrium conditions a Henry's law type of distribution

is implied or

$$\begin{aligned} m_i c_{i(aq_b)} &= c^*_{i(o)} \\ m_i c_{i(aq_{int})} &= c_{i(o_{int})} \\ m_i c^*_{i(aq)} &= c_{i(o_b)} \end{aligned} \tag{5.2}$$

and thereby the distribution coefficient is

$$m_i = \frac{c^*_{i(o)}}{c_{i(aq_b)}} = \frac{c_{i(o_{int})}}{c_{i(aq_{int})}} = \frac{c_{i(o_b)}}{c^*_{i(aq)}}. \tag{5.3}$$

Combining equations 5.1 and 5.3 we can solve for the interfacial concentrations and assuming the validity of the series of resistances for mass transfer i.e.[?]

$$\frac{1}{K} = f(R_{b1}, R_{b2}, R_m, m_i) \tag{5.4}$$

where R_{b1}, R_{b2} are the respective individual film transfer resistances to mass transfer and m_i is the solute distribution or partition coefficient and R_m is the mass transfer reisitance of the liquid filling the membrane pores. Thus the overall transfer coefficient based on the organic resistance can be determined

$$\frac{1}{K_o d_{i_t}} = \frac{1}{d_{t(o)} k_{i(o_s)}} + \frac{1}{d_{t(lm)} k_{i(m_o)}} + \frac{m_i}{d_{i_t} k_{i(aq_t)}} \tag{5.5}$$

or for the aqueous side overall transfer resistance

$$\frac{1}{K_{aq} d_{i_t}} = \frac{1}{m_i d_{t(o)} k_{i(o_s)}} + \frac{1}{m_i d_{t(lm)} k_{i(m_o)}} + \frac{1}{d_{i_t} k_{i(aq_t)}}. \tag{5.6}$$

Because of the different conditions or scenarios for the types of membrane properties (hydorphilic or hydrophobic) and the various fluid flow conditions, counter current or co-current, aqueous in the tube or organic inside th tube there are a number of overall mass transfer coefficients equations. These are listed in the table below (after Prasad and Sirkar[?], [?]:

Membrane Type and Form	$\frac{1}{K_o}=$	$\frac{1}{K_{aq}}=$
Hydrophobic MHF		
Aqueous in Tube	$\frac{d_{i_t}}{d_{t(o)}k_{i(o_s)}} + \frac{d_{i_t}}{d_{t(lm)}k_{i(m_o)}} + \frac{m_i d_{i_t}}{d_{i_t}k_{i(aq_t)}}$	$\frac{d_{i_t}}{m_i d_{t(o)}k_{i(o_s)}} + \frac{d_{i_t}}{m_i d_{t(lm)}k_{i(m_o)}} + \frac{d_{i_t}}{d_{i_t}k_{i(aq_t)}}$
Organic in Tube	$\frac{d_{t(o)}}{d_{i_t}k_{i(o_t)}} + \frac{d_{t(o)}}{d_{t(lm)}k_{i(m_o)}} + \frac{m_i d_{t(o)}}{d_{t(o)}k_{i(aq_s)}}$	$\frac{d_{t(o)}}{m_i d_{t(o)}k_{i(o_s)}} + \frac{d_{t(o)}}{m_i d_{t(lm)}k_{i(m_o)}} + \frac{d_{t(o)}}{d_{t(o)}k_{i(aq_s)}}$
Hydrophilic MHF		
Aqueous in Tube	$\frac{d_{t(o)}}{d_{t(o)}k_{i(o_s)}} + \frac{m_i d_{t(o)}}{d_{t(lm)}k_{i(maq)}} + \frac{m_i d_{t(o)}}{d_{i_t}k_{i(aq_t)}}$	$\frac{d_{t(o)}}{m_i d_{t(o)}k_{i(o_s)}} + \frac{d_{i_t}}{d_{t(lm)}k_{i(maq)}} + \frac{d_{t(o)}}{d_{i_t}k_{i(aq_t)}}$
Organic in Tube	$\frac{d_{i_t}}{d_{i_t}k_{i(o_t)}} + \frac{m_i d_{i_t}}{d_{t(lm)}k_{i(maq)}} + \frac{m_i d_{i_t}}{d_{t(o)}k_{i(aq_s)}}$	$\frac{d_{i_t}}{d_{i_t}k_{i(o_t)}} + \frac{d_{i_t}}{d_{t(lm)}k_{i(maq)}} + \frac{d_{i_t}}{d_{t(o)}k_{i(aq_s)}}$

The porous structure of the membrane is incorporated in the solute mass transfer coefficient $k_{i(m_o)}$ or $k_{i(m_{aq})}$. Estimation of the mass transfer coefficient for unhindered diffusion of species i through organic solvent filled microporous membrane is with the effective diffusivity $\mathcal{D}_{i_{eff}}$ [?]

$$k_{i(m_o)} = \frac{\mathcal{D}_{i_{eff}}}{l} = \frac{\varepsilon_m \mathcal{D}_{i_o}}{\tau_m l} \tag{5.7}$$

where ε_m is the membrane porosity and τ_m is the membrane tortuosity, l is the membrane thickness, and $\mathcal{D}_{i_o}$ is the free diffusion coefficient of solute i in the organic solvent. And for the aqueous phase

$$k_{i(m_{aq})} = \frac{\mathcal{D}_{i_{eff}}}{l} = \frac{\varepsilon_m \mathcal{D}_{i_{aq}}}{\tau_m l} \tag{5.8}$$

and replacing the thickness by l with $\frac{d_{t_o} - d_{t_i}}{2}$ the expressions above can be used for hollow fibers [?].

The assumption that make equations 5.7 and 5.8 valid is [?]

1. There is unhindered diffusion of solute
2. The membrane is symemtric and completely wetted by the designated phase
3. No two-dimensional effects occur.

A critical assumption is that the membrane is completely wetted or filled by the appropriate phase. If the excess pressure that keeps the wetting phase from flowing into the non-wetting phase region approaches the critical or breakthrough pressure, Δp_{cr}, then the interface is located inside the pores of the membrane and at least two phases are present in the pores. At this condition the location of the interface is uncertain and the membrane transfer coefficient expressions are unknown making the predictions of the solute concentrations unpredictable.

Effect of Pressure The effects of pressure have, in general, been shown to be negligible by Sirkar, Prasad and co-workers (cf [?] and [?]. This is a result of the magnitude of the term $\overline{V}_i \Delta p$ of the chemical potential equation

$$\Delta \mu_i = RT \Delta \ln c_i + \overline{V}_i \Delta p \tag{5.9}$$

generally being an order magnaitude smaller than the first term. This pressure independence, as has been mentioned, dissapears close to the critical pressure and immiscible displacement occurs of the liquid in the pores. This causes the membrane resistance, m_i, to

change consideribly (reference the overall extraction coefficient equations above). In hollow-fiber systems a change in Δp beyond a certain value will cause the membrane structure to deform. In a compression the pores may become smaller and restricted and the fiber walls "thinned". In tension pore sizes are increased reducing Δp_{cr}.

Critical pressure or breakthrough pressure is the pressure to ensure non-dispersive extraction with a microporous membrane. The pressure of the phase not in the pores must not exceed the pressure of the phase in the pores by more than a certain determained value for a specific system. Modeling the structure of a microporous membrane as a collection of parallel cylindrical poares of radius r_p, then the critical pressure can be determined by the Young-Laplace equation [?]

$$\Delta p_{cr} = \frac{2\gamma_{wo}\cos\theta_c}{r_p} \tag{5.10}$$

where γ_{wo} is the interfacial tension and θ_c is the contact angle measured from the pore wall to the tangent of the liquid-liquid interface drawn into the pore liquid. Correlation of models for membranes with noncylindrical pores have been studied (see the reference of [?, page 746]). In conventional extraction processes the interfacial tension is very critical. In the membrane based systems using two film theory γ_{wo} does not influence the mass transfer coefficients and only influences the value of Δp_{cr} [?]. This may not be so under circumstances or systems that have strong spontaneous convection terms, interfacial reactions reactions and non equilibrium conditions.

Distribution Coefficient The distribution coefficient, as defined by the equilibrium equation in equation 5.3, is an important relationship for the two film theory of membrane transport. It allows us to relate the phases without having to know anything about interfacial phenomenon; however, this relationship is only valid under equilibrium conditions. The magnitude of m_i allows a qualatative analysis of the extraction process:

- For $m_i \gg 1$ implies the solute prefers the organic phase and the aqueous phase resistance will control
- For $m_i \ll 1$ implies the solute prefers the aqueous phase and the organic resistance will control.

In the membrane system, the membrane resistance will be important if the membrane pores have the same fluid that is controlling the resistance. Thus in some instances the membrane resistance may not effect the mass transfer at all unless there is hindered diffusion or the membrane is exceptionally thick [?]. Under these conditions the membrane resistance may still be important regardless of the magnitude of m_i.

When $m_i \gg 1$ a hydrophobic membrane is much better where as for a $m_i \ll 1$ a hydrophilic membrane is preferred [?]. That is a hydrophobic membrane is preferred for a solute preferring the organic phase and a hydrophilic for solute preferring the aqueous phase. These factors in chosing the type of membrane to be used are a good first estimate of the membrane to be used. There may be other factors; for example, The use of polar-non-polar organic systems a hydrophobic membrane can be operated with the polar organic in the pores [?]. Hydrophylic membranes can also be operated with the organic phase in the pores [?].

Design Models and Correlations of the Extraction Device

There are basically two ways to model the hollow fiber membrane extraction device [?]

1. Determine an overall mass transfer coefficient for the extractor using correlations and use a mean concentration driving force across the extractor, calculate the total rate of solute extraction
2. Solve numerically two differential equations for concentration profiles on the tube side and shell side coupled through the boundary conditions of diffusive transport through the liquid-filled membrane pores.

Prasad, Sirkar and co-workers and most other workers have in the past used the first method. The second method has seen efforts from the Japanese school [?], [?] and others [?], [?], [?]. Except for the works of Yoshizuka *et al.* the interface complexities were not addressed to any degree. Chemical reactions were addressed usually by an effectiveness factor or modulus like the Hatta number, Thiele modulus, or the Damköhler group. There is actually a third way to model the membrane that is much more fundamental than any presented so far in the literature and we will develop the method for this study in later sections. For now the equations for the two film theory without chemical reaction are listed in the following table. These equations are derived using a simple differential solute material balance about the membrane (see Sirkar and co-workers) for countercurrent flow configuration the length of the membrane is calculated as

$$L = \frac{Q_{aq}}{\overline{K}_{aq}(\pi d_{i_t})} \frac{1}{\left\{1 - \left[\frac{Q_{aq}}{m_i Q_o}\right]\right\}} \ln \left[\frac{\left(c^{in}_{i(aq_b)} - \frac{c^{out}_{i(O_b)}}{m_i} \right)}{\left(c^{out}_{i(aq_b)} - \frac{c^{in}_{i(O_b)}}{m_i} \right)} \right] \tag{5.11}$$

For a given . $c^{in}_{i(aq_b)}, c^{in}_{i(O_b)}, \overline{K}_{aq}, Q_{aq}, Q_o, m_i, L$, and d_{i_t} , then the aqueous bulk effluent concentration can be obtained by using the overall balance equation to obtain

$$c^{out}_{i(aq_b)} = \frac{c^{in}_{i(aq_b)}\left(1-\frac{Q_{aq}}{m_i Q_o}\right) - \frac{c^{in}_{i(O_b)}}{m_i}\left[1-\exp\left(\frac{L\left\{1-\left[\frac{Q_{aq}}{m_i Q_o}\right]\right\}}{LTU}\right)\right]}{\exp\left(\frac{L\left\{1-\left[\frac{Q_{aq}}{m_i Q_o}\right]\right\}}{LTU}\right) - \frac{Q_{aq}}{m_i Q_o}} \tag{5.12}$$

where LTU is the length of transfer unit very similar to HTU in typical mass transfer operations and is defined by

$$LTU = \frac{Q_{aq}}{\overline{K}_{aq}(\pi d_{i_t})N} \tag{5.13}$$

where N is the number of fibers in the module. Typically one needs to know the length of a module to effect a certain effluent concentration. This is obtained by

$$L = LTU \times NTU \tag{5.14}$$

and the number of transfer units NTU is defined by

$$NTU = \frac{1}{\left\{1-\left[\frac{Q_{aq}}{m_i Q_o}\right]\right\}} \ln\left[\frac{\left(c^{in}_{i(aq_b)} - \frac{c^{out}_{i(O_b)}}{m_i}\right)}{\left(c^{out}_{i(aq_b)} - \frac{c^{in}_{i(O_b)}}{m_i}\right)}\right]. \tag{5.15}$$

This method is valid if a module averaged $\overline{K}_{aq}$ is available. The equation to be integrated is 5.6 and K_{aq} is available over the distance x along the flow direction if $k_{i(o_s)}$ and $k_{i(aq_t)}$ are available as function of x and the value $k_{i(m_o)}$ is known. Generally this is not the case and exact analytical expressions for these values are known as function of tube length for laminar flow conditions for constant wall concentration or constant wall flux. Neither represent the actual conditions in a hollow-fiber extractor. Prasad and Sirkar give a method to approximate these values assuming $K_{aq} \cong k_{i(aq_t)}$ for $m_i \gg 1$ and uniform wall concentration and laminar parabolic flow the analytical Graetz solution may be used. Two forms of the solution are given; one for the average Sherwood number based on arithmetic-mean driving force, and the other for local Sherwood number. Prasad and Sirkar [?]also use a more simplified Leveque solution to attempt to theoretically calculate film transfer coefficient on the tube side rather than the complex Graetz equation.

$$Sh\,|_{tube} = \frac{\overline{k}_{aq_t} d_{i_t}}{D_{i_{aq}}} = 1.6151\left[\frac{d_i}{L} Re_t Sc_i\right]^{0.33} \tag{5.16}$$

where $\int_0^L k_{i(aq_t)}dx = \overline{k}_{i(aq_t)}L$ and assuming $\overline{K}_w \cong \overline{k}_{i(aq_t)}$ and substituting this equation into equation 5.13 then and analytical expression can be obtained for LTU. In general, to use the Graetz correlation experimental data are needed to calculate empirical mass transfer coefficients and determine if the equation is valid to describe the mass transfer coefficients as a funtion of x.

Based on the Graetz solution for laminar parabolic flow and developing mass transfer for uniform wall concentration Prasad and Sirkar have found the following corrlations describe the tubeside coefficient for species i for hollow fibers of d_{i_t} ID and length L:

$$Sh_i = \frac{k_{i_t} d_{i_t}}{\mathcal{D}_{i_t}} = 0.5 \left(\frac{d_{i_t}}{L}\right) Re_t Sc_i \frac{1-\zeta}{1+\zeta}, \tag{5.17}$$

where

$$Re_t = \frac{d_{i_t} v_t}{\nu_t}, \tag{5.18}$$

$$Sc_i = \frac{\nu_t}{\mathcal{D}_{i_t}} \tag{5.19}$$

$$\zeta = \sum_{n=1}^{\infty} -4 \left(\frac{B_n}{\beta_n^2}\right) \left(\frac{d\phi}{dr_+}\right)_{r_+=1} \exp\left(\frac{-2\beta_n^2 L}{d_{i_t} Re_t Sc_i}\right), \tag{5.20}$$

$$\beta_n = 4(n-1) + 2.666, \quad n = 1, 2, 3, \ldots, \tag{5.21}$$

$$B_n = -(1)^{n-1} \times 2.84606 \beta_n^{\frac{-2}{3}}, \tag{5.22}$$

$$-B_n \left(\frac{d\phi}{dr_+}\right)_{r_+=1} = 2\left(1.01276 \beta_n^{-0.33}\right). \tag{5.23}$$

These correlations were developed with both hydrophobic and hydrophylic hollow fibers for $300 < Sc_i < 1000$ and $0 < Re_t < 60$.

The above were correlations for the tubeside mass transfer correlations the shell side as Given by Prasad and Sirkar [?] are listed now. For parallel flow

$$Sh_i = \frac{k_{i_s} d_e}{\mathcal{D}_{i_s}} = 5.85 (1-\phi) \left(\frac{d_e}{L}\right) Re_s^{0.66} Sc_s^{0.33} \tag{5.24}$$

where

$$Re_s = \frac{d_e v_s}{\nu_s}, \tag{5.25}$$

$$Sc_i = \frac{\nu_s}{\mathcal{D}_{i_s}} \tag{5.26}$$

ϕ is the packing density of the fibers in the module or shell, d_e is the hydraulic diameter of the shell (4× cross-sectional area/wetted perimeter). Cussler and co-workers used the following for parallel flow in the shell

$$Sh_i = \frac{k_{i_s} d_e}{\mathcal{D}_{i_s}} = 8.8 \left(\frac{d_e}{L}\right) Re_s Sc_s^{0.33} \tag{5.27}$$

and for the tubeside mass transfer

$$Sh_i = \frac{k_{i_t} d_{i_t}}{\mathcal{D}_{i_t}} = 1.5 \left(\frac{d_{i_t} v_t}{L \mathcal{D}_{i_t}}\right)^{1/3} \tag{5.28}$$

Chemical Reactions

Sirkar and co-workers have recently evaluated the perforamance of membrane solvent extraction with chemical reactions [?], [?]. For an instantaneous reaction at the phase interface of a hydrophobic membrane, then the aqueous film resistance (third term) of equation 5.5 will be missing; and, for a hydrophylic membrane the aqueous and pore filled resistance term will be missing [?, page 32]. This is basically the Hatta modified two film theory of mass transfer with a simultaneous reaction. Application requires a knowledge of the reaction plane. Basu [?] considered two cases in the extraction of (1) Citric Acid from a dilute aqueous solution using tri-n-octylamine in a diluent and (2) the extraction of copper

Case I Reaction plane is in the aqueous film

Case II Reaction plane is the phase interface.

In his study, Basu also used the contained hollow fiber liquid membrane. In this configuration the stripping and extraction phases are contained in different filaments with a facilitation fluid between them. Solute is extracted form a feed stream into the facilitation fluid and then back extracted or stripped from the facilitation fluid to a stripping fluid in another tube contained in the same bundle as the feed tube. Because of this both co-current and counter current flow is obtained relative to the facilitation fluid.

The concentrations vary down the length of the membrane and are modeled by a series of differential equations which are solved numerically using a Runge Kutta package form IMSL. An analytical solution to the system of algebraic differential equations defining this problem, like that obtained without a reaction in a single HFM, is not possible due to the reaction at the interface being non-linear. Basu solved it numerically.

In the absence of any chemical reaction the overall mass transfer coefficient will be a function of ~~coefficients~~ [?, page 46]

1. five individual transfer Coefficients
   (a) Two aqueous boundary layers
   (b) Two porous substrates
   (c) and the Contained Liquid membrane
2. the fiber dimensions
3. the distribution coefficients.

The prediction of mass transfer coefficients using methods previously discussed appear to work fairly well for the contained liquid membrane system without a chemical reaction. For a system with a chemical reaction the predictions of the mass transfer coefficients become inaccurate and appear to be dependent on the type of reaction (irreversible or reversible) and the direction that it occurs (from organic to aqueous or aqueous to organic). The ability to predict the mass transfer coefficients for the reacting species is necessary for the theoretical models. Calculations of mass transfer coefficients use the diffusion correlation of Wilke and Chang devided by the effective thicness of the HFCLM. The calculations of the effective membrane thickness from the experimental data and that using physical parameters of the porous membrane differ by 4.2 times [?, page 204]. Basu gives three possible explanations:

1. Actual values of the membrane thickness, δ_m, is much larger than that predicted theoretically
2. actual value of the tortuosity is larger than that obtained from the literature and manufacture's information
3. there may be interfacial resistance of mass transfer not accounted for in the calculations for the effective thickness using experimental data.

Basu, through gas permeation experiments, determined a value for the membrane thickness, δ_m, to be 76.2 to 452.1 μm. He states these are high compared to 110 μm that were theoretically determined based on a regular pattern development of the fibers in the module; but, does not explain the large differences in the calculated effective thicknesses for the HFCLM that are given by

$$t_{eff} = \frac{d_i}{d_{lm}} \left(\frac{\tau_s (d_o - d_i)}{\varepsilon_s} \right) + \left(\frac{d_i}{d_o} \right) \delta_m. \tag{5.29}$$

From this equation δ_m only effects one term. Thus the effect of δ_m is porbably not significant enough to cause the large difference in and of itself. Using the value for δ_m a value of tortuosity was determined to vary from 13.4 to 14.6. These values are approximately 4.5 to 7.5 higher than normal values for this same type of membrane given by Kiani *et al* [?] and Prasad and Sirkar [?]. Thus the higher values are attributed to interfacial effects.

This is a very relative and important conclusion for this study. As pointed out in other portions of this report and other authors [?],[?],[?], [?], [?], [?], [?], [?], [?], [?], [?][?], [?], [?], [?], [?], [?], [?], [?], [?], [?], [?], [?], [?], [?], [?], [?], the interfacial effects in solvent extraction, especially in metal extraction, is extremely important. It also illustrates a limitation of the film theory. The amount of citric acid removed, as for any solute transferred, is dependent upon flow. The percentage removed is shown for the experimental and theoretical values in Basu's table 4.6-4 and 4.6-5. Though not shown, the difference in the theoretical and experimental values varies from 14 to 36 percent. The theoretical value always being higher. The mass transfer rate was also higher approximately 14 to 35 percent higher than the experimental removal rates. Just observing the actual values they look close but do have significant error though the lower end could be within experimental error.

However, as Basu himself recognized, his model has inherent inadequecies [?, page 172] and the predicted or theoretical mass transfer coefficients values match the experimental values for some systems and for others they do not. An example of this phenomenon is that of acetic acid extracted from phenol-MIBK into water system and extraction of acetic acid from phenol-Deconol into water. In the first sytem the experimental and theretical values match fairly well. In the later they do not. Basu supposes that the the higher viscosity of the decanol then the solute diffusivities in the membrane are low and the fibers were different having a lower viscosity. The effects of diluent on extraction has been known for some time and studied fairly extensively [?], [?], [?], [?]. The effects of diluents may enhance the extraction by enhancing the chemical activity of the active organic consituant through solvation or other phenomenon.

Also noted in Basu's dissertation is the time dependent mass transfer rates. Depending on the sytem, the time to reach steady state took from 2 to over 12 hours . This in itself shows that a model based on a steady state assumption cannot be used until after the steady state is reached. As Higbie pointed out many years ago, the time of exposeure of a fluid to mass transfer is short and the concentration gradient of the film theory indicative of steady state does not have time to develop [?, page 50].

Summary of Film Theory Modeling of Hollow Fiber Membranes

The two film theory offers a simplier model and good insight into the performance evaluations of hollow fiber membrane transport processes. It provides a method to predict, albeit limited, effects of some process parameters. To do so, however, requires empirical correlations for each specific system. The most difficult disadvantage is that of the mass transfer coefficients and relating them as a function of position along the membrane length. The two film theory inherently assumes steady state concentration gradient conditions and the study of the effects of transient influences is not easily studied. The more complex the system is, the more difficult and less accurate the film theory becomes since it will lump a great deal of the physical system together. In fact, Prasad and Sirkar actually had to go to a more complete model, the Graetz solution to obtain correlations for the mass transfer coefficient correlations. This is somewhat ironic since the film theory is usually used as a predictive method for the mass transfer coefficients [?, page 50]. The two film theory allows no study of the effects of the interface, complex reactions, complex geometrical flow (i.e. random arrangement of fibers in the shell), or unsteady state non-qualibrium conditions. Basu, in his study also noted that the time to steady state was long indicating insantaneous reaction was not present or that the interfacial resistance was not negligible.

Additionally different equations for the mass transfer coefficients have to be formulated for each type of membrane (hydrophobic or hydrophilic), the fluid flow configuration (counter current or co-current), which phase is in the shell and which is in the tube, and what is the direction of mass transfer (aqueous to organic or *vice versa*. This gives a possibility of sixteen scenarios that have different modeling equations for the mass transfer coefficients.

Counter Current			
Hydrophobic		**Hydrophilic**	
Shell	**Tube**	**Shell**	**Tube**
organic	aqueous	organic	aqueous
organic→	aqueous	organic→	aqueous
aqueous→	organic	aqueous→	organic
aqueous	organic	aqueous	organic
organic→	aqueous	organic→	aqueous
aqueous→	organic	aqueous→	organic

Co-Current			
Hydrophobic		**Hydrophilic**	
Shell	**Tube**	**Shell**	**Tube**
organic	aqueous	organic	aqueous
organic→aqueous		organic→aqueous	
aqueous→organic		aqueous→organic	
aqueous	organic	aqueous	organic
organic→aqueous		organic→aqueous	
aqueous→organic		aqueous→organic	

Rahul Basu's[?] doctoral dissertation modeled and experimentally evaluated a contained hollow fiber liquid membrane with a chemical reaction. An anaylis of his dissertation reveals that the two film theory, though a simpler method for a first order evaluation to characterize the process, is inadequate to predict performance of this process. Most of the difficulty lies with the inability to realistically model the interface and the assumption of equilibrium conditions. This assumption allows for a simple partitioning analysis which is more than likely an oversimplification of a process that reacts at or near the interface. The interfacial reaction is heterogeneous and can cause a departure from equilibrium especially if the reaction is a slow reaction. This can lead to a reduction in mass-transfer rate. Conversely, the spontaneous convection or the Marangoni effect can increase the mass transfer rate (see section on Interfacial Phenomenon). Neither of these two deviations from equilibrium are placed in the two film model.

Other problems of spacial configuration and orientation of the fibers especially between the feed and strip fibers in the shell and the flow in the shell could be of significant importance. The location of the interface may not be at the pore mouth of the non-invading fluid and may be somewhere in the pore itself. Pore structure could be of high importance in the diffusional analysis especially if the membrane is not as symetrical as assumed.

Classic models that improve on the two film theory such as the penetration and surface renewal models may aid in obtaining a more representative model of the MHFM or HFCLM. They are not restricted to steady state and have a method of surface age distribution [?, page 51] and can be more readily modified to account for complexities of the system.. A combination of the film surface renewal theory like that presented by Dobbins and referenced by Treybal may give better mass transfer coefficients, but basically this would be the same as that presented by Basu and using Graetz correlations.

5.2.2 Penetration and Surface Renewal Theory

The penetration and surface renewal theory are basically the same except that the surface renewal assumes a probability function for time of exposure of a mass element to mass

diffusion. The penetration theory has a set time of exposure. Secor and Beutler [?] have used the pentration theory for diffusion accompanied by a reversible chemical reaction considering many geometries (plane sheets, flat plate with impervious edges, infinite cylinder, a cylinder with impervious ends, and a sphere; but not specifically a membrane. A generalized treatment of the the diffusion accompanied by a single, generalized, reversible, chemical reaction with the following assumptions:

1. The reaction is of the form
$$\gamma_A A + \gamma_B B - \gamma_M M + \gamma_N N \tag{5.30}$$
2. Concentration of A at the surface of the medium is constant
3. Concentration of B at is initially uniform throughout the medium
4. Species B, M, and N are novolatile.
5. Transport of all species is by molecular diffusion alone
6. The diffusion coefficient of each species is constant
7. Only a single reaction is kinetically significant
8. Heat effects are negligible

The differential material balance for each species yields:

$$\mathfrak{D}_A\left(\frac{\partial^2 A}{\partial x^2}+\frac{\lambda}{x}\frac{\partial A}{\partial x}\right) = \frac{\partial A}{\partial t}+\gamma_A\left(k_1A^\alpha B^\beta - k_2M^\mu N^\nu\right) \quad \text{(Chemical Potential Equation)}$$

$$\mathfrak{D}_B\left(\frac{\partial^2 B}{\partial x^2}+\frac{\lambda}{x}\frac{\partial B}{\partial x}\right) = \frac{\partial B}{\partial t}+\gamma_B\left(k_1A^\alpha B^\beta - k_2M^\mu N^\nu\right) \tag{5.31}$$

$$\mathfrak{D}_M\left(\frac{\partial^2 M}{\partial x^2}+\frac{\lambda}{x}\frac{\partial M}{\partial x}\right) = \frac{\partial M}{\partial t}-\gamma_M\left(k_1A^\alpha B^\beta - k_2M^\mu N^\nu\right) \tag{5.32}$$

$$\mathfrak{D}_N\left(\frac{\partial^2 N}{\partial x^2}+\frac{\lambda}{x}\frac{\partial N}{\partial x}\right) = \frac{\partial N}{\partial t}-\gamma_N\left(k_1A^\alpha B^\beta - k_2M^\mu N^\nu\right) \tag{5.33}$$

where $\lambda = 0$ for semi-infinite medium or an infinite plane, $\lambda = 1$ for an infinite cylinder, and $\lambda = 2$ for a sphere. The boundary conditions for these equations are

$$A = A_0, B = B_o, M = M_o, N = N_o, t = 0, \quad t = 0, 0 \le x \le x_0 \tag{5.34}$$

$$A = A_i, \frac{\partial B}{\partial x} = 0, \frac{\partial M}{\partial x} = 0, \frac{\partial N}{\partial x} = 0, \quad t > 0, x = 0 \tag{5.35}$$

$$\frac{\partial A}{\partial x} = 0, \frac{\partial B}{\partial x} = 0, \frac{\partial M}{\partial x} = 0, \frac{\partial N}{\partial x} = 0, \quad t > 0, x = x_0. \tag{5.36}$$

Secor and Beutler solved the dimensionless forms of these equations with finite difference scheme. By integrating the flux at the surface over the time of exposure and dividing by the time of exposure the average rate of diffussion or flux is obtained [?]

$$R = -\frac{1}{t}\int_0^t \mathfrak{D}_A \left(\frac{\partial A}{\partial x}\right)_{x=0} dt \,. \tag{5.37}$$

The concentration profiles, rate of diffussion of species through the interface, and the mass transfer coefficients as a function of time can be calculated and are presented by Secor and Beutler.

The model is comparable to the film theory at high values of time and when the diffusivity ratios are near unity. At large values of time the mass transfer coefficient ratio (coefficient with a chemical reaction to that of mass transfer without a chemical reaction) approaches a constant value where diffusion with an equilibrium reaction is represented. Olander [?] has presented a model for several reaction mechanisms under equalibrium conditions using the the two film theory and the surface renewal theory. These can be solved analytically and the equations for the mass transfer coefficients for the reactions above are

$$k_A = k_A^o \left[1 + \frac{\mathfrak{D}_M}{\mathfrak{D}_A}\frac{\phi}{A_i - A_L}\right] \tag{5.38}$$

where

$$\begin{aligned}\phi \;=\; & \frac{1}{2}\left\{\left[\left(\frac{\mathfrak{D}_N}{\mathfrak{D}_M} - 1\right)\sqrt{KB_LA_L} + \frac{\mathfrak{D}_N}{\mathfrak{D}_B}A_iK\right]^2 + 4\left[\frac{\mathfrak{D}_B}{\mathfrak{D}_M}B_L + \sqrt{KB_LA_L}\right]\frac{\mathfrak{D}_N}{\mathfrak{D}_B}A_iK\right\}^{\frac{1}{2}} \\ & -\frac{1}{2}\left[\frac{\mathfrak{D}_N}{\mathfrak{D}_M}\sqrt{KB_LA_L} + \frac{\mathfrak{D}_N}{\mathfrak{D}_B}KA_i\right]\end{aligned} \tag{5.39}$$

and

$$K = \frac{MN}{AB}. \tag{5.40}$$

The mass transfer coefficients are functions not only of the various diffusivities and equilibrium constants but of the concentrations at the interface and in the bulk of the reacting phase.

Cho and Ranz [?], [?] investigated diffusion controlled and slow reaction zones in two phase liquid reactions. Their approach is pertinent to the penetration model. Consider two stagnant semi-infinite phases brought into contact along a plane interface, phase I containing a dilute concentration of species A and phase II containing a dilute concentration of species B. Scriven [?] was referenced to have shown that the reaction zone would move into one

phase or the other, depending on the following ratio (assuming an instantaneous reaction)

$$\phi = \frac{c^{II}_{B\infty}}{c^{I}_{B-\infty}}\sqrt{\frac{\mathfrak{D}^{II}_{B}}{\mathfrak{D}^{I}_{B}}}. \tag{5.41}$$

If $\phi < 1$, the reaction zone moves into phase II, while $\phi > 1$, it moves into phase I, and for $\phi = 1$, the reaction take place at the interface. Scriven also gives the location of the reaction zone or zone front x^* for $\phi < 1$ as

$$x^* = 2\beta\sqrt{\mathfrak{D}^{II}_{A}t} \tag{5.42}$$

where β is determined by

$$\phi\left(1 + m_A\Lambda_A^{\frac{1}{2}}\operatorname{erf}\beta\right) = \exp\left[\beta^2\left(\frac{1}{\Delta} - 1\right)\right]\operatorname{erf}\left[\frac{\beta}{\Delta^{\frac{1}{2}}}\right] \tag{5.43}$$

where $\Delta = \frac{\mathfrak{D}^{II}_{B}}{\mathfrak{D}^{II}_{A}}$ and $\Lambda = \frac{\mathfrak{D}^{I}_{B}}{\mathfrak{D}^{II}_{A}}$ when the reaction is in phase I changing notation can result in the smae equation for $\phi > 1$. In this particular case (fast reactions) the system is in steady state practically from the initial contact of the phases [?]. For a system with a slow reaction a steady state is approached only after a period of contact. This system is dependent upon the reaction order and rates. A reaction zone characteristic length is estimated and an estimation of the raction zone thickness is obtained. Though this method is an interesting analytical limit, it appears to be similar nature to Secor and Beutlers method (which would be expected since it is built from the penetration model). The method becomes quite involved for first order reactions and any system with reactions of order greater than first order or pseudo-first order will be extrememly difficult albeit impossible to analyze. In addition, as Cho and Ranz point out, there is no direct way of using zone front data to estimate quantitatively the effects of interfacial turbulence on transfer rates and an indirect method to obtain "reasonable approximations" is presented [?].

5.2.3 Facilitated Transport to Model the Hollow Fiber Membrane — The Graetz–Nusselt Problem

Originally solved for heat transfer, this fromulation of the diffusion transport equation is also applicable to mass transfer across walls of a pipe containing a fluid in laminar flow [?, page 296]. The problem assumes a sparingly soluble solute and a parabolic velocity profile i.e. laminar flow in steady state conditions. A steady state balance equation written for a tube with microporous walls

$$\mathfrak{D}\left(\frac{1}{r}\frac{\partial}{\partial r}\left(r\frac{\partial c}{\partial r}\right) + \frac{\partial^2 c}{\partial z^2}\right) - v_z\frac{\partial c}{\partial z} = 0. \tag{5.44}$$

The Graetz problem assumes that the axial diffusion is small compared to the axial convection thus

$$\mathfrak{D}\frac{\partial^2 c}{\partial z^2} \ll v_z \frac{\partial c}{\partial z} \tag{5.45}$$

and therefor the term $\frac{\partial^2 c}{\partial z^2} \equiv 0$ and is neglected. There has been investigations as to the inclusion of the axial diffusion, primarily in heat transfer [?], [?]. The inclusion of the axial conduction term for heat transfer (axial diffusion for mass transfer) is referred to as the extended Graetz-Nusselt problem. The justification for ignoring the axial diffusion in mass transfer processes is that for short tubes, solute diffusion occurs mainly near the wall and the bulk of the fluid near the tube's axis is pure solvent therefore axial diffusion is small and can be ignored [?, page 299].

The governing equation for steady state Graetz equation for mass transfer in radial coordinates is

$$\mathfrak{D}_i\left(\frac{\partial^2 c_i}{\partial r^2} + \frac{1}{r}\frac{\partial c_i}{\partial r}\right) = v_z \frac{\partial c}{\partial z}. \tag{5.46}$$

v_z is written as the average velocity over the tube diameter. Thus [?, page 46 and 538]

$$\begin{aligned} v &= \langle v_z \rangle \\ &= \frac{1}{2} v_{z,\max} \end{aligned} \tag{5.47}$$

$$v_z = v_{z,\max}\left[1 - \left(\frac{r}{R}\right)^2\right] \tag{5.48}$$

$$v_z = 2\langle v_z \rangle \left[1 - \left(\frac{r}{R}\right)^2\right]$$

$$v_z = 2v\left[1 - \left(\frac{r}{R}\right)^2\right] \tag{5.49}$$

gives a relation for the local velocity in terms of the average velocity and the Graetz equation becomes [?]

$$\mathfrak{D}_i\left(\frac{\partial^2 c_i}{\partial r^2} + \frac{1}{r}\frac{\partial c_i}{\partial r}\right) = bv\left[1 - \left(\frac{r}{R}\right)^2\right]\frac{\partial c}{\partial z} \tag{5.50}$$

where a=0 and b=1.5 for parallel plates, a=1 and b=2 for cylindrical geometry [?], [?].

Kim [?] [?] solved the Graetz problem for the hollow fiber immobilized liquid membrane using four reaction configurations at the the interface:

1. Equilibrium of chemical reversible equilibrium reaction inside the membrane

$$A + B \underset{k_r}{\overset{k_f}{-}} AB \tag{5.51}$$

2. Coupled Transport

   (a) Counter Transport Membranes with the equilibrium reactions

   $$A + C - AC \tag{5.52}$$

   $$B + C - BC. \tag{5.53}$$

   Here the membrane is a supported liquid membrane with the species C (the carrier species) to be constrained to remain within the membrane (i.e. immobilized liquid membrane). The fluxes of the species A and B are opposite to each other.

   (b) Co Transport Membranes with the reversible equilibrium reactions

   $$A + B + C - ABC. \tag{5.54}$$

   Again the species C is constrained to remain in the membrane pores.

3. Facilitated Ion Pair Transport

$$A^+ + B^- - (AB)_M \tag{5.55}$$

$$(AB)_M + C - (ABC)_M \tag{5.56}$$

Three of the boundary conditions for two of his scenarios are:

B.C.	Facilitated Transport	Counter Transport
1	$c_A = c_i \quad z = 0$, all r	$\left.\begin{matrix} c_A = c_i \\ c_B = 0 \end{matrix}\right\} z = 0$, all r
2	$\frac{\partial c_A}{\partial r} = 0 \quad r = 0$, all z	$\left.\begin{matrix} \frac{\partial c_A}{\partial r} = 0 \\ \frac{\partial c_B}{\partial r} = 0 \end{matrix}\right\} r = 0$, all z
3	$-\mathcal{D}_A \frac{\partial c_A}{\partial r} = k_{wA}(1 + F_{eq}) s c_A \quad r = R$, all z	$\left.\begin{matrix} -\mathcal{D}_A \frac{\partial c_A}{\partial r} = k_{wA} s H [(1 + F_A)(c_A - c_{Ad}) \\ \quad + U(c_A c_{Bd} - c_B c_{Ad})] \\ -\mathcal{D}_B \frac{\partial c_B}{\partial r} = k_{wB} s H [(1 + F_B)(c_B - c_{Bd}) \\ \quad + U\tau(c_B c_{Ad} - c_B c_{Bd})] \end{matrix}\right\} r = 0$

$$F_{eq} = \frac{\mathcal{D}'_B K_{eq} c_T}{\mathcal{D}'_A (1 + K_{eq} c_A H)}$$

$$F_i = \frac{\mathcal{D}'_C K_i c_T}{\mathcal{D}'_i P} \qquad i = A \text{ and } B$$

$$U = \frac{\mathcal{D}'_C K_A K_B c_T H c_{Bd}}{\mathcal{D}'_A P}$$

$$P = (HK_A c_A + HK_B c_B + 1)(HK_A c_{Ad} + HK_B c$$

Kim presents the governing equation and boundary conditions for each of these different scenarios. The differences are in the third boundary condition at the internal membrane

wall where the reaction occurs. In comparison these boundary condition differences can show a remarkable affect in the amount of solute transferred to the "dialysate side" of the membrane. Kim shows the effects of the diffusion and reaction parameters changes due to this boundary condition of solute-fluid system on the mass transfer rate of the solute in terms of the wall Sherwood number, the dimensionless equilibrium constant, and the maximum facilitation factor, and the dimensionless mixing cup concentration. He shows theoretically, as others have shown experimentally, that the liquid membrane can significantly increase mass transfer and selectively separate ions and species in dilute concentrations.

Of critical importance is the fact that this is a modal of an immobilized liquid membrane system. Though similar to the membrane contactor of this study, it does not represent the hollow fiber membrane contactor in this study. It should also be noted that Kim used the equilibrium, steady state of the membrane process on one filament assuming that all other filaments will be the same and a multiplication factor is all that is neceassary to account for more fibers.. To assume equilibrium, the Damköhler number for diffusion and reaction for the species inside the membrane must be close to infinity. In many situations the equilibrium case is not valid thus the non-equailibrium case should be considered [?].

This model could be adopted to the contactor for any number of reactions, but the limits of equilibrium steady state reactions do not allow any complex computer simulation of the interfacial phenomenon. The Kims solution of the Graetz model for membrane transport, though a more thorough theoretical approach than the film theory, is still more of a performance evaluation of the membrane process than a predictive model. Design criteria can be obtained from the information that is presented and developed by this model; such as, for counter-transport the carrier species should be chosen to have a large K_A and a small K_B. This qualitative but valuable information is discussed in the thesis and are not reproduced here.

As is noted and has been discussed before the characterization of the diffusion and reaction rate parameters for the membrane itself, i.e. the diffusion constants and reaction rate constants, are effective parameters for a hetergeneous porous medium filled with reactive liquid. Thus the need for the membrane porous structure to be accounted for [?].

5.2.4 The Approach to a more Substantial Theoretical Model

Recently Yoshizuka *et al.* [?], [?] have developed a fundamental model attempting to account for the kinetics and mechanism of extraction and stripping through hollow fiber membranes. Since for a membrane extraction process

5.3 Modeling of Transport in Porous Structures

In microporous membranes most models assume constant uniform porosity. Howevr, in reality this is probably not so; though, for symetric membranes the pore size distribution is fairly uniform. The problem arises when pressures increase above the crititcal or breakthrough pressure then there will be penetration into some of the pores. However, if the pore size changes within the membrane thickness this does not create a situation of breakthrough. Partial penetration will result in the interface location not to be fixed and certainly not known and the membrane transfer coefficient expressions become unknown. Thus the solute transfer becomes unknown [?].

In the study of effective transport properties different approaches have been used to eliminate the microscale dependence of the local fields or intrinsic properties. There are a number of techniques to derive a macroscopic approximation model for the closure problem of a microscopic spatially periodic system. Whitiker, Stroeve and co-workers have presented extensively in the literature on volume averaging techniques of multiphase transport in porous media [?], [?], [?], [?], [?], [?], [?], [?], [?], [?], [?]. Soria and De Lasa [?] have also presented theoretical analysis on averaging techniques. Regalbuto [?] use a maximum principle for an approximate solution to nonlinear diffusion reaction boundary value problems. They used Langmuir Hinshelwood reaction kinetics within a porous catalyst. Moment matching, moment-difference expansion are mentioned in the references of Mauris' paper who uses homogination techniques to model the diffusion and convection of a solute through a packed bed. Few of the papers consider a reactions and those that do use an irreversible first order model. Mauri [?], following after Shapiro and Brenner [?] who used the matching of moments technique, model a reactive solute transport in a spatially periodic porous media. Hornung and Jager [?] use the homogination technique to model the diffusion, convection, adsorption and reaction of chemicals in porous media. Ochoa-Tapia and Whitaker [?] state that these methods produce the same macroscopic equation and the same closure problem that is used to determine the dispersion tensor. The correspondance between the method of averaging and of spatial homogination was compared in one of their references by Bourgeat. Ochoa-Tapia et al [?] use the averaging technique to model facilitated transport in porous media. and alos bu by Kim [?] and Kim and Stroeve [?]. The method of spatial homogination is popular among mathematicians.

The above techniques are approximations of complex systems that are assumed to be treatable theoretically. If the magnitude of the complexity of the microscopic system does not allow numerical simulation, one may be forced to use one of the aforementioned techniques. Averageing transport equations for multiphase systems seems to be the most widely used especially in engineering circles. This is probably due to the averaging of local instantaneous transport equations being valid inside each phase, interface and contact line. The

substantial advantage over other continuum approaches is that the physical meaning of the different averaged quantities is clearly extablished [?]. However, when certain constraints concerning the characteristic time, lengths, and the micropore Thiele modulus are not satisfied [?] then the diffusive transport can not be treated by the averaging technique and can only be described in terms of the separate transport equations for the macropore phase and the micropore phase if no other scaling technique is shown to be valid [?, page 217]. Most of the reported works thus far in the literature concerning the mapping of the microscale to the macroscale have contained limited if any non-linear reaction terms. Most of the reactions dealt with thus far are single, first order, irreversible homogenous reactions. At present, as far as I know, there has been no theoretical treatment of transport in complex geometric structures with complex reaction chemistry. Though initially these methods are appealling the theoretical basis is limited to a very select grouping of reactions. Thus we are proceeding with a more fundamental development of transport in porous membranes with reaction at an interface and in a homogenous fluid. Harada and Miyake [?] considered both homogeonus bulk phase reactions and heterogenous interfacial reactions in the extraction of copper(II) but not in a porous structure.

5.3.1 Geometrical Properties and Solute interactions due to Porous Structures

The modeling of membrane pore structure is difficult because of the unknown geometrical trajectories and connectivities of the pores inside the wall of the membrane. A medium can have a high degree of porosity but a low connectivity and the transport property is severly restricted. At the macroscale a regular array of spheres or cylinders is one of the most artificial and simplest models of a porous media. This concept is referred to as spatially periodic porous media. The spatially periodic structure is extremely unlikely to occur naturely at the macroscale but can and does occur at the atomic scale [?, page 10].

The structure of a porous media may allow the induction of a significant simplification in the media's modeling description and thus important consequences to the transport processes that occur in the porous media. This structure is an invarient geometric property that may induce symmetry or a relationship of characteristic correspondence, equivalence, or identity among constituents of an entity or between different entities. Two different types geometric symmetries are distinguished in the study of porous media [?, page 29]:

- *Translational Symmetry* is the classic concept that many materials look much the same at different locations. If the material has a well balanced population of constituents of the properties then it can be classed as translational invariant or homogeneous material of that property. Material that exhibit constant overall geometric properties such as porosity as one moves from one point to another by translation is classed in this category. Most material are not homogenous but their properties can be derived

from a finite sample. The whole medium is then reconstructed by the juxtaposition (side by side placement) of identical samples or cells in space and the spatially periodic structure model is born.

- *Dilatational Symmetry* is a scale or size similarity. Fractals or self-similarity are used to describe this symmetry. This type of symmetry is a fairly new concept.

There are three modern theories of porous media [?]:

1. PERCOLATION THEORY (ca. 1957) deals with completely random materials without any spatial correlation
2. FRACTALS (ca 1975) which characterize materials by self similarity at different scales
3. RECONSTRUCTED MEDIA (ca. 1990) where the porous materials with given statistical characteristics are reconstructed numerically. The local field equations are solved numerically inside these media with appropriate boundary conditions and the macroscopic transport equations are determined by spatial integration.

In to deal with a porous media or structure some definitions are essential. First and obviously fundamental for porous material is the concept or definition of porosity. The concept is simple enough — porosity is the void space within a solid that can be occupied by one or more fluid phase(s). Mathematically following after Adler [?, page 19] if a porous media occupies a volume, V, in $\mathbb{R}$ such that each spatial point $\mathbf{r}$ belongs to the solid phase (S) or pore (void or liquid) space (L).

$$\forall V \in \mathbb{R}^3, \exists\, \mathbf{r} \in \mathbf{S} \cup \mathbf{L} \tag{5.57}$$

Defining two phase functions $X_s(\mathbf{r})$ and $X_L(\mathbf{r})$ as

$$X_K(\mathbf{r}) = \begin{cases} 1 \text{ if } \mathbf{r} \in \text{ phase } K \\ 0 \text{ otherwise,} \end{cases} \tag{5.58}$$

where $K = L, S$ and the volume of the phase K is denoted by V_K. In general for porous media the interface between the two phases (i.e. the liquid and solid is assumed to be negligible. In this study this will be done also. However, it should be brought out that we have two different phases in the pores and thus an interface between these fluids. This fluid interface cannot be neglected since it is an integral part of the membrane process. Most of the attention in the transport in a porous media is focused on the pore space [?, page 19] as will be our focus in this study. Therefor,

$$X_L(\mathbf{r}) + X_S(\mathbf{r}) = 1 \tag{5.59}$$

and focusing only on the void space and dropping the L index

$$X(\mathbf{r}) = X_L(\mathbf{r}) \tag{5.60}$$

and using a distribution expression for the derivative of the phase functions

$$\nabla X_K(\mathbf{r}) = -\delta_S(\mathbf{r}) \cdot v_K \tag{5.61}$$

where $\delta_S(\mathbf{r})$ is a one-dimensional Dirac delta-function across the interface and v_K is the outwar normal to phase K.

Integrating the spatial properties of the phase function give us the porosity property

$$\varepsilon = \frac{1}{V}\int_V X_L(\mathbf{r}) \cdot dV(\mathbf{r}) \tag{5.62}$$

ε generally depends upon V but when V is large enough the ε is independent of V. As V tends to infinity the ε tends toward a limit.

$$\varepsilon = \lim_{V\to\infty} \frac{1}{V}\int_V X_L(\mathbf{r}) \cdot dV(\mathbf{r})$$

The interconnectivity of the pores of a media is the emphasis of most theories on modeling of porous media. The accounting for dead or closed porosity is problematic. Tortuosity was introduced by Carma (ca 1937) [?] and was defined as the sware of the ratio of the *effective average path length* L_e in the porous medium to the shortest distance L measured along a particular direction of macroscopic fluid flow.

$$\tau = \left(\frac{L_e}{L}\right)^2. \tag{5.63}$$

The geometric tortuosity can be defined by using the concept of connected components. If any two points $\mathbf{r}_1$ and $\mathbf{r}_2$ are a subset of the same connected component or subnetwork and $L_{\min}(\mathbf{r}_1, \mathbf{r}_2)$ is the length of the sohortes path in the fluid space that connects $\mathbf{r}_1$ and $\mathbf{r}_2$ then the geometric tortuosity of this particular set of points can be defined as [?, page 24]

$$\tau_G(\mathbf{r}_1, \mathbf{r}_2) = \left[\frac{L_{\min}(\mathbf{r}_1, \mathbf{r}_2)}{|\mathbf{r}_1 - \mathbf{r}_2|}\right]^2, \mathbf{r}_2 \in C_L(\mathbf{r}_1). \tag{5.64}$$

At this point the modeling of porous structure by necessity expands into the three theories of spatially periodic structures. The application of these theories to the study of the structure and effects on the transport process of porous membrane structure is important, fascinating, and tempting; however, the discussion and use is judged to be beyond the scope of this study at this time.

A common practice of modeling membrane transport is to treat the hetrogeneous membranes as if they were homogenous permeable membranes without considering the effects or

interaction between the pores and the subsequent distortion of the flux. This assumption that the pores are so closely spaced that the membrane is homogeneously permeable shows a diffusive resistance, R_m, related to its porosity ε

$$R_m = \frac{l}{\varepsilon \mathcal{D}_p} \tag{5.65}$$

where $\mathcal{D}_p$ is the pore diffusivity and l is the membrane thickness [?]. A phenomenological approach of the pore structure resistances (permeabilities) can be implemented if the experimental data is available. This treatment does not generally relate each term to the intrinsic characteristics that the irregular morphologies (variations in the proe sizes, sloping in their trajectories, etc.) present in a hetergenous membrane. These complex spatial variations require a more thorough analysis of the membrane structure and the introduction of these details in the flux models [?]. Another complexity is that of the streamlines of diffusive flux being distorted around the mouth of each pore. This distortion of the diffusional boundary layer has been recongnized as a potential factor in controlling the transfer rates in membranes [?].

The pore interaction has been modeled by Glandt [?], [?], as power series expression of Henry's Law for the partition coefficient for an equalibrium distribution of a solute between a bulk phase and very small pores. When Henry's law operates then the solute concentration is uiform across a section of the pore, exce[t for the inaccessible periphery where it is zero [?]. As the concentration of a species is increased the concentration inside the pore becomes spatially nonuniform near the pore walls due to solute-solute interactions. At or near the center of the pore the concentration is close to that of the bulk phase and a layering effect becomes apparent in the pore — an enriched region exists along the pore walls. Glandt notes that this preference of the solute molecule for being in contact with the walls is a result of the structure causing effect of the solid on the fluid and not by any attractive or adsorbing potential or mechanism associated with the walls of the pore. The partition coefficient, K, is a consequence of solute-solute interactions at finite concentrations and is no longer a constant function of the geometry. The virial-type power series dependence on the bulk concentration is given by Glandt as

$$K = K_0 + K_1 c_b + K_2 c_b^2 + \dots \tag{5.66}$$

where K, K_0 (Henry's law constant) are dimensionless and K_n has units of (molar volume)^n. The virial coefficients K_1, K_2, etc., can be calculated from the knowledge of the effective interactions between solute molecules with the pore walls. When the ration of the hard-sphere diameter d, which Glandt based his work, is small compared to the diameter of a

cylindrical pore D or $\lambda = \frac{d}{D} \rightarrow 0$ then the constants are

$$K_1^* \simeq \pi\left(\lambda - \frac{23}{15}\lambda^2\right) \quad \text{as } \lambda \rightarrow 0 \tag{5.67}$$

$$K_2^* \simeq \pi\left(\frac{-\lambda}{3} + \lambda^2\right) \quad \text{as } \lambda \rightarrow 0 \tag{5.68}$$

Glandt defined these in a dimensionless form using a reduced bulk concentraion and Avogadro's number N_A

$$c_b^* = c_b d^3 N_A \tag{5.69}$$

$$K_n^* = \frac{K_n}{(d^3 N_A)^n} \tag{5.70}$$

$$K_0 = \frac{V'}{V} \tag{5.71}$$

where V' and V are: the volume accessible to the center of the molecules, and the pore volume respectively and equation 5.66 becomes

$$K = K_0 + K_1^* c_b^* + K_2^* c_b^{*2} + \ldots \tag{5.72}$$

Glandt [?] shows that for a limiting situation of the pore diameter approaching the dimensions of the hard sphere molecule, $\lambda \rightarrow 1$, that the molecules behave effectively like hard rods and the centers lie very close to the pore axis. And, as such, the properties can be exactly solved for and the activity of particles in the pore is

$$a = \left(\frac{4\lambda^2}{(1-\lambda)^2}\right)\overline{c}\frac{\exp\left[\frac{\pi\overline{c}d^3}{4\lambda^2 - \pi\overline{c}d^3}\right]}{4\lambda^2 - \pi\overline{c}d^3} \tag{5.73}$$

where $\overline{c}$ is the average molar density $\frac{n}{V}$ inside the pore. When equated to the activity of the bulk fluid in equilibrium with the pore

$$a_b = c_b \exp\left[\frac{8\eta - 9\eta^2 + 3\eta^3}{(1-\eta)^3}\right] \tag{5.74}$$

a relationship between $\overline{c}$ and c_b can be obtained which determines $K(c_b)$.

The effect of pore size distributions on the effective diffusivities was studied by Cui et al [?]. Effective diffusivities are global parameters which lump complicated geometrical structure together with the diffusion process. Cui et al determined that the effective and mean diffusivities are not independent of the the geometries at a micro and macro scale and also have a coupling between the diffusional transport and other physico-chemical process such as adsorbtion. Determining the tortuosity without taking into account the adsorbtion phenomenon, when appropriate, of the actual solutes can lead to erroneous values. Defining diffusivites

- D $\equiv$ the diffusivity in the homogenous fluid
- D''_{app} $\equiv$ the effective diffusivity in the homogeneous fluid corrected by the internal porosity ϵ and the tortuosity τ
- D' $\equiv$ the effective diffusivity in the pseudo-homogeneous solid accounting for diffusion of molecules both in the fluid phase and on the adsorbed phase
- K_A $\equiv$ the adsorption equilibrium constant (m^3/kg)
- ρ_p $\equiv$ the particle or species density

$$D''_{\text{app}} = \frac{\varepsilon}{\tau} D \qquad D' = \frac{\varepsilon}{\tau(\varepsilon + \rho_p K_A)} D = \frac{D''_{\text{app}}}{\varepsilon + \rho_p K_A} \tag{5.75}$$

From these definitions a mean diffusivity determined by different techniques can be established. Further expounding on this work will not be fruitful since these authors have used a linear adsorption technique to arrive at an equation to determine the mean diffusivities. Using the above definitions as well as the reaction kinetics, interfacial adsorption kinetics, and transport equations developed subsequently in this study, basically accounts for the physico-chemical coupling that these authors discuss are so important.

Beeckman [?] gives an exression for the tortuosity factor as a function of the porosity for a catalystas:

$$\tau = \frac{\varepsilon}{1 - (1 - \varepsilon)^{\frac{1}{3}}} \tag{5.76}$$

He derives this from a statistical mathematical description of a heterogeneous catalyst and a travel and branching process. The tortuosity factors calcuated from the above equation, Beeckman claims, are within the range of values reported by Satterfield. At low porosities the tortuosity factor approaches three. The introduction of dead in pores lead to an increase in the tortuosity above three. For high porosities the factor approaches unity asymptotically.

Deepak and Bhatia [?] attribute higher than theoretically expected tortuosity to correlation effects arising because of meandering of the species being transported in the network result in the path being retraced. These authors also derive an equation from transport theory taking into account the pore geometry and effects of the medium using the correlated random walk theory. They report that the effective diffusivity is not significantly affected by chemical reactions which is in contrast with Hollewand and Gladden [?]. Hollewand and Gladden report that the effective diffusivity is significanly affected by chemical reactions in the pores, with the tortuosity decreasing with increase in the Thiele Modulus. According

to Deepak and Bhatia the effect that Hollewand and Gladden observed was due to finite pore level Thiele modulus under which the usual Fickian modal for transport is suspect [?].

5.4 The Diffusional Macroscopic Governing Equations for Membrane Interfacial Mass Transport

Consider two immiscibe phases, α and β phases, that are in contact and have different concentrations of chemical species in each respective bulk phase. From Bird et al. [?, page 557] the transport equation of species i in the β phase is given by

$$\frac{\partial c_{i_\beta}}{\partial t} + \left(\nabla \cdot c_{i_\beta} v^\star\right) = \left(\nabla \cdot \mathfrak{D}_\beta \nabla c_{i_\beta}\right) + R_{i_\beta} \tag{5.77}$$

and the transport of species i in the α phase is given by a like equation or

$$\frac{\partial c_{i_\alpha}}{\partial t} + (\nabla \cdot c_{i_\alpha} v^\star) = (\nabla \cdot \mathfrak{D}_\alpha \nabla c_{i_\alpha}) + R_{i_\alpha} \tag{5.78}$$

This assumes reaction occurs primarily in the bulk and therefore is reaction limited (reaction rate is slower than diffusion rate). Most cases of liquid/liquid extraction of metals are diffusion limited and the reaction takes place at the interface. The boundary conditions become the limiting step. From Ochoa et. al.[?] similar equations have been developed in general for cellular membranes.

$$\frac{\partial c_{i_\beta}}{\partial t} = \left(\nabla \cdot \mathfrak{D}_\beta \nabla c_{i_\beta}\right) \tag{5.79}$$

The above equation, which is Fick's second law of diffusion, assumes no velocity gradient normal to the species transport and thus does not contain the hydrodynamic flow of the β phase. The flow term is inserted in the equation below.

$$\frac{\partial c_{i_\beta}}{\partial t} + (\nabla \cdot c_i v^\star) = \left(\nabla \cdot \mathfrak{D}_\beta \nabla c_{i_\beta}\right) \tag{5.80}$$

Note that the reaction term is not in equation 5.79 or equation 5.80. The boundary conditions will incorporate this information for reaction at the interface. Equation 5.77 can be used with a reaction in the bulk and at the interface. If no reaction involving species i occurs in the bulk phase, $R_{i\alpha}$ is zero.

Rewriting equation 5.77

$$\frac{\partial c_{i\alpha}}{\partial t} + (\nabla \cdot c_{i\alpha} v^\star) = (\nabla \cdot \mathfrak{D}_\alpha \nabla c_{i\alpha}) + R_{i\alpha} \tag{5.81}$$

The general boundary conditions at the $\alpha - \beta$ interface

$$\textbf{B. C. 1} \quad \frac{\partial c_{i_s}}{\partial t} + (\nabla_s \cdot c_{i_s} v^*) = (\nabla_s \cdot \mathfrak{D}_s \nabla_s c_{i_s}) + R_{i_s} + \mathbf{n}_{\alpha\beta} \cdot \| \bar{\mathbf{j}}_{i_\alpha} \| \tag{5.82}$$

If we assume that there is no convective transport along the interface then equation 5.82 becomes

$$\textbf{B. C. 1-}\alpha \quad \frac{\partial c_{i_s}}{\partial t} = (\nabla_s \cdot \mathfrak{D}_s \nabla_s c_{i_s}) + R_{i_s} + \mathbf{n}_{\alpha\beta} \cdot \| \bar{\mathbf{j}}_{i_\alpha} \| \tag{5.83}$$

and the second boundary condition for the α phase is

$$\textbf{B. C. 2-}\alpha \quad c_{i_\alpha} = f(\mathbf{r}_{i_\alpha}, t) \tag{5.84}$$

note that $\mathbf{n}_{\alpha\beta}$ is the outwardly directed unit (normal) vector at the interface pointing from the α phase to the β phase and equation 5.83 reflect diffusion species i from one phase into the other at the interface and therefore there is no accumulation of species i in the interface. This is in keeping with the concept of a two dimensional surface for the definition of the interface. Where $\mathbf{r}$ in equation 5.84 is the position vector and t is time scalar.

The initial conditions are:

$$\left.\begin{array}{l} c_{i_\alpha} = c_{i_{\alpha_{in}}} \text{ for all } \mathbf{r} \\ c_{i_\beta} = c_{i_{\beta_{in}}} \text{ for all } \mathbf{r} \end{array}\right\} \text{ for } t = 0 \tag{5.85}$$

and in the β phase the transport equation is

$$\frac{\partial c_{i_\beta}}{\partial t} + \left(\nabla \cdot c_{i_\beta} v^*\right) = \left(\nabla \cdot \mathfrak{D}_\beta \nabla c_{i_\beta}\right) + R_{i_\beta} \tag{5.86}$$

and the boundary conditions are similar as in the α phase. At the interface the boundary condition is the same:

$$\textbf{B. C. 1-}\beta \quad \frac{\partial c_{i_s}}{\partial t} = (\nabla_s \cdot \mathfrak{D}_s \nabla_s c_{i_s}) + R_{i_s} + \mathbf{n}_{\alpha\beta} \cdot \| \bar{\mathbf{j}}_{i_\alpha} \| \tag{5.87}$$

and the second boundary condition for the β phase is

$$\textbf{B. C. 2-}\beta \quad c_{i_\beta} = f(\mathbf{r}_{i_\beta}, t) \tag{5.88}$$

5.4.1 Derivation of Governing Equations in Cylindrical Co-ordinates Non-Constant Diffusion Coefficient

The transport equations in cylindrical co-ordinates for hollow fiber membrane separation processes are developed from the general equation given in equation 5.81 and 5.86. These transport or balance equations and boundary conditions are a very general formulation in

vector notation. Since the problem at hand is to model the transport of a species from one phase to another via hollow fiber membranes a suitable coordinate system is the cylindrical co-ordinate system. Most work that has been accomplished in hollow fiber contactors has been to simplify by assuming a constant diffusion coefficient $\mathfrak{D}$ with concentration we will not, at this time, use this simplification. To transform the above equations into the appropriate useful equations we will use the relationships of spatial derivatives of unit vectors [?, page 737]

$$\begin{array}{lll} \frac{\partial}{\partial r}\delta_r = \mathbf{0} & \frac{\partial}{\partial r}\delta_\theta = \mathbf{0} & \frac{\partial}{\partial r}\delta_z = \mathbf{0} \\ \frac{\partial}{\partial \theta}\delta_r = \delta_\theta & \frac{\partial}{\partial \theta}\delta_\theta = -\delta_r & \frac{\partial}{\partial \theta}\delta_r = \mathbf{0} \\ \frac{\partial}{\partial z}\delta_r = \mathbf{0} & \frac{\partial}{\partial z}\delta_\theta = \mathbf{0} & \frac{\partial}{\partial z}\delta_z = \mathbf{0} \end{array} \tag{5.89}$$

and the properties of the dot products of the unit vectors

$$\begin{cases} (\delta_1 \cdot \delta_1) = (\delta_2 \cdot \delta_2) = (\delta_3 \cdot \delta_3) = 1 \\ (\delta_1 \cdot \delta_2) = (\delta_2 \cdot \delta_3) = (\delta_3 \cdot \delta_1) = 0 \end{cases} \tag{5.90}$$

The definition of the del operator (∇) or nabla for cylindrical co-ordinate system is

$$\nabla = \delta_r \frac{\partial}{\partial r} + \delta_\theta \frac{1}{r}\frac{\partial}{\partial \theta} + \delta_z \frac{\partial}{\partial z} \tag{5.91}$$

and the gradient is the operation of the nabla over a scalar quantity such as concentration (c) and is given here to be

$$\nabla c = \delta_r \frac{\partial c}{\partial r} + \delta_\theta \frac{1}{r}\frac{\partial c}{\partial \theta} + \delta_z \frac{\partial c}{\partial z} \tag{5.92}$$

and multiplying this gradient by the scalar diffusion coefficient $\mathfrak{D}$ gives

$$\mathfrak{D}\nabla c = \mathfrak{D}\delta_r \frac{\partial c}{\partial r} + \mathfrak{D}\delta_\theta \frac{1}{r}\frac{\partial c}{\partial \theta} + \mathfrak{D}\delta_z \frac{\partial c}{\partial z} \tag{5.93}$$

and since a scalar multiplying a vector is commutative

$$\mathfrak{D}\nabla c = \delta_r \mathfrak{D}\frac{\partial c}{\partial r} + \delta_\theta \frac{1}{r}\mathfrak{D}\frac{\partial c}{\partial \theta} + \delta_z \mathfrak{D}\frac{\partial c}{\partial z} \tag{5.94}$$

and the divergence given by the dot product of the ∇ operator over the above equation is represented by

$$\nabla \cdot \mathfrak{D}\nabla c = \left(\delta_r \frac{\partial}{\partial r} + \delta_\theta \frac{1}{r}\frac{\partial}{\partial \theta} + \delta_z \frac{\partial}{\partial z}\right) \cdot \left(\delta_r \left(\mathfrak{D}\frac{\partial c}{\partial r}\right) + \delta_\theta \frac{1}{r}\left(\mathfrak{D}\frac{\partial c}{\partial \theta}\right) + \delta_z \left(\mathfrak{D}\frac{\partial c}{\partial z}\right)\right) \tag{5.95}$$

$$= \delta_r \cdot \frac{\partial}{\partial r}\left[\delta_r \left(\mathfrak{D}\frac{\partial c}{\partial r}\right)\right] + \delta_r \cdot \frac{\partial}{\partial r}\left[\delta_\theta \frac{1}{r}\left(\mathfrak{D}\frac{\partial c}{\partial \theta}\right)\right] + \delta_r \cdot \frac{\partial}{\partial r}\left[\delta_z \left(\mathfrak{D}\frac{\partial c}{\partial r}\right)\right] +$$

$$\boldsymbol{\delta}_\theta \cdot \frac{1}{r}\frac{\partial}{\partial \theta}\left[\boldsymbol{\delta}_r\left(\mathfrak{D}\frac{\partial c}{\partial r}\right)\right] + \boldsymbol{\delta}_\theta \cdot \frac{1}{r}\frac{\partial}{\partial \theta}\left[\boldsymbol{\delta}_\theta \frac{1}{r}\left(\mathfrak{D}\frac{\partial c}{\partial \theta}\right)\right] + \boldsymbol{\delta}_\theta \cdot \frac{1}{r}\frac{\partial}{\partial \theta}\left[\boldsymbol{\delta}_z\left(\mathfrak{D}\frac{\partial c}{\partial z}\right)\right] +$$
$$\boldsymbol{\delta}_z \cdot \frac{\partial}{\partial z}\left[\boldsymbol{\delta}_r\left(\mathfrak{D}\frac{\partial c}{\partial r}\right)\right] + \boldsymbol{\delta}_z \cdot \frac{\partial}{\partial z}\left[\boldsymbol{\delta}_\theta \frac{1}{r}\left(\mathfrak{D}\frac{\partial c}{\partial \theta}\right)\right] + \boldsymbol{\delta}_z \cdot \frac{\partial}{\partial z}\left[\boldsymbol{\delta}_z\left(\mathfrak{D}\frac{\partial c}{\partial z}\right)\right] \tag{5.96}$$

Expanding the dot products of each of the terms above results in the following

$$\begin{aligned}
= \; & \left\{\left[\boldsymbol{\delta}_r \cdot \boldsymbol{\delta}_r \frac{\partial}{\partial r}\left(\mathfrak{D}\frac{\partial c}{\partial r}\right) + \boldsymbol{\delta}_r \cdot \mathfrak{D}\frac{\partial c}{\partial r}\left(\frac{\partial \boldsymbol{\delta}_r}{\partial r}\right)\right] + \right. \\
& \left[\boldsymbol{\delta}_r \cdot \boldsymbol{\delta}_\theta \frac{\partial}{\partial r}\left(\frac{1}{r}\mathfrak{D}\frac{\partial c}{\partial \theta}\right) + \boldsymbol{\delta}_r \cdot \frac{1}{r}\mathfrak{D}\frac{\partial c}{\partial \theta}\frac{\partial \boldsymbol{\delta}_\theta}{\partial r}\right] + \\
& \left.\left[\boldsymbol{\delta}_r \cdot \boldsymbol{\delta}_z \frac{\partial}{\partial r}\left(\mathfrak{D}\frac{\partial c}{\partial z}\right) + \boldsymbol{\delta}_r \mathfrak{D}\frac{\partial c}{\partial z}\frac{\partial \boldsymbol{\delta}_z}{\partial r}\right]\right\} + \\
& \left\{\left[\boldsymbol{\delta}_\theta \cdot \boldsymbol{\delta}_r \frac{1}{r}\frac{\partial}{\partial \theta}\left(\mathfrak{D}\frac{\partial c}{\partial r}\right) + \boldsymbol{\delta}_\theta \cdot \frac{1}{r}\left(\mathfrak{D}\frac{\partial c}{\partial r}\right)\left(\frac{\partial \boldsymbol{\delta}_r}{\partial \theta}\right)\right] + \right. \\
& \left[\boldsymbol{\delta}_\theta \cdot \boldsymbol{\delta}_\theta \frac{1}{r}\frac{\partial}{\partial \theta}\left(\frac{1}{r}\mathfrak{D}\frac{\partial c}{\partial \theta}\right) + \boldsymbol{\delta}_\theta \cdot \frac{1}{r}\frac{1}{r}\mathfrak{D}\frac{\partial c}{\partial \theta}\frac{\partial \boldsymbol{\delta}_\theta}{\partial \theta}\right] + \\
& \left.\left[\boldsymbol{\delta}_\theta \cdot \boldsymbol{\delta}_z \frac{1}{r}\frac{\partial}{\partial \theta}\left(\mathfrak{D}\frac{\partial c}{\partial z}\right) + \boldsymbol{\delta}_\theta \cdot \left(\frac{1}{r}\mathfrak{D}\frac{\partial c}{\partial z}\right)\frac{\partial \boldsymbol{\delta}_z}{\partial \theta}\right]\right\} + \\
& \left\{\left[\boldsymbol{\delta}_z \cdot \boldsymbol{\delta}_r \frac{1}{r}\frac{\partial}{\partial z}\left(\mathfrak{D}\frac{\partial c}{\partial r}\right) + \boldsymbol{\delta}_z \cdot \left(\mathfrak{D}\frac{\partial c}{\partial r}\right)\left(\frac{\partial \boldsymbol{\delta}_r}{\partial z}\right)\right] + \right. \\
& \left[\boldsymbol{\delta}_z \cdot \boldsymbol{\delta}_\theta \frac{\partial}{\partial z}\left(\frac{1}{r}\mathfrak{D}\frac{\partial c}{\partial \theta}\right) + \boldsymbol{\delta}_z \cdot \frac{1}{r}\mathfrak{D}\frac{\partial c}{\partial \theta}\frac{\partial \boldsymbol{\delta}_\theta}{\partial z}\right] + \\
& \left.\left[\boldsymbol{\delta}_z \cdot \boldsymbol{\delta}_z \frac{\partial}{\partial \theta}\left(\mathfrak{D}\frac{\partial c}{\partial z}\right) + \boldsymbol{\delta}_z \cdot \left(\mathfrak{D}\frac{\partial c}{\partial z}\right)\frac{\partial \boldsymbol{\delta}_z}{\partial z}\right]\right\}
\end{aligned} \tag{5.97}$$

Using the relations in equations 5.89 and 5.90 reduces equation 5.97 above to a substantially reduced form

$$\begin{aligned}
\nabla \cdot \mathfrak{D}\nabla c \; = \; & \left[\frac{\partial}{\partial r}\left(\mathfrak{D}\frac{\partial c}{\partial r}\right)\right] + [0] + [0] + \\
& \left[\boldsymbol{\delta}_\theta \cdot \frac{1}{r}\left(\mathfrak{D}\frac{\partial c}{\partial \theta}\right)\boldsymbol{\delta}_\theta\right] + \left[\frac{1}{r}\frac{\partial}{\partial \theta}\left(\frac{1}{r}\mathfrak{D}\frac{\partial c}{\partial \theta}\right)\right] + \left[\boldsymbol{\delta}_\theta \cdot \frac{1}{r^2}\mathfrak{D}\frac{\partial c}{\partial \theta}(-\boldsymbol{\delta}_r)\right] + [0] + \\
& [0] + [0] + \left[\frac{\partial}{\partial z}\left(\mathfrak{D}\frac{\partial c}{\partial z}\right)\right]
\end{aligned} \tag{5.98}$$

accounting for the commutative law of multiplication in vectors and scalars gives

$$= \frac{\partial}{\partial r}\left(\mathfrak{D}\frac{\partial c}{\partial r}\right) + \boldsymbol{\delta}_\theta \cdot \boldsymbol{\delta}_\theta \frac{1}{r}\mathfrak{D}\frac{\partial c}{\partial r} + \frac{1}{r}\frac{\partial}{\partial \theta}\left(\frac{1}{r}\mathfrak{D}\frac{\partial c}{\partial \theta}\right) + \boldsymbol{\delta}_\theta(-\boldsymbol{\delta}_r)\frac{1}{r^2}\mathfrak{D}\frac{\partial c}{\partial \theta} + \frac{\partial}{\partial z}\left(\mathfrak{D}\frac{\partial c}{\partial z}\right) \tag{5.99}$$

and applying the same relations of equations 5.89 and 5.90 gives

$$= \frac{\partial}{\partial r}\left(\mathfrak{D}\frac{\partial c}{\partial r}\right) + \frac{1}{r}\mathfrak{D}\frac{\partial c}{\partial r} + \frac{1}{r}\frac{\partial}{\partial \theta}\left(\frac{1}{r}\mathfrak{D}\frac{\partial c}{\partial \theta}\right) + \frac{\partial}{\partial z}\left(\mathfrak{D}\frac{\partial c}{\partial z}\right) \tag{5.100}$$

expanding the first, third, and fourth terms (no expansion is possible on the second term) gives

$$\begin{aligned} &= \left[\mathfrak{D}\tfrac{\partial^2 c}{\partial r^2} + \tfrac{\partial c}{\partial r}\tfrac{\partial \mathfrak{D}}{\partial r}\right] + \left[\tfrac{\mathfrak{D}}{r}\tfrac{\partial c}{\partial r}\right] + \left[\tfrac{1}{r}\mathfrak{D}\tfrac{\partial c}{\partial \theta}\tfrac{\partial}{\partial \theta}\left(\tfrac{1}{r}\right) + \tfrac{1}{r^2}\tfrac{\partial}{\partial \theta}\left(\mathfrak{D}\tfrac{\partial c}{\partial \theta}\right)\right] \\ &\quad + \left[\mathfrak{D}\tfrac{\partial^2 c}{\partial z^2} + \tfrac{\partial c}{\partial z}\tfrac{\partial \mathfrak{D}}{\partial z}\right] \end{aligned} \tag{5.101}$$

expanding the third term further

$$\begin{aligned} &= \left[\mathfrak{D}\tfrac{\partial^2 c}{\partial r^2} + \tfrac{\partial c}{\partial r}\tfrac{\partial \mathfrak{D}}{\partial r}\right] + \left[\tfrac{\mathfrak{D}}{r}\tfrac{\partial c}{\partial r}\right] + \left[\tfrac{1}{r}\mathfrak{D}\tfrac{\partial c}{\partial \theta}\left(-\tfrac{1}{r^2}\right)\tfrac{\partial r}{\partial \theta} + \tfrac{1}{r^2}\left(\tfrac{\partial c}{\partial \theta}\left(\tfrac{\partial \mathfrak{D}}{\partial \theta} + \mathfrak{D}\tfrac{\partial^2 c}{\partial \theta^2}\right)\right)\right] + \\ &\quad + \left[\mathfrak{D}\tfrac{\partial^2 c}{\partial z^2} + \tfrac{\partial c}{\partial z}\tfrac{\partial \mathfrak{D}}{\partial z}\right] \end{aligned} \tag{5.102}$$

It should be noted that the first term of the third bracketed term is zero since the r and θ co-ordinates are orthogonal and the equation for the divergence of the gradient of c becomes

$$= \left[\mathfrak{D}\frac{\partial^2 c}{\partial r^2} + \frac{\partial c}{\partial r}\frac{\partial \mathfrak{D}}{\partial r}\right] + \left[\frac{\mathfrak{D}}{r}\frac{\partial c}{\partial r}\right] + \left[\frac{1}{r^2}\left(\frac{\partial c}{\partial \theta}\frac{\partial \mathfrak{D}}{\partial \theta} + \mathfrak{D}\frac{\partial^2 c}{\partial \theta^2}\right)\right] + \left[\mathfrak{D}\frac{\partial^2 c}{\partial z^2} + \frac{\partial c}{\partial z}\frac{\partial \mathfrak{D}}{\partial z}\right] \tag{5.103}$$

rearranging the above equation

$$\nabla\cdot\mathfrak{D}\nabla c = \left[\mathfrak{D}\frac{\partial^2 c}{\partial r^2} + \frac{\mathfrak{D}}{r}\frac{\partial c}{\partial r} + \frac{\partial c}{\partial r}\frac{\partial \mathfrak{D}}{\partial r}\right] + \left[\frac{1}{r^2}\left(\frac{\partial c}{\partial \theta}\frac{\partial \mathfrak{D}}{\partial \theta} + \mathfrak{D}\frac{\partial^2 c}{\partial \theta^2}\right)\right] + \left[\mathfrak{D}\frac{\partial^2 c}{\partial z^2} + \frac{\partial c}{\partial z}\frac{\partial \mathfrak{D}}{\partial z}\right] \tag{5.104}$$

the terms in this equation can be reduced to

$$\nabla\cdot\mathfrak{D}\nabla c = \left[\frac{1}{r}\frac{\partial}{\partial r}\left(\mathfrak{D}\left(r\frac{\partial c}{\partial r}\right)\right)\right] + \left[\frac{1}{r^2}\frac{\partial}{\partial \theta}\left(\mathfrak{D}\frac{\partial c}{\partial \theta}\right)\right] + \left[\frac{\partial}{\partial z}\left(\mathfrak{D}\frac{\partial c}{\partial z}\right)\right] \tag{5.105}$$

if $\mathfrak{D}$ is assumed constant (i.e. $\frac{\partial \mathfrak{D}}{\partial r} = \frac{\partial \mathfrak{D}}{\partial \theta} = \frac{\partial \mathfrak{D}}{\partial z} = 0$ then equation 5.104 becomes

$$\mathfrak{D}\nabla\cdot\nabla c = \mathfrak{D}\left\{\left[\frac{\partial^2 c}{\partial r^2} + \frac{1}{r}\frac{\partial c}{\partial r}\right] + \left[\frac{1}{r^2}\left(\frac{\partial^2 c}{\partial \theta^2}\right)\right] + \left[\frac{\partial^2 c}{\partial z^2}\right]\right\} \tag{5.106}$$

or the reduced format equation

$$\mathfrak{D}\nabla\cdot\nabla c = \mathfrak{D}\left[\frac{1}{r}\frac{\partial}{\partial r}\left(r\frac{\partial c}{\partial r}\right) + \frac{1}{r^2}\left(\frac{\partial^2 c}{\partial \theta^2}\right) + \frac{\partial^2 c}{\partial z^2}\right] \tag{5.107}$$

which is the laplacian. Now, if the concentration is assumed not to vary in the circumferential direction i.e. with $\theta\ \frac{\partial c}{\partial \theta} = 0$ then equation 5.104 for $\nabla \cdot \mathfrak{D}\nabla c$ becomes

$$\nabla \cdot \mathfrak{D}\nabla c = \mathfrak{D}\frac{\partial^2 c}{\partial r^2} + \frac{\partial c}{\partial r}\frac{\partial \mathfrak{D}}{\partial r} + \frac{\mathfrak{D}}{r}\frac{\partial c}{\partial r} + \mathfrak{D}\frac{\partial^2 c}{\partial z^2} + \frac{\partial c}{\partial z}\frac{\partial \mathfrak{D}}{\partial z} \tag{5.108}$$

The term $\nabla \cdot c\boldsymbol{v}^\star$ of the general governing transport equation is expanded in cylindrical co-ordinates in a similar fashion to the divergence of the gradient derived above.

$$\nabla \cdot c\boldsymbol{v}^\star = \nabla c \cdot \boldsymbol{v}^\star + c(\nabla \cdot \boldsymbol{v}^\star) \tag{5.109}$$

from [?, page 739B table A.7-2]

$$c(\nabla \cdot \boldsymbol{v}^\star) = c\left(\frac{1}{r}\frac{\partial}{\partial r}(rv_r) + \frac{1}{r}\left(\frac{\partial v_b}{\partial \theta}\right) + \frac{\partial v_z}{\partial z}\right) \tag{5.110}$$

and $\nabla c \cdot \boldsymbol{v}^\star$ becomes

$$\nabla c \cdot \boldsymbol{v}^\star = v_r\frac{\partial c}{\partial r} + v_\theta\frac{1}{r}\frac{\partial c}{\partial \theta} + v_z\frac{\partial c}{\partial z} \tag{5.111}$$

adding these two equations together

$$\nabla \cdot c\boldsymbol{v}^\star = v_r\frac{\partial c}{\partial r} + v_\theta\frac{1}{r}\frac{\partial c}{\partial \theta} + v_z\frac{\partial c}{\partial z} + c\left(\frac{1}{r}\frac{\partial}{\partial r}(rv_r) + \frac{1}{r}\left(\frac{\partial v_\theta}{\partial \theta}\right) + \frac{\partial v_z}{\partial z}\right) \tag{5.112}$$

assuming that there is no bulk flow in the θ and r direction defines $\frac{\partial v_\theta}{\partial \theta} = \frac{\partial v_r}{\partial r} = v_r = v_\theta = 0$ and equation 5.112 reduces to

$$\nabla \cdot c\boldsymbol{v}^\star = v_z\frac{\partial c}{\partial z} + c\frac{\partial v_z}{\partial z} \tag{5.113}$$

Re-writing the general transport equation (equation 5.81 and/or equation 5.86) for convenient review

$$\frac{\partial c_i}{\partial t} + (\nabla \cdot c_i v^\star) = (\nabla \cdot \mathfrak{D}\nabla c_i) + R_i \tag{5.114}$$

and substituting the appropriate cylindrical terms in gives the transient transport with reaction equation in cylindrical co-ordinates for a non-constant diffusion coefficient

$$\frac{\partial c_i}{\partial t} + v_z\frac{\partial c_i}{\partial z} + c_i\frac{\partial v_z}{\partial z} = \mathfrak{D}_i\frac{\partial^2 c_i}{\partial r^2} + \frac{\partial c_i}{\partial r}\frac{\partial \mathfrak{D}_i}{\partial r} + \frac{\mathfrak{D}_i}{r}\frac{\partial c_i}{\partial r} + \mathfrak{D}_i\frac{\partial^2 c_i}{\partial z^2} + \frac{\partial c_i}{\partial z}\frac{\partial \mathfrak{D}_i}{\partial z} + R_i \tag{5.115}$$

The above equation has the homogenous reaction term R_i. Vandegrift and Horwitz [?] show that the extraction of Ca(II) with HDEHP is complexed at the interface which is the slow step of of the reaction. They also show that the kinetics are first order and that macro and tracer metal extraction studies showed equal mass transfer rates. According to Vandegrift and Horwitz these two facts as well as other data give strong support that the extraction of

metal by HDEHP is by a complex formed at the two phase interface and not in the aqueous phase. Thus the reaction is contained in the boundary condition for most metal extraction by HDEHP and the above equation becomes

$$\frac{\partial c_i}{\partial t} + v_z\frac{\partial c_i}{\partial z} + c_i\frac{\partial v_z}{\partial z} = \mathfrak{D}_i\frac{\partial^2 c_i}{\partial r^2} + \frac{\partial c_i}{\partial r}\frac{\partial \mathfrak{D}_i}{\partial r} + \frac{\mathfrak{D}_i}{r}\frac{\partial c_i}{\partial r} + \mathfrak{D}_i\frac{\partial^2 c_i}{\partial z^2} + \frac{\partial c_i}{\partial z}\frac{\partial \mathfrak{D}_i}{\partial z} \tag{5.116}$$

Liquid membranes inherently consist of two interfaces. The membrane contactor separates the interfaces into two operations— the extraction and the stripping stage. The interface between two immiscible phases is the most critical and complex part of the liquid membrane extraction process. Thus, considerable effort in this study will be directed to understanding the chemistry, the physics, and mathematical modeling of the interface in order to model and simulate the membrane contactor.

An interface is conveniently idealized as a two–dimensional, singular 'surface' possessing a microscopically defined location, configuration and orientation between a pair of contiguous, three–dimensional, immiscible bulk–fluid phases. The above definition could be viewed as verbal mathematician's rendition of a surface — a surface that has no thickness. A fluid interface is not a truly two–dimensional material entity. The interface is a three dimensional very thin region where the system's properties change rapidly [?, Chapter 7].

The transport processes at and through the interfacial transition zone is analogous to volumetric transport processes occurring in the bulk phases [?, page 41]. As pointed out by Edwards et al [?] two scales of analysis can be used to describe the transport processes through the interfacial zone between two phases.

The *macroscale*, or conventional view of the interface is described as a deformable, two–dimensional, singular surface model and uses phenomenological relation functions as boundary conditions imposed upon volumetric transport fields(gradients) at the interface. These constraints are derived from analogy similarities with existing conservation and constitutive transport laws for three–dimensional fluid continua. The ultimate characterization of the interface and it's fields cannot be understood without a thorough micro mechanical analysis of the interfacial transition region. For operational purposes macro mechanical phenomenological properties such as interfacial tension, interfacial viscosity, and interfacial elasticity may be sufficient to describe the transport phenomena between two different immiscible fluids.

The *mircroscale* model is a more rigorous, fundamental three dimensional interphase description. Thus the second scale is a first principles approach at the molecular level to model interfacial transport. The use of the micro scale theory in a liquid/liquid extraction process using micro porous hollow fiber membranes to stabilize the interface, is of interest and will be modeled and examined if time in this project permits. As a preliminary, since

the macro–analysis is inherent in the micro continuity equations, the transport, constitutive boundary equations are developed for a hollow fiber liquid/liquid membrane extractor. Thus, the interface of the membrane contactor will be the first boundary condition.

In general for fast reactions and in well stirred systems two assumptions hold for transport in liquid membranes

1. Steady State
2. Linear concentration gradient through the membrane

when the transport mechanism is simultaneously controlled by diffusion in the bulk phases, diffusion in and through the membrane, and by interfacial chemical reactions the theoretical treatment is complex [?]. Danesi et al as well as other workers have presented models for the extraction of various metal species using the simplifying assumptions:

1. Metal concentrations is much smaller than the extractant
2. Extractant is assumed to behave ideally
3. linear concentration gradients for the metal cations
4. negligible concentration gradient for the hydrogen ion
5. stationary state conditions (steady state)

Ideally the boundary condition one would like to use would be the overall extraction rate based on the controlling reactions. However, as has been discussed in the Kinetics chapter of this study an overall extraction rate is difficult at best even for very simple processes or imposing conditions on the extraction process that oversimplify the process. Assuming a controlling step or steps a priori allows a researcher in some instances to reduce the complexities to a manageable problem. This is not an incorrect scheme and requires a very intuitive understanding analysis of the the problem at hand. But it also restricts the model to a very specific sub–scheme of the larger model. We would like to avoid this if possible and model the extraction process in the most general method as our current capablities will permit.

For each phase i.e the aqueous (aq) and the organic (org) every specie that is involved in the extraction reaction will need to be modeled by a diffusion equation as given by equation 5.115. Equation 5.115 has a reaction term for reactions that occur in the bulk phase. These reactions are a result of partial distribution of the extractant between the organic and aqueous phases, the dimerization reaction, if any in the organic phase, and adduct

reactions in the organic phases. Primarily liquid liquid extraction reactions occur at the interface and this is in the boundary conditions. Thus for specie i in the aqueous phase

$$\frac{\partial c_i}{\partial t} + v_z\frac{\partial c_i}{\partial z} + c_i\frac{\partial v_z}{\partial z} = \mathfrak{D}_i\frac{\partial^2 c_i}{\partial r^2} + \frac{\partial c_i}{\partial r}\frac{\partial \mathfrak{D}_i}{\partial r} + \frac{\mathfrak{D}_i}{r}\frac{\partial c_i}{\partial r} + \mathfrak{D}_i\frac{\partial^2 c_i}{\partial z^2} + \frac{\partial c_i}{\partial z}\frac{\partial \mathfrak{D}_i}{\partial z} + R_i \quad (5.117)$$

and for specie i in the organic phase where the overbar indicates organic phase

$$\frac{\partial \overline{c}_i}{\partial t} + \overline{v}_z\frac{\partial \overline{c}_i}{\partial z} + \overline{c}_i\frac{\partial \overline{v}_z}{\partial z} = \overline{\mathfrak{D}}_i\frac{\partial^2 \overline{c}_i}{\partial r^2} + \frac{\partial \overline{c}_i}{\partial r}\frac{\partial \overline{\mathfrak{D}}_i}{\partial r} + \frac{\overline{\mathfrak{D}}_i}{r}\frac{\partial \overline{c}_i}{\partial r} + \overline{\mathfrak{D}}_i\frac{\partial^2 \overline{c}_i}{\partial z^2} + \frac{\partial \overline{c}_i}{\partial z}\frac{\partial \overline{\mathfrak{D}}_i}{\partial z} + \overline{R}_i \quad (5.118)$$

the transport equation in the pores of the membrane is given by the following note that there is no convective transport in the pores for this study and ε, is the porosity and τ, is the tortuosity.

$$\varepsilon\frac{\partial c_i}{\partial t} = \frac{\varepsilon}{\tau}\mathfrak{D}_i\frac{\partial^2 c_i}{\partial r^2} + \frac{\varepsilon}{\tau}\frac{\partial c_i}{\partial r}\frac{\partial \mathfrak{D}_i}{\partial r} + \frac{\varepsilon}{\tau}\frac{\mathfrak{D}_i}{r}\frac{\partial c_i}{\partial r} + \frac{\varepsilon}{\tau}\mathfrak{D}_i\frac{\partial^2 c_i}{\partial z^2} + \frac{\varepsilon}{\tau}\frac{\partial c_i}{\partial z}\frac{\partial \mathfrak{D}_i}{\partial z} + \varepsilon R_i \quad (5.119)$$

5.4.2 The Reaction Term

The reactions listed here are discussed in detail in the kinetics seciton of this report.

Homogenous Reactions

Aqueous Phase: The following reactions can occur in the aqueous phase:

DISSOCIATION OF THE EXTRACTANT IN THE AQUEOUS PHASE

$$m\,[\mathrm{HA}] \underset{k_{-a}}{\overset{k_a}{\rightleftharpoons}} m\,[\mathrm{H}^+] + m\,[\mathrm{A}^-] \quad (5.120)$$

FORMATION OF METAL EXTRACTION COMPLEXES

$$\begin{aligned} [\mathrm{M}^{m+}] + [\mathrm{HA}] &\underset{k_{-1}}{\overset{k_1}{\rightleftharpoons}} \left[\mathrm{MA}^{(m-1)+}\right] + [\mathrm{H}^+] \qquad K_1 = \frac{\left[\mathrm{MA}^{(m-1)+}\right][\mathrm{H}^+]}{[\mathrm{M}^{m+}][\mathrm{HA}]} \\ [\mathrm{M}^{m+}] + [\mathrm{A}^-] &\underset{k_{-1a}}{\overset{k_{1a}}{\rightleftharpoons}} \left[\mathrm{MA}^{(m-1)+}\right] \qquad K_{1a} = \frac{\left[\mathrm{MA}^{(m-1)+}\right]}{[\mathrm{M}^{m+}][\mathrm{A}^-]} \end{aligned} \quad (5.121)$$

$$\begin{aligned} \left[\mathrm{MA}^{(m-1)+}\right] + [\mathrm{HA}] &\underset{k_{-2}}{\overset{k_2}{\rightleftharpoons}} \left[\mathrm{MA}_2^{(m-2)+}\right] + [\mathrm{H}^+] \qquad K_2 = \frac{\left[\mathrm{MA}_2^{(m-2)+}\right][\mathrm{H}^+]}{\left[\mathrm{MA}^{(m-1)+}\right][\mathrm{HA}]} \\ \left[\mathrm{MA}^{(m-1)+}\right] + [\mathrm{A}^-] &\underset{k_{-2a}}{\overset{k_{2a}}{\rightleftharpoons}} \left[\mathrm{MA}_2^{(m-2)+}\right] \qquad K_{2a} = \frac{\left[\mathrm{MA}_2^{(m-2)+}\right]}{\left[\mathrm{MA}^{(m-1)+}\right][\mathrm{A}^-]} \end{aligned} \quad (5.122)$$

$$\begin{aligned}
&\left[MA_2^{(m-2)+}\right] + [HA] \underset{k_{-3}}{\overset{k_3}{-}} \left[MA_3^{(m-3)+}\right] + [H^+] \qquad K_3 = \frac{\left[MA_3^{(m-3)+}\right][H^+]}{\left[M^{(m-2)+}\right][HA]} \\
&\left[MA_2^{(m-2)+}\right] + [A^-] \underset{k_{-3a}}{\overset{k_{3a}}{-}} \left[MA_3^{(m-3)+}\right] \qquad K_{3a} = \frac{\left[MA_3^{(m-3)+}\right]}{\left[M^{(m-2)+}\right][A^-]}
\end{aligned} \tag{5.123}$$

$$\vdots$$

$$\begin{aligned}
&\left[MA_{m-1}^+\right] + [HA] \underset{k_{-m}}{\overset{k_m}{-}} [MA_m] + [H^+] \qquad K_m = \frac{[MA_m][H^+]}{\left[M_{m-1}^+\right][HA]} \\
&\left[MA_{m-1}^+\right] + [A^-] \underset{k_{-m_a}}{\overset{k_{m_a}}{-}} [MA_m] \qquad K_{m_a} = \frac{[MA_m]}{\left[M_{m-1}^+\right][A^-]}
\end{aligned} \tag{5.124}$$

Also the hydrolyzed metal ion can exist, though in some cases such high pH it may be small, and needs to be accounted for

$$[M^{m+}] + [H_2O] \underset{k^*_{-hyd}}{\overset{k^*_{hyd}}{-}} \left[M(OH)^{(m-1)+}\right] + [H^+] \tag{5.125}$$

$$\begin{aligned}
&\left[M(OH)^{(m-1)+}\right] + [HA] \underset{k_{-hyd}}{\overset{k_{hyd}}{-}} \left[MA^{(m-1)+}\right] + [H_2O] \\
&\left[M(OH)^{(m-1)+}\right] + [A^-] \underset{k_{-hyd_a}}{\overset{k_{hyd_a}}{-}} \left[MA^{(m-1)+}\right] + [OH^-]
\end{aligned} \tag{5.126}$$

and the rate equations mathematically describing or modeling these reactions are:

$$r_a = k_a [HA]^m - k_{-a} [H^+]^m [A^-]^m \tag{5.127}$$

$$r_1 = k_1 [M^{m+}] [HA] - k_{-1} \left[MA^{(m-1)+}\right] [H^+] \tag{5.128}$$

$$r_{1a} = k_{1a} [M^{m+}] [A^-] - k_{-1a} \left[MA^{(m-1)+}\right] \tag{5.129}$$

$$r_2 = k_2 \left[MA^{(m-1)+}\right] [HA] - k_{-2} \left[MA_2^{(m-2)+}\right] [H^+] \tag{5.130}$$

$$r_{2a} = k_{2a} \left[MA^{(m-1)+}\right] [A^-] - k_{-2a} \left[MA_2^{(m-2)+}\right] \tag{5.131}$$

$$r_{3a} = k_{3a} \left[MA_2^{(m-2)+}\right] [A^-] - k_{-3a} \left[MA_3^{(m-3)+}\right] \tag{5.132}$$

$$\vdots$$

$$r_m = k_m \left[MA_{m-1}^+\right] [HA] - k_{-m} [MA_m] [H^+] \tag{5.133}$$

$$r_{m_a} = k_{m_a} \left[MA_{m-1}^+\right] [A^-] - k_{-m_a} [MA_m] \tag{5.134}$$

$$r^*_{hyd} = k^*_{hyd}\left[M^{m+}\right] - k^*_{-hyd}\left[M(OH)^{(m-1)+}\right]\left[H^+\right] \tag{5.135}$$

$$r_{hyd} = k_{hyd}\left[M(OH)^{(m-1)+}\right]\left[HA\right] - k_{-hyd}\left[MA^{(m-1)+}\right]\left[H^+\right] \tag{5.136}$$

$$r_{hyd_a} = k_{hyd_a}\left[M(OH)^{(m-1)+}\right]\left[A^-\right] - k_{-hyd_a}\left[MA^{(m-1)+}\right] \tag{5.137}$$

Organic Phase: THE SELF ASSOCIATION OF THE EXTRACTANT OR POLYMERIZATION IN THE ORGANIC PHASE

$$[yHA]_{(org)} \underset{k_{-poly}}{\overset{k_{poly}}{-}} [H_yA_y]_{(org)} \qquad K_{poly} = \frac{[H_yA_y]_{(org)}}{[HA]^y_{(org)}} \tag{5.138}$$

$$r_{poly} = k_{poly}\left[\overline{HA}\right]^y - k_{-poly}\left[\overline{H_yA_y}\right] = k_{poly}\left[\overline{HA}\right]^y - k_{-poly}\left[\overline{HA}\right]_y \tag{5.139}$$

This POLYMERIZATION PHENOMENA can also occur between other types of extractants and cause a synergistic affect of extraction. The self adduct formation to satisfy the coordination saturation demand by adding one or several molecules of the undissociated acid HA. The complex formed is

$$[MA_m]_{org} + x\,[HA]_{org} \underset{k_{-add}}{\overset{k_{add}}{-}} [MA_m \cdot x\,(HA)]_{org} \quad K_{add\ (org)} = \frac{[MA_m \cdot x\,(HA)]_{org}}{[MA_m]_{org}\,[HA]^x_{org}} \tag{5.140}$$

$$r_{add} = k_{add}\,[MA_m]_{org}\,[HA]^x_{org} - k_{-add}\,[MA_m \cdot x\,(HA)]_{org} \tag{5.141}$$

Heterogenous Reactions at the Interface:

Partitioning of the Extractant between the organic carrier and aqueous phase: INTERFACIAL PARTITION OF THE ORGANIC EXTRACTANT BETWEEN THE ORGANIC AND AQUEOUS PHASES

$$[HA]_{org} \underset{k^*_{-part}}{\overset{k^*_{part}}{-}} [HA] \tag{5.142}$$

$$r^*_{part} = a_{org}k^*_{part}\,[HA]_{org} - a_{aq}k^*_{-part}\,[HA] \tag{5.143}$$

THE DISTRIBUTION OF THE METAL EXTRACTION SPECIES

$$[MA_m] \underset{k^*_{-d}}{\overset{k^*_d}{-}} [MA_m]_{org} \qquad K_{MA_m} = \frac{[MA_m]_{org}}{[MA_m]} \tag{5.144}$$

$$r^*_d = a_{org}k^*_d\,[MA_m] - a_{aq}k^*_{-d}\,[MA_m]_{org} \tag{5.145}$$

Interfacial reactions:

$$
\begin{aligned}
r_1^* &= k_1^* \left[\mathrm{M}^{m+}\right] \left[\mathrm{HA}\right]_{ad} - k_{-1}^* \left[\mathrm{MA}^{(m-1)+}\right]_{ad} \left[\mathrm{H}^+\right] \\
r_2^* &= k_2^* \left[\mathrm{MA}^{(m-1)+}\right]_{ad} \left[\mathrm{HA}\right]_{ad} - k_{-2}^* \left[\mathrm{MA}_2^{(m-2)+}\right]_{ad} \left[\mathrm{H}^+\right] \\
r_3^* &= k_3^* \left[\mathrm{MA}_2^{(m-2)+}\right]_{ad} \left[\mathrm{HA}\right]_{ad} - k_{-3}^* \left[\mathrm{MA}_3^{(m-3)+}\right]_{ad} \left[\mathrm{H}^+\right] \\
&\vdots \\
r_m^* &= k_m^* \left[\mathrm{MA}_{m-1}^{+}\right]_{ad} \left[\mathrm{HA}\right]_{ad} - k_{-m}^* \left[\mathrm{MA}_m\right]_{ad} \left[\mathrm{H}^+\right] \\
r_{des}^* &= a_{org} k_{des}^* \left[\mathrm{MA}_m\right]_{ad} - a_{aq} k_{-des}^* \left[\mathrm{MA}_m\right]_{\mathrm{org}} \\
r_{ad}^* &= a_{org} k_{ad}^* \left[\mathrm{HA}\right]_{org}^m - a_{aq} k_{-ad}^* \left[\mathrm{HA}\right]_{ad}^m \\
r_{hyd_{(int)}} &= a_{org} k_{hyd_{(int)}} \left[\mathrm{M(OH)}^{(m-1)+}\right] \left[\mathrm{HA}\right]_{ad} - a_{aq} k_{-hyd_{(int)}} \left[\mathrm{MA}^{(m-1)+}\right]_{ad}
\end{aligned}
$$

Reaction Rates of Species The reactions displayed above happen in different phases as well as accross the interfaces. Because of this, the change with time of the species depends on consecutive and/or parallel reactions occuring in other phases or at the interface.

Aqueous phase:

$$
\begin{aligned}
\frac{d\left[\mathrm{HA}\right]}{dt} &= r_{part}^* - \sum_1^m r_i - r_{hyd} - r_a \\
\frac{d\left[\mathrm{A}^-\right]}{dt} &= r_a - \sum_1^m r_{i_a} \\
\frac{d\left[\mathrm{MA}_i^{(m-1)+}\right]}{dt} &= r_1 + r_{hyd} + r_{1a} \\
\frac{d\left[\mathrm{MA}_i^{(m-i)+}\right]}{dt} &= r_i - r_{(i+1)} - r_{(i+1)_a} \\
\frac{d\left[\mathrm{MA}_m\right]}{dt} &= r_m - r_d + r_{m_a} \\
\frac{d\left[\mathrm{M(OH)}^{(m-1)+}\right]}{dt} &= r_{hyd}^* - r_{hyd} - r_{hyd_{(int)}} - r_{hyd_a} \\
\frac{d\left[\mathrm{M}^{m+}\right]}{dt} &= -(r_1 - r_{hyd}^* + r_1^* + r_{1a}^*)
\end{aligned}
$$

$$\frac{d[\mathrm{H}^+]}{dt} = \sum_1^m r_i + r_a + r^*_{hyd} + r_{hyd} + \sum_1^m r^*_i$$

The above is a convenient shorthand for the expanded equations listed below. The accumulation of [HA] in the aqueous phase is given by a mass balance

$$\begin{aligned}\frac{d[\mathrm{HA}]}{dt} = {} & \frac{a_{org}}{V_{org}} k^*_1 [\mathrm{HA}]_{org} - \frac{a_{aq}}{V_{aq}} k^*_{-1} [\mathrm{HA}] \\ & -k_{hyd}\left[\mathrm{M(OH)}^{(m-1)+}\right][\mathrm{HA}] + k_{-hyd}\left[\mathrm{MA}^{(m-1)+}\right] \\ & -k_1[\mathrm{M}^{m+}][\mathrm{HA}] + k_{-1}\left[MA^{(m-1)+}\right][H^+] \\ & -k_2\left[\mathrm{MA}^{(m-1)+}\right][\mathrm{HA}] + k_{-2}\left[MA^{(m-2)+}\right][H^+] \\ & -k_3\left[\mathrm{MA}_2^{(m-2)+}\right][\mathrm{HA}] + k_{-3}\left[MA_3^{(m-3)+}\right][H^+] \\ & -k_4\left[\mathrm{MA}_3^{(m-3)+}\right][\mathrm{HA}] + k_{-4}\left[MA_4^{(m-4)+}\right][H^+] \\ & \vdots \\ & -k_{m-1}\left[\mathrm{MA}_{m-2}^{2+}\right][\mathrm{HA}] + k_{1-m}\left[MA^+_{m-1}\right][H^+] \\ & -k_m\left[\mathrm{MA}^+_{m-1}\right][\mathrm{HA}] + k_{-m}[MA_m][H^+] \end{aligned} \tag{5.146}$$

$$\begin{aligned}\frac{d[\mathrm{M}^{m+}]}{dt} = {} & k_{-1}\left[\mathrm{MA}^{(m-1)+}\right][H^+] - k_1[\mathrm{M}^{m+}][\mathrm{HA}] + k^*_{-hyd}\left[\mathrm{M(OH)}^{(m-1)+}\right][\mathrm{H}^+] \\ & -k^*_{hyd}[\mathrm{M}^{m+}] \end{aligned} \tag{5.147}$$

$$\begin{aligned}\frac{d\left[\mathrm{M}^{(m-1)+}\right]}{dt} = {} & k_1[\mathrm{M}^{m+}][\mathrm{HA}] - k_{-1}\left[\mathrm{MA}^{(m-1)+}\right][\mathrm{H}^+] \\ & -k_2\left[\mathrm{MA}^{(m-1)+}\right][\mathrm{HA}] + k_{-2}\left[\mathrm{MA}_2^{(m-2)+}\right][\mathrm{H}^+] \end{aligned} \tag{5.148}$$

$$\begin{aligned}\frac{d\left[\mathrm{MA}_2^{(m-2)+}\right]}{dt} = {} & k_2\left[\mathrm{MA}^{(m-1)+}\right][\mathrm{HA}] - k_{-2}\left[\mathrm{MA}_2^{(m-2)+}\right][\mathrm{H}^+] \\ & -k_3\left[\mathrm{MA}_2^{(m-2)+}\right][\mathrm{HA}] + k_{-3}\left[\mathrm{MA}_3^{(m-3)+}\right][\mathrm{H}^+] \end{aligned} \tag{5.149}$$

$$\begin{aligned}\frac{d\left[\mathrm{MA}_3^{(m-3)+}\right]}{dt} = {} & k_3\left[\mathrm{MA}_2^{(m-2)+}\right][\mathrm{HA}] - k_{-3}\left[\mathrm{MA}_3^{(m-3)+}\right][\mathrm{H}^+] \\ & -k_4\left[\mathrm{MA}_3^{(m-3)+}\right][\mathrm{HA}] + k_{-4}\left[\mathrm{MA}_4^{(m-4)+}\right][\mathrm{H}^+] \end{aligned} \tag{5.150}$$

$$\vdots$$

$$\frac{d\left[\mathrm{MA}^{+}_{m-1}\right]}{dt} = k_{m-1}\left[\mathrm{MA}^{m+}_{m-2}\right][\mathrm{HA}] - k_{1-m}\left[\mathrm{MA}^{+}_{m-1}\right][\mathrm{H}^{+}] - k_{m}\left[\mathrm{MA}^{+}_{m-1}\right][\mathrm{HA}] + k_{-m}[\mathrm{MA}_{m}][\mathrm{H}^{+}] \quad (5.151)$$

Equations 5.148 through 5.151 can be reduced in form to

$$\frac{d\left[\mathrm{MA}^{(m-i)+}_{i}\right]}{dt} = k_{i}\left[\mathrm{MA}^{(m-i+1)+}_{i-1}\right][\mathrm{HA}] - k_{-i}\left[\mathrm{MA}^{(m-i)+}_{i}\right][\mathrm{H}^{+}] - k_{i+1}\left[\mathrm{MA}^{(m-i)+}_{i}\right][\mathrm{HA}] + k_{-(i+1)}\left[\mathrm{MA}^{m-(i+1)}_{i+1}\right][\mathrm{H}^{+}] \quad (5.152)$$

for $i = 1$ to $m-1$. The rate expression for the metal complex concentration in the aqueous phase is

$$-\frac{d[\mathrm{MA}_{m}]}{dt} = k_{m}\left[\mathrm{MA}^{+}_{m-1}\right][\mathrm{HA}] - k_{-m}[\mathrm{MA}_{m}][\mathrm{H}^{+}] - k^{*}_{d}[\mathrm{MA}_{m}] + k^{*}_{-d}[\mathrm{MA}_{m}] \quad (5.153)$$

For which the overall formation equalibrium constant is

$$K_{f} = K_{1}K_{2}K_{3}\cdots K_{m-1}K_{m} = \prod_{i=1}^{m} K_{i} = \frac{[\mathrm{MA}_{m}][\mathrm{H}^{+}]^{m}}{[\mathrm{M}^{m+}][\mathrm{HA}]^{m}} \quad (5.154)$$

Using the reaction rates for each specie and the continuity equation of equation 5.117 the concentration gradients in the aqueous phase can be determined.

Species balance in the organic phase:

$$\frac{d\left[\overline{\mathrm{HA}}\right]}{dt} = -(r_{poly} + r_{add} + r_{part} + r_{ad})$$

$$\frac{d\left[\overline{\mathrm{MA}_{m}}\right]}{dt} = r^{*}_{d} - r_{add}$$

$$\frac{d\overline{[\mathrm{MA}_{m}\cdot x\,(\mathrm{HA})]}}{dt} = r_{add}$$

$$\frac{d\left[\overline{\mathrm{H}_{y}\mathrm{A}_{y}}\right]}{dt} = r_{poly}$$

In this phase the above reactions or specie rates are inserted into equation 5.118.

5.5 The Diffusive Boundary Conditions

5.5.1 Initial State at $t = 0$, $0 \leq z \leq l$ and $r_0 \leq r \leq r_1$ where r_1 is the interface Location and r is the direction of diffusion and z is the distance along the axis of filament:

Aqueous Phase	Organic Phase	Interface
$[\mathrm{HA}] = [\mathrm{HA}]_0$	$\left[\overline{\mathrm{HA}}\right] = \left[\overline{\mathrm{HA}}\right]_0$	$[\mathrm{HA}]_{ad} = [\mathrm{HA}]_{ad_0}$
$[\mathrm{H}^+] = [\mathrm{H}^+]_0$	$\left[\overline{\mathrm{H}_y\mathrm{A}_y}\right] = \left[\overline{\mathrm{H}_y\mathrm{A}_y}\right]_0$	$\left[\mathrm{MA}_i^{(m-i)+}\right]_{ad} = \left[\mathrm{MA}_i^{(m-i)+}\right]_{ad_0}$
$[\mathrm{A}^-] = [\mathrm{A}^-]_0$	$\left[\overline{\mathrm{MA}_m}\right] = \left[\overline{\mathrm{MA}_m}\right]_0$	
$[\mathrm{M}^{m+}] = [\mathrm{M}^{m+}]_0$	$\left[\overline{\mathrm{MA}_m \cdot x\,(\mathrm{HA})}\right] = \left[\overline{\mathrm{MA}_m \cdot x\,(\mathrm{HA})}\right]_0$	
$\left[\mathrm{MA}_i^{(m-i)+}\right] = \left[\mathrm{MA}_i^{(m-i)+}\right]_0$		
$\left[\mathrm{M(OH)}_i^{(m-i)+}\right] = \left[\mathrm{M(OH)}_i^{(m-i)+}\right]_0$		
or	or	or
$c_i = c_{i_0}$ where	$\overline{c}_i = \overline{c}_{i_0}$ where	$c_i = c_{i_0}$ where
$c_i \equiv$ concentration of species i such as . HA, H^+, A^- ,M^{m+} etc	$\overline{c}_i \equiv$ concentration of species i such as HA, MA_m etc.	$c_i \equiv$ concentration of species i such as HA, MA_m etc.

for most species the initial concentration is zero except for the metal concentrations in the aqueous phase and the extractant concentration in the organic phase but here for generality we have left it to be a constant.

5.5.2 At $t > 0$ and $z > 0$ and $r = 0$

by symmetry argument

$\mathfrak{D}_i \frac{\partial c_i}{\partial r} = 0$

which says the flux for each specie at the center of each filiment is zero and is a function of r and z but not of θ.

5.5.3 At the outer surface or structure of the membrane fiber $r = r_2$, $t > 0$ and $z > 0$

For this study interactions between the hollow fiber solid material are assumed negligible and no penetration of the fiber wall material occurs. Thus the flux at the solid portions of the outside wall of the fibrous structure is

$$(1 - \varepsilon_o)\,\mathfrak{D}_i \frac{\partial c_i}{\partial r} = 0 \tag{5.155}$$

where $\varepsilon_o \equiv$ porosity of the outside wall of the membrane and $1 - \varepsilon_o$ is the surface area occupied by the solid material which nothing pentrates.

Equation 5.155 also reflects the boundary condition for pores at this point as the flux from and into the pore is

$$\mathfrak{D}_i \frac{\partial c_i}{\partial r}\bigg|_{r \to r_1^-} = \varepsilon_o \mathfrak{D}_i \frac{\partial c_i}{\partial r}\bigg|_{r \to r_1^+} \tag{5.156}$$

This equation states that the bulk flux of the concentration of specie i at the outer wall of a membrane fiber is equal to the concentration flux inside the pore of specie i at the outer surface or boundary. Also, the diffusivity $\mathfrak{D}_i$ is assumed the same in the pore as in the bulk phase in equation 5.156. The assumption is made that immediately outside and immediately inside the pore entrances the phases are the same. Implied with this assumption is that the pore concentrations just within the pores are essentially in equilibrium with the corresponding external concentrations. For homogenous long pore structures the mass transfer resistances associated with two-dimensional flows at the pore entrances can be neglected [?]. Membranes with irregularities in their morphologies or structure (i.e. variations in the pore sizes, sloping in their trajectories, tortuosities, or distributions) require a detailed characterization introduced in the membrane model. The lack of homogeniety on the surface of the membrane distorts the streamlines of the diffusive flux around the mouth of each pore [?].

The diffusivity on the right hand side of equation 5.156 is more accurately represented by $\mathfrak{D}_{i,p}$ denoting a difference in the pore diffusivity of the outside phase and the bulk diffusivity in the continuous phase outside the pore structure. Within pores of dimensions comparible to that of a solute molecule it is generally found that the ratio $\frac{\mathfrak{D}_{i,p}}{\mathfrak{D}_{i,\infty}} < 1$ where $\mathfrak{D}_{i,\infty}$ is the diffusivity of the bulk continuous phase outside the effects of the pores [?]. This difference between the diffusivity in the pore and the continuous phase comes about from the wall effects of the pores causing an increase in the hydrodynamic drag force and nonhydrodynamic interactions between the solute and pore walls expressible as potentials. For electrically charged solutes and /or pores, electrostatic interactions between solute and pore walls are important.

The interactions between the molecules of the fluid or solute in the pore and the pore walls is known as Knudson diffusion. The interaction between the molecules in the fluid is termed continuum diffusion. Generally the Knudsen diffusion has been assumed to be important in small gas filled pores (<0.1 μm). In liquid phases the number density of molecules is much higher and the interactions between the walls of the porous structure usiually are neglected [?]. These hindered diffusion effects are generally handled by a lumped parameter like an effective diffusivity or mass transfer coefficient as given by $k_M = \frac{\mathfrak{D}_{i,e}}{d} = \mathfrak{D}_i \frac{\varepsilon}{d\tau}$. Knowing the porosity, ε, the tortuosity, τ, and the thickness of the membrane, d, the diffusion coefficients can be calculated from mass transfer experiments assuming no chemical reactions occur. In the intermediate range both types of diffusion play a role.

In the case where the solute molecular size is small compared to the pore size, $\mathfrak{D}_{i,p}$, can be replaced with the free or continuum diffusion coefficient. For a membrane with cylindrical pores, the resistance of the membrane, R_M, is given by

$$R_M = \frac{L}{\mathfrak{D}_{i,p} n\pi r^2} \tag{5.157}$$

where n is the pore density $\frac{1}{cm^2}$, r is the radius of the pores, and L is the pore length. Note that $R_M = \frac{1}{k_M}$ with L assumed to be the membrane thickness; thus, the term $n\pi r^2$, is the membrane porosity.

5.5.4 At the inner surface or structure of the membrane fiber $r = r_1$, $t > 0$ and $z > 0$

The boundary condition at this radial distance has the same structure as that at the outer wall or position.

$$(1 - \varepsilon_1)\,\mathfrak{D}_i \frac{\partial c_i}{\partial r} = 0 \tag{5.158}$$

for the inner wall made up of the solid membrane fiber and

$$\mathfrak{D}_i \frac{\partial c_i}{\partial r} = \varepsilon_1 \mathfrak{D}_i \frac{\partial c_i}{\partial r} \tag{5.159}$$

for the pore mouth fluxes. Note that the porosities have been made different for generallity but in most transport studies in porous media the porosities are assumed, as will be here, to be equal on the outer and inner surfaces and thus throughout the porous structure.

5.5.5 At $t > 0$ and $z > 0$ and $r = r_0$ or the locale of the interface

The solution of the species transport equation across an interface requires the quantitative specification of the following three conditions [?]:

1. The bulk phase partitioning of the species across the fluid interface

2. The normal bulk phase species flux in the pore $\mathbf{n}_{\alpha\beta} \cdot \|\frac{\varepsilon}{\tau}\bar{\mathbf{j}}_i\| = \frac{\partial(\varepsilon\Gamma_i^s)}{\partial t} + \nabla_s \cdot \left(\frac{\varepsilon}{\tau}\mathbf{v}^o\Gamma_i^s\right) - \frac{\varepsilon}{\tau}\mathcal{D}_i^s\nabla_s^2\Gamma_i^s - \varepsilon R_i^s$ where the surface excess molar specie concentration is $\Gamma_i^s \stackrel{\text{def}}{=} \frac{c_i^s}{M_i}$ and R_i^s is the surface excess molar areal production rate, ε is the porosity, and τ is the toruosity. In cylindrical coordinates for a surface at $r = r_0(t)$. Note that $\mathbf{n}_{\alpha\beta}$ is the unit normal vector pointing from the α phase into the β phase and for radial coordinates this vector becomes a scaler .

$$\frac{\partial(\varepsilon\Gamma_i^s)}{\partial t} + \varepsilon\frac{v_r^o}{r_0}\Gamma_i^s + \frac{\partial}{\partial z}\left(\varepsilon v_z^o\Gamma_i^s\right) + \frac{1}{r_0}\frac{\partial}{\partial\phi}\left(\varepsilon v_\phi^o\Gamma_i^s\right)$$
$$= \mathcal{D}_i^s\left(\frac{\partial^2\varepsilon\Gamma_i^s}{\partial z^2} + \frac{1}{r_0}\frac{\partial^2\varepsilon\Gamma_i^s}{\partial\phi^2}\right) + \varepsilon R_i^s + \frac{\varepsilon}{\tau}\|\bar{\mathbf{j}}_{i\,r}\| \tag{5.160}$$

and assuming no spatial or time variation of porosity or tortuosity:.

$$\varepsilon\frac{\partial\Gamma_i^s}{\partial t} + \varepsilon\frac{v_r^o}{r_0}\Gamma_i^s + \frac{\varepsilon}{\tau}\frac{\partial}{\partial z}\left(v_z^o\Gamma_i^s\right) + \varepsilon\frac{1}{r_0}\frac{\partial}{\partial\phi}\left(\frac{\varepsilon}{\tau}v_\phi^o\Gamma_i^s\right)$$
$$= \varepsilon\mathcal{D}_i^s\left(\frac{\partial^2\Gamma_i^s}{\partial z^2} + \frac{1}{r_0}\frac{\partial^2\Gamma_i^s}{\partial\phi^2}\right) + \varepsilon R_i^s + \frac{\varepsilon}{\tau}\|\bar{\mathbf{j}}_{i\,r}\| \tag{5.161}$$

$$\varepsilon\frac{\partial\Gamma_i^s}{\partial t} + \varepsilon\frac{v_r^o}{r_0}\Gamma_i^s + \varepsilon\frac{\partial}{\partial z}\left(v_z^o\Gamma_i^s\right) + \varepsilon\frac{1}{r_0}\frac{\partial}{\partial\phi}\left(\frac{\varepsilon}{\tau}v_\phi^o\Gamma_i^s\right)$$
$$= \varepsilon\mathcal{D}_i^s\left(\frac{\partial^2\Gamma_i^s}{\partial z^2} + \frac{1}{r_0}\frac{\partial^2\Gamma_i^s}{\partial\phi^2}\right) + \varepsilon R_i^s + \left(\frac{\varepsilon}{\tau}\| - \mathcal{D}_i\frac{\partial c_i}{\partial r}\|\right) \tag{5.162}$$

or

$$\varepsilon\frac{\partial\Gamma_i^s}{\partial t} + \varepsilon\frac{v_r^o}{r_0}\Gamma_i^s + \varepsilon\frac{\partial}{\partial z}\left(v_z^o\Gamma_i^s\right) + \varepsilon\frac{1}{r_0}\frac{\partial}{\partial\phi}\left(v_\phi^o\Gamma_i^s\right)$$
$$= \varepsilon\mathcal{D}_i^s\left(\frac{\partial^2\Gamma_i^s}{\partial z^2} + \frac{1}{r_0}\frac{\partial^2\Gamma_i^s}{\partial\phi^2}\right) + \varepsilon R_i^s - \frac{\varepsilon}{\tau}\mathcal{D}_i\frac{\partial c_i}{\partial r} \tag{5.163}$$

A discussion of each of the terms above and their importance may be fruitful:

(a) $\frac{\varepsilon}{\tau}\mathcal{D}_i\frac{\partial c_i}{\partial r}$ — this term is the net diffusive flux of specie i toward the interface. In the equation initially presented above this flux is the dot product of the magnitude of the flux in the bulk phase inside the pore

(b) εR_i^s — this is the surface reaction term and is necessary when a reaction will occur either by adsorption, desorption, between adsorbed species, with one of the adsorbed species and a specie in the bulk, or a combination of any two or more of these reactions.

(c) $\frac{\varepsilon}{\tau}\mathcal{D}_i^s\left(\frac{\partial^2\Gamma_i^s}{\partial z^2} + \frac{1}{r_0}\frac{\partial^2\Gamma_i^s}{\partial\phi^2}\right)$ — the surface diffusion flux which is important in the surface tension at the interface and plays a role in the marangoni effect

(d) $\frac{\varepsilon}{\tau}\frac{v_r^o}{r_0}\Gamma_i^s + \frac{\varepsilon}{\tau}\frac{\partial}{\partial z}(v_z^o\Gamma_i^s)$ — are the surface velocity or convective terms. They are a result of the surface diffusion fluxes caused by the opposing surface tension gradients and concentration gradients induced by the adsorbtion of a surface active specie at the interface.

(e) $\varepsilon\frac{\partial\Gamma_i^s}{\partial t}$ — this is the surface accumulation term of specie i at the interface

These terms are necessary to account for the Marangoni effect at the interface. If we assume that the Marangoni effect is negligible i.e. the surface diffusive fluxes and the tension and concentration gradient effects are negligible and thus the surface convective velocity terms are non existent the equation is reduced to in the unsteady state equation

$$\varepsilon\frac{\partial\Gamma_i^s}{\partial t} = \varepsilon R_i^s + \left(\frac{\varepsilon}{\tau}\| - \mathfrak{D}_i\frac{\partial c_i}{\partial r}\|\right) = \varepsilon R_i^s - \frac{\varepsilon}{\tau}\mathfrak{D}_i\frac{\partial c_i}{\partial r} \tag{5.164}$$

if the bulk concentration fields on both sides of the interface i.e. $c_{i(0+)}$ and $c_{i(0-)}$ are known a priori then the flux boundary condition may be circumvented. In this study since bulk reactions in both phases are occuring, an a priori knowledge of the concentration or density fields is not possible.

3. Kinetic adsorption relation i.e. the adorption isotherm

   (a) Two limits exist in the development of the constitutive form for the relationship between the instantaneous value of the bulk-phase species density or concentration at the interface to the surface excess species density or concentration : Equilibrium and Nonequilibrium Adsorption.

      i. Under Equilibrium (or small departures from equilibrium) conditions the Frumkin or Langmuir Isotherms are used

      ii. Under dynamical, nonequilibrium conditions the immediately previous simple models are usually invalid and a kinetic expression for the normal component of the bulk phase flux $\bar{\mathbf{j}}_i^o$ at the interface in terms of the local adsorption rate $r_{i_{ad}}$.

$$\frac{\varepsilon}{\tau}\mathbf{n}\cdot\bar{\mathbf{j}}_i^o = \varepsilon r_{i_{ad}} \tag{5.165}$$

The bulk phase species flux at the interface

Is given by the equation

$$\varepsilon\frac{\partial\Gamma_i^s}{\partial t} = \varepsilon R_i^s + \left(\frac{\varepsilon}{\tau}\| - \mathfrak{D}_i\frac{\partial c_i}{\partial r}\|\right) = \varepsilon R_i^s + \frac{\varepsilon}{\tau}\|\bar{\mathbf{j}}_{i\,r}\| \tag{5.166}$$

where R_i^s is the molar reaction of species i at the interface given by the following reactions as $R_{[i]_{ad}}$ and $\|\bar{\mathbf{j}}_{i\,R}\|$ is the flux of species i in the bulk of the fluid and is equal to $-\mathfrak{D}_i\frac{\partial c_i}{\partial r}$.

$$
\begin{aligned}
R_{[\mathrm{HA}]_{ad}} &= \frac{d[\mathrm{HA}]_{ad}}{dt} = r^*_{ad} - \sum_1^m r_i - r_{hyd_{(int)}} \\
R_{\left[\mathrm{MA}_i^{(m-1)+}\right]_{ad}} &= \frac{d\left[\mathrm{MA}_i^{(m-1)+}\right]_{ad}}{dt} = r^*_1 - r^*_2 + r_{hyd_{(int)}} \\
R_{\left[\mathrm{MA}_i^{(m-i)+}\right]_{ad}} &= \frac{d\left[\mathrm{MA}_i^{(m-i)+}\right]_{ad}}{dt} = r^*_i - r^*_{(i+1)} \quad \text{for } i = 2 \text{ to } m \\
R_{[\mathrm{MA}_m]_{ad}} &= \frac{d[\mathrm{MA}_m]_{ad}}{dt} = r^*_m - r^*_{des}
\end{aligned}
$$

The interface or surface adsorption expression $\frac{\varepsilon}{\tau}\mathbf{n}\cdot\bar{\mathbf{j}}_i^o = \varepsilon r_i$

This relation reveals a two step process

1. specie is first transported to the interface by diffusion in the pore, and then
2. adsorbed to the interface by a change in state.

The interfacial adsorption reactions:

$$
\begin{aligned}
r^*_{des} &= a_{org}k^*_{des}\,[\mathrm{MA}_m]_{ad} - a_{aq}k^*_{-des}\,[\mathrm{MA}_m]_{\mathrm{org}} \\
r^*_{org} &= a_{org}k^*_{ad}\,[\mathrm{HA}]_{org} - a_{aq}k^*_{-ad}\,[\mathrm{HA}]_{ad} \\
r^*_{aq} &= a_{aq}k^*_{aq}\,[\mathrm{HA}]_{ad} - a_{aq}k^*_{-aq}\,[\mathrm{HA}]_{aq}
\end{aligned}
\tag{5.167}
$$

and assuming the flux is in one direction only i.e. in the r direction only the bulk phase diffusion is $-\mathfrak{D}_i\frac{\partial c_i}{\partial r}$ and that equals the local specie adsorption rate for the species MA_m and HA since these are the only species that are assumed to adsorb and desorb reversibly at the interface or surface of the liquid/liquid membrane.

$$
-\varepsilon\mathfrak{D}_i\frac{\partial c_i}{\partial r} = \frac{\varepsilon}{\tau}r^*_i \tag{5.168}
$$

Consider a particular species that partitions between the phases and also adsorbs at the interface. If we set the fluxes equal to each other the rates become equal and a relationship for the concentration of the adsorped specie can be obtained in .

$$
[\mathrm{HA}]_{ad} = \frac{k^*_{ad}\,[\mathrm{HA}]_{org} + k^*_{-aq}\,[\mathrm{HA}]_{aq}}{k^*_{-ad} + k^*_{aq}} \tag{5.169}
$$

This assumes a steady state flow of HA to the interface from the organic and a steady state flow away from the surface in the aqueous side. Equation 5.169 would represent surface

saturated with HA.

The partitioning relation

Normally the partition relation is given by a linear Henry's Law relationship such as:

$$c_{i(0+)} = K_i c_{i(o-)}$$

where $c_{i(0+)}$ and $c_{i(o-)}$ are the concentrations of specie i on either side of the interface and K_i is the partition coefficient. This equation describes the equilibrium condition of the the partitioning between contiguous phases and can only under speciefic circumstances (i.e. diffusion controlled transport) be used for dynamic conditions (Edwards Brenner and Wasan). Specifications of equilibrium or nonequilibrium adsorption relations implicitly specifies the partition relation. Thus using a nonequalibrium adsorption relation for one phase sets the other phase to the same type of evaluation. If one were to assume an equilibrium analysis between the phases, the fluxes and thus the rates of species HA in equation 5.168 are equal to zero and the two equations solved simultaneously for $r_i = 0$ gives the partition coefficient with the equilibrium constant as $K_i = \frac{k^*_{-ad} k^*_{-aq}}{k^*_{ad} k^*_{aq}}$.

5.5.6 The Zero Diffusive Flux Condition Between Fibers — B. C. 2

In the shell side of the membrane contactor the concentration flux of species i between any two fibers will be zero.

$$\frac{\partial c_i}{\partial r} = 0 \tag{5.170}$$

Determining the location of this boundary can be difficult. The determination of this boundary is discussed in the following section.

5.6 Longitudinal Flow over Lumen (shell side velocity profile — the momentum balance in a tube bundle)

5.6.1 Geometrical and Packing Considerations of Hollow Fiber Bundles

The hydrodynamics of the shell side of hollow fiber membrane contactors is assumed to be unbaffled longitudinal laminar fluid flow between cylinders. This can be analogized to a non-baffled shell and tube heat exchanger or nuclear fuel rod assembly with axial fluid flow over a rod bundle. The modeling of the velocity profiles of fluid flow between cylinders can be complex and has been reported to take considerable computer time [?, see reference 14]; though, with current computer technology this may not be as intractable as it once was. Considerable effort within the nuclear industry to model the flow over

fuel rod budles has proliferated over the last thirty years. Various tube bundle geometries have been investigated with the primary three being a square pitch, hexagonal (triagular), and concentric bundles. Shell side fluid velocity profiles and thus the transport thermal properties have been shown to be dependent on the wall spacing (distance between the channel wall and outermost rod ring cluster), rod pitch to rod diameter ratio, and distance between rod ring clusters. The modeling of the shell and tube heat exchangers or nuclear fuel rod assemblies usually incorporate a technique of "subchannel" modeling to divide the heat exchanger into finite grids that are characterized primarily by the geometry of the tube layout and shell geometry.

Packing Considerations

Though simularites exist between hollow fiber membrane and shell and tube heat exchangers fluid flow outside the tubes, the placement of the tubes are controlled in the shell and tube heat exchangers. The manufacturing of the the hollow fiber modules does not allow precise placement or knowledge of the placement of the hollow fiber filaments. Thus to a large degree, the packing of the hollow fiber modules is random (at low to moderate packing densities and amorphic (locally structured) at high packing densities). If the packing of the filaments inside a circular (cylindrical) shell is maximized there appears to be no global symmetrical structure (see figure ———) and there is no known simple accurate (exact) analytical mathematical relationship to calculate the maximum number of smaller cylinders of a given radius that can be placed in a cylinder of a larger radius. Kausch, Fesko and Tschoegl [?] state that the packing fraction of a given area A is defined as the fraction of the area which is covered by the smaller circles; and, the packing fraction depends upon the choice of the area to be inspected and on its size. The packing fraction is independent of these only in the limit as A becomes large.

Kravitz [?] and Goldberg [?] attempt to analytically ascertain the packing efficincy of containing n equal nonoverlapping circles of diameter d in a larger circle of diameter D. They are able to accomplish this for an ensamble of circles up to 20 elements; extrapolation to higher densities cannot be done since instabilites and amorphous behavior appears. The maximum efficiency is given for a 20 circle ensemble of 0.8405 and is dependent on the number of circles in contained in the larger circle which is dependent uppon the smaller diameter. They define the packing efficiency as the summation of the areas occupied by a hexaganol element circumscribed about each element devided by the area of the container or $\phi = \frac{2\sqrt{3}}{\pi} \frac{Nd^2}{D^2}$.

From figure ———, which is a cursory computer experiment and was generated using a computer drawing program, the close packing of small diameter circles in a larger circle varies from approximately 0.259 for a single innercircle with a diameter just slightly larger

Number of Elememts (n)	**Small Circle diameter (d)**	**Large Circle diameter (D)**	$\left(\frac{d}{D}\right)^2$	**Packing density** $n\left(\frac{d}{D}\right)^2$
1	1.9182	3.77037	0.2588	0.2588344
2	1.8528	3.77037	0.2473	0.494759
30	0.60528	3.81	0.02538	0.75715
91	0.9525	10.16	0.008789	0.7998
127	0.9525	11.9458	0.00635	0.80743

Table 5.1: Values for packing densities

than the radius of the larger circle to a packing density of 0.807 for 127 smaller circles of 0.9525 cm in a 11.9458 cm circle (see table 5.1). As the diameter of the smaller circles gets smaller or $d \rightarrow 0$ as compared with the larger diameter then the approach of hexagonal packing can be deduced to be approximated at least away from the walls of a circular shell or cylinder. These conclusions are coroborated by Kausch, Fesko and Tschoegl [?]

Many workers have given experimental and computer simulated evidence that there exists a random close packing limit.Originally the packing theory was proposed to model structures of liquids primarily with spheres ([?], [?], [?, and references within]). The packing in two dimensions applicable to many physical systems such as films has been investigated by Quickenden and Tan [?], Mason [?], Shahinpoor [?], and Berryman [?], to list a few, who give estimates of random close packing density approaching 82%. Kausch, Fesko and Tschoegl [?] used computer experiments to determine a range of 0.8207 to 0.8319 for the packing density of a large number of disks i.e. $\geq$ 1000 circles. From a number of these computer experiments they determined an average packing density of 0.8207 $\pm$0.0019. Quickenden and Tan [?] experimentally determined the critical packing to 0.83$\pm$0.015 that slowly increased to the maximum packing density of an ordered two dimensional array of 0.9069. Shahinpoor [?] calculates a close packing density using Voronoi cells and comes up with a value of 0.846 for a critical packing density. The maximum packing of non-overlaping circles that can exists in a planar structure of infinite domain or at least an unconstrained environment corresponds to a regular triangular array (hexagonal) of closely packed circles which is $\sqrt{3}\pi/6 = 09069\cdots$. The value of 0.82 is considered a random close packing and is defined by Berryman [?] as the minimum packing fraction for which the median nearest–neighbor radius equals the diameter of the spheres.

The computer simulations to model random close packing suffers from an upper bound for random placement using random number generators in that it is not possible to generate a disk configuration of non overlaping disks greater than the "jamming" limit of 0.547$\pm$ 0.003

(Feder [?], Hinrichsen, Feder and Jøssang [?] without any reorganization of the placed disks. The method used by Hinrichsen et al. [?] to generate an ensemble of randomly oriented disks on a surface is called Random Sequential Adsorption or addition (RSA) and no reordering takes place of the disks already placed on the surface. Leamître et. al [?] used the RSA method of placing disks on a surface along with Voronoi tesslelations to determine the arrangement sizes of geometric shapes formed under different packing densities. A method used by Livesley and Loveday [?] uses a computer technique first used by Bennet [?] to sequentially deposit disks next to and in contact with at least two other disks (except for the first two disks placed which are placed in contact with each other). The site to attach a disk is chosen to be one of lowest potential energy. To achieve a degree of dissorder disks of a different size were placed at random times. As the ratio of the radii of the two disks used approach unity a crystalline or structure assembly initially appears and as more disks are added a general amorphic structure is produced; though, localized cystaline structures are seen (i.e. triangular, hexagonal, and square). This is also seen in figure ——— .

Rubinstein and Nelson [?] also used Bennett's algorithm to accomplish a deterministic chaotic behavoir or controllable amount of randomness by using a finite number of particles or disks of a different diameter than the majority of the disks. This causes what Rubinstein and Nelson call "stacking faults" which interrupt the crytalline (hexatic) structure but does not detroy it; since on either side of the fault a crystal structure is present and occasionally the faults coelesce to form regions of square lattices. These authors also note that orientation of the local structure or crystals is only slightly effected by the stacking faults. These authors built their computer generated packings from the inside out i.e. setting a single disk of a varying size at the center and "adsorbing or growing" other disks of fixed sizes to this seed and its subsequent cluster. By doing this with disks of the same size a hexagonal packing is obtained; and, by using a random number of another sized disk an ensemble of different configurations resembling randomness is evidenced but is actually deterministic.

Other techniques to increase the packing above the jamming limit use an emulated shaking method that allows disks to approach, at a random angle, the center or origin of a geometric shape where a disk has initially been placed. When it contacts this fixed circle or any other disk that has been subsequently fixed it rotates around the fixed disk always seeking the origin of the larger geometric shape. Eventually a close packing density (hexagonal) is achived (i.e. crystalline), and, again as more disks are added then an amorphic structure is formed away form the center of the assembly. This method is used by Kausch et al [?] who describes it in detail. Mason [?] uses an expansion method of overlaping disks to determine packing densities.

Cowan [?] considered an ensemble of solid disks having equal radii so that they are fairly closely packed but not in an ordered or regular manner but in a seemingly random way.

to define packing fraction and linking to thermodynamic quantities such as fluid equation of state (cf. [?] and references) through a probablity function.

The discussion as presented here on the packing literature is motivated by the effect tube neighbors have on fluid flow in in the shell and the subsequent effectiveness on the diffusion and convection of thermal energy as has been evidenced in the modeling of heat exchangers. Thus it is hypothesized that the packing configuration and density may have significant impact on the diffusion and convective transport in the hollow fiber membrane module.

Recently work has been done on the effects of shell side hydrodynamics on the performance of axial flow in hollow fiber modules (Costello et al [?]. The radomness of the packing geometries is illustrated in figure 6 of Costello et al and is also presented in figure ——-== of this study. The packing density of the modules used by this study is approximately 31% (calculated by dividing the sum of the cross-sectional area of the filaments by the cross sectional area of the shell) which is the lower end of the packing density of Costello et al.

Using the estimated upper limit of a random close packing of 0.82 and the diameter of the hollow fiber filaments of 300 microns, the maximum number of filiments that can be placed in a 2.54 cm cylindrical shell is 5,950 (**NOTE:** this does not account for the end space needed for the epoxy potting to hold the fibers and segregate the two fluid flows). If a hexagonal shell of equal cross sectional area to the circular cylinder is used then the packing density should approach the maximum packing of a hexagonal or triangular geometry of 0.9069 to give a maximum of 6501 filaments (**NOTE:** again this does not account for the end space needed for the epoxy potting to hold the fibers and segregate the two fluid flows). From figure ——-== all three basic geometric configurations (i.e. hexagonal or triangular, square, and concentric circle) are present at all packing densities; though much more random at lower densities and more prevelent at higher densities. This is evident of the random close packing in two dimensions. An out growth of Costello et al work was the work of Chen and Hlavacek [?] on modeling the hollow fiber modules using Voronoi Diagrams (tessellations). This method seems to be a more rigorous fundamental approach given the randomness of the spatial orientation of fibers especially at low packing densities. Many authors studying the packing densities use Voronoi diagrams and tessellations to arrange elements in space in a more dense packing as well as define the geometry of the structures at the short range and long range metric scales.

Geometric Considerations

Voronoi Diagrams or Tessellations The Voronoi Diagrams or tessellation and its graph theory dual, Delaunay Tesselation or Triangulation, is a method to construct randomly sized and shaped subdivisions or "cells" (polygons) of space. Its application here is to theortically

build or emulate a tube cluster that has no specific geometric symmetry and associate with each tube a flow area that has one and only one tube in the Voronoi cell. The boundaries of the Voronoi "cells" are also the boundaries where the diffusive flux is zero. Coupling the fluid flow profile solution with the diffusive equations for each cell will provide a more rigorous solution of the transport problem for membrane contactors.

Voronoi Diagrams and Delaunay Tessellations are part of an encompassing field of Computational Geometry. Computational Geometry is a new field and was defined in the Ph.D. thesis by Shamos in 1978. The construction of Voronoi Diagrams and Delaunay Tessellations and recently the numerical solution of partial differential equations are applications of this field [?, page 7]. The theory of VDs is presented in a concise manner in LaBarre's Ph. D. dissertation and fairly extensively with proofs of the algorithms in Okabe et al [?] and Preparata and Shamos [?]. The purpose of this section is not to produce a thesis of the VDs, but to give sufficient background of the VDs for their use in this study.

The ability to describe the area of mass and momentum "flux, potential or gradient" flow around a hollow fiber membrane and thus the necessity to delineate the boundary between randomly and non-randomly distributed fibers is an integral portion of this study. The numerical solution to solve the convective and diffusive partial differential equations that model the hollow fiber membrane modules will by necessity use a gridding technique. The use of the Voronoi Diagrams in automatic mesh generation may be valuble in this numerical solution. To this end, two very integral portions of this study are addressed in Voronoi Diagrams.

In a previous section porous structure and its relevence to the study of membrane transport was discussed. The advent of faster and more efficient computer technology (hardware and algorithms) has created a relative explosion in use of Voroni Diagrams, particularly in the area of porous media. The necessary information to allow the use of VDs to characterize the porous structure of the hollow fiber membrane porous structure is insufficient to allow use in this study. However, the VDs can be utilized in another and similar way as to descrbe fluid flow in the annular region of the membrane module.

Voronoi Diagrams — Applications and Brief History The actual formal Voronoi diagram method has been known for a long time and historically can be traced back and credited to mathematicians around the turn of the century, G. L. Dirichlet (1850) and G. F. Voroni (1908) (see references in [?]). The Voronoi diagrams are quite possibly of greater antiquity. Okabe et al. [?, page 6] gives a historical pespective of the development of the the Voronoi diagrams. A reduced accounting is given here taken form Okabe et al. and also from other sources (see for example [?] as well as Shamos's 1978 Ph. D. dissertation on *Computatuional Geometry*).

Okabe et al report that Descartes used Voronoi-like diagrams to show the disposition of matter in the solar system. During the late 19^{th} and early 20^{th} centuries and in the time since, many workers in separate and varied fields have used and in many cases rediscovered the Voronoi diagrams independently and seemingly completely unknowledgable of any past or current work in their respective fields or other fields dealing with the tesselation of space. As a result many synonyms have been used to describe basically the same technique; Direchlet domain; proximal polygon; S cell; tile; Thiessen polygon (meteorology); area of influence polygons (mining geology or the estimation of ore reserves);Wigner-Seitz Regions (solid state physics);domain of the atom (modelling of complex alloy structures as packings of spheres); area of potentiality, and plant polygons (ecology); capillary domains (biology). In the late 1940's, Okabe et al. report that the Voronoi diagram concept had spread form the natural scientists to the social scientists to model marketing areas in the U. S. Geographers, anthropologists, and archaeologists have also used the concept to model other types of human territorial systems. By the 1960's the Voronoi concept was current in both the natural and social sciences.

The use of the Voronoi method up to this time was empirically applied by the construction of the cells by compass and ruler. During the early 1970's a number of algorithms had been developed to construct Voronoi diagrams in two and three dimensions primarily stimulated by the developments in the computer science fields. Over the next twenty plus years the concept of Voronoi diagrams and the associated algorithms, computer implementation, and applications have proliferated. Its use to model the structures of natural phenomenon continues to help develop theoretical understanding of complex, seemingly randomly distributed and amorphic behavoir in films, soap froths [?], crystallography, structure of glass and the amorphous solid state, metallurgy grain boundaries, ceramics and material studies, liquid behavoir [?] and [?] [?] in the fields of condensed-matter physics [?], biological cell structures, flow of fluids through porous media [?]. Most recently and of interest to us, is the application of Voronoi Diagrams to the random arrangement of porous hollow fiber filaments in hollow fiber membrane modules [?], and the application of Voronoi and Delaunay Tessellations to unstructured mesh generation for the numerical solution of partial differential equations [?][?].

Brief Theory of Voronoi Diagrams The concept of the Voronoi Diagrams or for a shorter and more preferable acronym, VD, is simple and can be defined and formalized easily. The analytical derivation of random VD is difficult [?]; although, the construction is not difficult when done by hand, though tedious. Computer implementation becomes extensive especially for three dimensional studies. For this study two dimensional VD simulation is sufficient since the two dimensional packing of disks in a circle can be extended very easily to our three dimensional cylinders or fibers. Assuming, of course, no twisting or overlapping

of fiber filaments in the axial direction. In fact, the two dimensional analysis of the disk packing represents the cross–section of the module.

Definition 1 The Generalized Voronoi diagram *in d dimensional Euclidean space, $\mathbb{E}^d$, is a set of unique convex regions or cells called Voronoi Polyhedrons (V_i). These polyhedrons contain only one nucleus (P_i) (not necessarily centered within the polyhedron) of a set of nuclii distributed within a larger space. The polygons under discussion bound or enclose a subset of space closer to a specific nucleus (P_i) than to any other nucleus (P_j). More formally:*

$$V(P_i) := \{x \in \mathbb{E} : d(x, P_i) \leq d(x, P_j), j = 1, 2, \ldots, n\} \tag{5.171}$$

where d denotes distance. The polyhedra partition $\mathbb{E}^d$ in a unique way.

In other words $V(P_i)$ is the locus of points x such that each point of a subset of $\mathbb{E}^d$, say S, is nearer to P_i than is any point not in S [?],[?], [?], [?].

In order to understand Voronoi Tessellations preliminary associated definitions are needed. Great detail is not extended here and the literature by [?], [?], [?] is recommended.

Definition 2 (Convex Set) *A body, set or domain D in Euclidean space $\mathbb{E}^d$ is referred to as* convex *or an* ovoid *if the line segment, $\overline{q_1 q_2}$, joining any two points, q_1 and q_2, contained within the domain lie entirely in the domain. The intersection of a convex domain is a convex domain. [?] ($D \subset \mathbb{E}^d$ and is convex if whenever $q_1, q_2 \in D$ and $\overline{q_1 q_2} \subseteq D$)*

Definition 3 (Convex Hull) *If a set of points, S, in $\mathbb{E}^d$ is contained in the smallest bounded convex domain in $\mathbb{E}^d$ the boundary of this domain is a* convex hull.

Definition 4 (Polygon) *A closed figure in $\mathbb{E}^2$ with a finite set of segments called straight edges such that every segment extreme, called* vertices *or* nodes, *shares exactly two edges are called* polygons. *They are classified by the number of vertices (number of vertices and edges are the same). If segments connecting any two points inside the polygon always lie inside the polygon, it is* convex. *The interior angles of a convex polygon are less than 180°. If the polygon has any corners inverted it is considered* concave *and any interior angle(s) exceed 180°. A polygon,* P, *partitions the plane into two disjoint regions; the interior (bounded) and exterior (unbounded). It is simple if its interior is convex.*

Definition 5 (kernal) *A polygon is star-shaped if there exists a point* z *not external to* P *such that for all points* p *of* P *— the line segment $\overline{zp}$ lies entirely within* P. *Thus each convex polygon is also star shaped. The locus of points* z *having this star shaped property is the* **kernal** *of* P *and the convex polygon coincides with its own kernal.*

Definition 6 (Planar graph) *A graph $G = (V, E)$, where V is the vertex set and E is the edge set, is planar if it can be embedded in the plane without crossings. A straight line embedding determines a partition of the plane called planar subdivsion or map. Let v, e, and f denote respectively the numbers of vertices, edges, and regions (including the single unbounded region) of the subdivision. Euler's polyhedron theoreum relates these parameters*

$$v - e + f = \chi \tag{5.172}$$

where χ is an integer of order 1 and is a topological invariant of the space i.e $\chi = 2$ for a sphere and 1 for a plane and 0 for a torus, doughnut or tea cup [?]

Definition 7 (Isomorphic) *Isomorphic groups have the same structure, and calculations in them follow the same laws and rules, even though they may have different kinds of elements, and the operations may be defined in different ways.*

Definition 8 (Polyhedron) *In $\mathbb{E}^3$ a* polyhedron *is defined as a set of polygons that bound a region of space such that every edge of a polygon is shared by exactly one other polygon and no subset of polygons has the same property. The* vertices *and* edges *of the polygons form the vertices and edges of the polyhedron; while the polygons themselves form the facets or faces of the polyhedron. Just as the polygon partitions $\mathbb{E}^2$ into two disjoint domains so to does the polyhedron partition $\mathbb{E}^3$ into two disjoint domains; the* interior *(bounded) and* exterior *(unbounded) regions. The surface of a polyhedron is isomorphic to a planar subdivision thus the numbers v, e, and f of its vertices, edges, and facets obey Euler's formula (equation 5.172).*

Definition 9 (Degree) *The number of links or segments that have a common extreme i.e. a node is referred to as the degree of the node or vertex.*

The Voronoi Diagram was defined above for a general m-dimensional case. The construction of the polygons that make up the VD consist of the the perpendicular bisectors between two points. Let s_i, $s_j \in S$. Then the perpindicular bisector of the segment $\overline{s_i s_j}$, denoted $PB(\overline{s_i s_j})$, divides the plane into two regions, one consisting of points closer to s_i than to s_j and one of points closer to s_j. The Voronoi polygon can be defined as half planes. The half plane itself is determined by the perpindicular bisector and H_j^i is the half plane containing s_i created by the bisector. Continuing in with this method and contructing the segment $\overline{s_i s_k}$ as s_k andvances through S with $k \neq i$, and form each perpendicular bisector $PB(\overline{s_i s_k})$ and its associated H_j^i, the common intersection of the H_j^i yields precisely the collection of all points in the plane closer to s_i than to any other s_k. Thus the following definitions for the Voronoi polygon and Voronoi Tessillation are given [?].

Definition 10 (Voronoi Polygon) *Let S be a finite collection of points in the plane. Let $s_i \in S$. The Voronoi polygon associated with s_i is given by :*

$$Vor(s_i) := \bigcap_{k \neq i} H_k^i \tag{5.173}$$

Definition 11 (Voronoi Tesssellation) *Let S be a finite collection of points in the plane. The Voronoi tessellation associated with S is*

$$VorT(S) := \bigcup_{s_i \in S} Vor(s_i) \tag{5.174}$$

For this study we will primarily be concerned with the two dimensional planar case. If we ignore the unbounded region or the area outside the Voronoi Diagram and for a planar graph Euler's theorem becomes

$$v - e + f = 1 \tag{5.175}$$

If we assume that each vertex contained within the diagram has a property of degree ≥ 3 thus the number of edges is equal to or greater than three times the number of vertices and that there are two vertices per edge meaning that each edge is counted twice:

$$3v \leq 2e \tag{5.176}$$

There are a great many properties of the Voronoi Diagrams and its graph dual Delaunay Triangulation. I will list a few of the most important, but direct the reader to the literature such as [?][?][?] for details of proofs and further investigation. Here, we are interested in making use of the methods, algorithms, and codes that have been developed to efficiently construct these spatial tesselations for use with transport theory. The properties are useful in the development and understanding of these algorithms and codes.

The properties listed below are taken from [?]:

Property 1 *The Voronoi Diagram is a unique tessellation for the set of distinct points of P where $P = \{p_1, \ldots, p_n\} \subset \mathbb{E}^2 \, (2 \leq n < \infty)$.*

Property 2 *A Voronoi Diagram generated by a like set of distinct points, a Voronoi polygon is infinite if and only if $p_i \in CH(P)$ where CH(P) is the complex hull of P*

Property 3 *For the Voronoi Diagram generated by a set of distinct points*

1. *Voronoi edges are infinite straight lines iff P is collinear*
2. *Voronoi edge $e(p_i,p_j)(\neq \emptyset)$ is half line iff P is non-collinear and p_i and p_j are consecutive generators of the boundary of CH(P)*

3. *A Voronoi Edge generated by these two points is a finite line segment iff P is non-collinear and at least one of the points is in the ineterior of CH(P).*

Property 4 *The nearest generator point of p_i generates a Voronoi edge of $V(p_i)$*

Property 5 *The nearest generator point from p_i exists in the generators whose Voronoi polygons share the Voronoi edges of $V(p_i)$.*

Property 6 *For every Voronoi vertex, $q_i \in Q$ in a Voronoi diagram, there exists a unique empty circle C_i centered at q_i which passes through three or more generators. Under the non-degeneracy assumption, C_i passes through exactly three generators.*

Assumption 1 **(the non-degeneracy assumption)** *Every Voronoi vertex in a Voronoi diagram has exactly three Voronoi edges (see also [?, page 21])*

Assumption 2 **(the non-cocirculatory assumption)** *Given a set of points $P = \{p_1, \ldots, p_n\} \subset \mathbb{E}^2$ $(4 \leq n < \infty)$, there does not exist a circle, C, such that $p_{i1}, \ldots, p_{ik} \in P, k \geq 4$, are on C, and all points in $P \backslash \{p_{i1}, \ldots, p_{ik}\}$ are outside C_o.*

Property 7 *Circle C_i is the largest empty circle among empty circles centered at the Voronoi vertex q_i. (C_i contains no point of S in its interior (see also [?, page 21-22]))*

Property 8 *Let n, n_e, n_v be the numbers of generators (number of face centers or single points that the Voronoi Polygons are developed around), Voronoi edges, and Voronoi vertices of a Voronoi Diagram in $\mathbb{E}^2$, respectively $(2 \leq n < \infty)$. Then Eulers rule $n_v - n_e + n = 1$ gives*

$$n_e \leq 3n - 6 \tag{5.177}$$

$$n_v \leq 2n - 5 \tag{5.178}$$

When a set of P generators satisfies the non-collinearity assumption whith $n \geq 3$ every finite Voronoi polygon has at least three Voronoi edges.

Property 9 *A Voronoi polygon is given by the intersection of n-1 half planes*

$$V(p_i) = \{x \mid \|x - x_i\| \leq \|x - x_j\| \text{ for } j \neq i, j \in I_n\} \tag{5.179}$$

$$= \bigcap_{j \in I_n \backslash \{i\}} H(p_i, p_j) \tag{5.180}$$

A Voronoi polygon thus has n-1 Voronoi edges at the maximum. At the minimum when generators are collinear the leftmost and the rightmost Voronoi polygons have only one Voronoi edge. From equation 5.177 and the fact that every Voronoi edge is shared by exactly

two Voronoi polygons, the average number of Voronoi edges per Voronoi polygon is less than or equal to $2(3n - 6/n)$.

Property 10 *Thus the average number of Voronoi edges per Voronoi Polygon does not exceed six. The maximum number of Voronoi vertices in a two-dimensional Voronoi diagram is* $2n - 5$.

Computer Algorithms for Voronoi Construction — Two Dimensional Case A number of algorithms and variations have been proposed to construct the Voronoi Tesselations. Fortune [?] divides these into three categories — incremental algorithms, divide-and-conquer algorithms, and Sweepline algorithms. Okabe et al [?] describe seven different methods but do not class them into the three categories of Fortune. In fact Okabe et al. view their seven methods as distinct different methods, but discuss the incremental, divide-and-conquer and Sweepline methods in detail. These three as pointed out by Fortune and Okabe et al. are the most important and the other methods appear as Fortune has defined as varitions of these classes or methods. I will discuss the three for background but will give the algorithms for only the incremental or iterative method since they seem to be the most efficient and popular. An algorithm for the Naive method is also given. Though not an efficient method, it develops the Voronoi diagram more directly from the definition of the Voronoi polygons and diagram.

In general the construction of the Voronoi Diagram takes at least $O(n \log n)$ time in the worst case and at least $O(n)$ time on average. The order ($O(n)$, $O(n \log n)$ etc.) represents the behavoir of an algorithm as $n \to \infty$. At small n the behavoir may be different than at large n. Though the concept of the Voronoi Diagrams and for the most part the algorithms describing them are relatively easy to understand, implementing them on the computer can be difficult especially when additional information about the contents of the Voronoi diagrams is needed. The primary difficulty is in handling the degenerate cases that can occur and the numerical errors inherent with computer round off; thus, the direct translation of an algorithm to a computer program does not necessarily give a numerically valid program. In the development of the algorithms — let $P = \{p_1, \ldots, p_n\}$ be a set of generators, and $\mathfrak{V} = \{V(p_1), \ldots, V(p_n)\}$ denotes the Voronoi diagram for P.

Incremental Methods The incremental algorithms to construct the Voronoi Diagrams are some of the easiest methods to conceptually visualize and perhaps simpliest to implement (thorugh not trivial). The average time complexity can be decreased from $O(n^2)$ to $O(n)$ with inginuity [?]. The technique constructs a Voronoi diagram of each generator and modifies the surrounding polygons if appropriate. A method of sorting or reordering

randomly spaced generators by quaternary trees or bucketing and using nearest neighbor search can reduce the time complexity to linear time $O(n)$.

Naive method:

The Naive or brute approach method. is a relatively straight forward and follows directly from the definition of the Voronoi diagram and can be classed as an incremental method. The intersection of the half planes defined by the perpendicular bisectors of p_i and the other generators and the diagram is formed by constructing the polygons one by one. Though it builds each polygon one by one it does not account for any descrepencies of surrounding polygons previously or subsequenly formed. Thus, topological inconsitencies can occur.

Input: n generators $p_1, p_2, \ldots, p_n$.

Output: Voronoi diagram $\mathfrak{V} = \{V(p_1), \ldots, V(p_n)\}$

Step 1: For each i such that $i = 1, 2, \ldots, n$, generate $n-1$ half planes $H(p_i,p_j), 1 \leq j \leq n, j \neq i$, and construct their common intersection $V(p_i)$.

Step 2: Report $\{V(p_1), V(p_2), \ldots, V(p_n)\}$ as output and stop.

The Naive method is an insufficient method. To be sufficient the algorithm must be

- Correct
- Efficient
- Robust against numerical errors.

The method has an efficiency over time of $O(n^3)$ which means that a computer program based on the Naive procedure becomes eight times larger as the size of the input data becomes twice as large. If the time to process an input data set of size n is given as $T(n)$ and some positive function $f(n)$ there exists a constant such that C such that

$$\frac{T(n)}{f(n)} < C \quad \text{for all } n \tag{5.181}$$

we can say that $T(n) = O(f(n))$ and say that $T(n)$ of *order* $f(n)$ [?, page 210]. An implication is that $T(n)$ does not increase nore rapidly than $f(n)$ does as n grows and the algorithm can be considered as being efficient if it satifies a slowly increasing function $f(n)$ satisfying the above equation [?, page 210]. An algorithm that has a time $T(n) = O(n)$ is sometimes called a *linear time* algorithm.

The Naive Method's construction of the intersection of $n-1$ half planes can be accomplished in $O(n \ln n)$ time with a more sophisticated technique. Thus, the time complexity can be

reduced to $O(n^2 \ln n)$ [?][?, page 206]. By computing the Voronoi polygons independently the numerical errors could result in a topologically inconsistent tessellation. If information is desired to be extracted from the Voronoi diagram or polygons, using the naive method is not suitable.

Quaternary Incremental Algorithm:

Because of its conceptual simplicity and its best time complexity of $O(n)$ this algorithm is an important method for developing the Voronoi Diagrams and extracting information from the individual Voronoi polygons. Two associated algorithms are necessary to make the method work [?]

Algorithm 1 (Nearest neighbor search)

Input: *l generators $p_1, p_2, \ldots, p_l$, Voronoi diagram $\mathfrak{V}_{l-1}$ and initial guess $p_i\,(1 \le i \le l-1)$.*

Output: *The generator (other than p_l) that is closest to p_l.*

1. *Among the generators adjacent to p_i, find the one , say p_j, whith the minimum distance to p_l:*

$$d(p_j, p_l) = \min_k d(p_k, p_l),$$

where the minimum is taken over all generators p_k whose Voronoi polygons are adjacent to $V(p_i)$.

2. *If $d(p_i, p_l) \le d(p_j, p_l)$, return p_i, else $p_i \leftarrow p_j$ and go to Step 1.*

Algorithm 2 (Incremental Method)

Input: *Set $\{p_4, p_5, \ldots, p_n\}$ of $n-3$ generators located in the unit square $S-\{(x,y) \mid 0 \le x, y \le 1\}$.*

Output: *Voronoi diagram $\mathfrak{V}$ for n generators $\{p_1, p_2, \ldots, p_n\}$, where p_1, p_2, and p_3 are the additional generators defined by*

$$p_1 = \left(0.5, 3\sqrt{2}/2 + 0.5\right),$$
$$p_2 = \left(-3\sqrt{6}/4 + 0.5, -3\sqrt{2}/4 + 0.5\right),$$
$$p_3 = \left(3\sqrt{6}/4 + 0.5, -3\sqrt{2}/4 + 0.5\right)$$

1. *Find positive integer k such that 4^k is closest to n, divide S into 4^k square buckets, and construct the quaternary tree having the buckets as leaves.*

2. *Renumber the generators by quaternary reordering, and let the relultant order be $p_4, p_5, \ldots, p_n$.*

3. *onstruct the Voronoi diagram $\mathfrak{V}_3$ for the three additional generators p_1, p_2, and p_3 defined by equations above.*

4. *For $l = 4, 5, \ldots, n$, do*

   (a) *By algorithm 1 with the initial guess given by quaternary initial guessing, find the generator $p_i\,(1 \leq i \leq l-1)$ closest to p_l.*

   (b) *Find the points w_1 and w_2 of intersections of the perpindicular bisector of p_i and p_l with the boundary of $V\,(p_i)$*

   (c) *By the boundary-growing procedure, construct the closed sequence*

   $$(\overline{w_1w_2}, \overline{w_2w_3}, \ldots, \overline{w_{m-1}w_m}, \overline{w_mw_1})$$

   of segments of perpendicular bisectors forming the boundary of the Voronoi polygon of p_l.

   (d) *Delete from $\mathfrak{V}_{l-1}$ the substructure inside the closed sequence, and name the resultant diagram $\mathfrak{V}_l$.*

5. *Return $\mathfrak{V} = \mathfrak{V}_n$.*

The detail explanation of this algroithm is in Okabe et al [?, pp. 223–232]. The complex timing of the above algorithm is $O(n)$ or linear time. LaBarre [?] uses the incremental method developed by Watson for automatic mesh generation constructing the grid connectivity via the Delaunay triangulation and then to determine the control regions (flux cells determined by the Voronoi polygons as a by-product. Labarre's (Watson's) method in 2D does not have an optimal time of $O(n \log n)$ but instead has the time complexity of $O(n^{\frac{3}{2}})$.

Divide-And-Conquer Labarre comments that this method was introduced by Shamos in his Ph. D. thesis in 1978 for construction of the Voronoi diagram [?, page 24]. The divide-and-conquer algorithms divides the collection of nodes or generators into two sets of roughly equal size by a vertical line; the solution is obtained by merging the separate regions after the Voronoi diagrams in each reagion have been recursively developed. Labarre comments that "conceptually this is a very easy algorithm to understand but programmatically it is difficult to implement especially in 3D". Implementation details are complicated and numerical errors are likely [?] which is of chief concern. The algorithms have a complex time of $O(n \log n)$, though an algorithm using the divide and conquer technique with an expected time of $O(n)$ has been developed for certain subsets (see references of [?]). As in other methods sorting and reordering of the generators plays a key role for efficient implementation of the procedure. In this particular algorithm the generators are sorted in

increasing order of the x coordinates by any suitable efficient sort routine. An algorithm listed by Okabe et al. is suggested for further investigation of this method along with more detailed explanations of the algorithms structure and examples. Because of the difficulty of implementation and the success of other more efficient algorithms discussion of this method will belabored no further and the presentation by Okabe et al. [?] is recommended.

Plane Sweep Method This method attributed to Fortune [?] is a fundamental algorithm used to solve two dimensional geometric problems. Conceptually the algorithm computes the Voronoi Diagram by "sweeping the plane" and intersecting the geometric regions and objects of the plane one by one. Since the location of the generator or node sites are not known *a priori* then a transformation of the Voronoi Diagram is actually calculated. The transformation image is a function that is a set of hyperbolic regions and the transformed diagram has the property that the lowest point of the transformed Voronoi region is the node or generator itself. The edges become curves. Thus when the sweepline sweeps the plane it encounters the site or node for each region first before intersecting the region. A plane sweep algorithm does not have to be applied from bottom up as Fortune originally proposed but can go from left to right as Okabe et al. outlines.

This method can be implemented in to run in time $O(n \log n)$ and space $O(n)$ (therorem 2.8 of [?]). Details of the algorithm can be found in the article by Fortune and page 242 of Okabe et. al. A source code for this method is on NETLIB.

5.6.2 Shell Side Fluid Flow

The equation of motion of a fluid to model the flow in the shell side is derived from theory of continuity and is presented in the classical books of transport (cf. [?, ?, ?, ?]. A general form of this equation as given by Happel [?]

$$\begin{aligned} \rho\left(\frac{\partial \mathbf{v}}{\partial t} + \mathbf{v}\cdot\nabla\mathbf{v}\right) &= -\nabla p + \mu\nabla^2\mathbf{v} + \frac{1}{3}\mu\nabla\left(\nabla\cdot\mathbf{v}\right) \\ &\quad +2\left(\nabla\mu\right)\cdot\nabla\mathbf{v} + \left(\nabla\mu\right)\times\left(\nabla\times\mathbf{v}\right) \\ &\quad -\frac{2}{3}\left(\nabla\mu\right)\left(\nabla\cdot\mathbf{v}\right) + \kappa\nabla\left(\nabla\cdot\mathbf{v}\right) \\ &\quad +\left(\nabla\kappa\right)\left(\nabla\cdot\mathbf{v}\right) + \rho\mathbf{g} \end{aligned} \tag{5.182}$$

This equation along with the equation of state for density $p = p\left(\rho, T\right)$, the density dependence of shear viscosity $\mu = \mu\left(\rho, T\right)$, the density dependence of bulk viscosity $\kappa = \kappa\left(\rho, T\right)$, and the boundary conditions, determines the pressure, density, and velocity components of a flowing fluid. Equation 5.182 is generally not used in its complete form, but in a simpified variation and generally at isothermal conditions. The dependency of the bulk viscosity, κ,

is often set equal to zero and assumming irrotational and incompressible flow:

$$\nabla \times \mathbf{v} = \mathbf{0} \quad \text{irrotational flow} \tag{5.183}$$

$$\nabla \cdot \mathbf{v} = \mathbf{0} \quad \text{incompressible fluids} \tag{5.184}$$

Which means that equation 5.182 becomes

$$\rho\left(\frac{\partial \mathbf{v}}{\partial t} + \mathbf{v}\cdot\nabla\mathbf{v}\right) = -\nabla p + \mu\nabla^2\mathbf{v} + 2\left(\nabla\mu\right) + \rho\mathbf{g} \tag{5.185}$$

and if constant viscosity is assumed $\nabla\mu = 0$ and no gravitational effects then one form of the Navier-Stokes equation

$$\rho\left(\frac{\partial \mathbf{v}}{\partial t} + \mathbf{v}\cdot\nabla\mathbf{v}\right) = -\nabla p + \mu\nabla^2\mathbf{v} \tag{5.186}$$

and in cylindrical coordinates along the axial direction [?, page 85]

$$\rho\left(\frac{\partial v_z}{\partial t} + v_r\frac{\partial v_z}{\partial r} + \frac{v_\theta}{r}\frac{\partial v_z}{\partial \theta} + v_z\frac{\partial v_z}{\partial z}\right) = -\frac{\partial p}{\partial z} + \mu\left[\frac{1}{r}\frac{\partial}{\partial r}\left(r\frac{\partial v_z}{\partial r}\right) + \frac{1}{r^2}\frac{\partial^2 v_z}{\partial \theta^2} + \frac{\partial^2 v_z}{\partial z^2}\right] + \rho g_z \tag{5.187}$$

assuming that the velocity in the z direction does not vary with z or position axially then

$$\frac{\partial v_z}{\partial z} = 0 \tag{5.188}$$

and that the velocity components in the θ and r direction are zero. Therfore equation ?? becomes

$$\rho\left(\frac{\partial v_z}{\partial t}\right) = -\frac{\partial p}{\partial z} + \mu\left[\frac{1}{r}\frac{\partial}{\partial r}\left(r\frac{\partial v_z}{\partial r}\right) + \frac{1}{r^2}\frac{\partial^2 v_z}{\partial \theta^2} + \frac{\partial^2 v_z}{\partial z^2}\right] + \rho g_z \tag{5.189}$$

Normally, in a cylindrical duct such as a pipe for example, the velocity gradient $\frac{\partial v_z}{\partial \theta}$ of the z component will not vary with θ and would be set to zero and Poiseuille equation of flow or velocity ditribution results. In our case it varies due to the effects of filament proximity and changes in flow area azmuthally. Thus, the term $\frac{1}{r^2}\frac{\partial^2 v_z}{\partial \theta^2}$ must remain in the model.

If the shell side fluid is assumed to be in fully developed laminar axial flow for an incompressible Newtonian Fluid, the velocity field is given by Poisson's equation in cylindrical co-ordinates

$$\frac{1}{r}\frac{\partial}{\partial r}\left(r\frac{\partial \mathfrak{v}}{\partial r}\right) + \frac{1}{r^2}\frac{\partial^2 \mathfrak{v}}{\partial \theta^2} = \frac{1}{\mu}\frac{\partial \mathfrak{p}}{\partial z} \tag{5.190}$$

The boundary conditions needed to be satisfied in order that either of these equations can be solved are:

1. zero velocity at every surface in the shell side or the no slip boundary condition is applied at the shell side wall of all filaments and to the shell wall containing the filament bundle i.e $\mathbf{n} \cdot \mathbf{v} = \mathbf{0}$ at all the tube walls. This is the no-slip boundary condition.
2. The velocity gradient is zero at the "line of symmetry " between the filaments. This is the Voronoi edge as described previously $\frac{\partial v}{\partial r}$.

Brief overview of Solutions in the literature

The above equations and boundary conditions for shell side flow pattern are well established, but these Navier-Stokes equations are difficult to solve especially in complex geometry. Solutions of the flow equations for tube bundles with the above boundary conditions have been reported many times. But, these solutions have been limited to mostly one ring problems i.e. the tube bundle is a central rod with six tubes surrounding it usually in a fixed square or triangular structure. In complex and congested geometry the requirement that $\mathbf{n} \cdot \mathbf{v} = \mathbf{0}$ at all tube walls can be prohibitive [?]. A perspective of the progress toward an effective solution is briefly presented.

An analytical solution for an arbitray number of rods with different radii placed in concentric rings of arbitrary radius from a central rod was developed by [?]. They assumed however that the bundle has a characteristic symmetry with respect to the angular direction. Their figure 1 is reproduced here as figure ———— for ease of explanation. Two different reference systems are used; (1) the (r, ϕ) polar coordinate system refers to the center of the central rod and (2) the $(b_l \rho_l, \theta_l)$ polar coordiante system associated with the centers of the individual periperl rods. Because of the angular symmetry they assumed the solution, though basically a multiplicity of a single symmetry unit dipicted in figure ———, is not trivial and is complexed by satisfying all of the boundary conditions simultaneously. Mattaghain and Wolf analytically solved the problem using superposition of solutions (see [?] for detail).

The solution of the the PDEs usng orthoganol grid line (cartesian, cylindrical or spherical) coordiantes do not always intersect orthoganally with boundaries. Meyder [?] solved the coupled conservation equations for mass, impulse, and enthalpy in a complicated geometry i.e. fuel rod bundle by curvilinear-orthogonal coordinates or potential theory analysis and thereby generated a grid that orthoganally intersected the boundaries. In descretizing the PDEs in cartesian coordinates the dimensions form one mesh to the other are the same; but, in curvilinear coordinates the lengths and angles can vary form one mesh to the next. Criteria that are to be considered are that the solution must be consistent across areas of symnetry and results for laminar flow should be comparable to results of other investigations.

Meyder's figure 10 shows a line of symmetry; and, also reflects a state of triangulation. This line of symmetry and triangulation , though not stated and apparently not realized or noted in Meyder's discussion (or any discussion on the flow of fluid parallel to a tube bundle) is the Voronoi edge and the triangulation is the Voronoi Diagram theoretical dual the Delaunay Triangulation. Chen et al [?] discusses the use of boundary fitted coordinate method facilitating accurate representation of the flow regions especially between the rods and the wall. The numerical solution of Poisson's equation with arbitraily shaped boundaries is discussed in the work by Miki and Takagi [?]. These authors also use boundary fitted coordinate transformations to numerically the 3-D Poisson's problem.

Though Meyder's method generated a grid that orthoganally intersected the boundaries the computational time may be extreme and the equations of mass, heat and momentum transfer must undergo transformation dependeing on the local slopes of grid lines [?][?]. Benodekar and Date solved the flow and heat equation in a tube bundle by a typical finite difference method using the sector approach where the smallest symmetry segment is considered for the characteristic flow area. This is a typical approach for a spacially periodic arranged pattern of tubes. They used a structure of an arbitrary number of rods placed on concentric rings around a central rod.

Sha [?] reviews the rod bundle thermal hydraulic analysis of (1) subchannel concept, (2) porous medium formulation approach, (3) bench mark rod bundle using boundary fitted coordiante system. As Sha points out a major obstacle to the use of numerical methods in rod-bundle thermal-hydraulic analysis has been the complex geometry. This obsticle, up to the printing of Sha's review, was being obviated by using boundary fitted coordinate transformations. The mixing lengths for subchannel thermal hydrodynamical analysis of Liquid Metal Fast Breeder Reactors (LMFBR) was studied by Yeung and Wolf [?, ?]. They found that the effective mixing length is a strong function of the subchannel geometry and is not equal to the normally assumed centroid-to-centroid distance. It is interesting to note that these authors in developing their symmetrical crossection into the various unit cells for their numerical routines were approaching the use of Voronoi polygons. They observed that ten different polygons or unit cells of varying geometries were developed in their symmetrical segment. The flow equations could be applied to these flow areas enabling them to perform multicell slug flow heat transfer analysis.

A particularly interesting literature work that parallels this study of mass tranfer is that of an axially varying heat transfer to a fluid flowing axially between cylinders [?]. The analogy is viewed from the fact that the mass transfer driving force will dimenish in this as the heat transfer did in their study. The difference is that axially along the periphery of the rod the wall temperature is held uniform where in the mass transfer fiber the mass transfer is not held uniform.

6. Interfacial Phenomenon —Boundary Conditions— Applied to Membrane Transport

6.1 Mathematical Transformation and Relationship Between 3—D and the 2—D Interface

There are three ways to model the interface between two phases. Two of these are continuum models and the third is a molecular model. The later is embodied in quantum chemistry and is a statistical approach at an atomic level. The former is a simpler approximation. It is based on the observations that the details at the atomic level are many times not necessary. To our physical perception of site and touch the world around us — and in many ways the phenomenon of molecular transport — behave as systems and bodies that are continuous without any voids; though, discontinuities such as the boundaries between the air and water and the surface of tables and the surroundings are perceived([?]). The continuum models to approximate the behavior of an interface are (reference figure 6.1 page 170):

1. As the three dimensional continuum — The interface between two phases is physically a three dimensional region of steeply varying gradients and inhomogeneities of fluid properties such as mass density of the fluid, species mass densities, and shear viscosity fields. This interface does not have a sharp delineation but is a diffuse separate phase. The three dimensional continuum model is appealing since it represents reality; but, the difficulties of studying the field distributions and obtaining experimental information of the properties within this small phase prohibits or at least severely limits its useful implementation in engineering endeavors.

2. As a two dimensional surface —This is a hypothetical model of the three dimensional physical region between two phases. This model was originally proposed by Gibbs for a phase interface in a body at rest or at equilibrium dividing two homogeneous phases ([?]). Gibbs suggested that the cumulative effects in the interfacial region be taken into account at a single two dimensional dividing surface as excess properties not accounted for by the adjoining homogeneous phases (where homogeneous phases are defined to have properties such as mass density and stress, that assume uniform values). This is extended to include dynamic phenomena if a constitutive equation to describe the material behavior throughout the homogenous phase can be defined. And, as in the static case, the cumulative effects of the interface upon the adjoining

phases can be described by associating densities and fluxes with the dividing surface. These densities and fluxes associated with a dividing surface are referred to as excess properties.

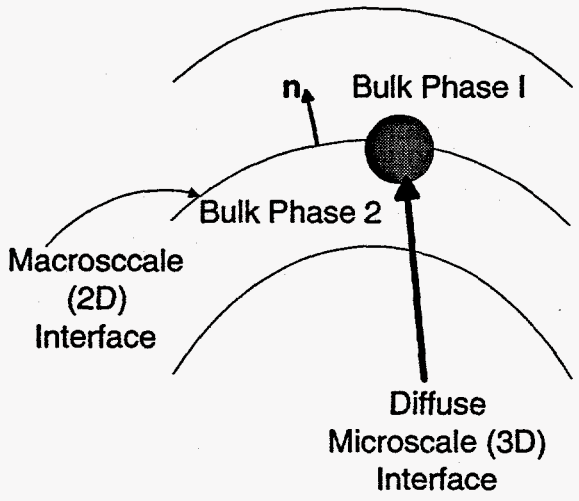

Figure 6.1: Visualization of the concepts between the two dimensional (macroscale) and three dimensional (microscale) models of the interface. The microscale is perceived to be a magnification of the macroscale 2–D surface between the two bulk phases

The literature works and reports on the study of interface phenomena is extensive. As one attempts to go through the literature of this subject it would appear that nearly all branches of science, mathematics, and engineering have contributed in some manner to this subject. In this section I will follow primarily two books that I find exceptionally beneficial — Slattery's book on Interfacial transport [?] and Edwards *et al.* book on Interfacial Transport Processes and Rheology [?]. The latter is especially beneficial from a visualization standpoint and is fairly well developed mathematically (though in places vague as textbooks tend to be) and will be followed fairly extensively. The former is a very extensive and rigorous work on the mathematical understanding of interfacial transport. As in other sections additional works will be referenced appropriately. The following of these books is done here since the interface is a very crucial and important part of the fundamental modeling of membrane separation processes and the theory has been fairly well developed thus far, especially for the dividing surface model. The need for an understanding of tensor analysis (cf. [?]) is fundamental since primarily I will look at the interface as a Riemannian Surface in non-Euclidean two dimensional curvilinear space.

6.1.1 Mathematic Preliminaries

In three dimensions we can use Euclidean space and its more understandable mathematical interpretations. For two dimensional surface flows the need for *non-Euclidean Riemannian* space arises. Riemannian space exists if a metric tensor exists and thus Euclidean space is a subset of Riemannian space. The fundamental metric tensor $g_{ij} \equiv \mathbf{e}_i \cdot \mathbf{e}_j$ (where e_α is the covariant base vector) describes the nature of a space, or manifold and associates a length with an infinitesimal vector whose components are the derivatives of the coordinate curves associated with the space. A space is Euclidean if the metric tensors are constant or a transformation can be found in which the metric tensors are constant. If it is not possible to find this mapping or transformation than the space is said to be non-Euclidean or *Riemannian* ([?, page 48]).

Transport phenomenon in the interface or surface is not merely a two dimensional analog of the three dimensional transport equations ([?]). The interface is a two dimensional space that can move in the higher three dimensional space surrounding it. The region of contact or interface between two bulk phases, as in this study, constitutes a two dimensional moving surface. The two dimensional model of an interface is a surface in Riemannian space. This two dimensional non Euclidean space demands a mathematical approach as a full general tensor treatment.

A surface, as considered from an intrinsic point of view or as observed from the perspective of an observer constrained to lie within the surface itself (independently of the three dimensional space in which the surface is embedded), is illustrated in figure 6.2 page 172. This is opposed to the extrinsic view, that is the perspective of the geometric description of an interface by an observer external to the surface constraints. The extrinsic view gives a connection between the three dimensional bulk phases and the two dimensional surface phase. This is done by utilizing vector and tensor transformations between the two dimensions.

The transformation from a rectangular cartesian coordinate system of x, y, z system to a curvilinear Riemannian Space is denoted by [?, page 46]

$$\begin{array}{rcccl} q^1 & = & q^1(x^1,x^2,x^3) & = & q^1(x,y,z) \\ q^2 & = & q^2(x^1,x^2,x^3) & = & q^2(x,y,z) \\ q^3 & = & q^3(x^1,x^2,x^3) & = & q^3(x,y,z) \end{array} \tag{6.1}$$

where the functions $q^1(x,y,z)$ =constant; $q^2(x,y,z)$ =constant; $q^3(x,y,z)$ =constant; and denote three surfaces in three dimensional space (cf. figure 6.3A, page 173). The intersection of any two defines a coordinate curve. When the transformation is non-linear the coordinate curves q^1, q^2, and q^3 are curved lines and when the coordinate curves are straight lines a linear transformation has been established. This linear transformation may and may

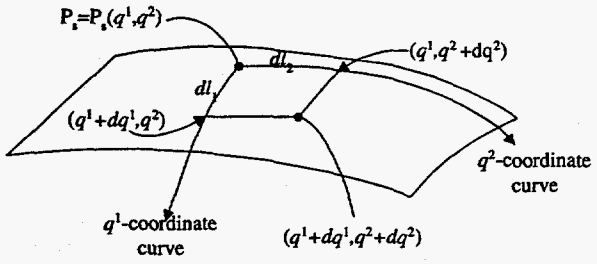

Figure 6.2: A two dimensional surface as considered from an intrinsic view or as observed from the perspective of an observer constrained to lie within or on the surface itself.

not be parallel to the original origin.

Slattery [?, page 13] gives a very good account of a dividing surface or interface and elucidates the above relationship.

> A dividing surface in three dimensional Euclidean space is the locus of a point whose position is a function of two parameters q^1 and q^2.

The two parameters, q^1 and q^2, are the surface curvilinear coordinates and uniquely determine a point on the surface and are independent functions of position within the surface.

$$q^\alpha = q^\alpha(\mathbf{x}_s) \qquad (\alpha = 1,2) \tag{6.2}$$

or

$$\begin{aligned} q^1 &= q^1(x,y,z) \\ q^2 &= q^2(x,y,z) \end{aligned} \tag{6.3}$$

where $\mathbf{x}_s$ is a position vector relative to an origin (see figure 6.3B page 173). The surface point P_s may be specified extrinsically as a function in cartesian coordinates with respect to a chosen origin as

$$\begin{aligned} F^0(\mathbf{x}_s) &= 0 \\ F^0(x^1,x^2,x^3) &= 0 \end{aligned} \tag{6.4}$$

[?, page 513]. The surface coordinates for this or at this point can be expressed as functions of the rectangular cartesian coordinate system relative to the origin O:

$$q^\alpha = f^\alpha\left(x^1,x^2,x^3\right) \qquad (\alpha = 1,2) \tag{6.5}$$

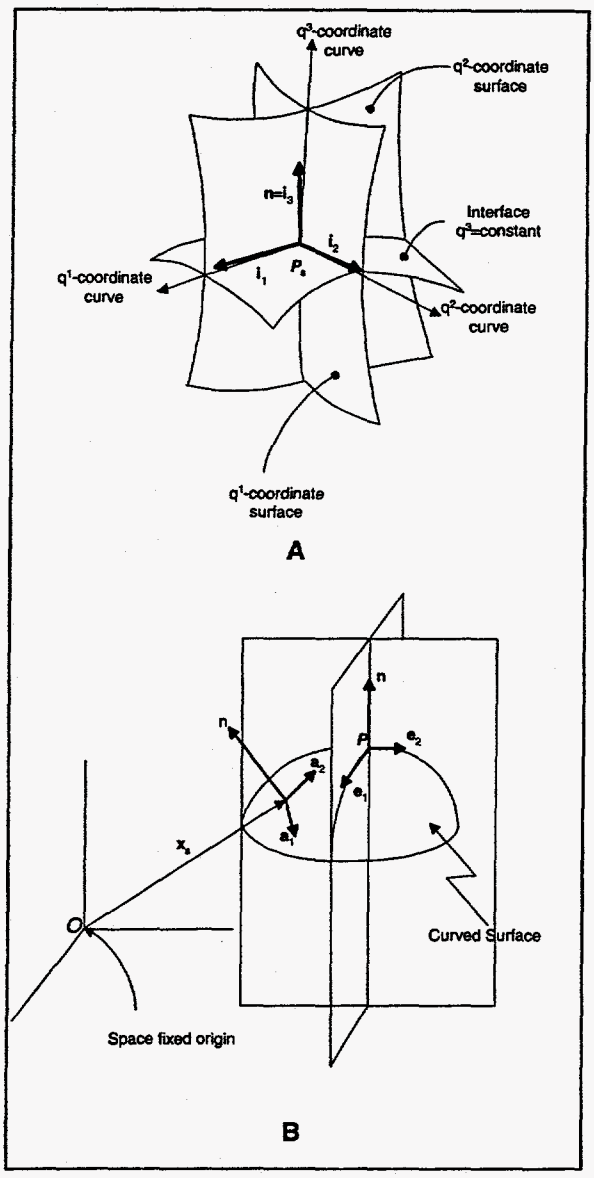

Figure 6.3: (A): Coordinate curves, surfaces and unit base vectors in an orthogonal parameterization of the interface in three dimensional space. The coordinate surface $q^3 =$ constant exemplifies the macroscale interface. The intersection of pairs of coordinate surfaces generate coordinate curves. (B): Curvilinear coordinate system in relation to the fixed cartesian coordinate system.

and therefore

$$q^{\alpha}(\mathbf{x}_s) - f^{\alpha}\left(x^1, x^2, x^3\right) = 0 \tag{6.6}$$

which if we equate F^{α} to be this difference then

$$F^{\alpha} \equiv q^{\alpha}(\mathbf{x}_s) - f^{\alpha}\left(x^1, x^2, x^3\right) = 0 \tag{6.7}$$

and in the canonical parametric form given by Aris [?, page 279]

$F_j(x, \ldots, x_m; y_1, \ldots, y_n) = 0, \qquad j = 1, \ldots, n$ then

$$\begin{array}{l} F^0\left(x^1, x^2, x^3; q^1, q^2\right) = 0 \\ F^1\left(x^1, x^2, x^3; q^1, q^2\right) = 0 \\ F^2\left(x^1, x^2, x^3; q^1, q^2\right) = 0 \end{array} . \tag{6.8}$$

If the Jacobian of the above functions does not vanish then, the functional transforms have a unique inversion given in this case by equation 6.9 [?], [?], [?], and [?, pages 86-89]:

$$\mathbf{x}_s = \mathbf{x}_s\left(q^1, q^2\right) \tag{6.9}$$

The interrelationship between the rectangular cartesian coordinates system of fixed origin and the curvilinear coordinate system of a curved surface is illustrated in figure 6.3B page 173. If $\mathbf{x}_s$, sometimes denoted as $\mathbf{r}$, is a two point vector field specifying the position of a point P_s in a two dimensional Riemannian surface relative to a fixed origin O then it is defined by $\mathbf{x}_s \equiv \mathbf{x}_s\left(q^1, q^2\right)$ on the surface. The differentiation of $\mathbf{x}_s$ with respect to the coordinate curve vectors or $d\mathbf{x}_s$ in two dimensional space can be written by the chain rule as

$$d\mathbf{x}_s = \frac{\partial \mathbf{x}_s}{\partial q^1} dq^1 + \frac{\partial \mathbf{x}_s}{\partial q^2} dq^2 = \frac{\partial \mathbf{x}_s}{\partial q^{\alpha}} dq^{\alpha} \tag{6.10}$$

where the partial derivatives

$$\frac{\partial \mathbf{x}_s}{\partial q^{\alpha}} \stackrel{def}{=} \mathbf{a}_{\alpha} \tag{6.11}$$

are the tangent to the coordinate curves as shown in figure 6.3A page 173. These partial derivatives are the surface base vectors, $\mathbf{a}_{\alpha}$, defined locally at P_s. They provide a relation between the two point differential displacement, $d\mathbf{x}_s$, between neighboring interfacial points $\mathbf{x}_s$ and $\mathbf{x}_s + d\mathbf{x}_s$ and the comparable differential displacement dq^{α} of the coordinates q^{α} [?, page 44-45].

To describe the two dimensional interface embedded in the three dimensional space the use of a semi-orthogonal curvilinear coordinate system is used (cf. [?]). In this geometrical

description two of the three coordinates lie on the surface of the interface and the third normal to the surface (cf. figure 6.3 page 173). The two coordinate vectors lying on the surface may and may not be orthogonal to each other but the third (normal to the surface) is always orthogonal to the other two. In terms of covariant base vectors $\mathbf{g}_3 \cdot \mathbf{g}_1 = 0$, $\mathbf{g}_3 \cdot \mathbf{g}_2 = 0$, and $\mathbf{g}_1 \cdot \mathbf{g}_2 \neq 0$.

The unit surface normal at a surface point $P_s \equiv P_s(q^1, q^2)$ also represent the tangent of the q^3 coordinate curve at P_s. The surface normal vector is defined as $\mathbf{n} = \frac{\mathbf{a}_1 \times \mathbf{a}_2}{\sqrt{a}}$ where $\mathbf{a}_\alpha$ are the surface base vectors and a is the determinant of the surface metric tensor and is defined as

$$a = \det a_{\alpha\beta} \equiv | \mathbf{a}_1 \times \mathbf{a}_2 |^2 \tag{6.12}$$

$$a_{\alpha\beta} = \mathbf{a}_\alpha \cdot \mathbf{a}_\beta \ (\alpha, \beta = 1, 2) \tag{6.13}$$

6.1.2 Derivation of the Interfacial Jump Equation

Simultaneous volumetric transport processes in the continuous bulk phases surrounding an interface accompany the areal transport process within and normal to fluid interfaces. The interdependence of these processes is apparent especially within the proximity of the interface. The volumetric physical properties (viscosity, density, solute diffusivity, etc.) and fields (velocity, pressure , solute concentration) are continuous within each phase but are generally discontinuous at the phase boundary separating the two phases. Thus the need to develop appropriate boundary conditions using the interfacial fields and physical properties.

Let Ψ denote the total amount of some generic, extensive physical property $\mathfrak{P}$ and be a function of time i.e. $\Psi = \Psi(t)$ contained within a domain of fluid ($V \equiv V(t)$) that convects with the fluid motion (cf. [?] and [?]). This property may be a scaler as in the case of mass or a vector in the case of momentum. The continuous spacial and time density field of this property is $\psi(\mathbf{x}, t)$ or the amount of the property $\mathfrak{P}$ per unit volume at a point $\mathbf{x}$ of V at time t such that

$$\Psi = \int_V dV \psi(\mathbf{x}, t) \tag{6.14}$$

and differentiating with respect to time

$$\frac{d\Psi}{dt} = \int_{V(t)} \left\{ \frac{\partial}{\partial t} \psi(\mathbf{x}, t) + \nabla \cdot [\mathbf{v}\psi(\mathbf{x}, t)] \right\} dV. \tag{6.15}$$

The rate of production of $\mathfrak{P}$ within V (denoted by $\mathbf{\Pi}$) may be expressed in terms of the

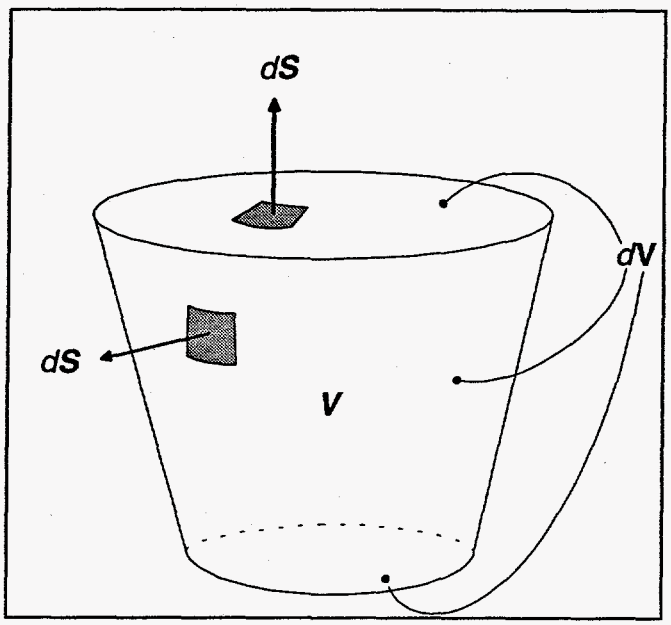

Figure 6.4: A single phase system or domain of convective fluid V(t) bounded by the closed surface $d\mathbf{V}$ or $\partial V(\mathrm{t})$ forming some portion of a three dimensional continuum. $d\mathbf{S}$ is the outwardly directed normal on $\partial \mathrm{V}$ that directs the flux of a property from the material volume.

volumetric production rate density field $\pi(\mathbf{x}, t)$

$$\mathbf{\Pi} = \int_V dV \pi(\mathbf{x}, t) \tag{6.16}$$

and the volumetric rate of supply density

$$\mathbf{Z} = \int_V dV \zeta(\mathbf{x}, t) \tag{6.17}$$

and defining $\phi(\mathbf{x}, t)$ the areal flux density (amount per unit area) of the property $\mathfrak{P}$ at a point $\mathbf{x}$ lying on the bounding surface denoted by $dV \equiv \partial V$ in figure 6.4 page 176. The time rate Φ at which property $\mathfrak{P}$ is transferred out of volume V through its surface is

$$\Phi = \oint_{\partial V} d\mathbf{S} \cdot \phi \tag{6.18}$$

where $d\mathbf{S}$ is the outward pointing normal of the bounding surface ∂V. Alternatively, using

the divergence theorem [?] given by

$$\iiint_R div\mathbf{A}d\tau = \oint_S \hat{\mathbf{n}} \cdot \mathbf{A}d\mathbf{S} \tag{6.19}$$

(note that $d\mathbf{S}$ in this equation is a differential element of surface; $\hat{\mathbf{n}}$ is the outward normal; $d\tau$ a differential volume element; and $\mathbf{A}$ is a vector function). Thus, equation 6.18 can be expressed as a volume integral

$$\mathbf{\Phi} = \int_V dV \nabla \cdot \phi \tag{6.20}$$

and by the generic overall balance the time rate of accumulation of, $\frac{d\Psi}{dt}$, of the property $\mathfrak{P}$ within V

$$\frac{d\mathbf{\Psi}}{dt} = -\mathbf{\Phi} + \mathbf{\Pi} + \mathbf{Z} \tag{6.21}$$

and substituting equations 6.15,6.16,6.17, and 6.20 into 6.21 to give the generic, volumetric balance equation for continuous three dimensional media at each point $\mathbf{x}$

$$\frac{\partial \psi}{\partial t} + \nabla \cdot (\mathbf{v}\psi + \phi) - \pi - \zeta = \mathbf{0}. \tag{6.22}$$

Note that the terms $\mathbf{v}\psi$ and ϕ are the convective and diffusive flux of the property $\mathfrak{P}$ respectively. When the specific variables (such as density, velocity, pressure, reaction rates, energy, entropy etc.) are substituted into equation 6.22 the familiar balance equations are obtained for the transport of mass, momentum, and energy for a continuous media (cf. [?, page 65] and [?, page 18]). For a discontinuity of a fluid phase boundary these equations must be supplemented by an appropriate equation quantifying the "jump" in the field across the discontinuity. This quantification for fluid interfaces is in the form of a surface excess balance equation at the macroscopic singular phase interface. This interface functions as a bounding condition imposed upon the discontinuous bulk field densities.

Consider a moving deforming fluid interface domain A in figure 6.5 page 178 that separates two bulk phases. Points within the total volume space bounded by the surfaces A_I, A_{II}, S_I, S_{II} may be identified by the space fixed position vector $\mathbf{x}$ or by the surface position vector $\mathbf{x}_s$. The normal coordinate to the surface is defined as

$$n \stackrel{def}{=} (\mathbf{x} - \mathbf{x}_s) \cdot \mathbf{n} \tag{6.23}$$

with $\mathbf{n}$ being the unit surface normal. Thus the space fixed position vector $\mathbf{x}$ is related to the surface vector $\mathbf{x}_s$ by

$$\mathbf{x} = \mathbf{x}_s + n\mathbf{n} \tag{6.24}$$

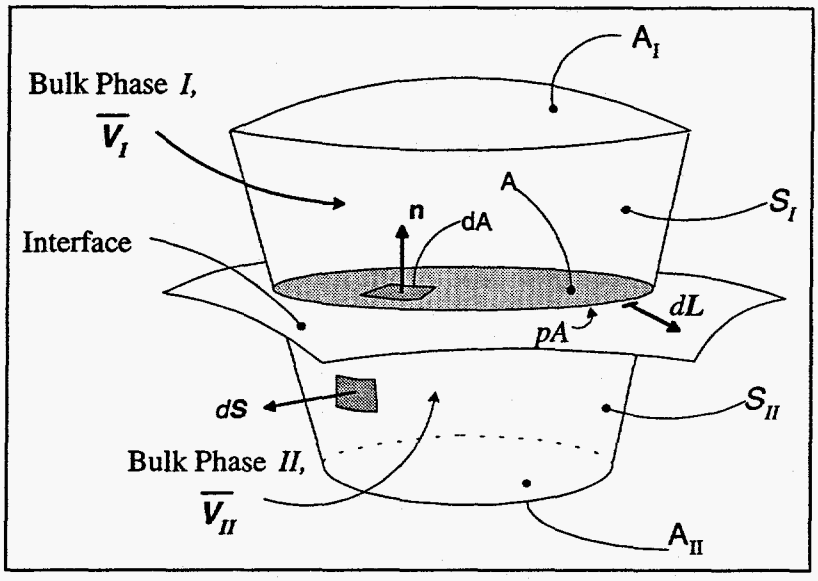

Figure 6.5: A visualization of the macroscale interface that separates two fluid phases I and II. Note that pA $\equiv \partial A$ and S$\equiv \Sigma$.

and $\mathbf{n}$ will always be directed in the positive direction away from the surface (cf. figure 6.6 page 179) i. e. originating at $\mathbf{P}_s$ on the interface and toward point $\mathbf{P}$ in space.

This allows for the generic parameterization of the three dimensional space into a two dimensional space.

$$\lambda(\mathbf{x};t) \equiv \lambda(\mathbf{x}_s, n; t) \tag{6.25}$$

Because of the two different continuum models (the three dimensional or real physical model or microscale and the two dimensional model or the macroscale) to describe an interface and thus two different length scales — a disparity exists. The two dimensional macroscale doesn't have the order of thickness of the interfacial transition region near the interface as does the microscale model. On the macroscale the total amount Ψ of $\mathfrak{P}$ in a specific bulk volume $\overline{V}$ (where the overbar denotes a bulk phase) can be expressed in terms of the generally discontinuous volumetric density field $\overline{\psi}(\mathbf{x},t)$ for each phase (i.e. amount of the property $\mathfrak{P}$ per unit volume at a point $\mathbf{x}$ of $\overline{V}$) such that

$$\Psi = \int_{\overline{V}} dV \overline{\psi}(\mathbf{x},t)\,. \tag{6.26}$$

The microscale viewpoint has a true field density $\psi(\mathbf{x},t)$ and is fully continuous over the

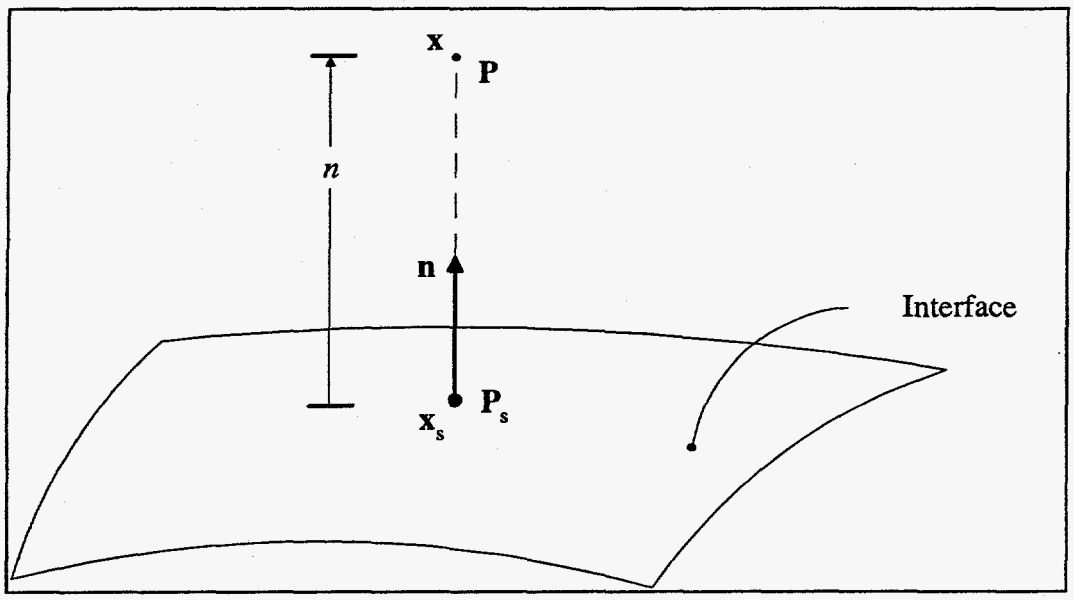

Figure 6.6: The relation between space and the surface fixed position vectors $\mathbf{x}$ and $\mathbf{x_s}$ respectively.

domain of the total volume of the system. Study of figure 6.7 page 181 elucidates this concept.

The true total amount Ψ of $\mathfrak{P}$ in V may be expressed in terms of the continuous volumetric density field $\psi(\mathbf{x},t)$

$$\Psi = \int_{\overline{V}} dV \psi(\mathbf{x},t) \tag{6.27}$$

Only in the vicinity of the fluid interface does the difference between the two length scales emerge. These differences are attributable to the large normal gradients $\frac{\partial \psi}{\partial n}$ in ψ existing within the interfacial transition one. To reconcile the discontinuous macroscale view with the true continuous microscale view the residual difference Ψ^s is defined

$$\Psi^s \stackrel{def}{=} \Psi - \overline{\Psi} \tag{6.28}$$

and is assigned to the macroscale surface A as representing the total 'surface excess' amount of the property $\mathfrak{P}$ in A. Assuming all subsequent intensive areal fields to be continuous within the interface this definition of the areally extensive variable maps the surface excess areal density field at each point $\mathbf{x}$ of A by the expression

$$\Psi^s = \int_A dA \psi^s(\mathbf{x}_s,t). \tag{6.29}$$

The generic areal field $\psi^s(\mathbf{x}_s,t)$ corresponds to the (excess) amount of the property $\mathfrak{P}$ per unit are at the point P_s of the two dimensional interfacial continuum, just as the volumetric field density $\psi(\mathbf{x},t)$ corresponds to the amount of property $\mathfrak{P}$ per unit volume at a point P of the three dimensional volumetric continuum. Ψ^s is *not* to be regarded as the actual amount of property $\mathfrak{P}$ per unit area at point P_s but rather represents the amount of property $\mathfrak{P}$ assigned to the interface as the intensive field representation of the extensive residual difference. For the macroscopic discontinuous domain the total amount $\Psi$of $\mathfrak{P}$ in V may be expressed via the above equations as

$$\Psi = \int_{\overline{V}} dV \overline{\psi} + \int_A dA \psi^s. \tag{6.30}$$

Likewise the molecular efflux Φ of the property $\mathfrak{P}$ through the boundaries of the macroscopically discontinuous volume element V can be obtained.

From the macroscale perspective the phase efflux $\overline{\Phi}$ of the property $\mathfrak{P}$ through the phase boundary $\partial\overline{V}$ may be expressed in terms of the generally discontinuous areal flux density $\overline{\phi}(\mathbf{x},t)$ (or the macroscopic length scaled amount the property $\mathfrak{P}$ per unit time flowing across a directed element centered at a point $\mathbf{x}$ lying on the bounding surface $\partial\overline{V}$) as

$$\overline{\Phi} = \oint_{\partial\overline{V}} d\mathbf{S} \cdot \overline{\phi}. \tag{6.31}$$

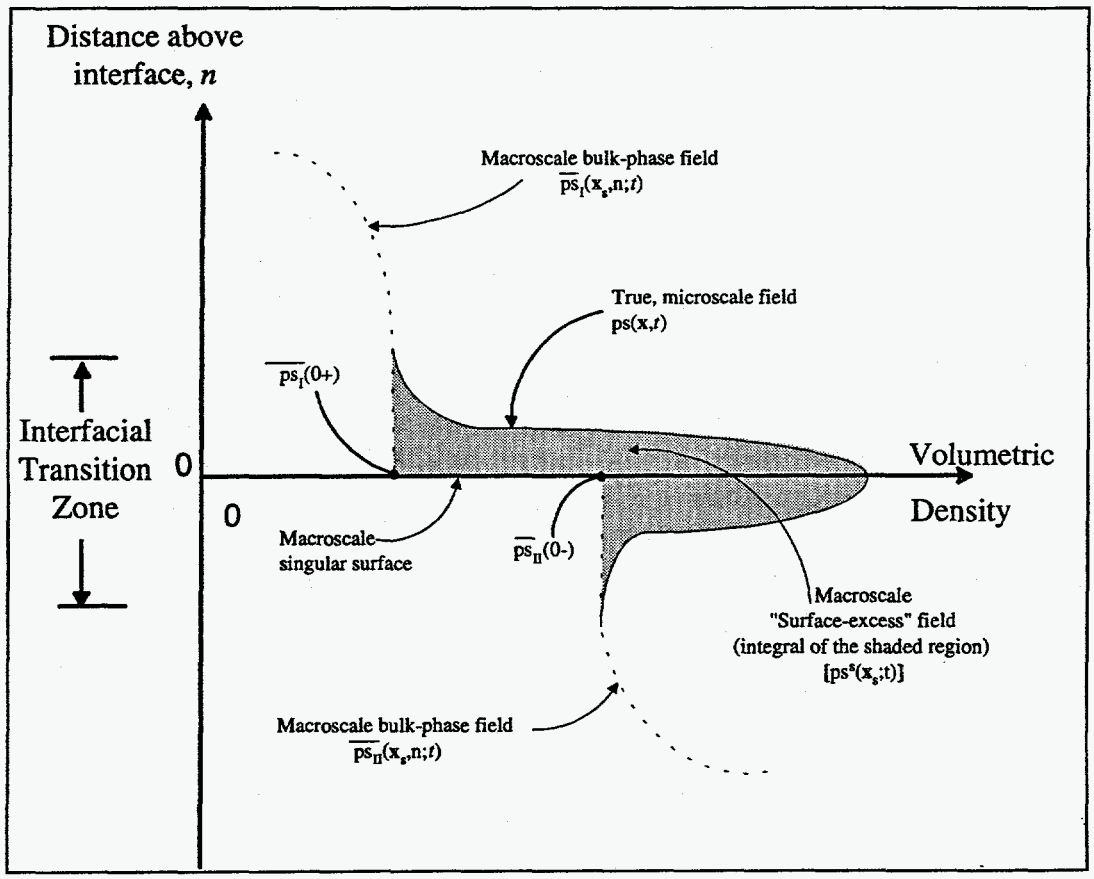

Figure 6.7: Illustration of difference in macroscale (two dimensional model) and the microscale (three dimensional model) fields at point $\mathbf{x}_s$. Note ps$\equiv \psi$.

For the microscale the true efflux $\mathbf{\Phi}$ through the material boundary ∂V for a continuous flux is expressed as

$$\mathbf{\Phi} = \oint_{\partial V} d\mathbf{S} \cdot \boldsymbol{\phi} \tag{6.32}$$

and the residual difference between these fluxes are

$$\mathbf{\Phi}^s \stackrel{def}{=} \mathbf{\Phi} - \overline{\mathbf{\Phi}}. \tag{6.33}$$

Which represents the total 'surface excess' molecular flux of the property out of A through the closed contour defined by the intersection of the interface with the total surface area bounding the system. From the assumption that all areal fields are continuous within the interface and the surface excess lineal density field $\boldsymbol{\phi}^s(\mathbf{x}_s, t)$ at each point $\mathbf{x}_s$ of the interface as

$$\mathbf{\Phi}^s = \oint_{\partial A} d\mathbf{L} \cdot \boldsymbol{\phi}^s \tag{6.34}$$

where $d\mathbf{L}$ is an outwardly directed differential lineal element along the surface. The generic field $\boldsymbol{\phi}^s(\mathbf{x}_s, t)$corresponds to the (excess) amount of the property $\mathfrak{P}$ per unit time per unit arc length flowing in a positive sense across the line element $d\mathbf{L}$ at point P_s of the two dimensional interfacial continuum. This is the two dimensional analog of the areal flux field $\boldsymbol{\phi}(\mathbf{x},t)$ corresponding to the flux of the property $\mathfrak{P}$ at a point P of the three dimensional volumetric continuum and represents flow along the surface or interface (cf. figure 6.5 page 178). The other volumetric relations are derived for

$$\frac{d\mathbf{\Psi}}{dt} = -\mathbf{\Phi} + \mathbf{\Pi} + \mathbf{Z} \tag{6.35}$$

where

$$\mathbf{\Pi} = \int_{\overline{V}} dV\overline{\pi} + \int_A d\mathbf{A}\pi^s \tag{6.36}$$

$$\mathbf{Z} = \int_{\overline{V}} dV\overline{\zeta} + \int_A d\mathbf{A}\zeta^s \tag{6.37}$$

π^s and ζ^s are the surface excess areal production and supply densities and the flux become

$$\mathbf{\Phi} = \int_{\partial\overline{V}} d\mathbf{S} \cdot \overline{\boldsymbol{\phi}} + \oint_{\partial\mathbf{A}} d\mathbf{L} \cdot \boldsymbol{\phi}^s \tag{6.38}$$

and by applying the divergence theorem ([?], [?], and [?])

$\int_R div\mathbf{F}d\tau = \oint_s \hat{\mathbf{n}} \cdot \mathbf{F}ds$
where

$d\tau$ ≡ differential volume element
$\mathbf{F}$ ≡ vector function
s ≡ surface that bounds region R
$\hat{\mathbf{n}}$ ≡ outwardly pointing normal
or

$$\int_R \nabla \cdot \mathbf{F} dV = \oint_s \mathbf{F} \cdot \mathbf{n} ds \tag{6.39}$$

which states that the flux of a vector function $\mathbf{F}$ through area S equals the triple or volumetric integral of the divergence over R.

over each of the continuous domains or bulk phases to obtain

$$\mathbf{\Phi} = \int_{\overline{V}} dV \nabla \cdot \overline{\phi} + \int_A dA \mathbf{n} \cdot \| \overline{\phi} \| + \int_A dA \nabla_s \cdot (\mathbf{I}_s \cdot \phi^s) . \tag{6.40}$$

where $\| \overline{\phi} \|$ is a denotation of the jump in discontinuous tensor field or in a generic form

$$\| \mathfrak{R} \| \stackrel{def}{=} \mathfrak{R}_I (0+) - \mathfrak{R}_{II} (0-) \tag{6.41}$$

where $\mathfrak{R}$ is a tensor field across a singular surface with $\mathfrak{R}_I (0+)$ and $\mathfrak{R}_{II} (0-)$ denoting the respective values of $\mathfrak{R}$ on the two sides of the interface, $n = 0+$and $n = 0-$.

By using the volumetric Reynolds transport theorem i.e.

$$\frac{d}{dt} \int_V \mathfrak{R} dV = \int_V \left[\frac{D\mathfrak{R}}{\partial t} + \mathfrak{R} \nabla \cdot \mathbf{v} \right] dV \tag{6.42}$$

where $\frac{D}{\partial t} \stackrel{def}{=} \frac{\partial}{\partial t} + (\mathbf{v} \cdot \nabla)$ (see [?, page 58, 72, and 86-87] and [?, page 725] and [?]) is the convected, material, or substantial derivative.

allows the following development from

$$\frac{d}{dt} \int\limits_{\overline{V}_I(t) \bigoplus \overline{V}_{II}(t)} dV \overline{\psi} = \int_{\overline{V}(t)} dV \left[\frac{\partial}{\partial t} \overline{\psi} + \nabla \cdot \left(\mathbf{v} \overline{\psi} \right) \right] \tag{6.43}$$

and using the surface Reynolds transport theorem for convected material surface [?, page 60] and [?, page 72-75] i. e.

$$\frac{d}{dt} \int_A \mathfrak{R} dA = \int_A \left[\frac{\partial \mathfrak{R}}{\partial t} + \nabla_s \cdot (\mathbf{v} \mathfrak{R}) \right] dA. \tag{6.44}$$

or in a more suitable form

$$\frac{d}{dt} \int_A dA \psi^s = \int_A dA \left[\frac{\partial}{\partial t} \psi^s + \nabla_s \cdot (\mathbf{v}^o \psi^s) \right] \tag{6.45}$$

and the combination of equations 6.43 and 6.45 with reference to equation 6.30 allows the development of

$$\frac{d\Psi}{dt} = \int_{\overline{V}(t)} dV \left[\frac{\partial}{\partial t}\overline{\psi} + \nabla \cdot \left(\mathbf{v}\overline{\psi}\right)\right] + \int_A dA \left[\frac{\partial}{\partial t}\psi^s + \nabla_s \cdot \left(\mathbf{v}^o\psi^s\right)\right]. \tag{6.46}$$

This comes about from the time rate of change of the amount, Ψ, of property $\mathfrak{P}$ given by the derivative of equation 6.30

$$\Psi = \int_{\overline{V}} dV\overline{\psi} + \int_A dA\psi^s \tag{6.47}$$

to give

$$\frac{d\Psi}{dt} = \frac{d\left(\int_{\overline{V}} dV\overline{\psi}\right)}{dt} + \frac{d\left(\int_A dA\psi^s\right)}{dt} \tag{6.48}$$

and substituting appropriately then equation 6.46 is obtained.

Recalling that

$$\frac{d\Psi}{dt} = -\Phi + \Pi + \mathbf{Z}$$

where

$$\begin{aligned} \Pi &= \textstyle\int_{\overline{V}} dV\overline{\pi} + \int_A d\mathbf{A}\pi^s \\ \mathbf{Z} &= \textstyle\int_{\overline{V}} dV\overline{\zeta} + \int_A d\mathbf{A}\zeta^s \\ \Phi &= \textstyle\int_{\overline{V}} dV\nabla \cdot \overline{\phi} + \int_A dA\mathbf{n} \cdot \| \overline{\phi} \| + \int_A dA\nabla_s \cdot (\mathbf{I}_s \cdot \phi^s) \end{aligned}$$

π^s and ζ^s are the surface excess areal production and supply densities and substituting accordingly

$$\begin{aligned} &\textstyle\int_{\overline{V}(t)} dV \left[\frac{\partial}{\partial t}\overline{\psi} + \nabla \cdot \left(\mathbf{v}\overline{\psi}\right)\right] + \int_A dA \left[\frac{\partial}{\partial t}\psi^s + \nabla_s \cdot \left(\mathbf{v}^o\psi^s\right)\right] \\ &= -\left(\textstyle\int_{\overline{V}} dV\nabla \cdot \overline{\phi} + \int_A dA\mathbf{n} \cdot \| \overline{\phi} \| + \int_A dA\nabla_s \cdot (\mathbf{I}_s \cdot \phi^s)\right) \\ &\quad + \textstyle\int_{\overline{V}} dV\overline{\zeta} + \int_A d\mathbf{A}\zeta^s + \int_{\overline{V}} dV\overline{\pi} + \int_A d\mathbf{A}\pi^s \end{aligned} \tag{6.49}$$

combining like terms and taking terms to the left hand side

$$\begin{aligned} &\textstyle\int_{\overline{V}} dV \left\{\frac{\partial}{\partial t}\overline{\psi} + \nabla \cdot \left(\mathbf{v}\overline{\psi} + \overline{\phi}\right) - \overline{\pi} - \overline{\zeta}\right\} \\ &+ \textstyle\int_A dA \left\{\frac{\partial}{\partial t}\psi^s + \nabla_s \cdot \left(\mathbf{v}^o\psi^s + \mathbf{I}_s \cdot \phi^s\right) - \pi^s - \zeta^s + \mathbf{n} \cdot \| \overline{\phi} \|\right\} \\ &= 0. \end{aligned} \tag{6.50}$$

The first integral term is the transport or continuity equation in a single phase or in this case one of the bulk phases and by the conservation of mass constraint at each point within

a phase is zero i.e.

$$\int_{\overline{V}} dV \left\{ \frac{\partial}{\partial t}\overline{\psi} + \nabla \cdot \left(\mathbf{v}\overline{\psi} + \overline{\phi} \right) - \overline{\pi} - \overline{\zeta} \right\} = 0 \tag{6.51}$$

[?, page 86-87]. Thus equation 6.50 reduces to

$$\int_A dA \left\{ \frac{\partial}{\partial t}\psi^s + \nabla_s \cdot (\mathbf{v}^o \psi^s + \mathbf{I}_s \cdot \phi^s) - \pi^s - \zeta^s + \mathbf{n} \cdot \| \overline{\phi} \| \right\} = 0 \tag{6.52}$$

and since the integrand is zero if an integral over an arbitrary portion of dividing surface is zero [?, page 88] then the jump mass balance is

$$\frac{\partial}{\partial t}\psi^s + \nabla_s \cdot (\mathbf{v}^o \psi^s + \mathbf{I}_s \cdot \phi^s) - \pi^s - \zeta^s + \mathbf{n} \cdot \| \overline{\phi} \| = 0 \tag{6.53}$$

or

$$\frac{d\psi^s}{dt} + \nabla_s \cdot (\mathbf{v}^o \psi^s + \mathbf{I}_s \cdot \phi^s) - \pi^s - \zeta^s = -\mathbf{n} \cdot \| \overline{\phi} \| . \tag{6.54}$$

Equation 6.54 is the point-wise generic interfacial equation valid for each point $\mathbf{x}_s$ of A. It must be true for every portion of a dividing surface excluding a common line (i.e. intersection of three phases) (cf. [?, page 87]).

π^s ≡ surface excess time rate of production of a generic property at a point on the interface
ζ^s ≡ surface excess time rate of supply of a generic physical property at a point on the interface
ϕ^s ≡ surface excess diffusion flux of generic property
$\mathbf{v}^o$ ≡ velocity at a point $\mathbf{x}_s$ of the material interface
$\mathbf{I}_s$ ≡ unit surface idemfactor
ψ^s ≡ surface excess amount of generic physical property at a point on the interface (field density per unit area)

If there is no mass transfer to or from the surface and the supply and production terms are zero ($\pi^s = \zeta^s = 0$) and the flux is zero ($\phi^s = 0$) and thus $-\mathbf{n} \cdot \| \overline{\phi} \| = 0$ the surface excess transport equation reduces to

$$\frac{d\psi^s}{dt} + \nabla_s \cdot (\mathbf{v}^o \psi^s) = 0 \tag{6.55}$$

and if the surface amount of the property, ψ^s, is held constant then $\nabla_s \cdot \mathbf{v} = 0$ which states that there is no local expansion (dilation) of the interface [?, page 87].

Except for the bulk phase molecular flux terms appearing on the right side a one to one correlation or analog is apparent between the terms of the three dimensional transfer equation

and the two dimensional surface jump equation. The flux term is a source or sink to the interface. A second distinction is the idemfactor $\mathbf{I}$ which is constant in a three dimensional space that is flat and the flux $\mathbf{I}\cdot\phi$ is constant throughout space and independent of $\mathbf{x}$. In contrast, the curvature of the interface may cause $\mathbf{I}_s$ not to be constant except for flat surfaces or interfaces and is a function of $\mathbf{x}_s$ [?, page 75].

Solute Mass Transfer Equation

For mass transfer there is no areal supply rate, ζ^s. This term comes about in momentum balance and energy balance equations. Letting

$$\begin{aligned} \psi^s &\equiv \rho_i^s \text{ (surface excess mass density for species } i) \\ \phi^s &\equiv j_i^s \text{ (surface excess mass flux for spcies } i) \\ \pi^s &\equiv R_i^s \text{ (surface excess areal production for spcies } i) \end{aligned}$$

then the mass balance becomes

$$\frac{d\rho_i^s}{dt} + \nabla_s \cdot (\mathbf{v}^o \rho_i^s + \mathbf{I}_s \cdot j_i^s) = R_i^s + \mathbf{n} \cdot \| \overline{j_i} \| \tag{6.56}$$

and defining j_i^s in the "surface Fickian " diffusive form

$$j_i^s \stackrel{def}{=} (\mathbf{v}_i^o - \mathbf{v}^o)\, \rho_i^s = -\mathfrak{D}_i^s \nabla_s \rho_i^s \tag{6.57}$$

the surface projection of $j_i^s = \mathbf{I}_s \cdot j_i^s$ thus

$$\frac{d\rho_i^s}{dt} + \nabla_s \cdot (\mathbf{v}^o \rho_i^s) - \nabla_s \cdot (\mathfrak{D}_i^s \nabla_s \rho_i^s) = R_i^s + \mathbf{n} \cdot \| \overline{j_i} \| \tag{6.58}$$

or for the case of constant surface diffusivity, $\mathfrak{D}_i^s$,

$$\frac{d\rho_i^s}{dt} + \nabla_s \cdot (\mathbf{v}^o \rho_i^s) - \mathfrak{D}_i^s \nabla_s^2 \rho_i^s = R_i^s + \mathbf{n} \cdot \| \overline{j_i} \| \,. \tag{6.59}$$

Placing terms more typical of surface excess molar species concentration

$$\Gamma_i^s \stackrel{def}{=} \frac{\rho_i^s}{M_i} \tag{6.60}$$

where here M_i is the molecular weight and Γ_i^s is the surface excess molar concentration. The surface excess species flux boundary condition is obtained

$$\frac{d\Gamma_i^s}{dt} + \nabla_s \cdot (\mathbf{v}^o \Gamma_i^s) - \mathfrak{D}_i^s \nabla_s^2 \Gamma_i^s = r_i^s + \mathbf{n} \cdot \| \overline{j_i} \| \tag{6.61}$$

where r_i^s is the surface excess molar areal production rate.

Equations of Motion

Recognition of the intimate coupling of surface flow with flow of the adjacent bulk fluids, requires the simultaneous solution of the equations defining these two flow regimes. Scriven [?] as well as Edwards et al. [?] derive these equations in detail in tensor formalism and using the theorems of differential geometry. This type of formal derivation is given in section 6.1 for the generic interfacial conservation equation. In the case at hand we desire the generic volumetric balance equation ?? page ??. Using the proper fields for the generic variables for linear momentum of $\overline{\Psi} = \rho\mathbf{v}$, $\overline{\phi} = -\mathbf{P}$, $\pi = 0$, and $\zeta = \mathbf{F}$ the linear momentum conservation equation is obtained.

$$\frac{\partial}{\partial t}(\rho\mathbf{v}) + \nabla\cdot(\rho\mathbf{v}\mathbf{v}) - \nabla\cdot\mathbf{P} - \mathbf{F} = \mathbf{0} \tag{6.62}$$

and for angular momentum $\overline{\Psi} = \mathbf{x}\times(\rho\mathbf{v}) + \rho\mathbf{a}$, $\overline{\phi} = \mathbf{P}\times\mathbf{x} - \mathbf{C}$, $\pi = 0$, and $\zeta = \mathbf{x}\times\mathbf{F} + \mathbf{G}$

$$\frac{\partial}{\partial t}(\rho\mathbf{x}\times\mathbf{v}) + \frac{\partial}{\partial t}(\rho\mathbf{a}) + \nabla\cdot(\rho\mathbf{v}\mathbf{x}\times\mathbf{v}) + \nabla\cdot(\rho\mathbf{v}\mathbf{a}) - \nabla\cdot(\mathbf{P}\times\mathbf{x}) - \nabla\cdot\mathbf{C} - \mathbf{x}\times\mathbf{F} - \mathbf{G} = \mathbf{0}. \tag{6.63}$$

Defining a pseudo-vector invariant $\mathbf{P}_\mathbf{x}$ of the antisymmetric portion $\frac{1}{2}\left(\mathbf{P} - \mathbf{P}^\dagger\right)$ of the pressure tensor as

$$\begin{aligned}\mathbf{P}_\mathbf{x} &= -\varepsilon:\frac{1}{2}\left(\mathbf{P} - \mathbf{P}^\dagger\right)\\ &\equiv -\varepsilon:\mathbf{P}\end{aligned} \tag{6.64}$$

where ε is the unit alternator. In terms of this pseudovector equation 6.63 may be arranged into

$$\mathbf{x}\times\left[\frac{\partial}{\partial t}(\rho\mathbf{v}) + \nabla\cdot(\rho\mathbf{v}\mathbf{v}) - \nabla\cdot\mathbf{P} - \mathbf{F}\right] + \frac{\partial}{\partial t}(\rho\mathbf{a}) + \nabla\cdot(\rho\mathbf{v}\mathbf{a}) - \mathbf{P}_\mathbf{x} - \nabla\cdot\mathbf{C} - \mathbf{G} = \mathbf{0}. \tag{6.65}$$

and as a result of equation 6.62 becomes

$$\frac{\partial}{\partial t}(\rho\mathbf{a}) + \nabla\cdot(\rho\mathbf{v}\mathbf{a}) - \mathbf{P}_\mathbf{x} - \nabla\cdot\mathbf{C} - \mathbf{G} = \mathbf{0}. \tag{6.66}$$

For non polar fluids the internal momentum and stress pseudovectors are zero thus $\mathbf{a} = \mathbf{C} = \mathbf{G} = \mathbf{0}$ and thus $\mathbf{P}_x = \mathbf{0}$ and therefore $\mathbf{P} = \mathbf{P}^\dagger$. This illustrates the symmetry of the pressure tensor.

$\mathbf{a}$ = internal angular momentum pseudovector
$\mathbf{C}$ =couple-stress pseudovector
$\mathbf{F}$ = external body force density vector
$\mathbf{G}$ = body couple density pseudovector
$\mathbf{P}$ = pressure dyadic
ρ = mass density
$\mathbf{v}$ = mass average velocity vector
$\mathbf{x}$ = space-fixed position vector
$\mathbf{P}^\dagger$ = transpose of the stress or pressure tensor

The pressure tensor can be written in a decomposed form into what Edwards *et al* refer tc as the isotropic or thermodynamic pressure, p, and deviatory part or viscous stress tensor, $\boldsymbol{\tau}$

$$\mathbf{P} = -p\mathbf{I} + \boldsymbol{\tau}. \tag{6.67}$$

The thermodynamic pressure is different than the *mean pressure* which is defined as

$$\overline{p} \stackrel{\text{def}}{=} -\frac{1}{3}\mathbf{I}\!:\!\mathbf{P} \tag{6.68}$$

This the pressure, p, at any point in a fluid is larger than the mean normal pressure by the additive term proportional to the rate of expansion, $\nabla \cdot \mathbf{v}$. For a Newtonian fluid $\boldsymbol{\tau}$ is a second order tensor given by [?, page 565]:

$$\boldsymbol{\tau} = \left(\kappa - \frac{2}{3}\mu\right)(\mathbf{I}\!:\!\mathbf{D})\,\mathbf{I} + 2\mu\mathbf{D} \tag{6.69}$$

where μ and κ are the shear and dilatational viscosities and $\mathbf{D}$ is the rate of deformation tensor defined as [?]

$$\mathbf{D} \stackrel{\text{def}}{=} \frac{1}{2}\left(\nabla\mathbf{v} + [\nabla\mathbf{v}]^\dagger\right). \tag{6.70}$$

κ is also referred to as the propotionality constant defined to be the bulk viscosity coefficient and relates stress to volumetric deformation rate in the same way that shear viscosity relates stress to linear deformation rate [?]. A compressible Newtonian fluid will have a relationship between the thermodynamic and mean pressures given by

$$\overline{p} - p = -\kappa\nabla \cdot \mathbf{v} \tag{6.71}$$

involving only the dilatational viscosity coefficient κ. For an incompressible Newtonian fluid $\mathbf{I}\!:\!\mathbf{D} \equiv \nabla \cdot \mathbf{v} = \mathbf{0}$ and the viscous stress tensor simplifies to

$$\boldsymbol{\tau} = 2\mu\mathbf{D}. \tag{6.72}$$

This implies that by the continuity equation that the mass density ρ is constant in space in time (note: this does not imply that the mass of species i is constant in space and time) and that the thermodynamic and mean pressures are equivalent. The whole point of this exercise was to obtain two important starting equations in modeling the Marangoni effects: the equation of continuity , and ; Navier-Stokes equation. By combining equations ??, 6.67, 6.69 and the continuity equation at constant fluid density $\nabla \cdot \mathbf{v} = \mathbf{0}$ the Navier-Stokes and continuity equation for a three dimensional, incompressible, nonpolar, Newtonian fluid continuum with ρ and μ constant throughout the fluid.

$$\rho\left(\frac{\partial \mathbf{v}}{\partial t} + \mathbf{v} \cdot \boldsymbol{\nabla}\mathbf{v}\right) = -\nabla p + \mu \nabla^2 \mathbf{v} \tag{6.73}$$

$$\nabla \cdot \mathbf{v} = \mathbf{0} \tag{6.74}$$

Note that the external body force vector represented by $\mathbf{F}$ is incorporated in the pressure term p. Generally this term is the gravitational vector $\rho \mathbf{g} \cdot \mathbf{z}$ and thus the pressure term $p' = p + \rho \mathbf{g} \cdot \mathbf{z}$ ($\mathbf{z}$ being the position vector) with the prime on the left hand side eventually dropped [?, page 28], [?, page 52]. In the section on Interfacial Turbulence section 6.2 the coupling between the interfacial solute transport, Navier-Stokes equation, the continuity equation as well as some constitutive equations will be combined to develop the model for the phenomena of spontaneous convection due to mass transfer and chemical reactions at an interface.

6.2 Interfacial Turbulence or Convection — The Marangoni Phenomena

6.2.1 Brief Background

Interfacial instabilities occur when two unequilibrated immiscible or partially miscible liquid phases containing a solute that is soluble in both phases are brought into contact. The term Marangoni phenomena effect or specifically the solutal Marangoni effect or soluto-capillary instability [?] is applied to the spontaneous interfacial flow induced by interfacial tension gradients. These interfacial tension gradients are caused by changes in solute concentrations, temperature and interfacial electrical potential [?, Chapter 3 by E. S. Perez de Ortiz]. Spontaneous interfacial flow results in an additional component to the interfacial flux that is not included in the general theories of mass transfer.

Two physical properties play important roles in this induced fluid motion [?]:

- solute diffusivity
- kinematic viscosity

Edwards *et al* [?, page 273] reports that Hennenberg *et al* [?] showed that the interfacial turbulence may be enhanced as Sternling and Scriven deduced by:

1. solute transfer from the phase of highest viscosity and lowest diffusivity
2. small viscosities and diffusivites, and
3. large interfacial tension gradients and small interfacial viscosities

Other effects on the instabilities may be caused by a wall or boundary, adsorption-desorption at the interface, and/or other chemical reactions. In systems with no chemical reactions a qualitative analysis of the effects of viscosity can be discussed as the references [?, page 162] and [?, page 275-278] have done. For a typical system without a chemical reaction with adsorption and similar values of solute diffusivities in both phases, interfacial convection is likely to be sustained when mass transfer takes place from the phase of higher viscosity [?, page 161]. A system with like diffusivities but unlike kinematic viscosities is predicted to be unstable when the solute is transferred from the phase of lower solute diffusivity [?, page 161].

In the case of a system with a chemical reaction it is not easy to predict the interfacial stability qualitatively. There has been little theoretical work done on the effects of the Marangoni phenomena accompanied by chemical reactions. Most of the works reported, though abundant, are phenomenological and are primarily experimental observations of the turbulence of mass transfer with chemical reaction. Recently Warmuziński *et al* [?] and previously Ruckenstein and Bebente [?] and [?] have attempted to distinguish the effects of the Marangoni effect and that of the chemical reaction on mass transfer processes.

Nakache *et al* [?], [?] observed reactions leading to emulsification, interfacial movements, and surface deformation. The different types of instabilities result from variation of interfacial tensions and pH with contact time. Oscillations of interfacial tension were experimentally observed to have a correlation between surface convection and adsorption density. Systems were always stable when the reactants were dissolved in the phases where they were less soluble. The type of organic solvent also effected the interfacial stability and was interpreted to be an effect of the dielectric constant of the solvent and the ionization of the reactants. Nakache *et al* proposed a mechanism of instability that included adsorption/desorption steps, reactant concentrations, and chemical, diffusional and convective steps [?]. In the extraction of copper Nakache as reported by Ortiz [?] saw interfacial movements and emulsion formation in the extraction of copper in di(2-ethylhexyl) phosphoric acid (DEPAH) and its sodium salt (DEPANa) in xylene. Extracting with DEPANa alone had a higher interfacial activity and deformation than when mixed with DEPAH.

Rogers and Thompson [?] and Thompson [?, page 180] observed interfacial instabilities

during extraction of uranyl nitrate, plutonium(IV) nitrate and nitric acid from aqueous solution into tributyl phosphate organic phase. Rogers and Thompson observed and reported that the systems that exhibit interfacial turbulence the value of the mass transfer coefficient depend on the time of contact and hence the age of the interface. This is in agreement with Nakache. Rogers and Thornton suggest that the dampening of interfacial turbulence with time is unresolved but proposes that it is not caused by a buildup of the interfacial complexes or contaminants as proposed by others. Ruckenstein suggests that the liquid elements taking part in the roll cells of the interfacial activity become progressively saturated and thereby reduce the concentration gradients [?]. Contrarily Kizim and Lańkov [?] experimentally determined that 20-30 percent of the initial amount of a lanthanide extraction in DEHP accumulates in the interfacial film 60 minutes after the initiation of their experiment. These authors feel that the higher accumulation during the first 5-10 minutes may be due to spontaneous surface convection. As the interfacial film develops the interfacial surface is shielded and decreases the rate of formation of the extracted compound. The discussion is primarily limited experimentally determining the formation of the presence of a film. Spontaneous convection is only briefly mentioned.

An experimentally verified molecular model of the interface is not yet available [?, page 176] though there is work underway to describe the interfacial parameters as described in the references [?], [?] and [?]. Figure **(((INTERFACE1)))** is a qualitative conception of the interface. This conception is echoed by Vandegrift and Horwitz description of the water or aqueous phase near the interface in a HDEHP extractant system. They describe the aqueous side of the interface as being a two layer system. The water forms hydrogen bonds with the HDEHP monolayer (organic reactant) and the interface on the aqueous side becomes "ice-like" with a very structured orientation with thickness being dependent upon temperature [?]. In concept this can explain the aging effect. As the layer develops with time and may grow thicker the "shielding" effect as Kizim and Lańkov noted may become more pronounced. However, it should be noted that as the reactions take place heat of reaction and heat of solution is present and could raise the temperature close to the interface. This heat probably locally restricted could cause "thawing" of the interface in these local areas and may effect oscillatory turbulence if not completely keep the system from reaching stability. This hypothesis has not been verified and is not, to my knowledge, contained in the literature. Vadegrift and Horwitz did comment on mechanical energy by low speed stirring could not "thaw" the icelike structure at low temperatures.

The intensity of the interfacial turbulence strongly depends on the magnitude of the gradient of interfacial tension as a result of the rates of mass and momentum transfer between the two phases. Surfactants have a tendency to reduce the interfacial tension possibly below a level that any perturbations of the solute concentration can change to induce instabilities [?]. An example of this calming effect is the placement of thin sheen of oil on a wavy pound.

Surfactants alter the structure of the interfaces rheological behavior and in the rate of mass transfer.

6.2.2 Mathematical Modeling of the Marangoni Effect

The characteristic method for mathematical modeling of the interfacial instabilities often referred to as the linear stability theory and widely used in the hydrodynamic stability analysis is [?]:

1. Initially the interface is along a planar or cylindrical geometry
2. Initially the system is in a stationary state (steady state) or at local equilibrium at the interface (undisturbed state)
3. The phases may be either stagnant or flowing
4. May be accompanied by heat of solution
5. Liquids are Newtonian (isotropic fluids in which stress depends linearly on rate of strain)
6. Liquids are incompressible
7. Physical properties are not dependent on concentration or temperature gradients
8. The equations governing the perturbed system are obtained by introducing infinitesimal increments to the physical variables that describe the flow
9. These equations are linearized and solved in order to obtain the evolution of the perturbations in time.

Additionally, most models make the following assumptions:

Sternling and Scriven first applied this approach [?] to two semi-infinite, quiescent fluid phases in contact along a plane interface in thermodynamic but not chemical equilibrium. Sternling and Scriven point out that interfacial forces generated by accounting for temperature variations are roughly a thousandfold less than those simultaneously generated by concentration variations in a typical system benzene-acetone-water. The simplified model that Sternling and Scriven introduced twenty-five years ago had several simplifications that make it unrealistic [?]:

1. Two dimensional disturbances were not accounted for
2. In reality the interface is not fixed in position

3. the system is not planar rather it is typically curved or even spherical
4. Solute transfer is not steady state
5. Solvents also interdiffuse along with the solutes
6. the diffusivities usually depend strongly on concentration

There are other modeling approaches. The Sørensen *et al* model accounts for variables that the Sternling-Scriven model neglects (i.e. the adsorbed mass, the normal deformations of the interface, heat effects (phases are in thermal equilibrium), and gravity). A variation of the Sorensen model also used an exponential estimation of the profile for the solute concentration distribution. The Hennenberg model is basically the same as the Sørensen model but the interfacial balances for the perturbed quantities are written at the location of the perturbed interface instead of at the non-perturbed interface [?].

Hennenberg [?][?], Sørensen and co-workers [?] and Sanfield and co-workers [?][?] considered the effects of non-linear concentration profiles, deformable interfaces, mass transfer with interfacial chemical reactions and electrical constraints [?, page 171]. Ortiz reports that the results differ from Sterling and Scriven model by negligible amounts for systems with interfacial tension greater than 1 mN/m. At lower interfacial tension, oscillatory instabilities appeared in regions predicted by Sternling and Scriven to be stable.

The governing equations for modeling spontaneous flow are the Navier-Stokes, continuity, and the convection diffusion equations with chemical reactions, for each bulk phase i

$$\rho\left(\frac{\partial \mathbf{v}_i}{\partial t} + \mathbf{v}_i \cdot \nabla \mathbf{v}_i\right) = -\nabla p_i + \mu_i \nabla^2 \mathbf{v}_i + \rho_i \mathbf{g} \cdot \mathbf{z} \tag{6.75}$$

$$\nabla \cdot \mathbf{v}_i = \mathbf{0} \tag{6.76}$$

$$\frac{\partial c_i}{\partial t} + \nabla \cdot (\mathbf{v}_i c_i) = \nabla \cdot \mathfrak{D}_i \nabla^2 c_i + R_i \; ; \tag{6.77}$$

the boundary conditions at the interface represented by the solute mass conservation and the surface momentum conservation equations [?], [?]

$$\frac{d\Gamma_i^s}{dt} + \nabla_s \cdot (\mathbf{v}^o \Gamma_i^s) - \mathfrak{D}_i^s \nabla_s^2 \Gamma_i^s = r_i^s + \mathbf{n} \cdot \| \overline{j_i} \| \tag{6.78}$$

$$\frac{\partial (\rho^s \mathbf{v}^o)}{\partial t} = -\nabla_s \cdot (\rho^s \mathbf{v}^o \mathbf{v}^o) - \nabla_s \sigma \cdot + 2h\sigma \mathbf{n} + \nabla_s \cdot \boldsymbol{\tau}^s - \mathbf{n} \|p\| + \mathbf{n} \cdot \|\boldsymbol{\tau}\| \, . \tag{6.79}$$

In arriving at equation 6.79 several items need to be illuminated. These can best be illustrated by a brief derivation starting from the generic surface excess balance equation,

equation ??:

$$\frac{d\psi^s}{dt} + \nabla_s \cdot (\mathbf{v}^o \psi^s + \mathbf{I}_s \cdot \phi^s) - \pi^s - \zeta^s = -\mathbf{n} \cdot \| \overline{\phi} \| \tag{6.80}$$

and substituting the proper variables for surface-excess linear momentum $\psi^s = \rho^s \mathbf{v}^o$, $\phi^s = -\mathbf{P}^s$, $\overline{\phi} = -\mathbf{P}$, $\pi^s = 0$, and $\zeta^s = \mathbf{F}^s$ results in

$$\frac{d(\rho^s \mathbf{v}^o)}{dt} + \nabla_s \cdot (\rho^s \mathbf{v}^o \mathbf{v}^o) - \nabla_s \cdot (\mathbf{I}_s \cdot \mathbf{P}^s) - \mathbf{F}^s = -\mathbf{n} \cdot \| \overline{-\mathbf{P}} \| . \tag{6.81}$$

The surface excess pressure tensor possesses the property $\mathbf{I}_s \cdot \mathbf{P}^s = \mathbf{P}^s$. Thus, $\nabla_s \cdot (\mathbf{I}_s \cdot \mathbf{P}^s) = \nabla_s \cdot \mathbf{P}^s$ [?, page 106]. Using this property and the decomposition of the surface excess pressure tensor in its isotropic and deviatory parts [?, page 108]

$$\mathbf{P}^s = \mathbf{I}_s \sigma + \boldsymbol{\tau}^s, \tag{6.82}$$

where $\boldsymbol{\tau}^s$ the surface excess stress tensor σ is the *thermodynamic* interfacial tension and is the hypothetical surface tension which would appear in an equilibrium equation of state that is governing the surface intensive variables $\sigma \equiv \sigma(\rho^s, T, x_i^s)$ results in

$$\begin{aligned} -\mathbf{n} \cdot \| \overline{-\mathbf{P}} \| &= \frac{d(\rho^s \mathbf{v}^o)}{dt} + \nabla_s \cdot (\rho^s \mathbf{v}^o \mathbf{v}^o) - \nabla_s \cdot \mathbf{P}^s - \mathbf{F}^s \\ &= \frac{d(\rho^s \mathbf{v}^o)}{dt} + \nabla_s \cdot (\rho^s \mathbf{v}^o \mathbf{v}^o) - \nabla_s \cdot (\mathbf{I}_s \sigma + \boldsymbol{\tau}^s) - \mathbf{F}^s \\ &= \frac{d(\rho^s \mathbf{v}^o)}{dt} + \nabla_s \cdot (\rho^s \mathbf{v}^o \mathbf{v}^o) - \nabla_s \cdot \mathbf{I}_s \sigma - \nabla_s \cdot \boldsymbol{\tau}^s - \mathbf{F}^s. \end{aligned} \tag{6.83}$$

From the general identities

$$\begin{aligned} \mathbf{I}_s &\stackrel{\text{def}}{=} \mathbf{I} - \mathbf{nn} && \text{(dyadic surface idemfactor)} \\ \nabla_s &\stackrel{\text{def}}{=} \mathbf{I}_s \cdot \nabla && \text{(Surface gradient operator)} \\ \mathbf{b} &\equiv -\nabla_s \mathbf{n} && \text{(Surface Curvature dyadic)} \\ H &\stackrel{\text{def}}{=} -\frac{1}{2} \nabla_s \cdot \mathbf{n} \\ &\equiv -\frac{1}{2} \mathbf{I}_s : \mathbf{b} && \text{(mean surface curvature)} \end{aligned}$$

which gives the identity [?, page 51]

$$\nabla_s \cdot \mathbf{I}_s \equiv 2H\mathbf{n}. \tag{6.84}$$

Expanding the third term of equation 6.83

$$\nabla_s \cdot \mathbf{I}_s \sigma = \mathbf{I}_s \cdot \nabla_s \sigma + \sigma \nabla_s \cdot \mathbf{I}_s \tag{6.85}$$

$$= \mathbf{I}_s \cdot \nabla_s \sigma + 2H\mathbf{n}\sigma \tag{6.86}$$

and noting that the bulk pressure tensor decomposed into its isotropic and deformatory parts alters the left hand side of this equation to

$$\begin{aligned} -\mathbf{n}\cdot\|\overline{-\mathbf{P}}\| &= \mathbf{n}\cdot\|-p\mathbf{I}+\boldsymbol{\tau}\| \\ &= \mathbf{n}\cdot\|-p\mathbf{I}\|+\mathbf{n}\cdot\|\boldsymbol{\tau}\| \\ &= -\|p\|\,\mathbf{n}\cdot\mathbf{I}+\mathbf{n}\cdot\|\boldsymbol{\tau}\| \\ &= -\mathbf{n}\|p\|+\mathbf{n}\cdot\|\boldsymbol{\tau}\| \end{aligned} \tag{6.87}$$

and thus equation 6.83 becomes

$$-\mathbf{n}\|p\|+\mathbf{n}\cdot\|\boldsymbol{\tau}\| = \frac{d(\rho^s\mathbf{v}^o)}{dt}+\nabla_s\cdot(\rho^s\mathbf{v}^o\mathbf{v}^o)-\nabla_s\sigma-2H\mathbf{n}\sigma-\nabla_s\cdot\boldsymbol{\tau}^s-\mathbf{F}^s. \tag{6.88}$$

This is identical to equation 8 of Bekki *et al* [?] where $\|\ \ \|$ denotes the jump of the bracketed quantity across the interface, $\boldsymbol{\tau}$ and $\boldsymbol{\tau}^s$ the bulk and interfacial stress tensors respectively and the other quantities have been defined previously.

The *dynamic* or *mean interfacial tension* is defined as

$$\overline{\sigma}\overset{\text{def}}{=}\frac{1}{2}\mathbf{I}_s{:}\mathbf{P}^s, \tag{6.89}$$

at the interfacial point $\mathbf{x}_s$ [?, page 109]. Interfacial phases are generally not incompressible in that $\nabla_s\cdot\mathbf{v}_s\neq 0$ even though $\nabla\cdot\mathbf{v}=0$ and a difference will generally exist between the dynamic interfacial tension $\overline{\sigma}$ and the thermodynamic interfacial tension σ[?].

6.3 Constitutive Equations — Interfacial adsorption and Surface Equations of State — Equilibrium or Non-equilibrium

All models on the Marangoni effect, presented in the literature that have been reviewed for this study, start with the Navier-Stokes and the continuity equation developed in section 6.1.2 for incompressible Newtonian fluids with boundary conditions at the interface given by the surface solute mass conservation equation, equation ??, and the surface momentum conservation equation, equation ??. Additionally as has been discussed, bulk concentration gradients in each liquid phase are assumed linear and the partition relationship between the contiguous bulk phases is in an equilibrium state as well as steady state transport across the interface. These simplifying assumptions are not present in the metal extraction with membranes though they can be assumed in certain circumstances.

6.3.1 Interfacial Adsorption

Basically to solve the species transport equation involving an active interface the following can be summarized [?]:

1. The bulk phase equilibrium partitioning of the species (generally a surfactant) across the fluid interface is

$$\overline{\rho}_i\left(0^+\right) = K_i \overline{\rho}_i\left(0^-\right) \tag{6.90}$$

The partition relationship cannot in a strict sense be used for non equilibrium circumstances.

2. The normal component bulk-phase flux [i.e. surface species flux equation (boundary condition)]

$$\frac{d\rho_i^s}{dt} + \nabla_s \cdot \left(\mathbf{v}^o \rho_i^s\right) - \nabla_s \cdot \left(\mathfrak{D}_i^s \nabla_s \rho_i^s\right) = R_i^s + \mathbf{n} \cdot \parallel \overline{j_i} \parallel \tag{6.91}$$

3. A kinetic adsorption relation like the Frumkin or Langmuir Isotherms. These represent equilibrium states and thermodynamically ideal bulk solutions. Non equilibrium adsorption is represented by a kinetic rate expression for the normal component of the bulk phase species flux at the interface in terms of the local surfactant adsorption rate as given by

$$\mathbf{n} \cdot \overline{\mathbf{j}}_i^o = \phi_i \tag{6.92}$$

(where ϕ_i is the local adsorption rate). Specification of the type of isotherm relationship i.e. equilibrium or non-equilibrium also specifies the partition relation. A kinetic rate expression developed Borwanker and Wasan [?] for Frumkin-like adsorption behavior in the equilibrium limit is

$$\phi_i = K_a \exp\left[\frac{A}{2}\left(\frac{\rho_i^s}{\rho_{i\infty}^s}\right)^2\right]\left[\overline{\rho}_i^o\left(\rho_{i\infty}^s - \rho_i^s\right) - \frac{\rho_i^s}{K_a}\exp\left(-A\frac{\rho_i^s}{\rho_{i\infty}^s}\right)\right] \tag{6.93}$$

and for ideality A=0, the Langmuir-type kinetic expression is

$$\phi_i = K_a\left[\overline{\rho}_i^o\left(\rho_{i\infty}^s - \rho_i^s\right) - \frac{\rho_i^s}{K_a}\right] \tag{6.94}$$

If the assumption is made, as do most analytical investigations of Marangoni effect, that small perturbations from the equilibrium adsorption state occur then the knowledge of interfacial tension variation with specie density over the entire range of interfacial composition would be unnecessary since the kinetic adsorption rate may be linearized about the equilibrium state to obtain

$$\begin{aligned}
\phi_i &= \phi_i^a - \phi_i^d \\
&= \left(\phi_i^a\right)_o - \left(\phi_i^d\right)_o + \left[\left(\frac{\partial \phi_i^a}{\partial \rho_i^s}\right)_o - \left(\frac{\partial \phi_i^d}{\partial \rho_i^s}\right)_o \left(\rho_i^s - \rho_{i\,o}^s\right) + \ldots\right] \\
&\approx \alpha_i\left(\rho_i^s - \rho_{i\,o}^s\right),
\end{aligned} \tag{6.95}$$

where (a) (d) represent adsorption and desorption and are equal at equilibrium state represented by o and the single adsorption parameter is

$$\alpha_i \equiv \left(\frac{\partial \phi_i^a}{\partial \rho_i^s}\right)_o - \left(\frac{\partial \phi_i^d}{\partial \rho_i^s}\right)_o . \tag{6.96}$$

If the specification of the bulk phase concentration fields in the proximity of the interface $\overline{\rho}_i(0^+)$ and $\overline{\rho}_i(0^-)$ is made or known *a priori* then the species flux boundary condition is not needed. Thus, under these circumstances the solution of the bulk phase species transport, the interfacial boundary condition reduces to a single equation (assuming the velocities are known) — the surface excess convection diffusion equation, equation 6.61.

Two limiting case solutions for equation 6.61 are [?] these controlling mechanisms are also discussed in more detail in chapter ?? page ??:

diffusion controlled species is transported slowly by diffusion through the bulk phase to the interface instantaneously relative to the diffusion step. An equilibrium adsorption relationship may therefore be assumed at the instantaneous conditions and the known bulk phase diffusion flux directly substitutes into the right hand side of equation 6.61 and upon solution furnish Γ_i^s (or ρ_i^s or c_i^s) without having to devote attention to details of adsorption kinetics.

Adsorption Controlled species transported rapidly to the interface by diffusion and/or convection and the adsorption steps become rate limiting. The surface excess species species balance equation may be regarded as being separate from the bulk-phase surfactant transport equation. Thus using an equation like 6.92 in the normal bulk species flux equation with an appropriate constitutive choice of kinetic rate expression provides a single equation for determining Γ_i^s (or ρ_i^s or c_i^s).

There is also the possibility of mixed regime along with chemical reactions in the bulk. This may strongly effect the interfacial tension gradients and their effects on the Marangoni Phenomena. The mixed regime is also discussed in chapter ??. A thorough knowledge of the kinetics is needed in a mixed regime.

6.3.2 The Surface Equation of State

The surface equation of state is generally a phenomenological relationship between the interfacial tension and the state of the interface i.e. its composition. The equation is developed under equilibrium conditions and is assumed to be equally applicable under non equilibrium conditions as long as the properties at each point do not change very rapidly closely generating a discontinuity [?, page 20]. This does not mean that the state variables

do not change just not in a jump condition. The Gibbs surface equation of state is useful in interfacial studies as long as the amount of a species is not high generally only in trace amounts and not applicable to concentrated monolayers[?, page 171]. Two surface equations of state developed from the Frumkin and Langmuir isotherms for the surface pressure[?, page 171]

$$\pi \stackrel{\text{def}}{=} \sigma_o - \sigma \equiv -\frac{RT}{M}\rho^s_{i\infty}\left[\ln\left(1-\frac{\rho^s_i}{\rho^s_{i\infty}}\right)+\frac{A}{2}\left(\frac{\rho^s_i}{\rho^s_{i\infty}}\right)^2\right] \tag{6.97}$$

and with $A \to 0$ (A is a parameter which measures the degree of non-ideality of the interface $A = 0$ for ideality),

$$\pi = \sigma_o - \sigma \equiv -\frac{RT}{M}\rho^s_{i\infty}\left[\ln\left(1-\frac{\rho^s_i}{\rho^s_{i\infty}}\right)\right] \tag{6.98}$$

where R and T are the gas constant and temperature. Combining equation 6.98 with the ideal Langmuir isotherm

$$\frac{\rho^s_i}{\rho^s_{i\infty}-\rho^s_i} = K_a\overline{\rho}^o_i \tag{6.99}$$

the *Szyskowsky-Langmuir* equation is obtained [?], [?].

$$\pi = \sigma_o - \sigma \equiv -\frac{RT}{M}\rho^s_{i\infty}\ln\left(1+K_a\overline{\rho}^o_i\right). \tag{6.100}$$

For small deviations from equilibrium the linearization of the interfacial tension can be used to give

$$\begin{aligned}\sigma &= \sigma_o + \left(\frac{\partial\sigma}{\partial\rho^s_i}\right)_o(\rho^s_i-\rho^s_{i\,o})+\ldots\\ &\approx \sigma_o - \frac{1}{\rho^s_o}E^i_o\left(\rho^s_i-\rho^s_{i\,o}\right),\end{aligned} \tag{6.101}$$

where

$$E^i_o \stackrel{\text{def}}{=} -\left(\frac{\partial\sigma}{\partial\ln\rho^s_i}\right)_o \tag{6.102}$$

Note that $\overline{\rho}^o_i$ can be chosen to be either $\overline{\rho}_i(0^+)$or $\overline{\rho}_i(0^-)$ since K^+_a and K^-_a will differ by the required amount necessary to make $K_a\overline{\rho}^o_i$ independent of the choice [?].

6.4 Summary of the Interfacial Boundary Conditions to incorporate the Marangoni Phenomena

To properly model a system of two phase mass transfer the interfacial effects must be applied. In this chapter the equations to incorporate the interface in a two dimensional fundamental approach have been presented. The development of the Marangoni Effects using the equations of motion i.e. the Navier-Stokes equation was presented as well as the constitutive equations for the surface properties and the surface equation of state. Care must be exercised in the application of these constitutive equations since most are derived from equilibrium systems and the membrane system as has been repeated several times is a non-equilibrium system. With simplifications the membrane can be modeled as an equilibrium system. Such simplifications will be kept to a minimum in this study and the membrane modeled at unsteady state with a non-equilibrium interface.

To summarize the interfacial modeling the table below will help as a map of the boundary equations (note after Edwards *et al* [?, page 473]):

Summary of Interfacial Transport Boundary Conditions

Mass	
Continuity of velocity	Equation 6.74
Hydrodynamics	
Interfacial stress boundary condition	Equation 6.88
Species Transport	
Surface Excess formulations of phenomenological coefficients	
Interfacial species flux	Equation 6.56
for Fickian Flux	Equation 6.61
Non-equilibrium adsorption kinetic realtion	
Frumkin	Equation 6.93
Langmuir	Equation 6.94
small departure from equilibrium	Equation 6.95
general non-equilibrium	intrinsic chemical kinetic adsorption equations of the system
Surface Equation of State	
Frumkin	Equation 6.97
Langmuir	Equation 6.98
Szyskowsky	Equation 6.100
small diviations from equilibrium	Equations 6.101 and 6.102

6.5 Nomenclature for Chapter 6

A	interfacial surface area between phases
$\mathbf{a}_\alpha$	surface co-variant unit vector ($\alpha = 1, 2$)
$\mathbf{a}^\alpha$	surface contra-variant unit vector ($\alpha = 1, 2$)
$\mathfrak{D}_i$	diffusivity of species i
$d\mathbf{A}$	differential element of surface or interface
$d\mathbf{S}$	outward pointing normal on ∂V
$\mathbf{e}_\alpha$	mutually perpendicular co-variant unit vector ($\alpha = i, j, k$)
$\mathbf{e}^\alpha$	mutually perpendicular contra-variant unit vector ($\alpha = i, j, k$)
$\mathbf{g}_i$	spatial covariant base vectors
g_{ij}	metric tensor
$\mathbf{I}$, $\mathbf{I}_s$	unit spatial Idemfactor or unit surface Idemfactor (identity tensor that transforms every vector into itself
i_i	unit orthogonal base vectors ($i = 1, 2, 3$)
n	normal coordinate to the surface
$\mathbf{n}$	outwardly pointing normal
P_s	Point on a surface
$\mathfrak{P}$	generic physical property
q^i	three dimensional curvilinear coordinates ($i = 1, 2, 3$)
q^3	curvilinear coordinate normal to the surface
q^α	two dimensional curvilinear coordinates ($\alpha = 1, 2$)
V, V(t)	time dependent domain of fluid volumetric element of fluid
∂V, dV	surface area bounding a single phase volumetric element (see figure 6.4 page 176)
$\mathbf{v}$	mass average velocity
x^i, x, y, z	$i = 1, 2, 3$ rectangular coordinates

$\mathbf{x}_s$ surface position vector

$\mathbf{x}$ spatial position vector

$\mathbf{Z}$ extensive volumetric rate of supply

Greek Letters

ζ intensive volumetric rate of supply of generic physical property (amount of property per unit volume) $\zeta \equiv \zeta(\mathbf{x}, t)$

Γ_i molar species concentration

$\boldsymbol{\lambda}$ generic volumetric variable used in parameterization form three dimensional to two dimensional region

$\mathbf{\Pi}$ rate of production of property $\mathfrak{P}$ within a volume element V. Extensive time rate of production of generic physical property within a fluid volume

π intensive volumetric production rate density: time rate of production of generic physical property at a point of fluid (amount of the property $\mathfrak{P}$ per unit volume)

$\mathbf{\Phi}$ extensive diffusive flux out of the bounding surface of a fluid volume; time rate at which property $\mathfrak{P}$ a fluid volume is transferred out of the volume V through a surface.

$\boldsymbol{\phi}$ areal diffusive flux density : intensive diffusive flux of generic property (amount of the property $\mathfrak{P}$ per unit time per unit volume)

$\mathbf{\Psi}$ time dependent total amount of generic, extensive physical property $\mathbf{\Psi} \equiv \mathbf{\Psi}(t)$

$\boldsymbol{\psi}$ volumetric density field (intensive amount of a generic property at a point of fluid) [amount of property $\mathfrak{P}$ per unit volume] $\boldsymbol{\psi} \equiv \boldsymbol{\psi}(t)$

Operators

∇ gradient

$\nabla\cdot$, *div* divergence operator

$\| \mathfrak{R} \|$ discontinuous tensor field or jump condition for field $\mathfrak{R}$

$\frac{D}{Dt}$ convected, material or substantial derivative

Superscripts

(overbar)	bulk phase or discontinuous property
s	surface excess quantity

Subscript

s	property assigned to the surface

7. THERMODYNAMIC CONSIDERATIONS

$\Delta H = -10.9 \frac{kcal}{mole}$
$\Delta G = +3.32 \frac{kcal}{mole}$
$\Delta S = -44$ e.u.

Thermodynamic paramters as determined by Vandegrift and Horwitz J. of Nucl Chem 1977 vol 19 pp 1425-1432 for the extraction of calcium from intric acid with HDEHPA in dodecane.